Controlled radical polymerization of vinyl esters and vinyl amides : experimental and theoretical studies

Aurélie Morin

Université de Toulouse

THÈSE

En vue de l'obtention du

DOCTORAT DE L'UNIVERSITÉ DE TOULOUSE

Délivré par :

Institut National Polytechnique de Toulouse (INP Toulouse)

Présentée et soutenue par :
Aurélie MORIN

le 06 novembre 2013

Titre :

Controlled Radical Polymerization of Vinyl Esters and Vinyl Amides: Experimental and Theoretical Studies

Polymérisation Radicalaire Contrôlée d'Esters et d'Amides de vinyle: Etudes Expérimentales et Théoriques

---

École doctorale et discipline ou spécialité :

ED SDM : Chimie organométallique de coordination - CO 043

Unité de recherche :

Laboratoire de Chimie de Coordination - LCC - CNRS - UPR 8241

Directeur(s) de Thèse :

Rinaldo POLI

Jury :

Pr. Rinaldo POLI	Directeur de thèse
Dr. Karine COSTUAS	Rapporteur
Pr. Sylvain MARQUE	Rapporteur
Pr. Mathias DESTARAC	Examinateur
Pr. Albert DEMONCEAU	Examinateur
Pr. Tomislav PINTAUER	Invité

En mémoire de toi, papa…

AVANT-PROPOS

Ces trois années passées au Laboratoire de Chimie de Coordination ont été riches tant d'un point de vue scientifique que de celui des relations humaines. Je tiens à exprimer mes remerciements à l'Ensemble du personnel du LCC dirigé par Azzedine Bousseksou, Denis Neibecker et Noël Lugan.

Je remrcie les membres du service de RMN : David Paryl, Francis Lacassin et Christian Bijani, du service de RPE : Jean-François Meunier et Lionel Rechignat, du service commun de spectrométrie de masse de l'université Paul Sabatier. J'adresse mes remerciements à Regis Laurent pour son aide en GPC.

Je tiens à remercier très chaleureusement mon directeur de thèse Rinaldo Poli. Il est un scientifique hors pair qui m'a beaucoup appris et qui m'a encouragée vers la réussite. Je remercie également tous les membres passés et présents de l'équipe G, une équipe soudée, pleine d'humour et de sympathie: Jean-Claude Daran, Eric Manoury, Agnès Labande, Sandrine Vincendeau, Florence Gayet, Eric Deydier, Catherine Audin, Dominique Agustin, Audric Michelot, Pauline Loxq, Aurélien Bethegnies, Andrès Cardozo, Zhigang Xue, Si Chen, Muh-Mei Wei et Katia Kozinets. Je remercie énormément Yohan Champouret qui a été un encadrant formidable lors de ma première année de thèse et qui malgré son changement d'équipe a suivi mes travaux et m'a aidée jusqu'au bout de cette expérience.

J'aimerais remercier mes collègues de l'équipe A: Vincent César, Guy Lavigne, Stéphanie Bastin, Dmitry Valyaev, Cécile Barthes, Rémy Brousses, Ludovik Noël-Duchesneau, Yin Zhang, Mirko Ruamps ainsi que Chiara Dinoi, Michel Etienne, Christine Lepetit, Corentin Poidevin, Heinz Gornitzka, Catherine Hemmert, Emmanuel Gras et Anne Robert. Je remercie également mes collègues enseignants de l'IUT de Chimie de Castres ainsi que mes collègues de l'IUT de Mesures Physiques de Toulouse. Merci de votre aide pour mes premiers pas en tant qu'enseignante.

Je remercie aussi « l'administration » du LCC et plus particulièrement Patricia Fouquereau et Isabelle Boutonnet qui malgré leur charge de travail ont toujours fait de leur mieux pour répondre à mes demandes, Mélanie Bégué pour ses talents culinaires et sa motivation sportive, Michel Griessinger et ses deux princesses. Je souhaite remercier Fabrice Candau, Jérôme Colombet, Michel Maupomé, Philippe Prono, Jean-Michel Van Butsele et Abdel Zouak ainsi que toute l'équipe de la cantine qui avec sa bonne humeur quotidienne (ou

presque) a fait de ma pause déjeuner un moment agréable. J'aimerais remercier Martine Morin pour sa joie de vivre quotidienne.

J'ai passé de très bon moments au LCC durant ces trois années, j'y ai rencontré de nombreuses personnes formidables qui sont devenues pour certaines de sincères ami(e)s. Pauline, Nadia, Ch'ti mi, Andrès et Cendrine, Tahiti douche vanille, stagiaire Hameau, Hélène la récessive et Kévin, Sabrina, Hanna, Kévin le coquin et Jérémy, Marlène, Justine, Daniel, Julien, Manel, Rémy le marseillais, Mélanie, Audric, Luca, Eric dit le mi-roux et Eric dit le petit, directrice Agnès, Arnaud el mafioso, Mirko de Montcuq, président Michelot, je vous remercie pour votre bonne humeur. Je remercie ma chéwi de mon coeur élo, johnny le gitan et mimi pour m'avoir kidnappée un weekend du mois d'août.

Enfin, je remercie plus que tout ma maman et ma soeur qui ont toujours été là pour moi ainsi que mon loulou qui a supporté chaque jour mes humeurs.

Je vous remercie toutes et tous très sincèrement.

ABBREVIATIONS and SYMBOLS

Symbols

%w	Weight percentage
κ	Chelate species
λ	Spin-orbit coupling constant
μ_B	Bohr magneton
a	Hyperfine coupling constant in EPR spectra
B	Magnetic field
C_{tr}	Chain transfer constant
Đ	Dispersity
E	Electronic energy
g	g factor
h	Planck constant
H	Enthalpy
k	Rate constant
K	Equilibrium constant
M	Monomer
M_n	Number-average molecular weight
$M_{n,exp}$	Experimental number-average molecular weight
$M_{n,theor}$	Theoretical number-average molecular weight
M_S	Secondary spin quantum number
M_w	Weight-average molecular weight
T_{melt}	Melting temperature
X_n	Degree of polymerization

Abbreviations (except chemical compounds listed below)

ARGET	Activators regenerated by electron transfer
ATRA	Atom transfer radical addition
ATRP	Atom transfer radical polymerization
BDE	Bond dissociation energy
BIRP	Organobismuthine-mediated radical polymerization
CA	Controlling agent

CCT	Catalyzed chain transfer
CERM	Center for education and research on macromolecules
CMRC	Cobalt-mediated radical coupling
Co-MRP	Cobalt-mediated radical polymerization
CSIRO	Commonwealth scientific and industrial research organization
CTA	Chain transfer agent
Cu-MRP	Copper-mediated radical polymerization
DSC	Differential scanning calorimetry
DFT	Density functional theory
DT	Degenerative transfer
ED	Electron donor
EPR	Electron paramagnetic resonance
FRP	Free radical polymerization
GC	Gas chromatography
GGA	Generalized gradient approximation
GPC	Gel permeation chromatography
H	Head
H-H	Head-to-head
H-T	Head-to-tail
ITP	Iodine transfer polymerization
LCST	Lower critical solubility temperature
LDA	Local density approximation
LRM	Less reactive monomer
LUMO	Lowest unoccupied molecular orbital
MADIX	Macromolecular design via the interchange of xanthates
MALLS	Multiangle laser light scattering
MRM	More reactive monomer
MW	Molecular weight
NMP	Nitroxide-mediated polymerization
NMR	Nuclear magnetic resonance
OMRP	Organometallic-mediated radical polymerization
RAFT	Reversible addition-fragmentation chain transfer
RDARP	Reversible dissociative activation radical polymerization
RDRP	Reversible deactivation radical polymerization

RITP	Reverse iodine transfer polymerization
ROP	Ring opening polymerization
SBRP	Organostibine-mediated radical polymerization
SEC	Size exclusion chromatography
SQUID	Superconducting quantum interference device
T	Tail
TERP	Organotellurium-mediated radical polymerization
TOFMS	Time-of-flight mass spectrometry

Chemical compounds abbreviations

1-PEI	1-PhenylEthyl Iodide
2-N(CH_3)CTPPH	2-Aza-2-methyl-5,10,15,20-tetraphenyl-21-carbaporphyrin
2VP	2-Vinyl Pyridine
AA	Acrylic acid
Acac	Acetylacetonate anion
AIBN	Azo-*bis*-isobutyronitrile
AM	Acrylamide
AMBS	Sodium 3-acrylamido-3-methylbutanoate
AMPS	Sodium 2-acrylamido-2-methylpropane-1-sulfonate
AN	Acrylonitrile
BA	*N*-Butylacrylate
bPy	2,2'-bipyridine
BzMA	Benzyl methacrylate
Cp	Cyclopentadienyl
CPD	α-Cumyl peroxyneodecanoate
CPM	2,4,4,6-Tetrakis(ethoxycarbonyl)hepta-1,6-diene
$CTPPH_2$	2-Aza-5,10,15,20-tetraphenyl-21-carbaporphyrin
DCDPS	Diethyl 2,3-dicyano-2,3-diphenylsuccinate
DCM	Dichloromethane
Dipp	2,6-Diisopropylphenyl
DMA	*N,N*-dimethylacrylamide
DMAEMA	*N,N*-(dimethylamino)ethyl methacrylate
DMF	Dimethylformamide
DMSO	Dimethylsulfoxide

DPCM	Diphenyldithiocarbamate of diethylmalonate
dTbpy	Di-*tert*-butyl-2,2′-bipyridine
EBP	Ethylbromopropionate
EHMA	2-ethylhexyl methacrylate
EMA-TeMe	Ethyl 2-methyltellanyl-2-methylpropionate
Et	Ethyl
GMA	Glycidyl methacrylate
HDPE	High-density polyethylene
*i*BMA	*iso*Butyl methacrylate
Im	Imidazole
iPr	*iso*Propyl
LDPE	Low-density polyethylene
LLDPE	Linear low-density polyethylene
MA	Methyl acrylate
MAH	Maleic anhydride
MANTU	*N*-Meth-acryloyl-N'-(α-naphthyl)thiourea
MCP	Methyl-2-chloropropionate
Me	Methyl
MeCN	Acetonitrile
Me_6TREN	Tris[2-(dimethylamino)ethyl]amine
MMA	Methyl methacrylate
$NacNac^{RR'}$	*N*-[3-[(alkyl')amino]-1-methyl-2-buten-1-ylidene]-alkylamine
NHC	*N*-heterocyclic carbene
NIPAM	*N*-isopropyl acrylamide
NMVA	*N*-methyl-*N*-vinylacetamide
NVA	*N*-vinyl acetamide
NVCl	*N*-vinyl caprolactam
NVF	*N*-vinyl formamide
NVP	Vinyl pyrrolidone
NVPip	*N*-vinyl-2-piperidone
OTf	Trifluoromethanesulfonate or triflate
PCl	Poly(ε-caprolactone)
PE	Poly(ethylene)
PEA	Poly(ethylacrylate)

PEG	Poly(ethyleneglycol)
PMDETA	*N,N,N′,N″,N″*-pentamethyldiethylenetriamine
PMMA	Poly(methylmethacrylate)
PNMVA	Poly(*N*-methyl-*N*-vinylacetamide)
PNVCl	Poly(*N*-vinyl caprolactam)
PNVF	Poly(*N*-vinyl formamide)
PNVP	Poly(vinyl pyrrolidone)
PS	Poly(styrene)
PVA	Poly(vinyl amide)
PVAc	Poly(vinyl acetate)
PVOH	Poly(vinyl alcohol)
Py	Pyridine
SSO3Na	Sodium styrene-4-sulfonate
St	Styrene
*t*BA	*tert*-Butylacrylate
*t*Bu	*tert*-Butyl
TCE	2,2,2-Trichloroethanol
TEMPO	2,2,6,6-Tetramethylpiperidin-1-yl)oxyl
THF	Tetrahydrofuran
TMP	Tetramesitylporphyrin
Tp*	Hydrotris(3,5-dimethylpyrazol-1-yl)borate anion
Tp^{CF3}	Hydrotris(3,5-bis(trifluoromethyl)pyrazol-1-yl)-borate anion
TPED	1,1,2,2-tetraphenylethane-1,2-diol
Tp^{H}	Hydrotris(pyrazol-1-yl)borate anion
Tp^{iPr}	Hydrotris(3,5-diisopropylpyrazol-1-yl)borate anion
TPMA*	Tris((4-methoxy-3,5-dimethylpyridin-2-yl)methyl)amine
TPTM	Tris(2-pyridylthio)methanide
tPy	2,2’;6’,2’’-Terpyridine
V-601	2,2’-Azobis(2-methylpropionate)
V-70	2,2'-Azobis(4-methoxy-2,4-dimethyl valeronitrile)
VAc	Vinyl acetate
VBz	Vinyl benzoate
Xyl	2,6-Dimethylphenyl or xylyl

TABLE OF CONTENTS

RÉSUMÉ EN FRANÇAIS

INTRODUCTION GÉNÉRALE

1) Les polymérisations radicalaires contrôlées

Les deux dernières décennies ont montré une réelle explosion du nombre de publications relatives aux polymérisations radicalaires contrôlées (PRC). La polymérisation radicalaire est une polymérisation en chaîne qui peut être décrite par quatre étapes fondamentales : l'amorçage, la propagation, la terminaison et les transferts de chaînes. Lorsque les réactions de terminaisons et de transferts de chaînes sont absentes, on parle alors de « polymérisation vivante » et le contrôle de la masse molaire, de la dispersité et des fonctionnalités de bout de chaînes des polymères synthétisés est ainsi possible. Une polymérisation radicalaire vivante est impossible car les radicaux sont sujets aux terminaisons bimoléculaires spontanées par couplage et/ou dismutation. Née en 1994,[1] l'expression "Polymérisation Radicalaire Contrôlée" se réfère aux polymérisations radicalaires dont la proportion de réactions de terminaisons et de transferts de chaînes par rapport à la croissance des chaînes est si faible que les caractéristiques de la polymérisation sont proches de celles attendues pour une polymérisation vivante. Il y a deux manières de contrôler la croissance des chaînes de polymère. La première est basée sur la réduction de la concentration en radicaux dans le milieu de telle sorte que les réactions de terminaison soient minimisées (la vitesse de terminaison est proportionnelle au carré de la concentration en radicaux alors que la vitesse de propagation est proportionnelle à la concentration en radicaux). Cette stratégie, appelée polymérisation radicalaire par activation dissociative réversible (RDARP), repose sur un piégeage dynamique et réversible des chaînes radicalaires en croissance par un agent de contrôle (CA) et formant une espèce dormante (Scheme 1), bénéficiant ainsi de l'effet radical persistant. L'équilibre doit être déplacé vers l'espèce dormante pour assurer un bon contrôle. La deuxième stratégie pour contrôler la polymérisation est appelée polymérisation radicalaire par transfert dégénératif (DTRP) (Scheme 2) car l'énergie de Gibbs totale se conserve (elle est identique des deux côtés de l'équation). La seule différence est la longueur des chaînes P et P'. La vitesse d'échange doit être idéalement beaucoup plus rapide que la vitesse de propagation pour obtenir un bon contrôle de la formation des polymères.[2] L'avantage des procédés radicalaires est leur grande tolérance à de nombreux groupes fonctionnels (alcool, amines…), et aux impuretés (en particulier à l'eau), et la large gamme de monomères polymérisables. Aujourd'hui, des polymères fonctionnalisés et à architectures complexes ont

[1] S. Gaynor, D. Greszta, D. Mardare, M. Teodorescu, K. Matyjaszewski, *J. Macromol. Sci., Pure Appl. Chem*., **1994**, *A31*, 1561-1578
[2] A. H. E. Müller, R. Zhuang, D. Yan, G. Litvinenkos, *Macromolecules*, **1995**, *28*, 4326-4333

été obtenus par PRC alors qu'il y a 15 ans, un tel contrôle ne pouvait être assuré que par polymérisation anionique ou cationique. De nombreux agents de contrôle ont été découverts et de nombreux monomères ont été polymérisés avec succès par PRC. Toutefois, il n'existe toujours pas de méthode satisfaisante pour le contrôle de la polymérisation de monomères peu réactifs (*i.e.* monomères donnant un radical très réactif). La raison principale est la haute énergie requise pour casser la liaison polymère-CA.

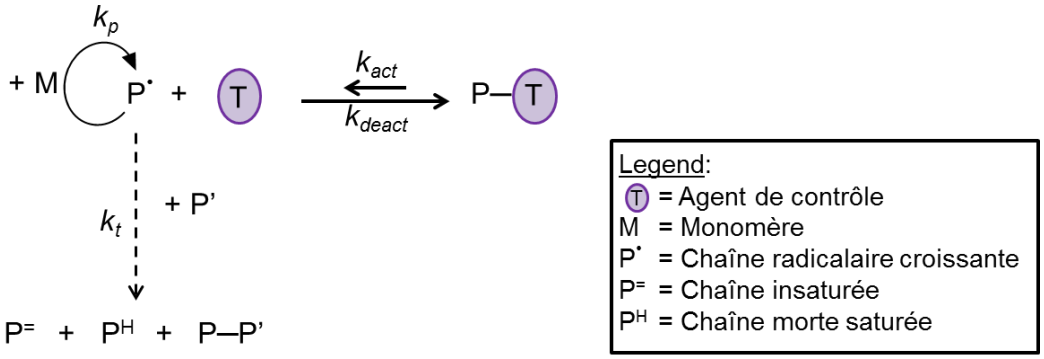

Schéma 1: Mécanisme général d'une polymérisation radicalaire par activation dissociative réversible.

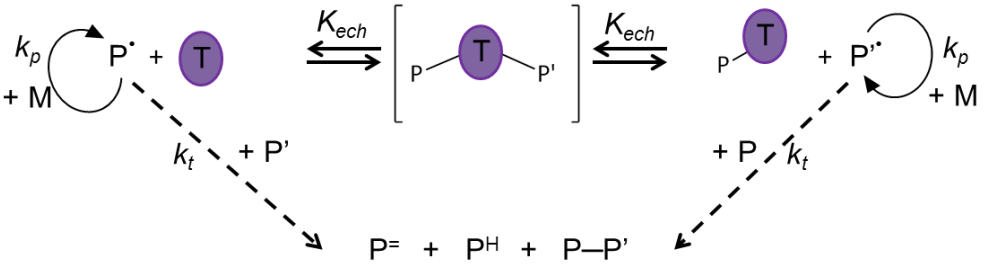

Schéma 2 : Mécanisme général d'une polymérisation radicalaire par transfert dégénératif.

Dans les polymérisations ayant un mécanisme de désactivation réversible, on retrouve la Polymérisation Contrôlée par des Nitroxides (NMP), la Polymérisation Radicalaire par Transfert d'Atome (ATRP) et la Polymérisation Radicalaire Contrôlée par voie Organométallique (OMRP).

L'agent de contrôle en NMP est un nitroxide stable comme, par exemple le TEMPO représenté dans la Figure 2.[3] L'ATRP quant à elle, a été découverte simultanément par Matyjaszewski[4] et Sawamoto[5] en 1995. L'étape clef est le transfert d'un atome d'halogène (le plus souvent un atome de chlore) depuis un complexe métallique dans un état d'oxydation (n+1) sur la chaîne radicalaire croissante pour former une chaîne terminée par un atome d'halogène et le complexe métallique dans un état d'oxydation n. De nombreux agents de

[3] D. H. Solomon, E. Rizzardo, P. Cacioli, CSIRO, **1985**, EP0135280A2
[4] K. Matyjaszewski, J.-S. Wang, *J. Am. Chem. Soc.*, **1995**, *117*, 5614-5615
[5] M. Kato, M.Kamigaito, M. Sawamoto and T.Higashimura, *Macromolecules*, **1995**, *28*, 1721-1723

contrôle ont été découverts permettant le contrôle en ATRP ou NMP de nombreux monomères tels que le styrène et ses dérivés, les (meth)acrylates, les (meth)acrylamides, les (meth)acrylonitriles, les vinylpyridines, le butadiène, les vinyl férrocéniques…[6,7,8,9] Toutefois, tous ces monomères sont classifiés comme "monomères activés". Les "monomères peu réactifs" comme l'acétate de vinyle, l'ethylène ou la pyrrolidone de vinyle ont été longuement étudiés mais sans succès.[10,11] Ces échecs ont été expliqués par une liaison carbone-CA trop forte.

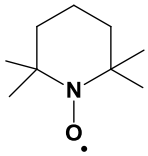

Figure 1: Structure du 2,2,6,6-tetramethylpiperidin-1-yl)oxyl ou TEMPO.

L'OMRP[12,13] a été introduite par Wayland en 1994.[14] La Polymérisation Radicalaire Contrôlée par des complexes de Cobalt (Co-MRP) est de loin la plus étudiée, en particulier l'agent de contrôle cobalt(II) acétylacétonate ([$Co(acac)_2$],

Figure 2),[15] mais des OMRP avec des complexes de vanadium,[16] chrome,[17] et osmium[18] ont également été rapportées. Jérôme réussit à contrôler la polymérisation de l'acétate de vinyle utilisant du [$Co(acac)_2$] (commercialement disponible) et du V-70 (

Figure 2) comme amorceur, à 30°C. Du poly(acétate de vinyle) (PAcV) ayant des masses molaires de plus de 99 000 g/mol et un faible indice de polymolécularité (Đ = 1.33) fût synthétisé. Il fût montré plus tard que dans les conditions rapportées par Jérôme, le mécanisme de polymérisation était en fait un mécanisme par transfert dégénératif (DT) plutôt

[6] [a] G. Moad, E. Rizzardo, *Macromolecules*, **1995**, *28*, 8722-8728; [b] S. Grimaldi, J. P. Finet, A. Zeghdaoui, P. Tordo, D. Benoit, Y. Gnanou, M. Fontanille, P. Nicol, J. F. Pierson, *Polym. Prep*., **1997**, *38*, 651-652; [c] N. L. Hill, R. Braslau, *Macromolecules*, **2005**, *38*, 9066-9074 ; [d] A. Fischer, A. Brembilla, P. Lochon, *Macromolecules*, **1999**, *32*, 6069-6072 ; [e] W. A. Braunecker, K. Matyjaszewski, *Prog. Polym. Sci*., **2007**, *32*, 93-146; [f] F. Chauvin, P.-E. Dufils, D. Gigmes, Y. Guillaneuf, S. R. A. Marque, P. Tordo, D. Bertin, *Macromolecules*, **2006**, *39*, 5238-5250
[7] D. Xiao, M. J. Wirth, *Macromolecules*, **2002**, *35*, 2919-2925
[8] K. Matyjaszewski, S. Mu Jo, H.-J. Paik, S. G. Gaynor, *Macromolecules*, **1997**, *30*, 6398-6400
[9] J. Xia, X. Zhang, K. Matyjaszewski, *Macromolecules*, **1999**, *32*, 3531-3533
[10] J.-F. Lutz, P. Lacroix-Desmazes, B. Boutevin, C. Le Mercier, D. Gigmes, D. Bertin, P. Tordo, *Polym. Prep*., **2002**, *43*, 287-288
[11] P. Bilalis, M. Pitsikalis, N. Hadjichristidis, *J. Polym. Sci Part A: Polym. Chem*., **2006**, *44*, 659-665
[12] A. Debuigne, J.-R. Caille, R. Jérôme, *Macromolecules*, **2005**, *38*, 5452-5458
[13] B. B. Wayland, L. Basickes, S. L. Mukerjee, M. Wei, M. Fryd, *Macromolecules*, **1997**, *30*, 8109-8112
[14] B. B. Wayland, G. Poszmik, and S. L. Mukerjee *J. Am. Chem. Soc.*, **1994**, *116*, 7943-7944
[15] A. Debuigne, J.-R. Caille, R. Jérôme, *Angew. Chem. Int. Ed*., **2005**, *44*, 1101-1104
[16] M. R. Perry, L. E. N. Allan, A. Decken, M. P. Shaver, *Dalton Trans*., **2013**, *42*, 9157-9165
[17] Y. Champouret, K. C. MacLeod, U. Baisch, B. O. Patrick, K. M. Smith, R. Poli, *Organomet*., **2010**, *29*, 167-176
[18] W. A. Braunecker, Y. Itami, K. Matyjaszewski, *Macromolecules*, **2005**, *38*, 9402-9404

qu'un mécanisme par désactivation réversible.[19] Cependant, une véritable RDARP a lieu lorsqu'un ligand se coordinant sur le cobalt est additionné.[20]

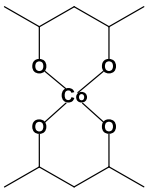

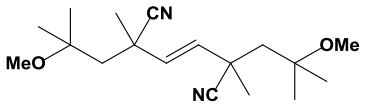

Figure 2 : Cobalt(II) acétylacétonate [$Co(acac)_2$] et V-70 ou 2,2'-Azobis(4-methoxy-2.4-dimethyl valeronitrile).

D'un point de vue industriel, l'OMRP est problématique car elle nécessite une quantité stœchiométrique en métal (contrairement à l'ATRP où le métal est en quantité catalytique) donc nécessite un traitement post-opératoire pour éliminer toute trace de métal des chaînes de polymère. Cet inconvénient pourrait être outrepassé par l'immobilisation des agents de piégeages sur surface ou par recyclage du métal après section des bouts de chaînes.[21]

Les complexes de cobalt sont sujets à la catalyse par transfert de chaînes (CCT) qui implique l'abstraction d'un atome d'hydrogène en position alpha du carbone portant le radical. Ce processus d'abstraction d'un atome d'hydrogène par LCo^{II} est généralement l'étape cinétiquement déterminante en CCT. Elle se produit à des vitesses égales ou proches des limites de diffusion ce qui indique que la barrière d'activation de ce processus est extrêmement basse. Il a été proposé que le mécanisme d'abstraction de l'atome d'hydrogène soit (dans la majorité des cas) une abstraction directe via un intermédiaire à trois centres. Puis, l'espèce de cobalt hydrure, très réactive, transfèrerait l'hydrogène au monomère.

a) Mécanisme par transfert dégénératif

Le transfert de chaîne par addition-fragmentation réversible (RAFT)[22,23] est assuré par un composé thiocarbonylthio (Z-C(S)S-R) ou par un xanthate (Z'-O-C(S)S-R) et l'on parle alors de conception macromoléculaire par échange de xanthate (MADIX). La réaction principale permettant la croissance des chaînes est représentée dans le Schéma 3. Le choix de l'agent RAFT est crucial car il influence profondément la cinétique des différentes étapes et permet ainsi le contrôle de la polymérisation de monomères particuliers.[24,25,26] La polymérisation

[19] S. Maria, H. Kaneyoshi, K. Matyjaszewski, R. Poli, *Chem. Eur. J*., **2007**, *13*, 2480-2492
[20] A. Debuigne, Y. Champouret, R. Jérôme, R. Poli, C. Detrembleur, *Chem. Eur. J*. **2008**, *14*, 4046-4059
[21] C. Detrembleur, R. Jérôme, Y. Piette, A. Debuigne, V. Sciannamea, *Chem. Comm.* **2006**, *40*, 4180
[22] J. Chiefari, Y. K. Chong, F. Ercole, J. Krstina, J. Jeffery, T. P. T. Le, R. T. A. Mayadunne, G. F. Meijs, C. L. Moad, G. Moad, E. Rizzardo, S. H. Thang, *Macromolecules*, **1998**, *31*, 5559-5562
[23] D. Colombani, P. Chaumont, *Prog. Polym. Sci*., **1996**, *21*, 439-503
[24] M. Destarac, C. Brochon, J.-M. Catala, A. Wilczewska, S. Z. Zard, *Macromol. Chem. Phys*., **2002**, *203*, 2281-2289

RAFT est l'une des techniques de PRC la plus universelle au niveau de la gamme de monomères polymérisables. Toutefois, la polymérisation des oléfines n'est toujours pas contrôlée par la méthode RAFT.

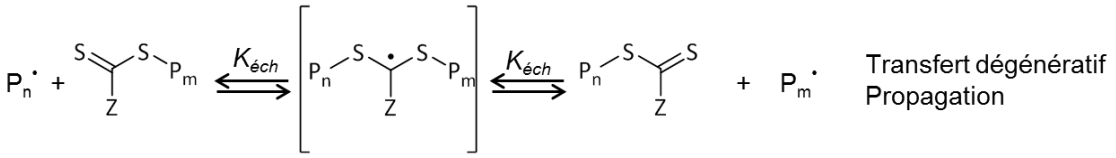

Schéma 3: Equilibre principal en RAFT après amorçage.

La polymérisation par tranfert d'iode (ITP) fût la première PRC découverte à la fin des années 1970 par Tatemoto.[27] Le mécanisme de contrôle est un transfert dégénératif où l'agent de transfert est un atome d'iode. Des analogues de chlore et brome ont été testés comme agent de transfert sans succès. L'ITP est l'une des rares méthodes capable de contrôler la polymérisation de fluoroalcènes comme le tetrafluoroethylène ou le fluorure de vinylidène.[28] Parmi les monomères non-halogénés, seulement quelques-uns ont été polymérisés avec contrôle via ITP : principalement des dérivés du styrène, des acrylates et l'acétate de vinyle. Du poly(acétate de vinyle) a été obtenu avec une faible dispersité mais les bouts de chaîne iodés étaient instables et se décomposaient en aldéhyde.[29]

Découverte en 1999 par Yamago,[30,31] la polymérisation radicalaire contrôlée par des organotellures (TERP) permet de maîtriser la polymérisation du styrène, des (meth)acrylates, des acrylamides et de l'acrylonitrile.[32] Comme en NMP, l'efficacité de l'agent de contrôle est fortement influencée par l'énergie de dissociation de la liaison (EDL) entre le carbone terminal de la chaîne croissante et l'agent de contrôle.[33] Des investigations cinétiques ont montré que le mécanisme principal de TERP du styrène, du methylacrylate et du butylacrylate était en fait une interaction entre un mécanisme de DTRP et de RDARP (Scheme 12).[34] Suivant l'exemple de la TERP, d'autres organo-hétéroatomes ont été testés comme agent de

---

[25] J. Chiefari, R. T. A. Mayadunne, C. L. Moad, G. Moad, E. Rizzardo, A. Postma, M. A. Skidmore, S. H. Thang, *Macromolecules*, **2003**, *36*, 2273-2283
[26] Y. K. Chong, J. Krstina, T. P. T. Le, G. Moad, A. Postma, E. Rizzardo, and S. H. Thang, Macromolecules, 2003, 36, 2256-2272
[27] M. Tatemoto, Y. Yutani, K. Fujiwara, European Patent 272698, **1988**
[28] C. Boyer, D. Valade, P. Lacroix-Desmazes, B. Ameduri, B. Boutevin, *J. Polym. Sci. Part A: Polym. Chem*., **2006**, *44*, 5763-5777
[29] M. C. Iovu, K. Matyjaszewski, *Macromolecules*, **2003**, *36*, 9346-9354
[30] S. Yamago, H. Miyazoe, J. Yoshida, *Tetrahedron Lett*., **1999**, *40*, 2339-2342
[31] S. Yamago, K. Iida, J.-I. Yoshida, *J. Am. Chem. Soc*., **2002**, *124*, 2874-2875
[32] S. Yamago, K. Iida, and J.-I. Yoshida, J. Am. Chem. Soc., 2002, 124, 13666-13667
[33] [a] G. Moad, E. Rizzardo, *Macromolecules*, **1995**, *28*, 8722-8728; [b] W. G. Skene, S. T. Belt, T. J. Connolly, P. Hahn, J. C. Scaiano, *Macromolecules*, **1998**, *31*, 9103-9105
[34] A. Goto, Y. Kwak, T. Fukuda, S. Yamago, K. Iida, M. Nakajima, and J.-I Yoshida, J. Am. Chem. Soc., 2003, 125, 8720-8721

transfert avec des succès modérés. Il s'agit des composés contenant un atome d'antimoine donnant naissance à la polymérisation radicalaire contrôlée par des organostibines (SbRP),[35] ou de bismuth avec la polymérisation radicalaire contrôlée par des organobismuthines (BiRP). Les TERP, SbRP et BiRP procèdent via des mécanismes de transfert dégénératif et de terminaison réversible.[119,36]

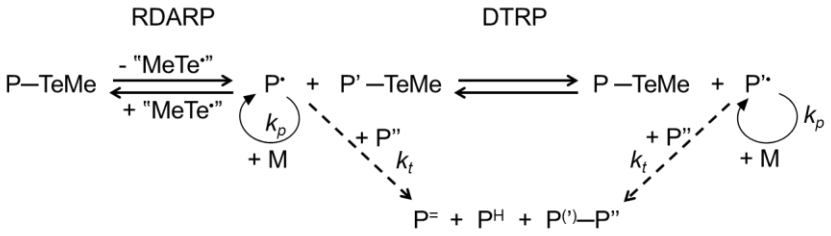

Schéma 4: Mécanisme proposé de la TERP.

2) Polymérisations (radicalaires) contrôlées de monomères peu réactifs

Les monomères sont appelés peu réactifs lorsque le radical correspondant n'est pas stabilisé par une délocalisation électronique donc est très réactif et difficilement contrôlable. L'acétate de vinyle, les amides de vinyle et l'éthylène appartiennent à ce groupe.

a) Etat de l'art de la polymérisation contrôlée de l'acétate de vinyle

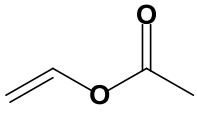

Figure 3: Le monomère acétate de vinyle (AcV).

L'acétate de vinyle, monomère peu réactif à vitesse de propagation très élevée (kp ~ 3 000 $L.mol^{-1}.s^{-1}$ à 20°C),[37] peut uniquement être polymérisé par un procédé radicalaire. Le poly(acétate de vinyle) (PAcV) est particulièrement intéressant car il peut être facilement hydrolisé en poly(alcool de vinyle) qui est le matériau hydrosoluble produit et commercialisé en plus grande quantité.[38]

Le premier exemple "d'ATRP" de l'acétate de vinyle a été rapporté en 1994[39,40] mais à ce jour, l'ATRP de l'AcV n'est toujours pas très satisfaisante. Les liaisons carbone-halogène (C─Br, C─Cl) de l'espèce dormante sont trop fortes pour être activées homolytiquement même par l'un des meilleurs catalyseurs d'ATRP. Bien que la NMP soit largement employée,

[35] S. Yamago, B. Ray, K. Iida, J.-I. Yoshida, T. Tada, K. Yoshizawa, Y. Kwak, A. Goto, T. Fukuda, *J. Am. Chem. Soc*., **2004**, *126* , 13908 -13909
[36] Y. Kwak, A. Goto, T. Fukuda, Y. Kobayashi, S. Yamago, Macromolecules 2006, 39, 4671-4679
[37] R. A. Hutchinson, J. R. Richards, M. T. Aronson, *Macromolecules*, **1994**, *27*, 4530-4537
[38] E. Chiellini, A. Corti, S. D'Antone and R. Solaro, *Prog. Polym. Sci*., **2003**, *28*, 963-1014
[39] K. Matyjaszewski, D. Mardare, *Macromolecules* **1994**, *27*, 645.
[40] C. Granel, R. Jérôme, P. Teyssié, C. B. Jasieczek, A. J. Shooter, D. M. Haddleton, J. J. Hastings, D. Gigmes, S. Grimaldi, P. Tordo, D. Greszta, K. Matyjaszewski, *Macromolecules*, **1998**, *31*, 7133-7141

à notre connaissance, il n'a pas été rapporté de nitroxides capables de contrôler la polymérisation de l'AcV. En revanche, la RAFT est l'une des techniques les plus étudiées pour la polymérisation de l'AcV.[41,42] La RAFT permet maintenant un très bon contrôle de l'AcV avec la synthèse de PAcV dépassant les 50 000 g/mol ayant des dispersités aussi basses que 1.24.[43] En général, il a été remarqué que, en RAFT, la dispersité des PAcV était basse à basse conversion (<1.2) puis augmentait. Ce phénomène a été expliqué par un transfert de chaîne au monomère et aux polymères. La TERP de l'AcV utilisant l'ethyl 2-methyltellanyl-2-methylpropionate (EMA-TeMe) et un amorceur azo, donne des polymères à faible dispersité pour des degrés de polymérisation faibles (M_n = 3.100, Đ = 1.28) mais ce contrôle diminue pour des degrés de polymérisation plus élevés (M_n = 8 500, Đ = 1.5).[44] Cette augmentation de la dispersité est expliquée par la formation d'adduit primaire (-CH_2-TeMe) qui se réactive plus lentement que l'adduit secondaire plus fréquent (-$CH(CH_3)$-TeMe). Les organostibines ont aussi été utilisés avec succès (conv. = 92%, M_n = 2 800, Đ = 1.26). Le mécanisme radicalaire a été confirmé mais les mêmes limitations que celles rencontrées pour la TERP ont été rapportées.[45] La dispersité des PAcV augmente avec la masse molaire à cause des évènements d'enchaînement tête-à-tête.[46] Du PAcV ayant une faible dispersité a été synthétisé grâce à l'utilisation d'iodo acétate comme agent de transfert (M_n = 20 000, Đ < 1.5).[47] L'analyse des bouts de chaîne a montré que les groupes terminaux iodés n'étaient pas stables et se décomposaient en groupement aldéhyde.[48,49,50] De plus, les enchaînements tête-à-tête formant des iodures d'alkyle primaires (plus stables que les iodures d'alkyle secondaires) ralentissent la polymérisation.

Jusqu'à présent, la meilleure méthode de contrôle de polymérisation de l'AcV est l'OMRP avec le complexe cobalt(II)acétylacétonate [$Co(acac)_2$] découverte par Jérôme.[51] Des PAcV de haute masse molaire ont été synthétisés (M_n = 99 000 g/mol, Đ = 1.33). Les auteurs proposent un mécanisme de RDARP. Toutefois, Poli a révélé une interaction jusque-là non suspectée des mécanismes de RDARP dissociatif et de DTRP associatif en OMRP.[52] La polymérisation radicalaire contrôlée par le cobalt (Co-MRP) de l'AcV en présence de

[41] P. Vana, T. P. Davis, G. E. Roberts, L. Cummins, M. H. Stenzel, *Macromol. Chem. Phys.* **2003**, *204*, 1160
[42] M. L. Coote, L. Radom, *Macromolecules*, **2004**, *37*, 590-596
[43] S. Perrier, P. Takolpuckdee, *J. Polym. Sci. Part A: Polym. Chem.* **2005**, *43*, 5347.
[44] S. Yamago, Y. Kobayashi, T. Fukuda, A. Goto, Y. Kwak, *Macromolecules* **2006**, *39*, 4671.
[45] A. K. Srivastave, A. K. Chaurasia, S. Sharma, G. Mishra, *J. Sci. Indus. Res*., **2006**, *65*, 514-517
[46] S. Yamago, *J. Polym. Sci. Part A: Polym. Chem*., **2006**, *44*, 1-12
[47] K. Matyjaszewski, M. C. Iovu, *Macromolecules,* **2003**, *36*, 9346-9354
[48] B. Boutevin, J. P. Hugon, Y. Pietrasanta, A. Sideris, *Eur. Polym. J*., **1978**, *14*, 353-356
[49] R. Adams, W. V. Wirth, H. E. French, *J. Am. Chem. Soc*., **1918**, *40*, 424-431
[50] E. K. Euranto, A. Noponen, T. Kujanpää, *Acta Chem. Scand*., **1966**, *20*, 1273-1280
[51] R. Jérôme, J.-R. Caille, A. Debuigne, *Angew. Chem. Int. Ed*., **2005**, *44*, 1101-1104
[52] R. Poli, K. Matyjaszewski, H. Kaneyoshi, S. Maria, *Chem. Eur. J.,* **2007**, *13*, 2480-2492

$Co(acac)_2$ passe d'un mécanisme de DT à un mécanisme de piégeage réversible si une molécule électro-donneuse (comme l'eau ou la pyridine) est ajoutée au milieu. La Co-MRP est le système le plus étudié en OMRP mais d'autres métaux ont également montré un contrôle effectif de la polymérisation de l'AcV. Le composé de chrome(III) alkyle [CpCr(nacnac^{Xyl,Xyl})(CH_2CMe_3)] donne un bon contrôle à température ambiante (M_n = 16 200, Đ = 1.46) même si la polymérisation est plutôt lente et les études cinétiques montrent un ralentissement attribué à la formation de liaison Cr─C plus forte dans l'espèce dormante issue d'un enchaînement tête-à-tête.[53,54]

b) Monomères amides de vinyle

Les amides de vinyles (Figure 26) possèdent une unité alcène qui n'est pas conjuguée avec le groupement carbonyle C=O et font donc partie de la famille des monomères peu réactifs ; le contrôle de leur polymérisation est difficile. Les poly(amides de vinyle) (PAmV) ont un intérêt principalement parce qu'ils sont biocompatibles et non-toxiques. Les PAmV sont généralement des matériaux à réponse thermique (*i.e.* ils peuvent subir un changement drastique de solubilité en fonction de la température).[55,56] Les PAmV ont reçu beaucoup d'attention pour leurs applications potentielles dans le domaine de la vectorisation de médicaments,[57,58,59] de procédés de séparation[60] et d'ingénierie des tissus.[61]

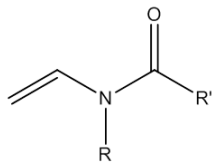

Figure 4 : Formule générale d'un amide de vinyle (R, R' = groupement alkyle).

A ce jour, la PRC de six amides de vinyle a été rapportée (Figure 27). Les homopolymérisations radicalaires contrôlées du formamide de vinyle (NVF), de la pyrrolidone de vinyle (NVP), de la 2-pipéridone de vinyle (NVPip) et du caprolactame de vinyle (NVCl) ont été rapportées. En revanche, l'acétamide de vinyle (NVA) et la *N*-methyl-

[53] K. M. Smith, J. L. Conway, L. Tang, R. Poli, U. Baisch, Y. Champouret, *Angew. Chem. Int. Ed.,* **2008**, *47*, 6069-6072
[54] Y. Champouret, K. C. MacLeod, U. Baisch, B. O. Patrick, K. M. Smith, R. Poli, *Organomet*., **2010**, *29*, 167-176
[55] S. Dai, P. Ravi, K. C. Tam, *Soft Matter*, **2009**, *5*, 2513-2533
[56] C. de las Heras Alarcón, S. Pennadam, C. Alexander, *Chem. Soc. Rev*., **2005**, *34*, 276-285
[57] A. B. Lowe, C. L. McCormick, *Prog. Polym. Sci*., **2007**, *32*, 283-351
[58] D. Schmaljohann, *Adv. Drug Delivery Rev*., **2006**, *58*, 1655-1670
[59] A. K. Bajpai, S. K. Shukla, S. Bhanu, S. Kankane, *Prog. Polym. Sci*., **2008**, *33*, 1088-1118
[60] A. Kikuchi, T. Okano, *Prog. Polym. Sci*., **2002**, *27*, 1165-1193
[61] G. Chan, D. J. Mooney, *Trends Biotechnol*., **2008**, *26*, 382-392

N-acétamide de vinyle (NMVA) ont uniquement été copolymérisés avec la NVCl par Co-MRP.[62] Parmi ces monomères, la NVP est de loin la plus étudiée.

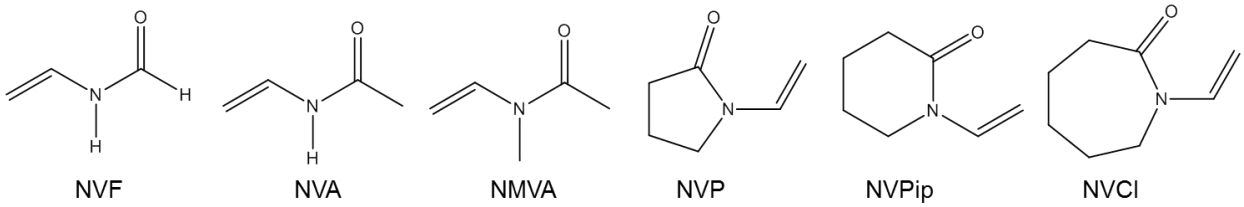

Figure 5 : Structures des amides de vinyle pour lesquels une PRC a été rapportée dans la littérature: formamide de vinyle (NVF), acétamide de vinyle (NVA), N-methyl-N-acétamide de vinyle (NMVA), pyrrolidone de vinyle (NVP), 2-piperidone de vinyle (NVPip) et caprolactame de vinyle (NVCl).

La polymérisation radicalaire de la pyrrolidone de vinyle a été contrôlée avec des organostibines[63] et des organobismuthines[64] mais la formation d'enchaînements tête-à-tête serait responsable de la perte de contrôle quand la quantité de NVP utilisée augmente (Đ = 1.1 pour Mn = 15 000 et Đ = 1.3 pour Mn = 100 000). De plus, la forte liaison C─Bi de l'espèce dormante est difficilement rompue pour libérer la chaîne radicalaire. Ce même phénomène d'augmentation de la dispersité des chaînes de Poly(pyrrolidone de vinyle) (PNVP) est observé pour l'ATRP[65] et la NMP.[66] La Co-MRP avec le [$Co(acac)_2$] permet d'atteindre de hautes conversions (55%) par comparaison aux autres méthodes et des valeurs de dispersités relativement faibles (Đ = 1.3 - 1.7).[67] Des copolymères statistiques PAcV-co-PNVP ont pu être préparés de manière contrôlée bien que le contrôle de la NVP soit inférieur à celui de l'AcV.[68]

Le poly(formamide de vinyle) (PNVF) est un matériau hydrosoluble et surtout un précurseur des poly(vinyle amines). Un unique article, publié en 2003 par Beckman, parle de la PRC du NVF.[69] Les auteurs ont essayé l'ATRP sans succès. Cependant, après avoir synthétisé un macro-amorceur de poly(ethylene glycol) (PEG) par RAFT (M_n = 2 100, Đ = 1.09) ils réussirent à synthétiser un copolymère à bloc PEG-*b*-PNVF (M_n = 6 100, Đ = 1.7). La large

[62] A. Kermagoret, C.-A. Fustin, M. Bourguignon, C. Detrembleur, C. Jérôme, A. Debuigne, *Polym. Chem*., **2013**, *4*, 2575-2583
[63] B. Ray, M. Kotani, S. Yamago, *Macromolecules*, **2006**, *39*, 5259-5265
[64] S. Yamago, E. Kayahara, M. Kotani, B. Ray, Y. Kwak, A. Goto, T. Fukuda, *Angew. Chem. Int. Ed*., **2007**, *46*, 1304-1306
[65] X. Lu, S. Gong, L. Meng, C. Li, S. Yang, L. Zhang, *Polymer*, **2007**, *48*, 2835-2842
[66] P. Bilalis, M. Pitsikalis, N. Hadjichristidis, *J. Polym. Sci. Part A: Polym. Chem*., **2006**, *44*, 659-665
[67] H. Kaneyoshi, K. Matyjaszewski, *Macromolecules*, **2006**, *39*, 2757-2763
[68] A. Debuigne, N. Willet, R. Jérôme, C. Detrembleur, *Macromolecules*, **2007**, *40*, 7111-7118
[69] L. Shi, T. M. Chapman, E. J. Beckman, *Macromolecules*, **2003**, *36*, 2563-2567

dispersité du bloc PNVF est attribuée aux nombreux transferts de chaîne du radical PNVF au monomère et au polymère.[70]

O'Reilly a publié une série de poly(2-piperidone de vinyle) (PNVPip) synthétisée en MADIX (M_n = 4 500- 83 000 g/mol, Đ < 1.3) mais si la masse moléculaire augmente linéairement avec la conversion, la vitesse de polymérisation subit dans chaque cas une accélération après 70% de conversion.[71] Les auteurs ont aussi réalisé un polymère amphiphile à bloc PNVPip-*b*-PAcV (M_n = 11 400 g/mol, Đ 1.27) par extension d'un bloc PNVPip de masse moléculaire 7 600 g/mol (Đ = 1.28).

La polymérisation du caprolactame de vinyle est contrôlée par RAFT/MADIX[72,73] ou par Co-MRP.[74,75] En RAFT/MADIX, des polymères de masse molaire allant de 3 100 jusqu'à 150 000 g/mol ont été synthétisés avec contrôle (Đ = 1.1 - 1.5). En revanche, lorsque ces polymères terminés par un groupement dithiocarbamate sont prolongés d'un bloc PAcV, la dispersité du polymère à bloc résultant est plus grande (Đ = 1.6-1.7). Une partie des chaînes de poly(caprolactame de vinyle) (PNVCl) sont mortes par couplage radicalaire ; elles ne portent donc pas de groupement fonctionnel en bout de chaîne et ne peuvent pas être allongées. La Co-MRP de la NVCl a été rapportée par Detrembleur qui utilisa un macro-amorceur PAcV-$Co(acac)_2$ pour former des polymères à bloc PAcV-*b*-PNVCl jusqu'à 87 000 g/mol et avec une faible dispersité (Đ = 1.1).

c) Bilan actualisé du poly(éthylène)

Le poly(éthylène) (PE) est l'un des plastiques les plus largement produits dans le monde avec 50 à 110 millions de tonnes selon les sources.[76] Le matériau brut est peu cher (~ 500 – 1 500 €/t) et représente moins de 1% de la production totale de gaz naturel et de pétrole. Il existe deux procédés de production industrielle majeurs : le procédé dit « à haute pression » qui produit du PE basse densité (LDPE) par polymérisation radicalaire libre avec une très large dispersité et une proportion importante de branches (une branche tous les 20-50 atomes de carbone) et le procédé dit « à basse pression » qui utilise un métal de transition comme catalyseur (Ti, V, Cr, Fe, Co, Ni…) bien souvent activé par un co-catalyseur ou déposé sur

[70] L. Gu, S. Zhu, A. N. Hrymak, R. H. Pelton, *Macromol. Rapid Commun*., **2001**, *22*, 212-214
[71] N. S. Ieong, M. Redhead, C. Bosquillon, C. Alexander, M. Kelland, R. K. O'Reilly, *Macromolecules*, **2011**, *44*, 886-893
[72] D. Wan, Q. Zhou, H. Pu, G. Yang, *J. Polym. Sci. : Polymer Chem*., **2008**, *46*, 3756-3765
[73] M. Beija, J.-D. Marty, M. Destarac, *Chem. Commun*., **2011**, *47*, 2826-2828
[74] M. Hurtgen, J. Liu, A. Debuigne, C. Jérôme, C. Detrembleur, *J. Polym. Sci. Part A : Polymer Chem*., **2012**, *50*, 400-408
[75] A. Kermagoret, C.-A. Fustin, M. Bourguignon, C. Detrembleur, C. Jérôme, A. Debuigne, *Polym. Chem*., **2013**, *4*, 2575-2583
[76] E. Jonhson, M. Arne, Chemistry & Industry (London, United Kingdom) **2009**, 14, 23-24

solide. Il existe de nombreuses versions du procédé à basse pression ; on l'appelle procédé Ziegler-Natta ou Phillips lorsque le titane ou le chrome sont respectivement employés. Le mécanisme proposé est un mécansime de coordination-insertion de l'éthylène dans la liaison métal-alkyle activée.[77,78] Les PE issus de ce procédé sont de haute densité (HDPE) et leur densité de branches est faible (moins de une branche pour 200 atomes de carbone). La formation des branches durant le processus de polymérisation radicalaire est due à deux types de réaction. La première, appelée, « backbiting », est un transfert de chaîne intramoléculaire où la chaîne radicalaire arrache un atome d'hydrogène de sa propre chaîne par repliement sur elle-même formant un cycle à six ou sept chaînons et conduisant ainsi à la formation de courtes branches (butyl ou pentyl).[79,80] La deuxième possibilité est un transfert d'hydrogène intermoléculaire conduisant à de longues branches.

Un défi majeur dans le contrôle de la polymérisation de l'éthylène est la maîtrise de sa copolymérisation avec des monomères polaires. Aujourd'hui, ce type de matériau est produit par polymérisation radicalaire non contrôlée ce qui limite les performances du copolymère. La PRC pourrait résoudre ces problèmes. Or on ne trouve qu'un nombre très limité de publications sur la (co)polymérisation contrôlée de l'éhylène. [81]

La polymérisation aléatoire d' α-olefines n'a été étudiée qu'avec le methyl (meth)acrylate en ATRP,[82,83,84] RAFT,[85] TERP[86] et ITP.[85] Des polymères bien contrôlés ont été obtenus avec de faibles dispersités mais seulement pour des degrés de polymérisations faibles et pour une proportion d'oléfine insérée faible. La dispersité des polymères augmente avec la masse molaire car il y a accumulation d'espèces dormantes terminées par une unité oléfine qui sont moins facilement réactivées que celles terminées par une unité arylate.[87] Toutefois, cette réaction parasite n'est pas significative, probablement à cause du phénomène de polymérisation croisée avec les acrylates qui est plus rapide que la réaction de terminaison. Les copolymérisations sont donc « contrôlées » avec des valeurs de dispersité aussi faible que 1.07 pour des copolymères methyl acrylate/1-hexene de faible poids moléculaire.

---

[77] D. P. Gates, S. A. Svejda, Enrique Oñate, C. M. Killian, L. K. Johnson, P. S. White, M. Brookhart, *Macromolecules*, **2000**, *33*, 2320-2334
[78] L. Deng, P. Margl, T. Ziegler, *J. Am. Chem. Soc*., **1999**, *121*, 6479-6487
[79] D. E. Dorman, E. P. Otocka, F. A. Bovey, *Macromolecules*, **1972**, *5*, 574-577
[80] R. S. Lehrle, C. S. Pattenden, *Polym. Degrad. Stab*., **1999**, *63*, 153-158
[8181] M. L. Coote, E. I. Izgorodina, G. E. Cavigliasso, M. Roth, M. Busch, C. Barner-Kowollik, *Macromolecules*, **2006**, *39*, 4585-4591
[82] S. Liu, A. Sen, *J. Polym. Sci., Part A: Polym. Chem*., **2004**, *42*, 6175-6192
[83] S. Borkar, A. Sen, *Macromolecules*, **2005**, *38*, 3029-3032
[84] R. Venkatesh, B. Klumperman, *Macromolecules*, **2004**, *37*, 1226-1233
[85] S. Liu, B. Gu, H. A. Rowlands, A. Sen, *Macromolecules*, **2004**, *37*, 7924-7929
[86] E. Mishima, T. Tamura, S. Yamago, *Macromolecules*, **2012**, *45*, 2989-2994
[87] R. Venkatesh, S. Harrisson, D. M. Haddleton, B. Klumperman, *Macromolecules*, **2004**, *37*, 4406-4416

En conclusion, il n'existe toujours pas de système capable de contrôler la (co)polymérisation de l'éthylène à un niveau proche de la polymérisation vivante.

CHAPITRE II: LES COMPLEXES FURTIFS DE CUIVRE(II)-ALKYLE

Le mécanisme de polymérisation radicalaire contrôlée par le cuivre (Cu-MRP) implique la formation d'un composé organométallique de cuivre(II) (LCu^{II}-P) comme espèce dormante (Schéma 5). La liaison cuivre-carbone doit être photolitiquement ou thermiquement labile pour avoir une activation suffisamment rapide et permettre aux chaînes radicalaires de se propager mais elle doit être suffisamment stable pour déplacer l'équilibre vers l'espèce dormante. Nous avons exploré les possibilités de synthèse d'un composé organométallique modèle. La chaîne de polymère (P) a été modélisée par un radical methyl ($CH_3^{\bullet}$) qui devrait se lier plus fortement au cuivre qu'une chaîne poly(acétate de vinyle) ou poly(amide de vinyle). L'isolement de tels complexes de cuivre(II) serait de grand intérêt car ils pourraient servir d'amorceur unimoléculaire en Cu-MRP et pourraient également nous permettre d'étudier les cinétiques d'activation. Cette synthèse visée est promise à des difficultés puisque les complexes de cuivre(II) souhaités contiennent une liaison métal-carbone faible.

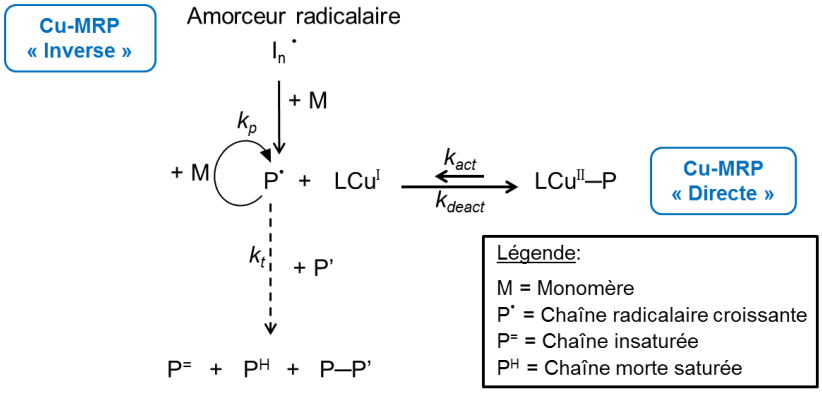

Schéma 5 : Mécanisme proposé de la polymérisation radicalaire contrôlée par le cuivre (Cu-MRP).

1) Etat de l'art des complexes orgaométalliques de cuivre(II)

Contrairement au cuivre(I), seulement quelques exemples de composés organométalliques de cuivre(II) ont été rapportés dans la littérature. Les adduits éphémères de cuivre(II)-σ-alkyle ont été postulés dans de nombreuses réactions organiques catalysées par le cuivre.[88,89,90,91] De

[88] G.-C. Kuang, P. M. Guha, W. S. Brotherton, J. T. Simmons, L. A. Stankee, B. T. Nguyen, R. J. Clark, L. Zhu, *J. Am. Chem. Soc*., **2011**, *133*, 13984-14001
[89] L. Fomina, B. Vazquez, E. Tkatchouk, S. Fomine, *Tetrahedron*, **2002**, *58*, 6741-6747
[90] A. E. King, T. C. Brunold, S. S. Stahl, *J. Am. Chem. Soc*., **2009**, *131*, 5044-5045
[91] E. Sperotto, G. P. M. van Klink, G. van Koten, J. G. de Vries, *Dalton Trans*., **2010**, *39*, 10338-10351

plus, la réaction des radicaux alkyles avec les ions cuivreux en solution aqueuse a été étudiée intensivement par Meyerstein qui a conclut que des espèces $[Cu^{II}\text{-}CH(CH_3)OH]^+$ et $[Cu^{II}\text{-}C(CH_3)_2OH]^+$ étaient formées mais que leur faible stabilité rendait leur observation impossible.[92,93,94,95]

Sept collections de données cristallographiques de composés organométalliques de cuivre(II) possédant une liaison cuivre-carbone sont publiées dans la littérature. Lorsque le cuivre est entouré d'une pseudo-porphyrine, la géométrie est plan carré dans les quatres cas (Figure 47, Figure 48, Figure 50, et Figure 51). En revanche, les géométries bipyramidale (Figure 56) et tétrahèdrale distordue (Figure 53) ou pseudo-octahédrale (Figure 54) sont rapportées dans les cas respectifs d'un atome de cuivre coordiné par les ligands anioniques tris(2-pyridylthio)méthanide et NHC neutre. Il faut noter que, puisque le ligand carbyl est un ligand donneur de 2 électrons (de type L selon la nomenclature de Green) contrairement aux radicaux organiques de type X (donneur d'un électron), ces complexes ne peuvent pas servir de modèle de l'espèce dormante ni d'amorceur unimoléculaire en OMRP.

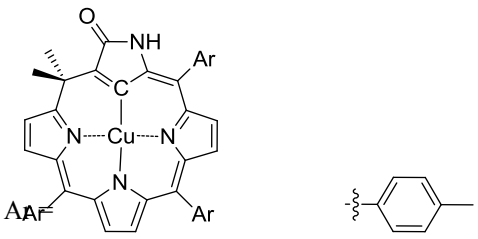

Figure 6 : Première structure RX contenant une liaison cuivre(II)-carbone publiée par Furuta.[96] A l'état solide, ce complexe forme un dimère par liaison hydrogène entre les groupements amides périphériques.

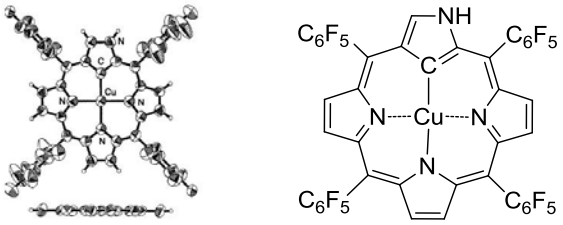

Figure 7 : Structure du complexe de cuivre(II) décrit par Furuta[97] (vue de haut et vue de coté de la structure RX et représentation schématique). Les paramètres de RPE (giso = 2.09, $g_{\parallel}$ = 2.12, $[A_{\parallel}]$ = 168 Gauss) dans le toluène à 77 K sont cohérents avec une géométrie plan-carrée

[92] M. Freiberg, W. A. Mulac, K. H. Schmid, D. Meyerstein, *J. C. S. Faraday I*, **1980**, *76*, 1838-1848
[93] H. Cohen, D. Meyerstein, *Inorg. Chem*., **1987**, *26*, 2342-2344
[94] H. Cohen, D. Meyerstein, *Inorg. Chem*., **1986**, *25*, 1505-1506
[95] N. Navon, G. Golub, H. Cohen, D. Meyerstein, *Organometallics*, **1995**, *14*, 5670-5676
[96] H. Furuta, T. Ishizuka, A. Osuka, Y. Uwatoko, Y. Ishikawa, *Angew. Chem. Int. Ed*., **2001**, *40*, 2323-2325
[97] H. Maeda, A. Osuka, Y. Ishikawa, I. Aritome, Y. Hisaeda, H. Furuta, *Org. Lett*., **2003**, *5*, 1293-1296

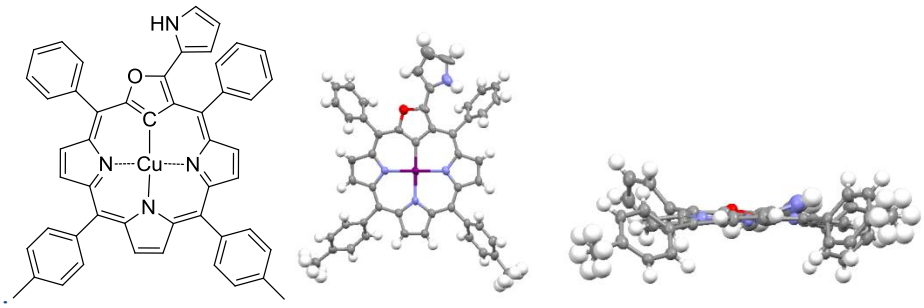

Figure 8 : Structure du complexe de cuivre(II) publiée par Latos-Grażyński[98] (représentation schématique; vue de haut et vue de coté de la structure RX). La distance Cu(II)-C est de 1.939(4) Å.

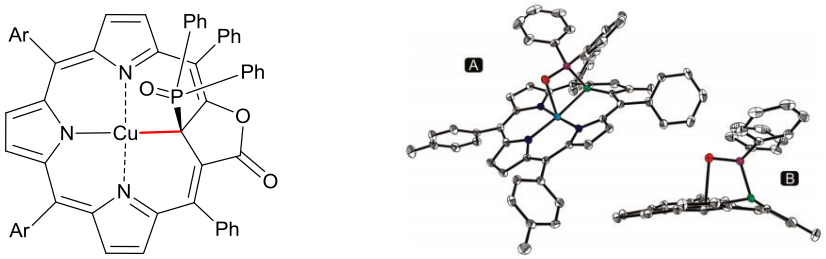

Figure 9 : Représentation schématique et structure RX du complexe de cuivre(II) possédant une liaison faible Cu-C (2.2322 Å). Le cuivre possède une géométrie pyramidale à base carrée dont la position apicale est occupée par un atome d'oxygène issu du groupe O=P≡. Caractéristiques RPE: $g_{\parallel} = 2.158$, $g_{\perp} = 2.041$, $g_{\circ} = 2.082$, $A_{\parallel}^{Cu} = 164$ Gauss, $A_{\perp}^{Cu} = 25$ Gauss, $A_{\circ}^{Cu} = 65.9$ Gauss, $A_{\circ}^{N} = 13.7$ Gauss.[99]

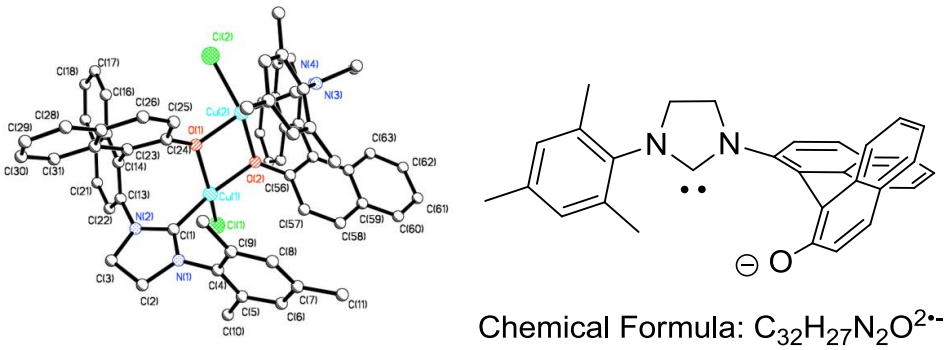

Figure 10 : Structure du complexe dimère de cuivre(II) et représentation du ligand NHC. Les atomes de cuivre sont de géométrie intermédiaire entre un plan carré et un tétrahèdre. Les liaisons cuivre-carbone sont de 1.926(8) and 1.964(8) Å.[100]

[98] M. Pawlicki, I. Kańska, L. Latos-Grażyński, *Inorg. Chem*., **2007**, *46*, 6575-6584
[99] N. Grzegorzek, M. Pawlicki, L. Szterenberg, L. Latos-Grażyński, *J. Am. Chem. Soc*., **2009**, *131*, 7224-7225
[100] A. O. Larsen, W. Leu, C. N. Oberhuber, J. E. Campbell, A. H. Hoveyda, *J. Am. Chem. Soc*., **2004**, *126*, 11130-11131

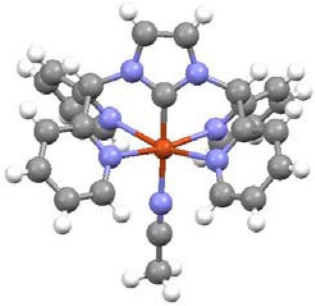

Figure 11 : Vue du cation issu du composé [(NHC)Cu(MeCN)](CF_3SO_3)$_2$. Deux molécules de THF ont été omises par souci de clarté. La liaison Cu-C de 1.889(4)Å est, à ce jour, la plus courte rapportée pour un complexe organométallique de cuivre(II). Le spectre RPE possède une symétrie apparente axiale avec $g_\perp \approx 2$ .23 and $g_\parallel \approx 2.08$.[101]

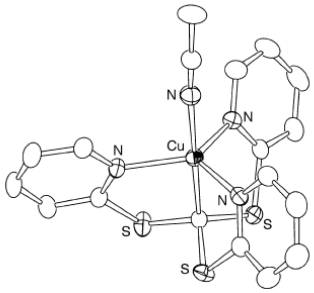

Figure 12 : Structure RX du complexe [Cu(TPTM)MeCN]PF_6, (PF_6 non représenté) qui possède une liaison Cu(II)-C(sp3) et ayant une structure bipyramidale à base triangulaire.[102,103] Elle possède une liaison Cu-C de 2.004(3) Å et une forte élongation axiale conduisant à un état fondamental dz^2.

2) Etudes sur les alkyles de cuivre (II)

Malgré de nombreux efforts, nous n'avons pas réussi à isoler un complexe de cuivre(II) alkyle. L'ensemble des expériences ont été réalisées à basse température et suivies par des mesures RPE. Elles sont décrites ci-dessous avec les spectres RPE correspondant. Nous avons essayé d'échanger un atome de chlore porté par un complexe chlorure de cuivre(II) par un groupement methyl à l'aide d'un réactif de Grignard (Figure 13) ou de methyl lithium (Figure 14). Des complexes cationiques de cuivre ont également été testés pour la réaction d'alkylation visée car ils ont une sphère de coordination moins encombrée (Figure 15, 16).

[101] J. M. Smith, J. R. Long, *Inorg. Chem*., **2010** , *49*, 11223-11230
[102] I. Kinoshita, L. J. Wright, S. Kubo, K. Kimura, A. Sakata, T. Yano, R. Miyamoto, T. Nishioka, K. Isobe, *Dalton Trans*., **2003**, 1993-2003
[103] R. Miyamoto, R. Santo, T. Matsushita, T. Nishioka, A. Ichimura, Y. Teki, I. Kinoshita, *Dalton Trans*., **2005**, 3179-3186

[Tp*CuCl] + MeMgBr $\xrightarrow{-40°C}$

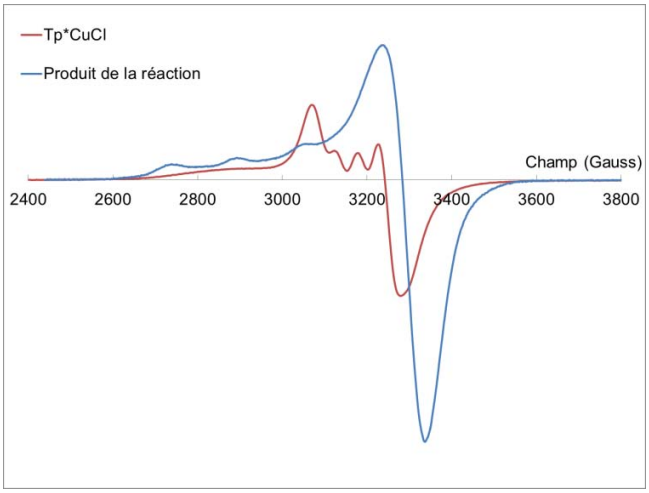

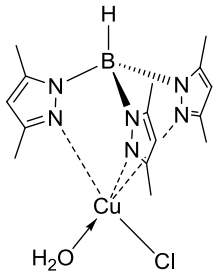

[Tp*CuCl] hydraté

Figure 13 : Spectres RPE de [Tp*CuCl] et du produit de methylation (en solution dans le THF, 150K).

Il n'y a pas de preuve directe de la présence d'un groupement methyl directement attaché à l'atome de cuivre (i.e. pas de constante de couplage hyperfin avec des atomes d'hydrogène) mais il est évident qu'une réaction entre [Tp*CuCl] et MeMgI s'est produite.

[(TPTM)CuCl] + MeLi $\xrightarrow{-30°C}$

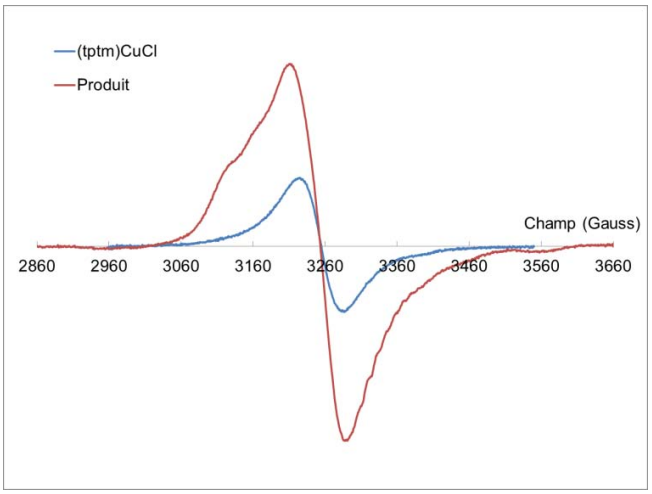

Figure 14 : Spectres RPE de [(TPTM)CuCl] et du produit de methylation (en solution dans le THF, 150K).

Nous n'avons pas observé de changement de couleur. Le spectre RPE du produit est de symétrie sphérique et ne montre qu'une différence mineure avec le spectre du chlorure de cuivre de départ. Ceci nous suggère qu'aucune réaction n'a eu lieu.

$$[(TPTM)Cu(MeCN)]BF_4 + MeLi \xrightarrow{-50°C}$$

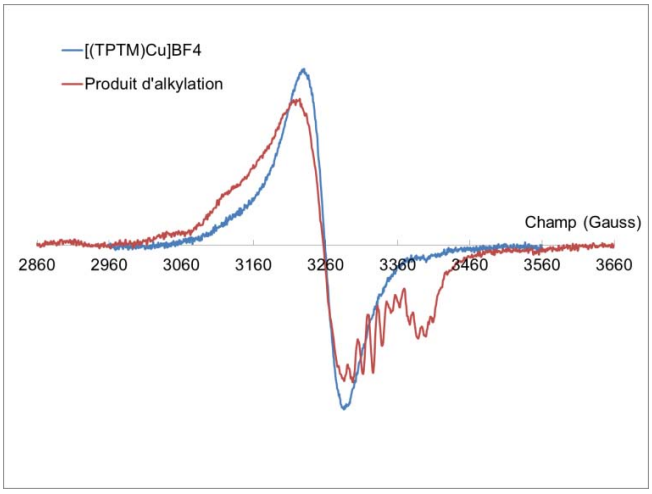

Figure 15 : Spectres RPE de $[(TPTM)Cu(MeCN)]BF_4$ et du produit de methylation (en solution dans le THF, 150K).

Le spectre de $[(TPTM)Cu(MeCN)]BF_4$ révèle un tenseur g de symétrie presque sphérique (g_{iso} = 2.083) alors que le spectre du produit possède une symétrie axiale ($g_{\perp}$ = 2.084, $g_{\parallel}$ = 1.995) avec des constante de couplage hyperfin de 11 à 15 Gauss. Cette structure hyperfine riche est cohérente avec une interaction de l'électron non apparié avec les trois atomes d'azote et/ou avec les atomes d'hydrogène du groupement methyl.

$$[(TPMA^*)CuCl]PF_6 + MeMgBr \xrightarrow{-50°C}$$

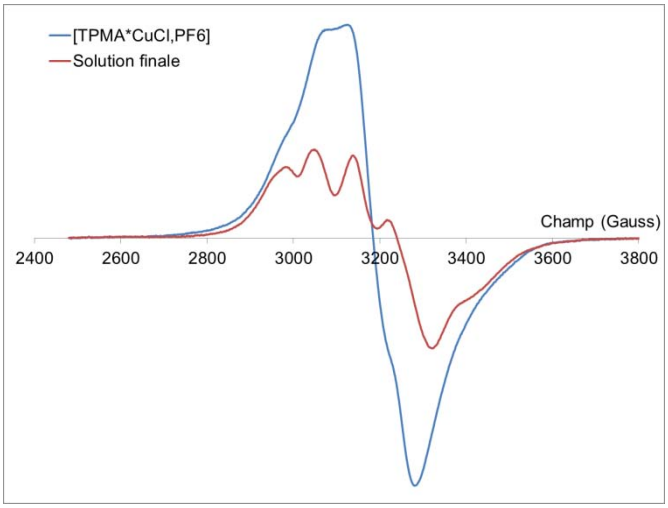

Figure 16 : Spectres RPE de $[(TPMA^*)CuCl]PF_6$ et du produit de methylation (en solution dans le THF, 150K).

Une comparaison des deux spectres montre une intensité globale qui a diminué de moitié environ et une amélioration de la résolution mais les minimums et maximums des deux spectres sont identiques. Il est proposé qu'une réaction de stoechiométrie 2 :1 se produit (2

molécules de MeMgBr pour chaque ion $[(TPMA^*)CuCl]^+$) et que le produit de la réaction n'est pas visible sur le spectre car diamagnétique.

En conclusion, selon la nature du ligand coordinant l'atome de cuivre, des preuves spectroscopiques plus ou moins évidentes de la formation d'une liaison cuivre-carbone ont été obtenues suite à l'alkylation d'un précurseur de chlorure de cuivre(II) cationique ou neutre. Bien que nous n'ayons pas réussi à isoler un complexe cuivre(II)-alkyle, nous sommes maintenant convaincus qu'une telle espèce peut se former et que l'on peut établir, dans des conditions appropriées, un équilibre d'OMRP avec les complexes étudiés.

CHAPITRE III : POLYMERISATIONS RADICALAIRES DE MONOMERES PEU REACTIFS CONTROLEES PAR LE CUIVRE

Dans ce chapitre, des complexes de cuivre(I) sont, pour la première fois, examinés comme agent de contrôle pour la polymérisation de l'acétate de vinyle et de l'éthylène en conditions OMRP (Schéma 5, page 14). Notre but est d'obtenir une polymérisation vivante qui est indiquée par une dispersité idéale des polymères (*i.e.* aussi proche que possible de Đ = 1), la prévisibilité de la masse molaire en fonction du rapport agent de contrôle/amorceur, un profil masse molaire-conversion linéaire (*i.e.* une concentration en radicaux constante) et la possibilité de synthétiser des polymères à bloc ou de plus haute masse molaire par addition supplémentaire de monomère.

1) Polymérisation de l'acétate de vinyle

Les complexes de cuivre sont largement utilisés en ATRP. Quelques publications signalent la possibilité d'interaction entre un radical organique et un complexe de cuivre(I) en l'absence d'atome d'halogène.[56]

Nous avons décidé dans le cadre de notre étude sur la polymérisation de l'AcV en conditions OMRP de considérer les complexes de cuivre(I) décrits dans la Figure 71. Tous les complexes choisis ne contiennent pas d'atome d'halogène pour éviter toute réaction d'ATRP.

Considérons le complexe **(1)** (Figure 71), si des chaînes radicalaires de PAcV sont piégées par ce complexe de cuivre(I) à la géométrie trigonale plane, une espèce dormante organométallique cuivre(II) sera formée ayant un nombre de coordination de trois ou quatre (selon la chélation possible d'une molécule de solvant). Les complexes de cuivre(II) tricoordiné et tétracoordiné adoptent généralement une géométrie trigonale ou un plan carré distordu respectivement. Dans les deux cas, le réarrangement de la sphère de coordination

sera minime lors du processus de piégeage des radicaux. Les polymérisations ont été réalisées dans le toluène en utilisant le V-70 comme amorceur radicalaire. Démarrée à 30°C, la température a été changée de 30°C à 50°C car la vitesse de polymérisation était trop lente. La couleur de la solution a changé et est passée d'un jaune pâle à marron, ce qui indique potentiellement la transformation du cuivre(I) en cuivre(II). De plus, après consommation totale de l'amorceur radicalaire, l'AcV était toujours consommé, ce qui implique que des radicaux continuent d'être générés réversiblement à partir de l'espèce dormante. Toutefois, les masses molaires obtenues sont d'environ dix fois supérieures à celles attendues. Le contrôle de la polymérisation de l'AcV est donc médiocre avec ce complexe.

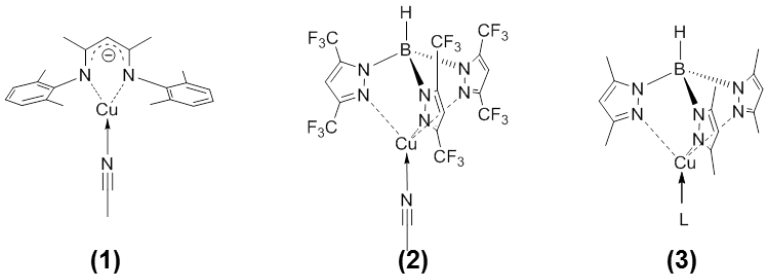

Figure 17 : Complexes de cuivre(I) testés en OMRP, (1) = hydrotris(3,5-dimethylpyrazol-1-yl)-borato] cuivre(I) avec L = H_2O, MeCN, THF [CuTp*L] ou sans L donne le dimère $[CuTp^*]_2$; (2) = hydrotris(3,5-bis(trifluoromethyl)pyrazol-1-yl)-borato](acétonitrile) cuivre(I) $[CuTp^{CF3}(MeCN)]$; (3) = (*N*-[3-[(2,6-dimethylphenyl)amino]-1-methyl-2-buten-1-ylidene]-2,6-dimethyl-benzenamine)(acétonitrile) cuivre(I) $[CuNacNac^{XylXyl}(MeCN)]$.

Le complexe **(2)** portant le ligand scorpionate tricoordinant est de géométrie tétrahédrale distordue.[104] Les vitesses de polymérisation avec et sans le complexe **(2)** sont identiques donc nous ne pouvons pas faire de conclusion quant au piégeage des chaînes de PAcV par le complexe $[Cu(Tp^{CF3})(MeCN)]$. La dispersité des PAcV obtenus en présence du complexe est faible et reste faible tout au long de la polymérisation (Đ = 1.2-1.3), ce qui indique potentiellement qu'un faible degré de contrôle de la polymérisation peut être imparti au complexe.

De meilleurs résultats ont été obtenus avec le complexe $[CuTp^*]_2$,[105] un analogue du précédent. Les trois atomes d'azote sont coordinés plus fortement au centre métallique que dans le cas du ligand Tp^{CF3} dû aux effets électro-donneurs des groupements methyl. Or, si le ligand est plus électro-donneur, l'espèce cuivre(II) devrait être mieux stabilisée donc l'équilibre d'OMRP est déplacé vers l'espèce dormante et la polymérisation est plus lente. En effet, la vitesse de polymérisation apparente avec le $[CuTp^*]_2$ est plus lente que celle observée en présence de $[Cu(Tp^{CF3})(MeCN)]$ et est plus lente que celle de l'expérience de contrôle

[104] M. N. C. Balili, T. Pintauer, *Acta Cryst*., **2007**, *E63*, m988-m990
[105] C. Mealli, C. S. Arcus, J. L. Wilkinson, T. J. Marks, J. A. Ibers, *J. Am. Chem. Soc*., **1976**, *98*, 711-718

réalisée sans cuivre (voir Figure 77). De plus, il y a une corrélation linéaire entre $\ln([Vac]_0/[Vac])$ et le temps de réaction (*i.e.* une concentration en radicaux constante) mais la variation des masses moléculaires avec la conversion et les hautes valeurs de dispersité démontrent un faible contrôle de la polymérisation avec $[CuTp^*]_2$.

En conclusion, nous avons montré pour la première fois que, même si le contrôle était parfois médiocre, les complexes de cuivre(I) sont capables de ralentir la polymérisation de l'acétate de vinyle et donnent des PAcV de basse dispersité (Đ < 1.5). Le ligand scorpionate tridente encombré fournit une efficacité de piégeage modérée résultant en un faible contrôle et le ligand β-diketiminate bidente produit une espèce dormante beaucoup plus stable qui ne se réactive pas très efficacement. Deux complexes (trispyrazolylborato)cuivre(I) ont été étudiés et le meilleur contrôle est obtenu avec le ligand substitué par des groupements methyl en comparaison avec son analogue portant des groupements électro-attracteurs trifluoromethyl.

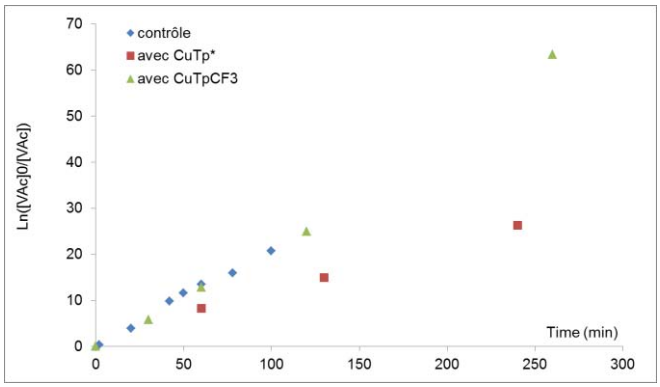

Figure 18 : Corrélation linéaire entre $\ln([VAc]_0/[VAc])$ et le temps. Polymérisations en masse de l'AcV avec $[Cu(Tp^{CF3})(MeCN)]$, $[CuTp^*]_2$ et sans cuivre (30°C, [Cu] / VAc / V-70 = 1 : 500 : 0.7).

Finalement, un réglage plus précis de la force de liaison cuivre-carbone pourrait être réalisé par des modifications stériques sur la sphère de coordination du ligand.[66]

2) Polymérisation de l'éthylène

En principe, une liaison PE-Métal est plus forte qu'une liaison PAcV-Métal. Quatre complexes différents de cuivre(I) ont été étudiés pour la polymérisation radicalaire de l'éthylène en conditions OMRP : $[CuTp^*]_2$, $[CuTp^{CF3}(MeCN)]$ et $[Cu(NacNac^{XylXyl})MeCN]$ qui ont été discutés dans la section précédente et $[CuTp^{H}(THF)]$ qui est un autre ligand scorpionate mais sans substituents sur les trois groupes pyrazolyl (voir Figure 82). Les conditions opératoires ont été inspirées du récent travail de Monteil.[196] Les résultats de ces polymérisations de l'éthylène en présence de complexes de cuivre(I) comme agent de contrôle

sont résumés dans le Tableau 1. La masse totale de PE isolée, après polymérisation dans des conditions identiques, est très différente selon le complexe de cuivre utilisé.

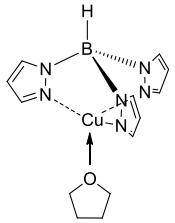

Figure 19: Hydrotris(pyrazol-1-yl)-borato]cuivre(I) adduit THF, [CuTp^{H}].

La polymérisation en présence de [Cu(NacNac^{XylXyl})(MeCN)] suggère que la polymérisation est ralentie par la présence du complexe métallique. De plus, on peut conclure qualitativement que les chaînes produites sont plus longues que lors de la polymérisation en l'absence de l'agent de contrôle.

Lorsque l'on utilise des complexes de cuivre(I) coordinés par des ligands scoprionates, la masse totale de PE isolée est plus grande et diminue avec les substituents du ligand CF_3 > H > CH_3. Comme pour la tendance observée précédemment pour la polymérisation de l'AcV en présence de complexes de cuivre scorpionates. Le ligand Tp* montre une efficacité de piégeage plus grande que Tp^{CF3}. La diminution de la contrainte stérique avec Tp^{H} n'a pas eu l'effet escompté puisque le contrôle semble moins bon qu'avec le ligand Tp* qui, encore une fois, entraîne une plus grande diminution de la vitesse de polymérisation.

Tableau 1: OMRP de l'éthylène avec des complexes de cuivre(I) (conditions: [Cu] ≈ 1.7 mM dans le THF, 90°C, 55-60 bars) solide isolé = chaînes de PE solides; masse totale de PE = masse de PE solide + masse des oligomères.

Entrée	Ligand	LCu / AIBN	Pression initiale d'éthylène (bar)	Temps de réaction (h)	Masse de PE solide (g)	Masse totale de PE (g)	DSC T_{fus} (°C)	Cristallinité
1	Tp^{H}	1 : 1.4	60	24	1.28	1.88	97.1	56.8%
2	Tp^{CF3}	1 : 1.4	55	24	0.84	2.04	96.5	70.1%
3	NacNac^{XylXyl}	1 : 0.7	55	24.5	0.34	0.94	nd	-
4	Tp*	1 : 0.0	58	24	0.11	0.62	89.6	40.6%
5		1 : 1.4	58	24	0.77	1.57	89.3	42.9%
6		1 : 1.4	60	2	0.02	0.61	97.3	79.5%

Afin de mieux explorer le caractère « vivant » de la polymérisation de l'éthylène contrôlée par des complexes de cuivre, une expérience d'extension de chaîne a été réalisée. En effet, les oligomères (fraction liquide du polyéthylène, chaînes courtes de moins de 30 carbones) issus d'une polymérisation en présence de [CuTp*]$_2$ ont été isolés sous atmosphère inerte puis

réintroduit dans un autoclave en présence de THF et d'éthylène uniquement. Les résultats de cette expérience suggèrent que les chaînes de PE produites sont terminées par le complexe de cuivre [PE-CH_2─Cu^{II}Tp*] et sont capables de relarguer des chaînes radicalaires $PE^{\bullet}$ pour permettre une polymérisation supplémentaire sans addition d'amorceur radicalaire.

Etonnamment, l'expérience de contrôle réalisée sans amorceur radicalaire ni complexe de cuivre (*i.e.* éthylène et THF seulement) nous a révélée la formation de PE initiée par des impuretés du THF ou du gaz. Cette expérience a été reproduite plusieurs fois mais souffre d'une faible reproductibilité dans la quantité de PE produite. Les liaisons α C-H du THF sont les plus faibles dans la molécule et peuvent être cassées homolytiquement pour former le radical tetrahydrofuryle qui peut amorcer la polymérisation.[197,106,107] L'influence de la température et de la pression sur la formation de PE par auto-amorçage dans le THF a été étudiée. Ces investigations ont permis de conclure que l'auto-amorçage de la polymérisation de l'éthylène se produisait dans nos conditions expérimentales. Toutefois, les expériences de polymérisations en présence de $[CuTp^*]_2$ et de l'amorceur radicalaire ont été réalisées à 90°C et 50 bars, où la quantité de PE produite par auto-amorçage dans les expériences précédentes est en moyenne de 70 mg. Cette quantité est faible comparée au PE produit en présence de cuivre et d'amorceur donc l'effet modérateur du cuivre sur la production de PE est bien réel.

CHAPITRE IV : ETUDES THEORIQUES A L'AIDE DE LA THEORIE DE LA FONCTIONNELLE DE LA DENSITE

Par l'utilisation de la théorie de la fonctionnelle de la densité (DFT), nous aspirons à mieux comprendre pourquoi la polymérisation radicalaire contrôlée par le cobalt (Co-MRP) donne, à ce jour, les meilleurs résultats dans le cas de l'acétate de vinyle et à rationnaliser certaines tendances de réactivité observées en PRC des amides de vinyle. Ceux chapitre est divisé en deux parties. La première révèle la généralisation du phénomène de chélation intramoléculaire découverte pour l'acétate de vinyle aux poly(amide de vinyle)s. La deuxième partie concerne l'étude des enchaînements tête-à-tête et tête-à-queue de l'acétate de vinyle en Co-MRP.

[106] M.-K. Wang, Z.-L. Zhou, R.-Y. Tang, X.-G. Zhang, C.-L. Deng, *Synlett*, **2013**, *24*, 737-740
[107] H. Sun, Y. Zhang, F. Guo, Z. Zha, Z. Wang, *J. Org. Chem*., **2012**, *77*, 3563-3569

1) Chélation au métal intramoléculaire et liaisons hydrogènes

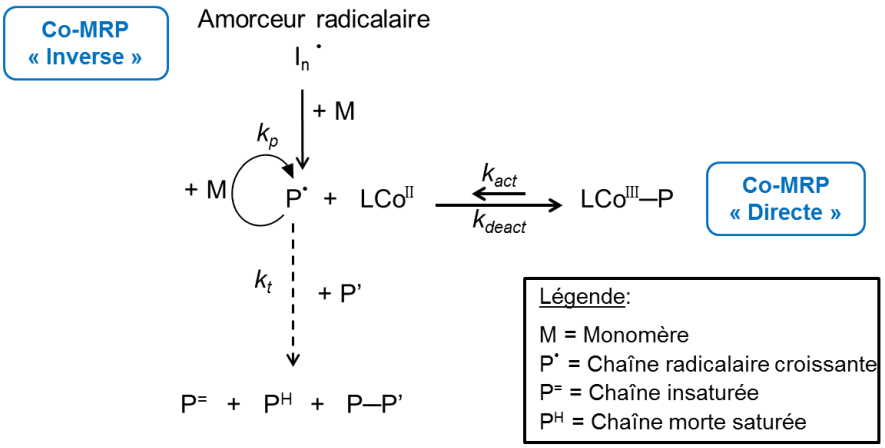

Schéma 6 : Mécanisme simplifié de la polymérisation radicalaire contrôlée par le cobalt (Co-MRP).

En l'absence d'agents de coordination extérieurs, il a été montré, dans le cas de la polymérisation de l'acétate de vinyle (AcV) contrôlée par le complexe bis(acetylacetonato)cobalt(II) ([$Co(acac)_2$]), qu'un phénomène de chélation du cobalt par coordination du groupement carbonyle de la dernière unité de la chaîne poly(acétate de vinyle) (PAcV) était possible (voir Figure 90).[108] Une telle double liaison entre l'agent de contrôle et la chaîne de polymère n'a été démontrée dans le domaine des PRC que dans ce cas particulier de l'AcV contrôlé par le [$Co(acac)_2$]. C'est une propriété très importante qui permet un ajustement précis de l'équilibre entre les espèces dormante et active mises en jeu en PRC. Une étude DFT a montré que la coordination du groupement carbonyle de la chaîne de PAcV crée un cycle à cinq chaînons qui stabilise la liaison cobalt-polymer de 3 kcal.mol^{-1} supplémentaires.

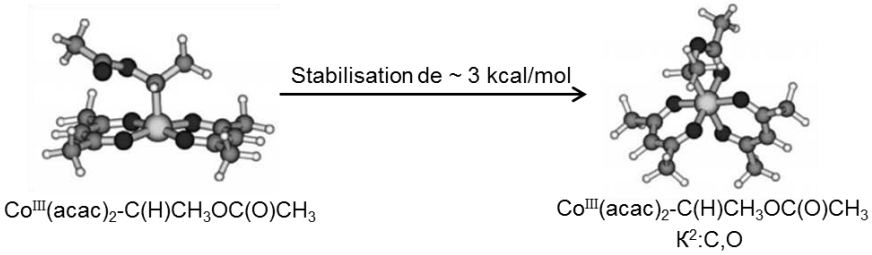

Figure 20 : Géométries optimisées en DFT du composé modèle AcV–$Co(acac)_2$ issues de la référence 108.

Bien que les amides soient connus pour être des bases de Lewis plus fortes que les esters en raison de leur groupement carbonyle plus riche en électrons, la possibilité d'une chélation intramoléculaire sur le cobalt n'a jamais été envisagée pour le cas de la polymérisation de la

[108] A. Debuigne, Y. Champouret, R. Jérôme, R. Poli, C. Detrembleur, *Chem. Eur. J.*, **2008**, *14*, 4046-4059

N-pyrrolidone de vinyle (NVP) et du N-caprolactame de vinyle. Quelque soient les conditions, la Co-MRP de ces monomères a toujours été présentée comme un simple piégeage réversible des chaînes par le métal selon un équilibre entre les espèces 1 et 2 représentées sur le Schéma 7.

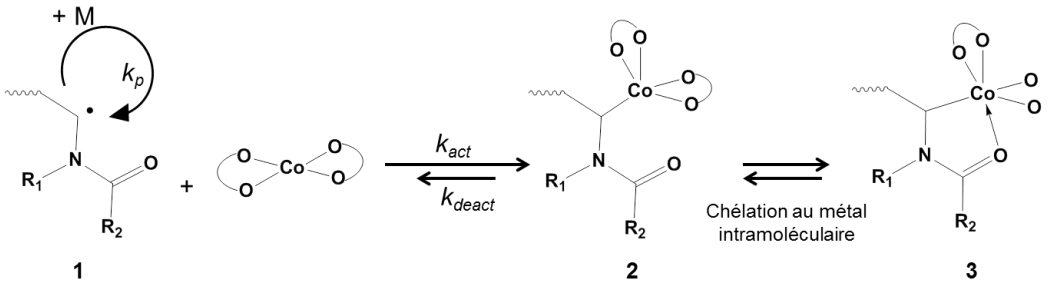

Schéma 7 : Equilibre de la Co-MRP d'amides de vinyle et phénomène de chélation sur le cobalt (= anion acétylacétonate).

En collaboration avec Antoine Debuigne, membre de l'équipe de Christine Jérôme du Centre d'Etude et de Recherche sur les Macromolécules (CERM) situé à Liège (en Belgique), nous avons étudié, sur des bases cinétiques et théoriques, la Co-MRP d'une série d'amides de vinyles (Figure 91) pour mettre en évidence la prépondérance de l'espèce chélatée dans le mécanisme de polymérisation.

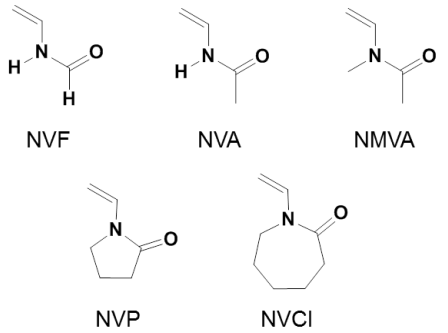

Figure 21 : Structure des cinq *N*-amides de vinyle non conjugués étudiés par Debuigne et ses collègues (NVF = *N*-formamide de vinyle, NVA = *N*-amide de vinyle, NMVA = *N*-méthyl-*N*-acétamide de vinyle, NVP = *N*-pyrrolidone de vinyle, NVCl = *N*-caprolactame de vinyle).

Debuigne et ses collègues ont réalisé les polymérisations en masse de ces cinq amides de vinyle dans des conditions d'OMRP en présence de $[Co(acac)_2]$.[109] Ils ont utilisé un amorceur de type cobalt-alkyle ($[(acac)_2Co^{III}\text{-}(AcV)_n\text{-}C(CH_3)(CN)\text{-}CH_2\text{-}C(CH_3)_2(OCH_3)]$ avec n ~4) qui, par traitement thermique, subit une rupture homolytique de la liaison Co-C et relargue à la fois l'agent de contrôle $[Co(acac)_2]$ et l'amorceur radicalaire (Co-MRP directe, Schéma 6). Bien que les mécanismes de transfert de chaîne dégénératif et de terminaison réversible sont

[109] A. Debuigne, A. N. Morin, A. Kermagoret, Y. Piette, C. Detrembleur, C. Jérôme, R. Poli, *Chem. Eur. J.*, **2012**, *18*, 12834-12844

rapportés pour la Co-MRP, le premier nécessite un flux de radicaux tout au long de la polymérisation, ce qui n'est pas le cas lorsque l'on utilise un dérivé cobalt-alkyle comme amorceur unimoléculaire. Les cinq monomères polymérisent à des vitesses très différentes dans des conditions similaires malgré leur structure électronique proche (CH2=CH-N(R^1)-CO-R^2). La polymérisation en masse est de plus en plus rapide selon l'ordre NMVA < NVCl < NVP < NVA < NVF (Figure 92).

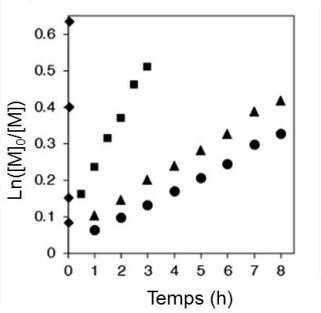

Figure 22 : ln([M]$_0$/[M]) (M = monomère) par rapport au temps de polymérisation pour la Co-MRP en masse de l'AcV (●), NVP (♦), NVCl (■), et NMVA (▲) amorcée à 40°C par un adduit cobalt-alkyle de faible masse molaire; [M]/[Co(acac)$_2$(PAcV)] = 380 (données issues de la référence 108).

Pour rationaliser cette ordre de vitesse de polymérisation, nous avons réalisé des études DFT pour chacun de ses systèmes et comparé les résultats avec ceux déjà publiés dans le cas de l'AcV.[110,111] La première question fût la force relative des liaisons Co^{III}-polymère et la présence ou non d'une extra-stabilisation par chélation intramoléculaire. Comme dans le cas de l'AcV, les chaînes ont été modélisées par un atome d'hydrogène au-delà de la première unité de monomère (Figure 94). Les calculs d'optimisation de géométries ont été effectués sur les trois procédés illustrés sur le Schéma 8 pour les cinq monomères et ont donné les résultats résumés dans le Table 13. L'enthalpie de dissociation de la liaison Co-C du complexe [Co(acac)$_2$(CH$_3$)] a également été calculée pour comparaison.

La force intrinsèque de la liaison Co-C des cinq modèles étudiés (enthalpie de formation de la liaison Co-C pour former le produit K^1:C) varie entre 7.3 et 10.0 kcal/mol et n'est que légèrement inférieure au modèle [Co(acac)$_2$(AcVH)] mais beaucoup plus faible que dans le cas [Co(acac)$_2$(CH$_3$)]. Toutefois, le phénomène de chélation du groupement carbonyle change radicalement les valeurs des forces de liaison Co-C totales (enthalpies de chélation entre 3.0 et 7.8 kcal/mol). Les enthalpies totales de formation de liaison Co-C produisant le produit K^2:C,O le plus stable sont toutes plus grandes que dans le cas de l'AcV (13.0 kcal/mol) excepté pour le radical NVPH (entre 11.6 et 16.5 kcal/mol). Finalement, la différence

[110] A. Debuigne, R. Poli, R. Jérôme, C. Jérôme, C. Detrembleur, *ACS Symp. Ser.*, **2009**, *1024*, 131-148.
[111] A. Debuigne, Y. Champouret, R. Jérôme, R. Poli, C. Detrembleur, *Chem. Eur. J.*, **2008**, *14*, 4046-4059

d'enthalpie entre l'espèce dormante et l'espèce radicalaire activée (Scheme 26) est de plus en plus faible selon l'ordre NMVAH > NVClH > NVAH > NVFH = VacH > NVPH.

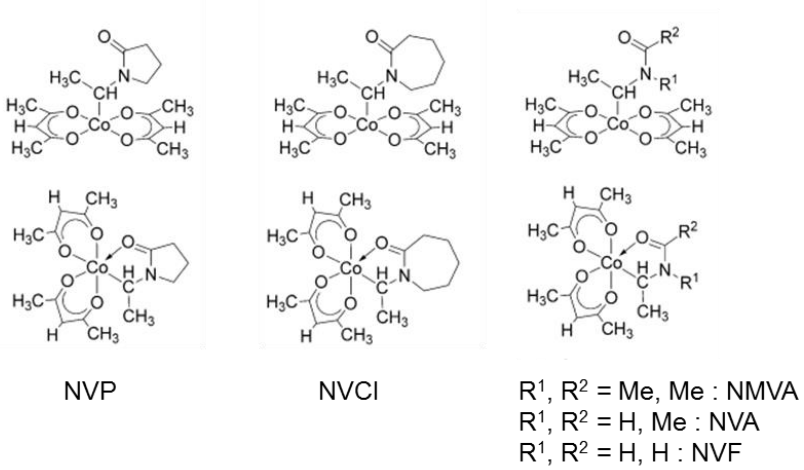

Figure 23 : Modèles des espèces dormantes de cobalt(III) penta- et hexa-coordiné pour la polymérisation des amides de vinyle.

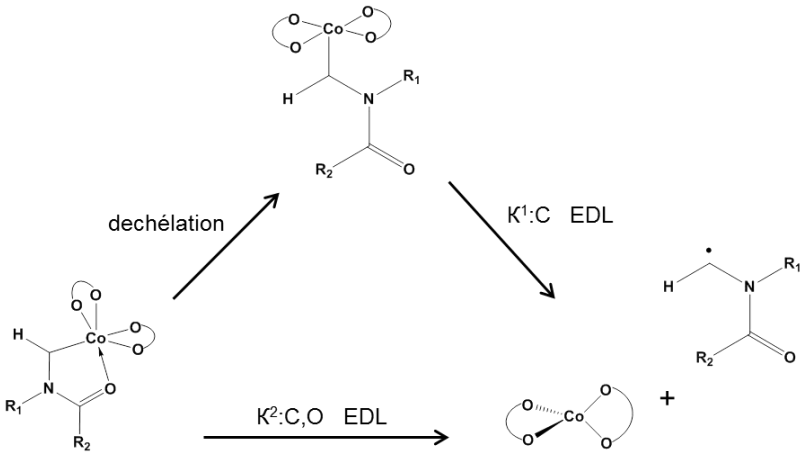

Schéma 8 : Procédés de déchélation et de rupture homolytique des liaisons de l'espèce dormante en Co-MRP des amides de vinyle avec le [Co(acac)$_2$] (O,O = acac).

Tableau 2 : Changements d'enthalpie (en kcal.mol^{-1}) calculés pour les procédés décrits dans le Scheme 26.

Complexe	Dechél.	K^1:C EDL	K^2:C,O EDL
[Co(acac)$_2$(NVPH)]	4.3	7.3	11.6
[Co(acac)$_2$(NVClH)]	5.2	9.5	14.7
[Co(acac)$_2$(NMVAH)]	7.8	8.7	16.5
[Co(acac)$_2$(NVAH)]	4.7	9.4	14.1
[Co(acac)$_2$(NVFH)]	3.0	10.0	13.0
[Co(acac)$_2$(VAcH)]	3.0	10.0	13.0
[Co(acac)$_2$(CH$_3$)]	-	20.1	-

Nous avons aussi étudié la possibilité de coordination du monomère sur les complexes de cobalt(II) et de cobalt(III). Les résultats montrent que la coordination d'une molécule de

monomère sur l'espèce de cobalt(III)aklyle n'est pas favorisée pour les cinq monomères étudiés. Le meilleur paramètre pour décrire l'équilibre de contrôle radicalaire est donc la différence d'enthalpie entre le complexe chélaté [K^2:C,O -$Co(acac)_2$(MH)] et le [$Co(acac)_2$] et le radical $MH^{\bullet}$ séparés (i.e., l'EDL K^2:C,O dans la dernière colonne du Table 13), à l'exception peut-être des systèmes NVA et NVF pour lesquels la stabilisation du Co^{II} par coordination d'une molécule de monomère (-1.8 et -2.2 kcal/mol respectivement) doit engendrer un effet accélérateur. Finalement, les différences d'enthalpie entre les espèces dormantes et activées sont classées dans l'ordre suivant (valeurs en kcal/mol): NMVA (16.5) > NVCl (14.7) > NVA (12.3) > NVP (11.6) > NVF (10.8).

La seule contradiction entre l'ordre des forces de liaisons et les vitesses de polymérisations (la plus lente NMVA < NVCl < NVP < NVA < NVF la plus rapide) apparait être la position relative de la NVP. Ceci s'explique par l'intervention de liaisons hydrogène N─H···O=C avec le monomère libre, qui stabilisent la chaîne dormante piégée (par son effet donneur de proton) et stabilise la chaîne radicalaire en croissance (à la fois comme donneur de proton et comme accepteur de proton). L'équilibre est donc déplacé vers la formation de la chaîne radicalaire en croissance.

2) Addition tête-à-tête de l'acétate de vinyle

Malgré les nombreux progrès réalisés pour la PRC de l'acétate de vinyle, tous les systèmes rapportés montrent une augmentation de la dispersité des PAcV avec la conversion ou un ralentissement de la vitesse de polymérisation (dans certains cas, la polymérisation s'arrête) à l'exception de l'agent de contrôle [$Co(acac)_2$] utilisé en Co-MRP qui permet d'obtenir une croissance des chaînes bien contrôlée jusqu'à de hauts degrés de polymérisation et des hautes conversions. Parmi de nombreuses explications proposées, on retrouve souvent la formation d'une liaison PAcV-CHOAc-CH2-X plus forte présente dans l'espèce dormante après l'insertion inversée d'un monomère par addition tête-à-tête et formant un radical primaire plus réactif. Cette liaison plus forte avec l'agent de contrôle rend l'espèce dormante plus difficile à réactiver et rationalise donc le ralentissement de polymérisation et l'augmentation de la dispersité mais cela n'explique pas pourquoi le ralentissement est plus prononcé pour certains systèmes (e.g., TERP, ATRP avec certains complexes de cuivre) que pour d'autres (e.g., RAFT/MADIX) et surtout pourquoi le système [$Co(acac)_2$] en OMRP ne souffre d'aucun ralentissement.

Il y a deux possibilités : soit [$Co(acac)_2$] d'une manière modifie la réactivité du radical et diminue la propension d'enchaînements tête-à-tête, soit l'espèce dormante permet une

réactivation plus facile du radical primaire piégé. La première explication a été écartée par des analyses RMN de PAcV synthétisés en OMRP avec le [$Co(acac)_2$] qui ont montré une fraction d'enchaînements tête-à-tête identiques avec et sans cobalt.[112]

Par conséquent, la réactivation du radical primaire piégé doit être aussi rapide que celle du radical secondaire (issu d'un enchaînement « normal » tête-à-queue). Nous avons donc étudié en DFT les modèles de ces deux espèces dormantes et calculé les EDL relatives des liaisons R-X des espèces dormantes générées en ATRP, RAFT, ITP et TERP afin de mieux comprendre les effets de ces inversions de monomères en PRC. Le polymère au-delà de la dernière unité de monomère a été simplifié par un atome d'hydrogène (voir Scheme 29). Dans le cas de la Co-MRP, les EDL calculées sont basées sur les espèces chélatées plus stables (vide supra). Les calculs ont été réalisés à l'aide de cinq fonctionnelles différentes (BPW91, BPW91*, B3PW91, M06 et M06L). Ils sont résumés dans le Table 16. Les calculs prédisent, en accord avec les données expérimentales, un ralentissement moins prononcé pour la RAFT que pour la ATRP, la TERP ou l'ITP. Le point le plus intéressant est la valeur de Δ très différente pour le système [$Co(acac)_2$] (proche de zéro). Cela signifie que le coût énergétique de la réactivation des deux types d'espèces dormantes est quasi identique donc l'absence de ralentissement de polymérisation avec le [$Co(acac)_2$] est rationalisée.

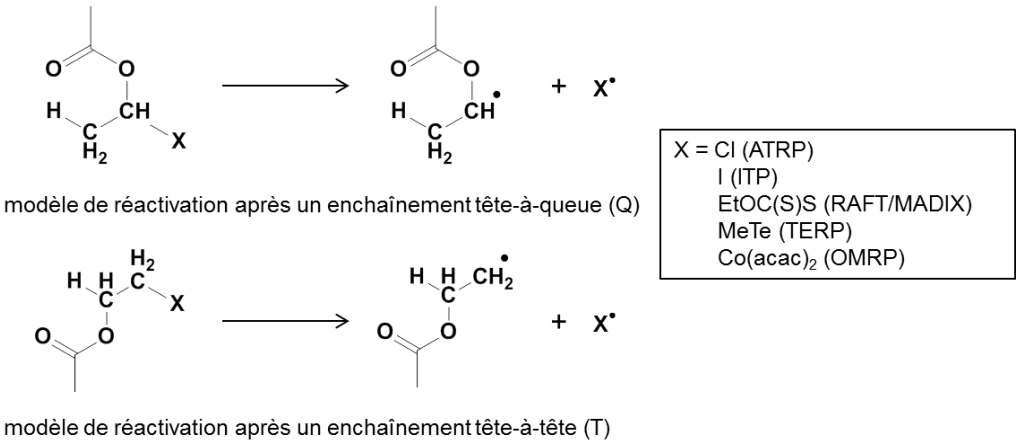

Schéma 9 : Modèles utilisés pour les calculs en DFT.

Afin de comprendre cette grande différence de stabilisation dans le cas du [$Co(acac)_2$], nous avons analysé plus en détail le processus de relargage du radical. Les résultats sont décrits graphiquement dans la Figure 103. En allant du [$Co(acac)_2$] (en haut, au milieu) vers l'espèce dormante [$AcVH{-}Co^{III}(acac)_2$] (isomère T-Q normal vers la droite et isomère inversé T-T vers la gauche), on peut diviser le processus en deux étapes : premièrement, la formation d'une liaison produisant un intermédiaire cobalt(III)-alkyle pentacoordiné qui possède un spin

[112] A. N. Morin, C. Detrembleur, C. Jérôme, P. De Tullio, R. Poli, A. Debuigne, *Macromolecules*, **2013**, *46*, 4303-4312

S=0 à l'état fondamental et une géométrie pyramidale à base carrée avec le groupe alkyle en position apicale. Le changement de spin se produit en engendrant un réorganisation des deux ligands acac d'un plan à un arrangement papillon. Ce qui permet un changement du site de coordination vacant de la position trans à cis par rapport au groupe alkyle et ainsi de permettre la coordination de la fonction carbonyle. Les calculs montrent que la formation de la liaison est, comme prévu, plus exothermique pour le radical primaire que pour le radical secondaire (16.0 kcal/mol pour l'isomère T-T *vs* 11.1 kcal/mol pour l'isomère T-Q). Toutefois, la chélation est plus favorable pour l'isomère T-Q formant un cycle à cinq chaînons (6.2 kcal/mol) que pour l'isomère T-T formant un cycle à six chaînons (2.3 kcal/mol). Donc la compensation d'une liaison C-Co plus faible par une chélation plus stable rend la stabilisation de l'espèce dormante T-Q équivalente à celle de l'isomère plus réactif T-T et les deux isomères sont réactivés à des vitesses similaires.

Tableau 3 : Enthalpies de dissociation de liaison calculées (en kcal/mol) pour les liaisons HAcV-X. T-Q = modèle de piégeage tête-à-queue (radical secondaire) ; T-T = modèle de piégeage tête-à-tête (radical primaire) ; Δ = EDL(T-T) – EDL(T-Q).

X		BPW91	BPW91*	B3PW91	M06	M06L
-	Δ[a]	8.2	7.7	7.3	7.2	6.6
Cl (ATRP)	T–Q	74.2	75.7	73.9	79.4	78.7
	T–T	81.8	83	81	85.8	84
	Δ	7.6	7.3	7.1	6.4	5.3
I (ITP)	T–Q	47.1	46.2	46.6	54.2	51.7
	T–T	56.3	55.5	55.7	62.7	59
	Δ	9.2	9.3	9.1	8.5	7.3
MeTe (TERP)	T–Q	41.8	43.5	42.5	52.8	50.2
	T–T	50.1	50.9	49.8	58.9	55.4
	Δ	8.3	7.4	7.3	6.1	5.2
EtOC(S)S (RAFT)	T–Q	46.8	51.3	50.6	57.7	54.7
	T–T	52.4	56.4	55.3	61.5	57.9
	Δ	5.6	5.1	4.7	3.8	3.2
$[Co(acac)_2]$ (OMRP)	T–Q	28.2	17.3	9.3	18.5	34.2
	T–T	29.1	18.3	10.2	19.9	34.3
	Δ	0.9	1	0.9	1.4	0.1

[a] Δ = Différence d'enthalpie entre les deux isomères du radical libre.

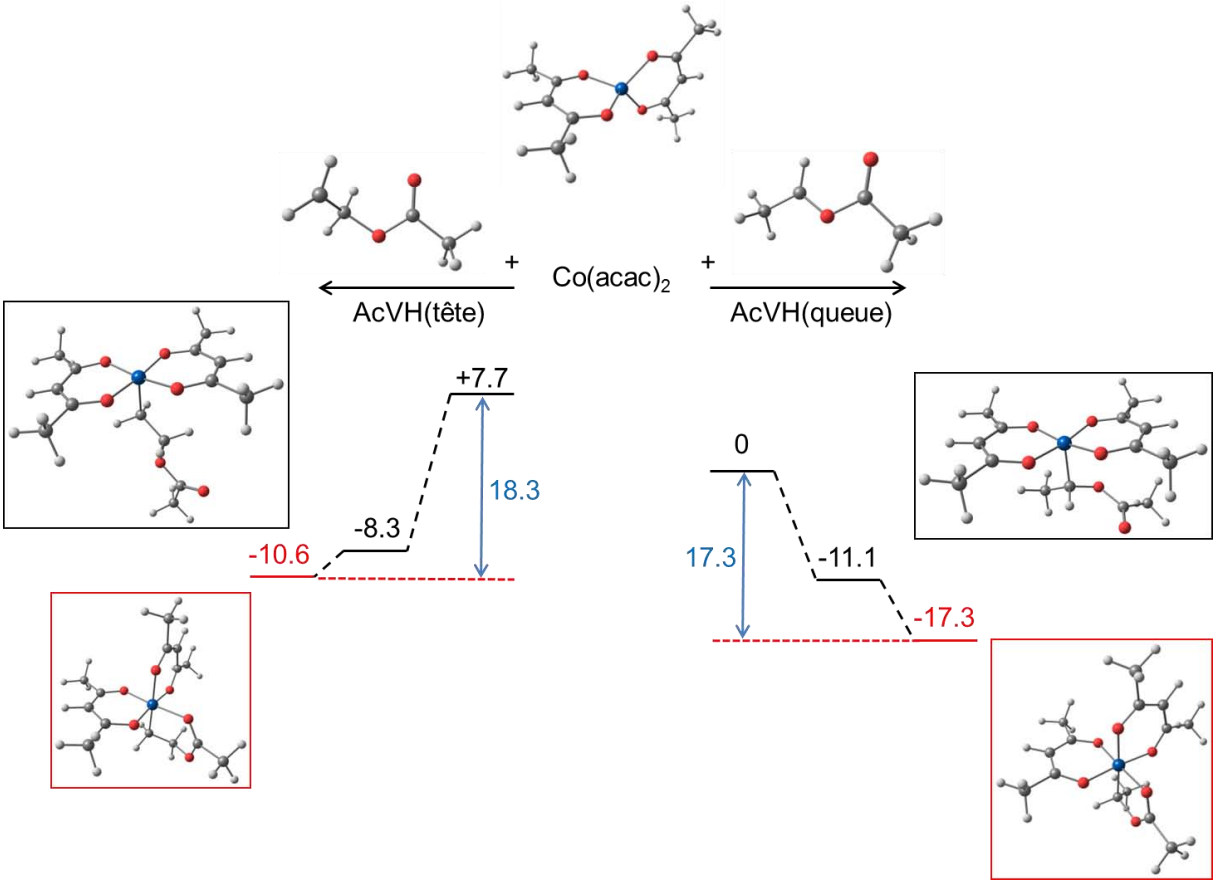

Figure 24 : Enthalpies relatives (en kcal/mol, BPW91*) et géométries optimisées des espèces impliquées dans le processus de désactivation en OMRP des modèles de PAcV radicalaire tête et queue (X = $[Co(acac)_2]$).

CONCLUSION GENERALE

En conclusion, nous avons pour la première fois démontré l'utilisation de complexes de cuivre comme agent de contrôle pour la polymérisation radicalaire (OMRP) de l'acétate de vinyle (AcV) et de l'éthylène. Nous nous sommes intéressés au couple cuivre(I)/cuivre(II) coordiné par des ligands azotés : β-dikétimines (NacNac), scorpionates substitués (Tp), tris(pyridylméthyl)amine (TPMA) et tris(pyridylthiométhanide) (TPTM). Bien que nous n'avons pas pu isoler d'espèce de cuivre(II)-alkyle, nous avons montré via des études spéctroscopiques EPR des preuves de formation de liaison cuivre-carbone par alkylation de comple es précurseurs de cuivre(II) appropriés. Nous sommes maintenant convaincus qu'une espèce organométallique de cuivre(II) peut être formée et qu'un équilibre d'OMRP peut être établi avec les complexes étudiés. Tous les complexes de cuivre(I) examinés ont montré un effet de retardement plus ou moins prononcé sur la polymérisation de l'AcV et de l'éthylène. Dans le cas de l'AcV, les meilleurs résultats ont été obtenus avec le ligand tris-(3,5-diméthyl-pyrzolyl)borate (Tp*) dont le complexe de cuivre a montré un certain degré de contrôle et les

poly(acétate de vinyle)s formés de faible dispersité (1.2 < Đ < 1.5). De plus, le fait que la formation de polymère continue après le temps nécessaire à la décomposition totale de l'amorceur radicalaire démontre la présence d'un piégeage dynamique réversible des chaînes de polymère par les complexes de cuivre(I) pour former une espèce dormante labile. D'après nos expériences préliminaires de polymérisation de l'AcV et de l'athylène, nous pouvons conclure que la structure du ligand a un effet sur l'équilibre d'OMRP : i) les substituants électro-donneurs donne un piégeage plus efficace. ii) par rapport au ligand scorpionate tridente, le nombre de coordination du ligand NacNac bidente conduit à la formation de liaisons PAcV-Cu^{II} plus fortes.

Par ailleurs, nous avons réalisé des calculs théoriques afin de mieux comprendre le succès de la polymérisation radicalaire contrôlée (PRC) par le complexe de cobalt acétylacétonate ([$Co(acac)_2$]). Nous avons étudié l'impact des enchaînements tête-à-tête en polymérisation radicalaire contrôlée de l'AcV. Bien que cet enchaînement « inversé » soit peu fréquent, les radicaux primaires tête-à-tête conduisent à une espèce dormante plus stable que pour les radicaux « normaux » secondaires tête-à-queue. Du fait de la réactivation de l'adduit primaire plus difficile, les polymérisations sont ralenties voire stoppées et la dispersité des PAcV augmente. Toutefois, la PRC de l'AcV en présence de [$Co(acac)_2$] ne semble pas être affectée par ce problème. En collaboration avec Antoine Debuigne et ses associés, nous avons donné une interprétation à ce phénomène exceptionnel remarqué pour le [$Co(acac)_2$]. En effet, le cobalt n'a pas d'effet sur la fréquence d'enchaînements tête-à-tête mais d'après les calculs de DFT, les deux formes d'espèces dormantes (adduits primaires et secondaires) sont réactivées à des vitesses similaires du fait de la singulière chélation du groupement carbonyle de la dernière unité de monomère des chaînes piégées sur le cobalt. La plus forte liaison σ Co−C formée par l'adduit primaire tête-à-tête est compensée par une plus faible stabilisation par coordination du groupement carbonyle formant un cycle à six chaînons. D'un autre côté, l'espèce dormante tête-à-queue possède une liaison σ Co−C plus faible mais la formation d'un cycle à cinq chaînons par coordination du groupement carbonyle sur le cobalt est plus stabilisante. La combinaison des deux effets (liaison σ et chélation) produit une vitesse similaire de réactivation pour les deux espèces dormantes. Cette caractéristique est spécifique aux chaînes dormantes terminées par le [$Co(acac)_2$], contrairement aux autres chaînes dormantes PAcV−X issues d'autres PRC comme l'ATRP, la RAFT, l'ITP ou la TERP pour lesquelles la liaison C−X de l'adduit primaire tête-à-tête est plus forte et donc plus difficile à réactiver.

Bien que les amides soient connus pour être des bases de Lewis plus fortes que les esters, l'OMRP avec le [$Co(acac)_2$] de ces monomères a toujours été présentée comme un simple piégeage réversible des chaînes par le complexe. A la lumière des résultats précédents avec l'AcV, nous avons étudié l'effet d'une possible coordination intramoléculaire sur le cobalt pour une série d'amides de vinyle : *N*-vinyle formamide (NVF), *N*-vinyle amide (NVA), *N*-méthyl-*N*-vinyle acétamide (NMVA), *N*-vinyle pyrrolidone (NVP), *N*-vinyle caprolactame (NVCl). Les vitesses de polymérisation expérimentales obtenues par Debuigne et ses collègues (la plus faible NMVA < NVCl < NVP < NVA < NVF la plus rapide) ont été rationnalisées par des études DFT. En fait, la force de liaison intrinsèque Co−C des modèles de chaînes dormantes (entre 7,3 et 10,0 kcal/mol) est légèrement plus élevée que celle du modèle [$Co(acac)_2$(AcVH)] mais la coordination du groupement carbonyle change totalement les forces de liaison totales (enthalpie de chélation entre 3,0 et 7,8 kcal/mol). Finallement, lorsque la chélation du groupement carbonyle est prise en compte, l'enthalpie totale de formation de liaison conduisant au produit K^2:C,O plus stable est de plus en plus faible selon l'ordre NMVAH > NVClH > NVAH > NVFH = AcVH > NVPH. La seule différence entre l'ordre des forces de liaison et les vitesses expérimentales de polymérisation réside dans le positionnement du monomère NVP. En fait, les différences d'enthalpie calculées ci-dessus sont surrévaluées pour les monomères NVA et NVF à cause de liaisons hydrogène. Les calculs prévoient en effet que les liaisons hydrogène avec le monomère stabilisent plus le radical libre + [$Co(acac)_2$] (13,1 et 15,1 kcal.mol^{-1} pour les modèles NVA et NVF, respectivement) que la forme chélatée dormante (2,4 et 3,2 kcal.mol^{-1} pour les modèles NVA et NVF, respectivement) ce qui conduit à une accélération de la polymérisation.

CONTROLLED RADICAL POLYMERIZATION OF VINYL ESTERS AND VINYL AMIDES : EXPERIMENTAL AND THEORETICAL STUDIES

GENERAL INTRODUCTION

GENERAL INTRODUCTION

1) Controlled radical polymerizations

The last two decades have witnesses a real explosion of publications related to reversible deactivation radical polymerization (RDRP) (Figure 1). Radical polymerization is a chain-growth polymerization which includes four fundamentals processes: chain initiation, chain propagation, chain termination and chain transfer. When termination and transfer are absent, a "living polymerization" process occurs, with important consequences on our ability to obtain polymers with controlled molecular weights, low dispersity, and controlled chain-end functionality. Living polymerizations have first been developed for anionic polymerization, then for cationic and coordination polymerizations. A living radical polymerization is of course impossible, since radicals undergo spontaneous bimolecular termination processes by coupling and/or by disproportionation. Born in 1994,[1] the expression "Controlled Radical Polymerization" refers to the radical polymerizations where the incidence of termination and transfer reactions on the polymer chain growth can be reduced to such a low level that the characteristics of the chain growth follow closely those expected for a living polymerization. IUPAC has recently recommended that this term be abandoned and replaced by the expression "Reversible-Deactivation Radical Polymerization" (RDRP).[2]

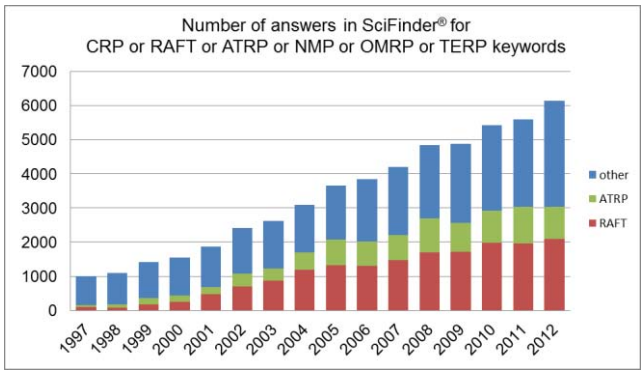

Figure 1: Results for "Controlled radical polymerization" concept in SciFinder. RAFT, ATRP, NMP, OMRP and TERP are controlled radical polymerization techniques detailed in this chapter.

There are two different ways to control chain growth of polymers. The first one is based on the reduction of the radical concentration in the medium through a reversible equilibrium through trapping by a controlling agent (CA), yielding a dormant species from which the active radical can dissociate again (Scheme 1), so that the unwanted termination reactions are lowered to a minimum (the termination rate is proportional to the square of the radical concentration whereas the propagation rate is proportional to the radical concentration). This

strategy, which we'll refer to in this thesis as Reversible Dissociative Activation Radical Polymerization (RDARP), benefits from the persistent radical effect. The equilibrium must be shifted toward the dormant state to allow good control. The second way to achieve control of polymerization is through a degenerative transfer (Scheme 2), because the overall Gibbs energy is identical on both sides of the equation. The difference is found in the chain length of P and P'. This strategy will be defined as Degenerative Transfer Radical Polymerization (DTRP). The dormant chain in this strategy acts also as transfer agent and relative to RDARP, which yields the active radical dissociatively, activation by DTRP consists in an associative exchange of active radicals. The exchange rate must ideally be much faster than the propagation rate to yield well controlled polymers.[3] This technique needs the continuous influx of new radicals from a conventional radical initiator, allowing the exchange and growth processes to continue. Controlled growth stops when no new radicals are injected into solution, whereas an RDARP process continues in the absence of an external radical source because the growing radical chains are generated dissociatively from the dormant species. In addition, the chain-length dependent termination rate constant (shorter chains terminate faster than longer ones) permits the longer chains to continue to grow in a pseudo-living manner whereas the short chains that are continuously generated from the initiator, while allowing the exchange and the controlled growth of the longer chains, terminate preferentially.

The advantages of radical processes are the high tolerance towards many functional groups (alcohol, amines…), impurities (especially water) and the large range of polymerizable monomers. Nowadays complex architectures and functional polymers have been obtained by RDRP whereas 15 years ago a high degree of control could only be reached via anionic or cationic polymerizations. To date, several controlling agents have been discovered and many monomers have been successfully polymerized via RDRP. However, suitable methods to accomplish the RDRP of less reactive monomers (LRM), *i.e.* monomers giving highly reactive radicals) with a satisfactory degree of control are still underdeveloped. The main reason is the strong energy required to break the polymer-CA bond. Advantages and limitations of each RDRP approach are summarized in the following section.

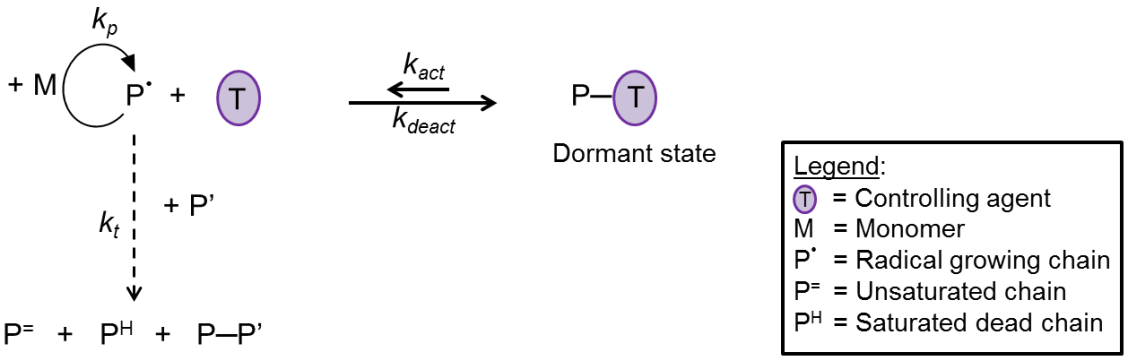

Scheme 1: General mechanism of radical polymerization controlled by reversible dissociative activation.

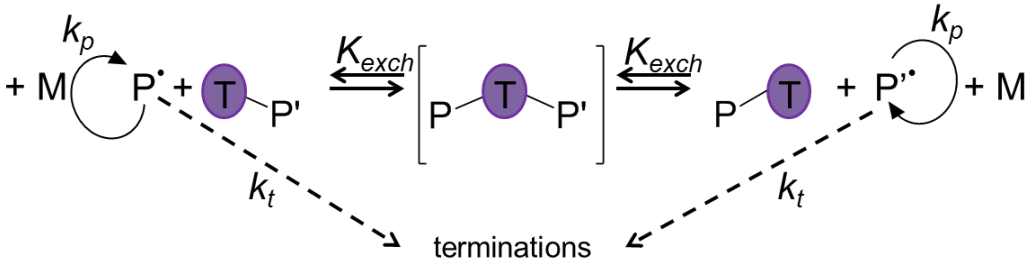

Scheme 2: General mechanism of the degenerative transfer radical polymerization (DTRP).

a) Reversible dissociative activation pathways

Within the reversible deactivation pathways are found Nitroxide-Mediated Polymerization (NMP), Atom Transfer Radical Polymerization (ATRP) and Organometallic-Mediated Radical Polymerization (OMRP). The advantages and limitations of each one of these methods which are the three main RDARP techniques will be presented in this section. These three mechanisms can sometimes interplay or be disturbed by others mechanisms.

NMP is based on a dynamic equilibrium between the propagating radical plus a stable nitroxide radical and an alkoxyamine (end-capped radical) as a dormant species (Scheme 3). As early as in 1983, Solomon and Rizzardo patented the use of alkoxyamines to control the oligomerization of styrene, (meth)acrylates, vinyl acetate and (meth)acrylonitrile[4] but the study which demonstrated the viability of the NMP pathway involved the use of 2,2,6,6-tetramethylpiperidin-1-yl)oxyl (better known as TEMPO, Figure 2) as a trapping agent for styrene polymerization.[5] TEMPO remains effective for styrene polymerization only because of the slow dissociation rate (homolytic cleavage of the alkoxyamine). Fine tuning of the nitroxide CA by polar, steric and electronic effects, the steric one being the predominant one, allows the control of others monomers.[6]

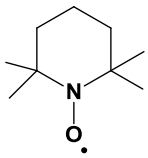

Figure 2: Chemical structure of TEMPO.

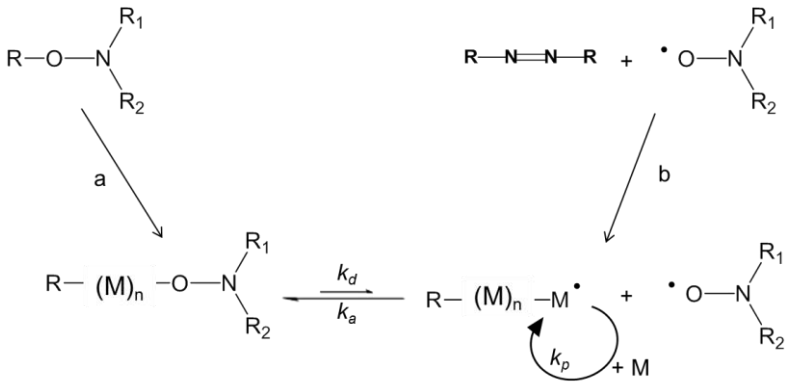

Scheme 3: Activation-deactivation equilibrium in NMP. Monocomponent (a) and bicomponent (b) initiating system.

Figure 3 shows some well-known NMP CA. Among them, cyclic nitroxides N1, N3 and N4 can control both styrene (St) and *n*-butylacrylate (*n*BA) whereas cyclic nitroxide N2 give the best results for styrene polymerization (M_n ~ 100 000 g/mol, Đ < 1.5).[7] The breaktrough in nitroxide adjustment was reported by Tordo and coworkers with TIPNO (N5) being able to control for the first time a wide range of monomers (St, acrylates, dienes etc…).[8] Later, N6 (water soluble in its protonated form) was shown to be more efficient than TIPNO for *n*BA polymerization which is explained, among other factors, by a lower radical concentration when using nitroxide N6.[9] Also N7 and SG1 were shown to be more efficient for St and *n*BA polymerization.[10,11] DPAIO (N9) showed efficient control of methyl methacrylate (MMA) and remains so far unique in this capacity.[12] Bis-nitroxides were also investigated as they may allow the synthesis of the symmetrical triblock copolymers AB-N-BA (N = bis-nitroxide), simplified as triblock ABA, previously inaccessible by NMP. Indeed, it is possible to add either a polystyrene or a polyisoprene B block to a polyacrylate or polyacrylamide macroinitiator, but a polystyrene or polyisoprene macroinitiator will not readily add a polyacrylate or polyacrylamide B block with adequate control. TIPNO derivatives (N10) demonstrated good control over styrene and *tert*-butylacrylate (*t*BA) and allow synthesis of the amphiphilic P*t*BA-*b*-PS-*b*-P*t*BA triblock with hydrophilic ends.[13] Alkoxyamines were investigated since Rizzardo4 and Hawker[14] displayed the monocomponent initiating system. For example N11 shows successful control for the polymerization of *n*BA.[15] Finally, NMP allows controlled polymerization of styrene or styrenic derivatives and vinylpyridines,[16,17,18] acrylic esters with TIPNO derivatives,[19] acrylonitrile in a low "livingness" character with

P*n*BA-SG1 macroalkoxyamine initiator,[20] acrylic acid with SG1-based alkoxyamine,[21] acrylamides with either SG1[22] or bisnitroxide N10,[23] butadiene or isoprene with TIPNO[24] or SG1,[25] methyl methacrylate with DPAIO (N9),[12] miscellaneous monomers like vinyl ferrocene with TEMPO[26] and other specific monomers for particular targeted applications.[27]

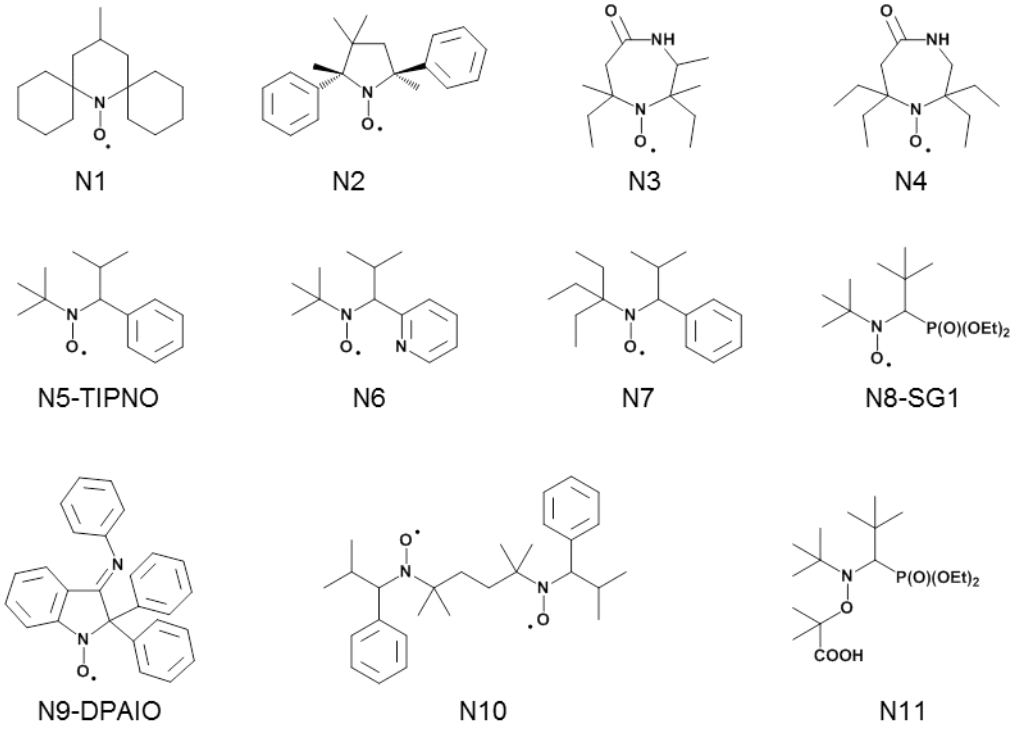

Figure 3: Nitroxides used as controlling agents in NMP of various monomers.

However, all of the afore-mentioned monomers are classified as "more reactive monomers" (MRM). Less reactive monomers (LRM) like vinyl acetate (VAc) or vinylpyrrolidone (NVP) have been extensively studied in NMP but all attempts resulted in poor or no control.[28,29] As alkoxyamines resulting from MRM need temperature ranging from 100°C to 130°C to be homolytically cleaved, one would guess that LRM yielding more reactive radicals will form stronger carbon-oxygen bond, thus demanding even higher temperature to break the C-ON bond. The bond dissociation energy (BDE) for VAc-based alkoxyamines has been calculated and reported by Tordo and coworkers.[30] Compared to MA-based alkoxyamines (MA = methyl acrylate, a similar sterically demanding monomer) the C-ON BDE in vinyl acetate derivatives is much higher because of a hyperconjugation between a lone pair of the nitroxyl oxygen and the adjacent antibonding σ* (C,O) orbital.[31,32]

Reversible deactivation is also the key process in atom transfer radical polymerization (ATRP), a mechanism independently discovered by Matyjaszewski[33] and Sawamoto[34] in 1995. Matyjaszewski and coworkers found out that atom transfer radical addition (ATRA) catalysts could also control radical polymerization. The use of 1-phenylethylchloride as

initiator and copper chloride complexed with 2,2'-bipyridine [CuCl(bPy)] as a chlorine atom transfer agent allows controlled polymerization of styrene (M_n = 4 000, Đ = 1.45) (Scheme 4). Sawamoto and coworkers, while working on living cationic polymerization of vinyl compounds, discovered the reversible formation of carbocations from the HCl─vinyl ether adducts and the rapid exchange process between them (Scheme 5). Therefore, by analogy with the living cationic polymerization, they explored the possibility of living radical polymerization where a dormant intermediate with a carbon-chlorine terminal bond might reversibly be converted into a radical growing species by coordination compounds (P─Cl $\rightleftharpoons$ P$^{\bullet}$). They used tetrachloromethane as initiator, bis(triphenylphosphine)-dichlororuthenium(II) with bis-(2,6-di-*tert*-butylphenoxido)methylaluminum for the polymerization of MMA and obtained good control (M_n = 5 200, Đ = 1.32).[34]

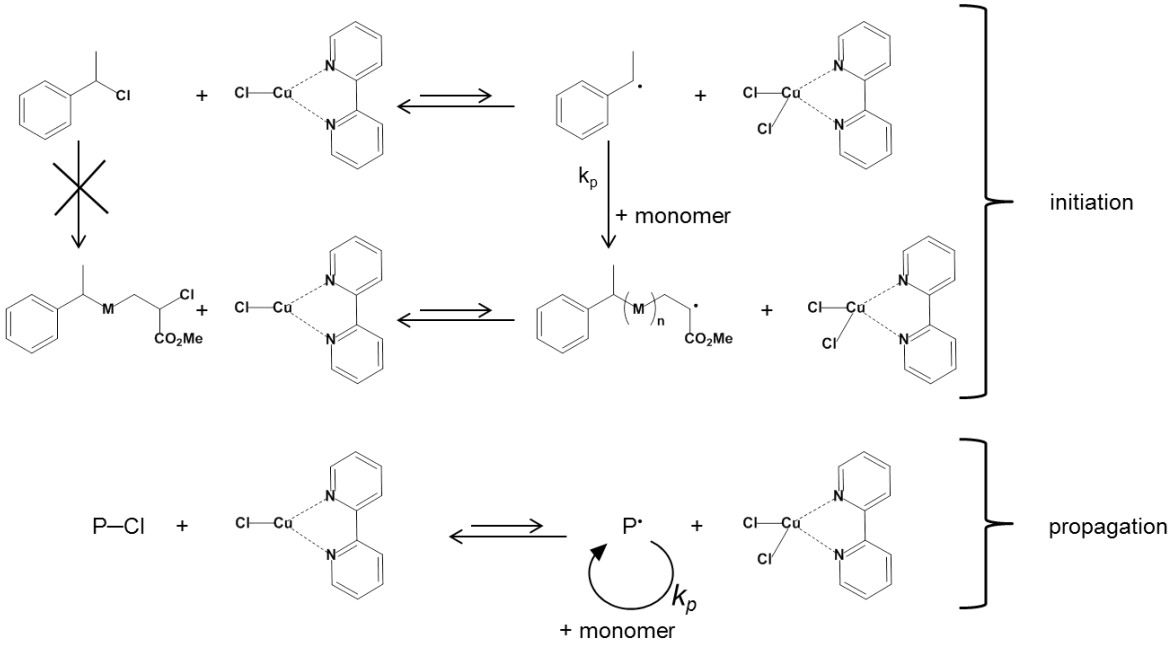

Scheme 4: ATRP mechanism proposed by Matyjaszewski's group at its discovery (reference 33).

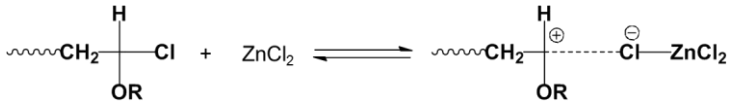

Scheme 5: Exchange process between the HCl─vinyl ether adduct and the carbocation discovered by Sawamoto and coworkers (reference 34).

Nowadays, nearly 20 years after its discovery, ATRP is one of the most widely used RDRP techniques. This is explained by the commercial availability of ATRP reagents (transition metal complexes, ligands and alkyl halide initiators) and the large range of controlled monomers. Controlled monomers include styrenes, (meth)acrylates, (meth)acrylamides,[35] acrylonitrile[36] and vinylpyridine[37] (Figure 4). Copolymerization of methyl acrylate and isobutene or isobutyl vinyl ether was also successfully realized using copper complexes.[38]

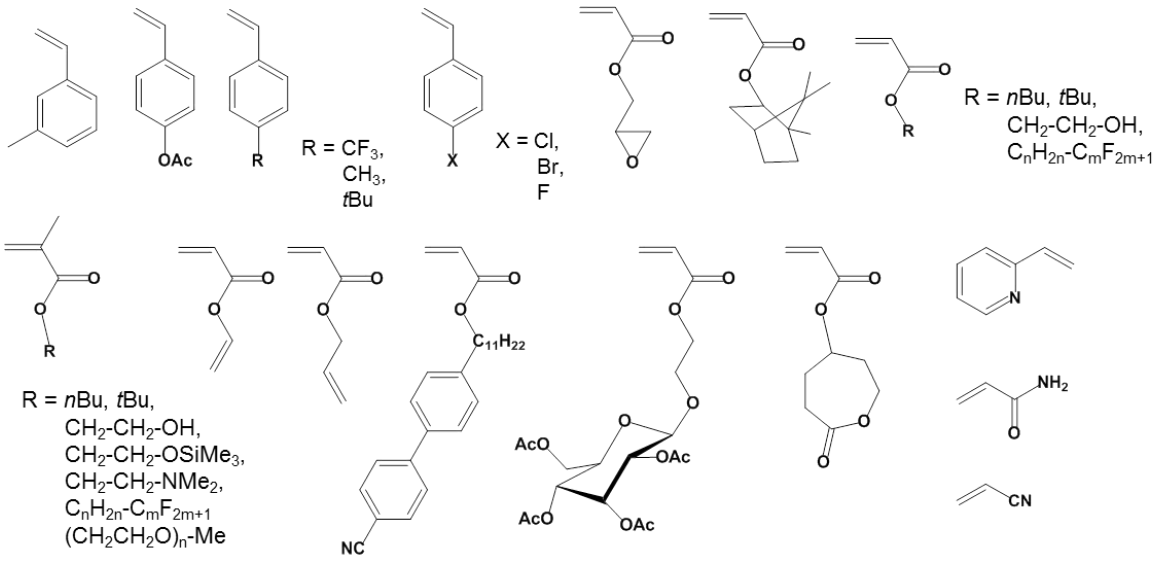

Figure 4: Styrenics, acrylates, acrylamides and other monomers controlled in ATRP.

Moreover, ATRP can equally well be carried out in bulk, in solution or in heterogeneous system (emulsion, suspension). Depending on the initiation, two polymerization protocols are recognized: "normal ATRP" when the initiating radicals are generated from an alkyl halide in the presence of a transition metal complex in the reduced state and "reverse ATRP" when conventional radical initiators are employed (AIBN, TPED, DCDPS, Figure 5) together with the transition metal in its higher oxidation state (Scheme 6).

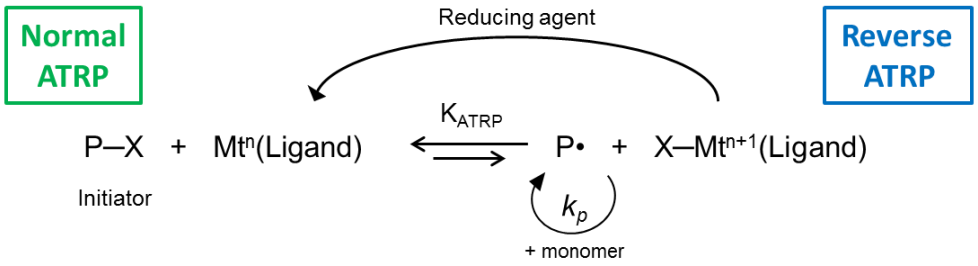

Scheme 6: General Scheme for normal/reverse ATRP.

Due to its versatility and low cost, copper is the most explored metal in ATRP (Figure 6).[39,40] However, St and MMA have been successfully polymerized with numerous other metallic complexes based on molybdenum,[41] rhenium,[42] iron,[43] ruthenium,[44] nickel,[45] palladium,[46] or rhodium.[47] Perhaps one of the greatest challenges in ATRP is the catalyst removal and recycle (either its immobilization or the use of biphasic systems with water, ionic liquids or fluorinated solvents),[48,49] or reducing its amount in order to leave it in negligible quantity into the final polymer. The latter strategy has been developed in the ARGET (Activators Regenerated by Electron Transfer) ATRP (Scheme 7).[50] The key of this process relies on the fact that the ATRP rate depends only on the ratio of concentrations of Cu^{I} to X-Cu^{II} and does not depend on the absolute concentration of the copper complexes. Thus, in principle, one

could reduce the amount of copper to ppb but a sufficient amount of deactivating species (i.e., X-Cu^{II}) is always needed for well-controlled polymerization since the dispersity is inversely proportional to the deactivator concentration. In ARGET, activating Cu^{I} complexes are generated in situ from oxidatively stable Cu^{II} species by the action of reducing agents such as tin(II) 2-ethylhexanoate,[51,52] ascorbic acid,[53] glucose,[54] or even an excess of the ligand.[55]

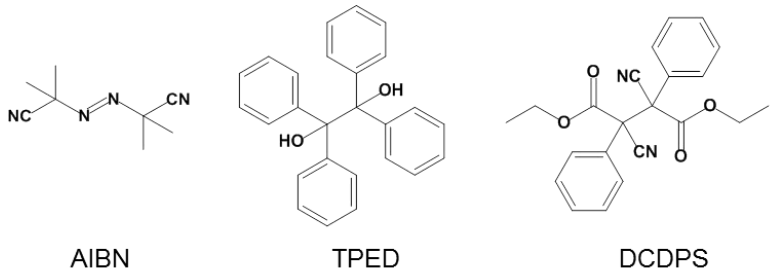

Figure 5: Chemical structures of radical initiators azo-bis-isobutyronitrile (AIBN), 1,1,2,2-tetraphenylethane-1,2-diol (TPED), diethyl 2,3-dicyano-2,3-diphenylsuccinate (DCDPS).

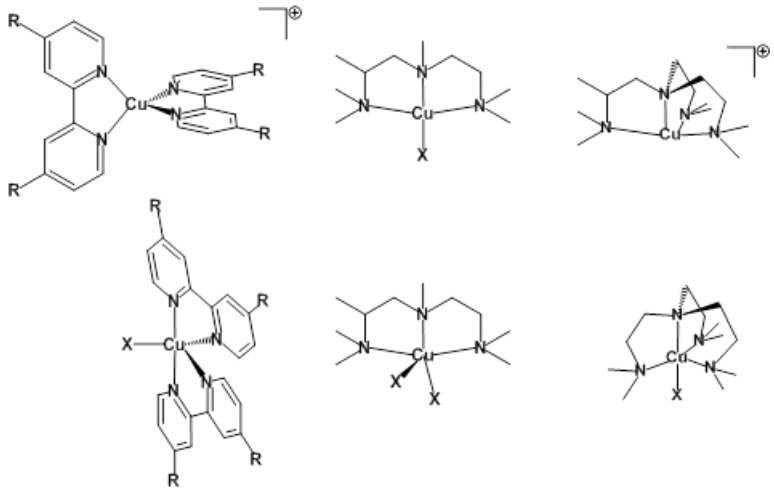

Figure 6: Copper complexes used in ATRP, X = Cl, Br.

In the early stages of ATRP discovery, it was accepted that there were no formation of direct copper-carbon bond.[56] However, Poli and coworkers have shown in 2001 that molybdenum complexes (Figure 7) used as ATRP catalyst could also control the polymerization via the direct formation of molybdenum-carbon bond (what we would call today OMRP), as well as undergo catalyzed chain transfer (CCT).[57] Later, Gibson and coworkers revealed that also α–diimine iron complexes act via both ATRP and CCT[58,59] and/or ATRP and OMRP.[60] More recently, Shaver and coworkers have reported a similar ATRP/OMRP interplay for the polymerization of either St or MMA with an iron aminebis(phenolate) catalyst.[61]

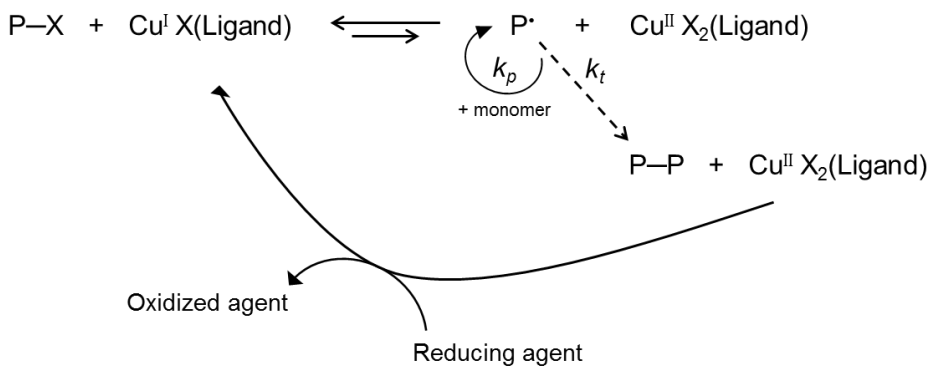

Scheme 7: General scheme for ARGET ATRP.

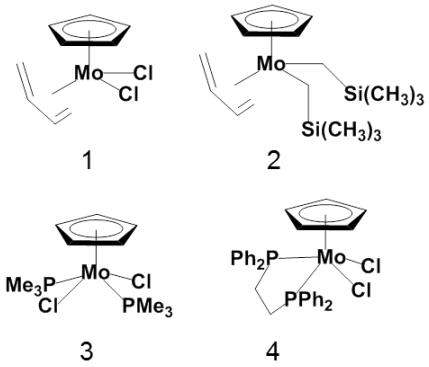

Figure 7: Molybdenum complexes able to form Mo-C bonds (from reference 57).

Organometallic-mediated radical polymerization (OMRP)[62,63] has been introduced by Wayland and coworkers in 1994 when they reported the first controlled radical polymerization of acrylates using (tetramesitylporphyrinato)cobalt(III) organo complex which act as the initiator and the CA (Figure 8).[64] They observed a linear increase of the polymer molecular weight with the monomer conversion along with a low dispersity (Đ = 1.1 - 1.3). Poly(methyl acrylate)-*block*-poly(butyl acrylate) were successfully synthesized (M_n = 131 400, Đ = 1.29) and the polymerization could be stopped and restarted by cycling the reaction temperature between 5°C and 60°C. The level of control was negatively affected by the inherent bimolecular radical termination and by β-H transfer reactions to monomer, polymer, solvent and the reduced cobalt complex. Cobalt-mediated radical polymerization (Co-MRP) is by far the most studied process but OMRP with vanadium,[65] chromium,[66] and osmium[67] have also been reported. It must be mentioned that catalytic chain transfer (CCT) polymerization in the presence of cobalt complexes has been known since the pioneering studies of Smirnov and Marchenko and quickly implemented at the industrial level.[68] Formation of cobalt(III)-alkyl adducts have been first proposed as a side reaction in CCT with π-conjugated macrocylic cobalt complexes (see more on cobalt CCT below).[69] The use of alkylcobaloximes (Figure 9) has also been reported[70] but as for porphyrin ligands, the polymerizations were restricted to acrylates monomers.

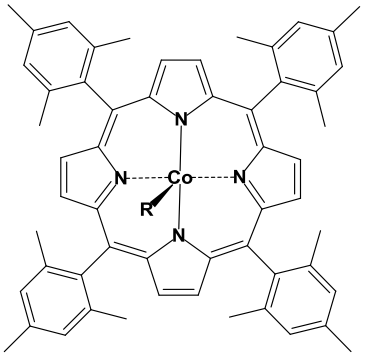

Figure 8: tetramesitylporphyrinato)cobalt(III), R = $CH(CH_3)$-CO_2CH_3.

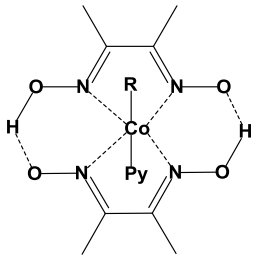

Figure 9: alkylcobaloxime (R = $CH(CH_3)_2$, Py = Pyridine).

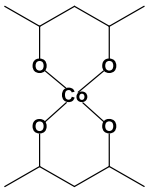

Figure 11: Cobalt(II)acetylacetonate $[Co(acac)_2]$.

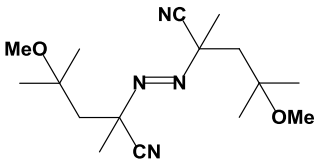

Figure 10: 2,2'-Azobis(4-methoxy-2.4-dimethyl valeronitrile) [V-70].[a]

A breakthrough progress in Co-MRP was the discovery of cobalt(II)acetylacetonate ($[Co(acac)_2]$, Figure 11) as a CA.[71] Jérôme and coworkers successfully controlled the radical polymerization of vinyl acetate using the commercially available $[Co(acac)_2]$ and V-70 (Figure 10) as initiator at 30°C. Poly(vinyl acetate) (PVAc) with a M_n as high as 99 000 g/mol was synthesized with low dispersity (Đ = 1.33). An induction period of 12 hours was observed corresponding to the time needed to convert Co^{II} into Co^{III}-R. The medium color changed from purple to dark brown-green consistent with the change in cobalt oxidation state. It has later been demonstrated that under these conditions the polymerization is in fact controlled by a DT mechanism rather than by a RDARP mechanism.[72] Indeed, in 2006, it was demonstrated that the mechanism of the polymerization process mediated by Co^{II}/Co^{III}-R could be switched from RDARP to DT depending on the ratio of radicals to cobalt complex.[73] After the induction period required to transform Co^{II} into the active Co^{III}-alkyl, during which a slower RDARP process takes place, the continued influx of radicals from the azo-initiator triggers the faster organocobalt-mediated DT mechanism. Finally, when the influx of azo-initiator has ended the polymerization reaction reverts to the slower RDARP pathway. However, a genuine RDARP process takes place upon addition of coordinative ligands to the cobalt center.[72] A linear increase of the molar mass with monomer conversion as well as the

[a] Azo-initiator commercially available and the abbreviation in brackets [V-70] is its trade name. This compound is a mixture of diastereomeric isomers whose melting point are 58 and 107 °C and should be stored below -10 °C to prevent any decomposition. V-70 is stable in a refrigerator for a few months.

successful restart of the polymerization from a preformed Co^{III}-PVAc macroinitiator are two evidences in favor of a Co-MRP. It has to be noticed that increasing the polymerization temperature to 60°C increases the irreversible chain termination to yield high dispersity PVAc (Đ = 2-3). Finally, ^{13}C NMR analysis of the PVAc demonstrated that [$Co(acac)_2$] had no influence on the stereoregularity of the polymer. The PVAc chains prepared by Co-MRP were easily end-capped by a bromine atom (by reaction of the $Co(acac)_2$-terminated PVAc with an α-bromoester functionnalized nitroxide) and used as macroinitiator for the ATRP of St, ethyl acrylate and MMA,[74] leading to the corresponding block copolymers (Table 1). Finally those copolymers can be hydrolyzed into the corresponding polymers containing poly(vinyl alcohol) blocks.

Table 1: Characteristics of the block copolymers prepared by chain extension of PVAc─Br macroinitiator via ATRP (PS = poly(styrene), PEA = poly(ethyl acrylate), PMMA = poly(methyl methacrylate)).

	PVAc macroinitiator Mn (g/mol)	Copolymer	
		$Mn_{,SEC}$	Đ
PVAc-b-PS	6 700	18 500	1.15
PVAc-b-PEA	6 700	23 500	1.50
PVAc-b-PMMA	8 800	33 500	1.10

Recently, Mahanthappa and coworkers used again [Co(acac)2] to synthesized block copolymers of vinyl acetate and vinyl pivalate or vinyl benzoate (Figure 12).75 They obtained copolymers with a molecular weight from 2 500 to 27 000 g/mol with a relatively low dispersity ranging around 1.2 - 1.3.

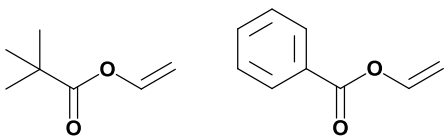

Figure 12: Chemical structure of vinyl pivalate and vinyl benzoate.

The limitation of Co-MRP toward standardization is the use of the azo-initiator V-70 which has to be stored at temperature below -20°C. Jérôme's group solved this problem by using a redox initiating system which consists of lauroyl peroxide or benzoyl peroxide as oxidant and ascorbic acid or citric acid as reducing agent.[76] Controlled PVAc with molecular weights as high as 79 000 g/mol and dispersity below 1.4 were obtained. From an industrial point of view, the drawbacks of OMRP are the need to use a stoichiometric amount of metal complex (one metal complex molecule per chain, contrary to ATRP where the metal complex is catalytic) and the necessary post-treatment to remove the metal from the polymer chains.

These limitations may be overcome by an immobilization of the metal trapping agent supported on a surface, with metal recycling after cleaving off the polymer chains.[77]

This literature survey will end with a few words on the interplay between Co-MRP and CCT. As early as in the 70's, substituted cobalt porphyrins or phtalocyanines (Figure 13) were found to drastically reduce the molecular weight of polymethacrylates with little to no reduction in overall polymerization rate.[68] The control of methacrylate polymerization was realized by enhanced chain transfer to monomer. The polymethacrylate chains were characterized as having one saturated and one unsaturated chain end per macromolecule. Cobalt complexes are prone to CCT reactions which involved the abstraction of a hydrogen atom in the alpha position of the carbon radical center (Scheme 8). The process of hydrogen abstraction by LCo^{II} from a propagating radical is usually the rate-determining step in CCT. It occurs at diffusion-controlled or close to diffusion-controlled rates indicating that the activation energy for the process must be extremely low. The mechanism involved for the hydrogen abstraction is proposed to be (in major cases) a direct abstraction via a three-centered intermediate. Then the very reactive cobalt hydride species transfer the hydrogen atom to a monomer.

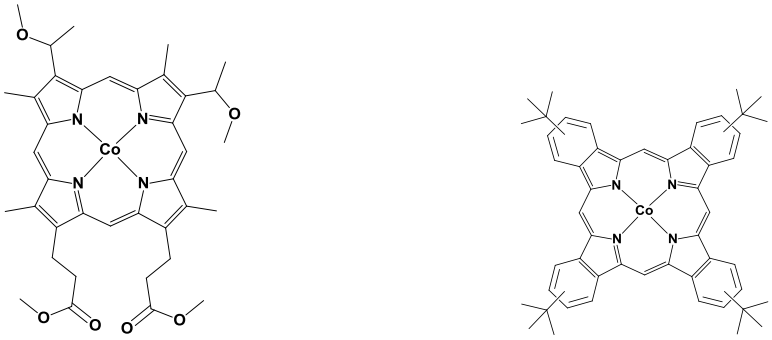

Figure 13: First cobalt complexes discovered as active CCT catalysts.

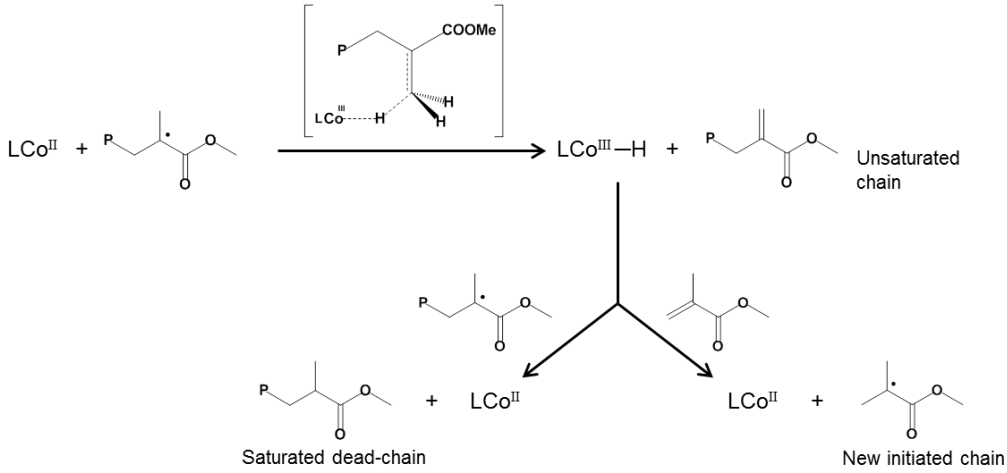

Scheme 8: Catalytic Chain Transfer (CCT) mechanism applied to methyl methacrylate.

The best known CCT catalyst is a cobaloxime (Figure 14) where the equatorial bis(oxime)rings are almost perfectly planar. In fact, the hydrogen atom bridges between the two parts of the ligand are sufficient to confer structural rigidity and chemical stability. The axial ligands play a crucial role as they tune the catalyst activities over a range of 3 orders of magnitude. Two types are recognized: type A, monoanionic ligands that bring Co to the oxidation state +3 (halides, alkyls, hydride); and type E, electron-donating neutral ligands (Lewis bases) like water. Empirically it was observed that a core of four nitrogen atoms in the coordination center incorporated into an extended system of conjugated π-bonds is needed to ensure the CCT activity. If two nitrogen atoms are replaced by oxygen or sulfur atoms, the ability of the cobalt complex to abstract hydrogen from free radicals is decreased.[69] Moreover, it seems that the chain transfer constant increases with the ligand field strength of the cobaloxime which depends more on the A type axial ligand than on the E type or on the equatorial ligand. The same observation is valid for cobalt porphyrins altough the effect is less pronounced. For cobalt porphyrins, the A ligands giving the highest activities are halides, especially chloride. In addition, when electron-withdrawing groups are added to the ligand, Cc increases with some complexes whereas it is lowered with others. Therefore, a certain extent of electron density may be needed on the cobalt center for good activity as a CCT catalyst. In addition, it was suggested that a low-spin configuration for the cobalt(II) complexes is a necessary (but not sufficient) condition for CCT activity. Finally, the higher the reduction potential for LCo^{III} to LCo^{II}, the greater the catalytic activity.

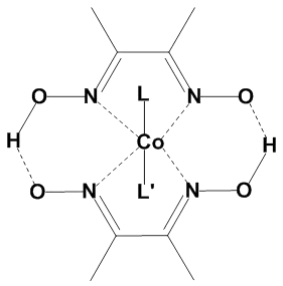

Figure 14: Chemical structure of a cobaloxime active as a CCT catalyst (L, L' = type A: halides, alkyls, hydride or type E: pyridine, water).

Early experiments with porphyrin complexes of Fe, Ni, V, Sn, Cu, Zn, Mg, Pd, Pt, and Mn demonstrated no activity. Only few chromium complexes or heterobimetallic chromium-molybdenum complexes showed CCT activities: $[CpCr(CO)_3]_2$; $[Cp(CO)_3Cr\text{-}Mo(CO)_3Cp]$; $[CpCr(CO)_2(PPh_3)]_2$;[78,79] $[(\eta^5\text{-}C_5Ph_5)Cr(CO)_3]_2$[80,81,82] ($Cp = \eta^5\text{-}C_5H_5$).

Finally, the role of the metal coordination sphere in regulating the proportion of the complex toward catalytic chain transfer and reversible deactivation is not fully understood. We can

only say that this is actually a kinetic issue, determined by the relative height of two reaction barriers: the radical trapping by the complex to form an organometallic-alkyl species and the hydrogen atom transfer to form a metal hydride complex with an unsaturated chain and a saturated dead chain.

b) Degenerative transfer mechanism

Reversible addition-fragmentation chain transfer (RAFT) was discovered by Moad, Rizzardo and Thang at the Commonwealth Scientific and Industrial Research Organisation (CSIRO) in 1998.[83,84,85] The accepted RAFT mechanism is described in Scheme 9. It comprises an initiation step where radicals are formed and give, after a few monomer additions, polymer chains $P_m^{\bullet}$. Those polymer chains $P_m^{\bullet}$ add to the RAFT agent 1 to form an intermediate radical species 2. The leaving group $R^{\bullet}$ is expulsed to give compound 3. Then $R^{\bullet}$ initiates new chains and gives $P_n^{\bullet}$. After all the initial RAFT agent 1 has been consumed, the degenerative transfer is the main reaction allowing propagation of the chains. Finally, the radicals undergo termination by bimolecular coupling or disproportionation.

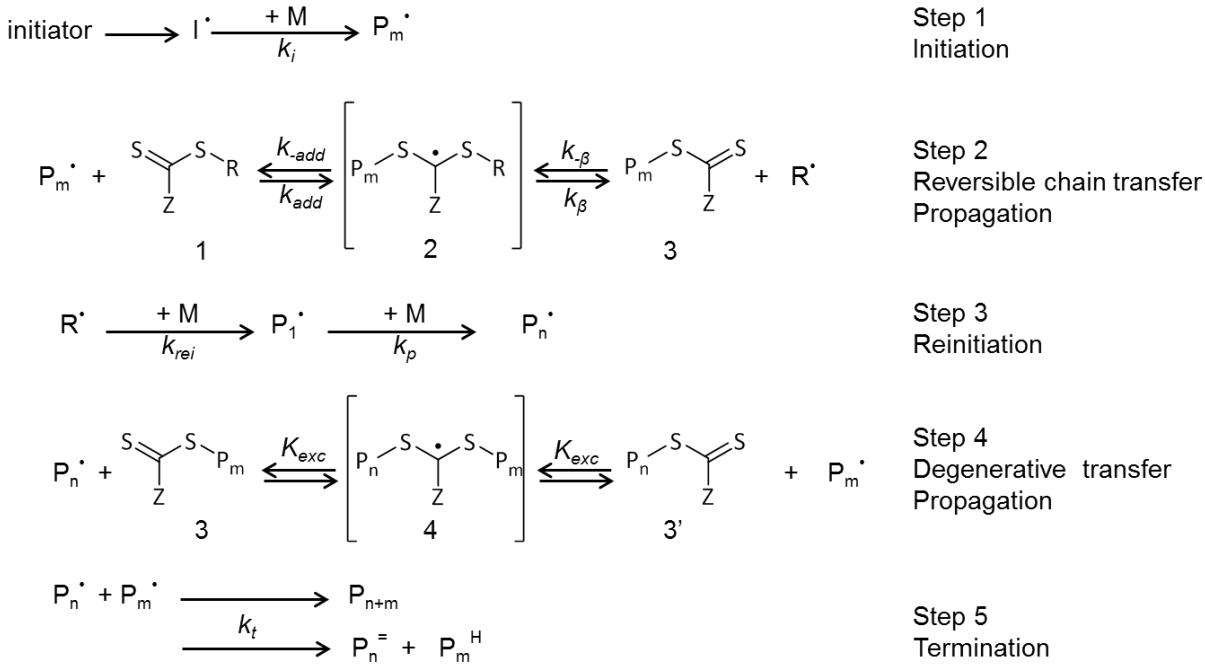

Scheme 9: Accepted RAFT mechanism.

The choice of RAFT agent is of crucial importance for tuning the kinetics of the different steps resulting in precise control of a particular monomer polymerization (Scheme 10). When Z is an alkoxy group (-OR') the RAFT agent R'OC(S)SR is a xanthate and the polymerization has also been called "macromolecular design via the interchange of xanthates" (MADIX).[86]

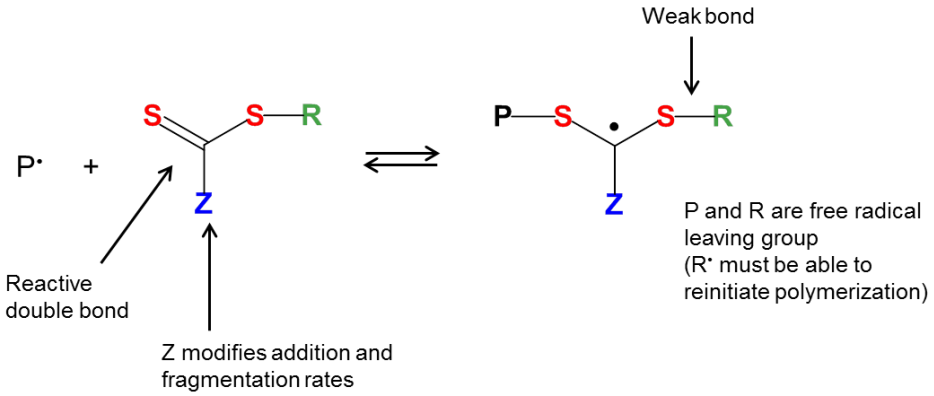

Scheme 10: Structural features of the RAFT agent and the pre-equilibrium intermediate.

The nature of the Z group modifies the addition and fragmentation rates in step 2.[87] Experimental studies show that the transfer coefficient ($C_{tr} = \frac{kexc}{kp}$) of RAFT agents is slow when Z possesses an electrophilic group with a lone pair directly attached to the C=S bond (-O, -N=). This is explained by different mesomeric forms that decrease the double bond reactivity. However, the reactivity can be completely changed if electron-withdrawing groups are attached to the oxygen or nitrogen atom. The best way to predict RAFT agent effectiveness seems to be molecular orbital calculations that estimate the LUMO energies or the heats of reaction. The greater the C=S double bond character or the lower the LUMO energy, the more efficient the radical addition to the C=S double bond. Finally, no influence of the Z group on the overall polymerization rate is observed. On the other hand, the R group is also decisive because it must be a good free radical leaving group and must be able to reinitiate the polymerization.[88] Its influence is crucial on methyl methacrylate polymerization, whereas styrene and butyl acrylate polymerizations are more tolerant and compatible with a wider range of R groups. Steric factors, radical stability and polar factors all appear important in determining the leaving group ability of R (more stable, more electrophilic, bulkier radicals are better leaving groups).

RAFT polymerization is the most versatile RDRP technique in terms of polymerizable monomers. The non exhaustive Table 2 shows the monomer scope of a few RAFT agents. Finally, most monomers can be polymerized by one or two RAFT agents. For example the tertiary cyanoalkyl trithiocarbonate is able to control either (meth)acrylate, (meth)acrylamide, and styrenic monomers. Due to the development of the RAFT technique, most of the RAFT agents are now commercially available. The controlled radical homopolymerization of simple olefins, however, is not possible by a RAFT process as well as by any other method. However, the synthesis of RAFT agents is usually done in good yields with straightforward methods.[89]

Concerning the reaction conditions, the reported temperature of RAFT polymerizations ranges from room temperature to 140°C. The RAFT process is compatible with different media such as alcohols, water,[90] ionic liquids[91] and supercritical carbon dioxide.[92] Polymerizations in emulsion[93,94] and miniemulsion[95,96] are also feasible. RAFT polymerizations have been reported at very high pressure (> 5 000 bar) which decreases the bimolecular termination and allows the synthesis of very high molecular weight polymers.[97,98]

Table 2: Monomer scope of a few RAFT agents.

Z	R	Homopolymers	Copolymers
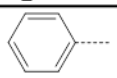		AA	-
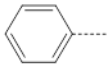		St, AA, MA, MMA, XMA, VBz, *MMA, BMA, EHMA*	NIPAM-*co*-XMA, St-*co*-MAH, *EHMA-b-St, EHMA-b-MMA-MA*
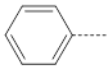		AN	-
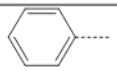	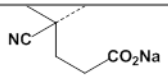	SSO_3Na, AMPS	AMPS-*co*-AMBS, AMPS-*b*-AMBS
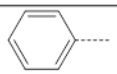		SAc, BA	
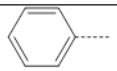	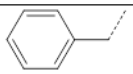	St, MA, BA, DMA, NIPAM, *S*, *MMA*	St-*b*-DMA, St-*b*-SMe, *MMA-b*-St, St-*co*-MAH
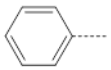	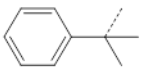	St, MA, BA, MMA, BzMA, DMAEMA, XMA, AM, DMA, NIPAM, 2VP, 4VP, CPM, *MMA, BMA*	St-*co*-AN, St-*co*-MMA, MMA-*co*-HEMA, MMA-*co*-BA, HEMA-iBMA-MMA-St, MMA-b-St, BzMA-b-DMAEMA, BzMA-b-MAA, 2VP-b-4VP, *MMA*-b-St, *BMA*-b-St
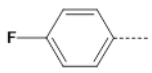	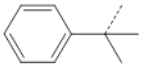	MA	-
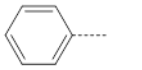	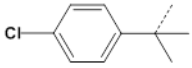	MMA	-
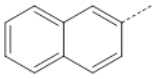		St, MMA, GMA	MMA-b-St

Abbreviations: AA, acrylic acid; AM, acrylamide; AMBS, sodium 3-acrylamido-3-methylbutanoate; AMPS, sodium 2-acrylamido-2-methylpropane-1-sulfonate; AN, acrylonitrile; BA, butyl acrylate; BzMA, benzyl methacrylate; CPM, 2,4,4,6-tetrakis(ethoxycarbonyl)hepta-1,6-diene; DMA, *N,N*-dimethylacrylamide; DMAEMA, N,N-(dimethylamino)ethyl methacrylate; EHMA, 2-ethylhexyl methacrylate; GMA, glycidyl methacrylate; iBMA, *iso*butyl methacrylate; MA, methylacrylate; MAH, maleic anhydride; MMA, methyl methacrylate; NIPAM, *N*-isopropyl acrylamide; St, styrene; Sac, 4-acetoxystyrene; SMe, 4-methylsturene; SSO_3Na, sodium styrene-4-sulfonate; VBz, vinyl benzoate; XMA, functional methacrylate;[99] 2VP, 2-vinyl pyridine; 4VP, 4-vinyl pyridine. Emulsion or miniemulsion experiments in italics.

Polymers synthesized by the RAFT technique are terminated by a thiocarbonylthio function which absorbs visible light. Thus the polymers are colored and might need, depending on the

final application, a post-treatment to remove or transform the end groups. This can be done either by a treatment with primary or secondary amines which gives thiol functionalized end groups or by a treatment with tributyltin hydride which gives saturated chains or by a thermal treatment which gives unsaturated chain ends.[89,100] Moreover, sulfur compounds are not desired for commercial applications as they can release an unpleasant smell.

Although RAFT is the more explored and the more used RDRP technique that relies on a degenerative transfer mechanism, other techniques also exist such as Iodine Transfer Polymerization (ITP) and Organoheteroatom (tellurium, antimony, bismuth)-mediated polymerization. ITP was the first RDRP discovered in the late 1970' by Tatemoto (Scheme 11).[101] The transfer reaction should ideally be neutral from a thermodynamic point of view (transfer of the iodine atom from the dormant polymer chain to the radical growing chain should exert no or little change in free energy). A way to approach the ideal case is to use alkyl iodide transfer agents that have a structure similar to the end of the propagating chain. For example, 1-phenylethyl iodide (1-PEI) will be employed for styrene polymerization. Another important consideration is the rate of the iodine atom exchange which has to be at least equal to or greater than the propagation rate constant. This is achieved when the transfer agent possesses groups able to stabilize the radical resulting from iodine abstraction. The stabilization can be ensured by polar or resonance effects.

Chlorine and bromine analogues of the transfer agents have been tested with no or poor control of the polymerization. It seems that the iodine atom is the only halogen able to form sufficiently strong carbon-halogen bonds in a hypervalent intermediate of the associative exchange so that the iodine transfer rate constant is high enough compared to the propagation rate constant. A drawback of alkyl iodides is that they are unstable upon prolonged storage, especially in the presence of light. Iodine transfer polymerization is one of the scarce methods that makes it possible to control the polymerization of fluoroalkenes such as tetrafluoroethylene or vinylidene fluoride (or 1,1-difluoroethylene).[102]

Barnes patented the use of iodoform to decrease the molar mass of polyvinyl chloride but the possible controlled nature of the polymerization was not mentioned.[103] Among the non-halogenated monomers, only few have been successfully polymerized in a controlled manner by ITP: mainly styrenics, (meth)acrylates and vinyl acetate. Poly(vinyl acetate) was obtained with low dispersity but the iodo end groups were unstable and decomposed into aldehyde.[104] The use of 1-PEI, iodoform or iodoacetonitrile to control the polymerization of styrene, methyl acrylate and butyl acrylate was first reported by Matyjaszewski's group.[105]

The dispersity was low for polystyrene but broader for acrylates monomers. The reason of the poor control with acrylates was attributed to a slower degenerative transfer. Furthermore, ITP of monomers involving tertiary propagating radicals (such as methacrylates) was not successful because it would require iodoalkyl compounds with better leaving groups, which are inherently even less stable. To overcome this limitation, Lacroix-Desmazes proposed a new process based on the direct reaction of radicals with molecular iodine, I_2. It is called, by analogy with ATRP, "reverse iodine transfer polymerization" (RITP). Several patents based on the RITP process have been recently published by Solvay[106] and Akzo[107]. RITP allows the controlled polymerization of methyl acrylate, butyl acrylate[108] and more interestingly methyl methacrylate.[109] Several investigations have shown that ITP can also occur under emulsion,[110] solution, or later mini-emulsion conditions.[111]

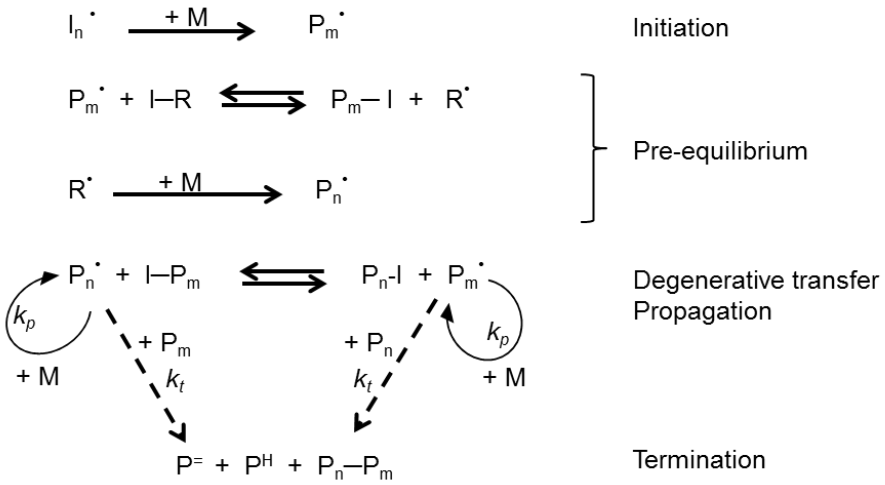

Scheme 11: Iodine Transfer Polymerization (ITP) mechanism.

In 1999, as Yamago and coworkers discovered the facile homolysis of tellurium-carbon bonds,[112] they decided, by analogy with NMP to look at organotellurium compounds as monomolecular initiators and CAs for styrene polymerization.[113] This polymerization process is called Organotellurium-mediated Radical Polymerization (TERP). Like in NMP, the CA efficiency is strongly related to BDE of the propagating chain carbon-CA bond.[6,114] Therefore, these authors calculated the carbon-tellurium BDEs of the six investigated tellurium compounds (Figure 15) by density funcional theory (DFT) and tested their controlling ability in styrene bulk polymerization at 105°C (Table 3).

The best results were obtained with initiator 1 which gives polystyrene with low dispersity (Đ = 1.17) at high conversion (conv.= 96%, M_n = 9 200). More interestingly, para-methoxystyrene, which is poorly controlled by ATRP, was successfully polymerized with low dispersity using initiator 1 (Đ = 1.17, conv. = 94%, M_n = 10 900). Six months later, the same

group reported that one and the same organotellurium compound (initiator 4 in Figure 15) could effectively control the polymerization of styrene along with acrylates, methacrylates, acrylamides and acrylonitrile.[115] The synthesis of di- and triblock copolymers was illustrated with acrylates or methyacrylates and styrene. The obtained copolymers had low dispersities ranging from 1.1 to 1.3. Note that these initial polymerizations were conducted under RDARP conditions.

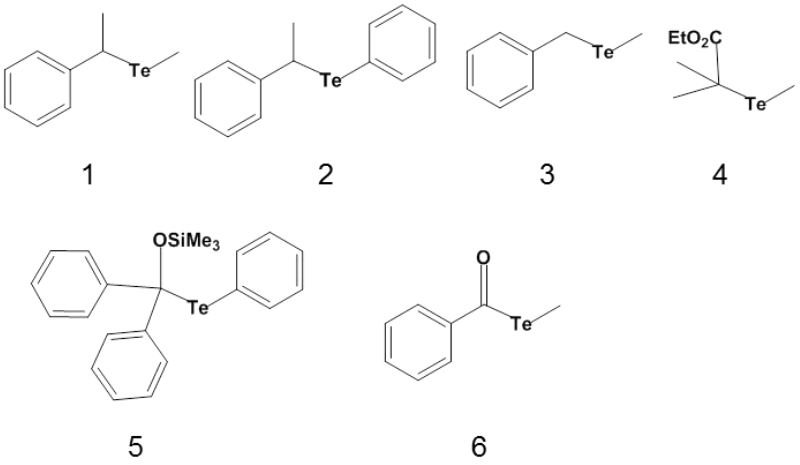

Figure 15: Tellurium initiators studied by Yamago and coworkers.

Table 3: Study on styrene bulk polymerization using organotellurium initiators (reference 114).

Tellurium initiator	conversion (%)	Mn (g/mol)	Đ	BDE (kJ/mol)
1	96	9 200	1.17	123
2	91	15 900	1.45	112
3	89	9 000	1.46	142
4	79	9 000	1.15	114
5	76	50 700	1.80	25
6	83	25 400	1.58	182

The effectiveness of dimethyl ditelluride (MeTe-TeMe) strongly suggested that the control was ensured by a reversible thermal dissociation of the tellurium end-capped chains (RDARP). However, further kinetic investigations showed that the main mechanism of the styrene, methyl acrylate and butyl acrylate TERP was in fact a DT with some interplay of RDARP mechanism (Scheme 12).[116]

An important advantage of TERP is the ease of end-group polymer transformations.[115] Thus, trapping the radical propagating chains with ethyl tributylstannylmethacrylate yielded an enoate functionalized polymer with 61 % yield (Scheme 13a) or the tellurium-capped chains can be transformed via a tellurium-lithium transmetallation with butyllithium followed by carboxylation with carbon dioxide and hydrochloric acid to give a carboxylic acid end function (Scheme 13b).

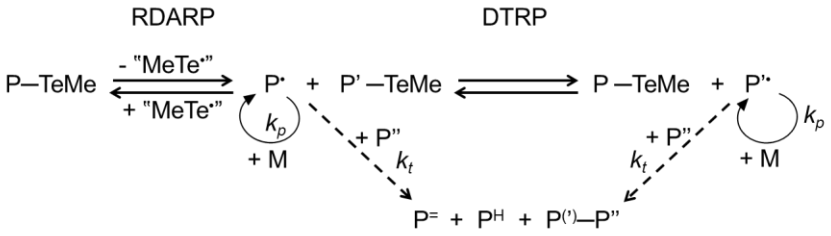

Scheme 12: Proposed mechanism in TERP.

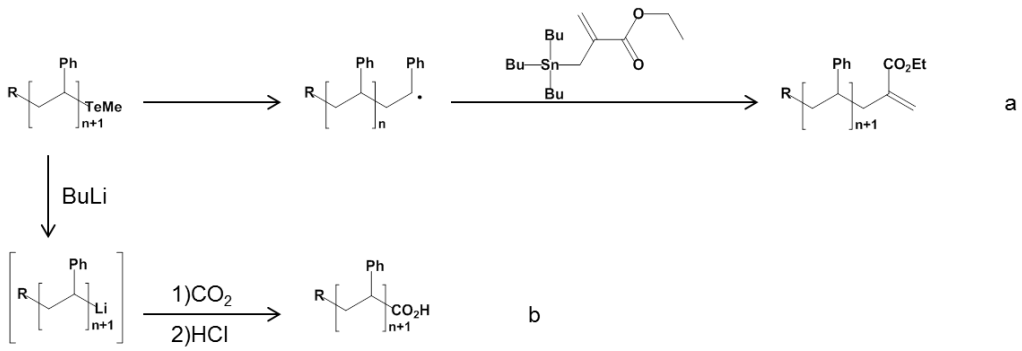

Scheme 13: End-group transformations of polystyrene formed by TERP.

Another family of organoheteroatom compounds able to mediate radical polymerization are the organostibines leading to the so-called organostibine-mediated radical polymerization (SBRP), which was discovered by Yamago and coworkers in 2004. Trialkylstibines (SbR_3) were first reported as sources of carbon centered radicals which act as radical polymerization controlling agents.[117] The first antimony compound studied (see Figure 16) allows polymerization of both conjugated and unconjugated monomers under mild conditions. High conversions were reached and well-defined polymers with narrow molecular weight distributions were obtained (see Table 4).

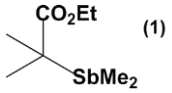

Figure 16: Organostibine used as a controlling agent for the RDRP of styrene in reference 117.

Table 4: SBRP using (1) at 60°C. Data taken from reference 117.

Entry	Monomer[a]	T (°C) / t (h)	yield (%)	Mn (g/mol)[b]	Đ[b]
1	St[c]	100 / 48	82	7 700	1.14
2	St[d]	60 / 36	65	49 400	1.23
3	BA[e]	60 / 1	96	12 400	1.13
4	MMA[e]	60 / 4	100	11 000	1.24
5	NIPAM[f]	60 /12	99	26 700	1.09
6	AN[g]	60 /18	81	15 000	1.05
7	NVP[h]	60 /1	92	42 100	1.22
8	VAc[i]	60 /5	92	2 800	1.26

[a]St, styrene; BA, *N*-butyl acrylate; MMA, methyl methacrylate; NIPAM, *N*-isopropyl acrylamide; AN, acrylonitrile; NVP, vinyl pyrrolidone; VAc, vinyl acetate.[b]Number-average molecular weight (M_n) and dispersity (Đ) were obtained by SEC calibrated by PS standards for entry 1-2 and PMMA standards for others. [c]St/(1) = 100:1. [d]St/(1)/AIBN = 100:1:0.5. [e]BA or MMA/(1)/AIBN= 100:1:0.3. [f]NIPAM/(1)/AIBN = 200:1:0.3 in DMF. [g]AN/(1)/AIBN = 100:1:0.1in DMF. [h]NVP/(1)/AIBN = 500:1:0.5. [i]VAc/(1)/AIBN = 25:1:0.1.

The molecular weight of PNVP increased linearly with the amount of NVP used. The existence of a dimethyl stibanyl polymer-end group was assessed by NMR and MS.[118] The synthesis of block copolymers was also successful. When PS (M_n = 4 400, Đ = 1.05) and PMMA (M_n = 4 700, Đ = 1.27) macroinitiators were treated with NVP in the presence of AIBN, the desired PS-*b*-PNVP and PMMA-*b*-PNVP were obtained in good yields (respectively M_n = 27 400, Đ = 1.05 and M_n = 20 500, Đ = 1.31). Kinetic studies on styrene polymerization have revealed that SBRP proceeds exclusively by the degenerative transfer mechanism.[119] The rate of degenerative transfer of the dimethylstibanyl group in SBRP is approximately two times faster than that of the methyl-tellanyl group in TERP.

Group transfer and atom transfer reactions are faster with heavier heteroatoms within a group of elements in the periodic table.[116] Therefore, Yamago and coworkers explored the reactivity of organobismuthines as RDRP mediator. Indeed, the level of control in organobismuthine-mediated radical polymerization (BIRP) is considerably higher than that in organostibine-, tellurium-, and iodine-mediated radical polymerizations (SBRP, TERP, and ITP, respectively).[120] The bulk polymerization of St, MMA, *n*BA, NIPAM and NVP was realized using either the organobismuthine Bi-1 or Bi-2 represented in Figure 17. The characteristics of the polymers obtained by BIRP are summarized in Table 5. Polymers with predictable chain length (depending on the ratio Monomer/Bi-x) and low dispersity values were obtained, although the M_n deviated slightly from the theoretical one and the dispersity value increased as the targeted M_n value increased.

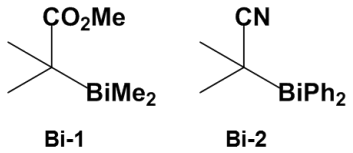

Figure 17: Organobismuthine used as controlling agent in reference 120.

Table 5: BIRP using organobismuthine Bi-1 and Bi-2. Data taken from reference 120.

Entry	Monomer (equiv.)	CTA	T (°C) / t (h)	Conv. (%)[a]	Mn (g/mol)[b]	Đ[b]
1	St (100)	Bi-1	100 / 4	99	10 500	1.07
2	St (1 000)	Bi-1	100 / 24	98	86 900	1.21
3	St (100)	Bi-2	100 /1	85	10 900	1.08
4	MMA (1 000)	Bi-1	100 / 5	100	107 200	1.14
5	BA[c] (1 000)	Bi-1	60 / 8	95	52 000	1.11
6	NIPAM[c] (1 000)	Bi-1	60 / 16	93	98 700	1.15
7	NVP[c] (500)	Bi-1	60 / 2	100	60 000	1.12

[a]Monomer conversion was determined by ^{1}H NMR. [b]Number-average molecular weight (M_n) and dispersity (Đ) were obtained by SEC calibrated by PS standards for entry 1-3 and PMMA standards for others. [c]0.1 equivalent of AIBN added.

Finally, organoheteroatom-mediated radical polymerizations (i.e. TERP, SBRP, BIRP) are highly versatile for polymerizing different families of monomers in a controlled manner by using the same chain-transfer agent. TERP, SBRP, and BIRP were found to proceed through both degenerative transfer and reversible termination.[119,121] The drawbacks of those methods are the oxygen sensitivity of the chain transfer agents which have to be stored under nitrogen and the basic conditions needed for their synthesis which are not compatible with many polar functional groups.

2) Controlled (radical) polymerizations of less reactive monomers (LRM)

Monomers are called less reactive when their corresponding radicals are not stabilized by electronic delocalization and are therefore very reactive and hardly controllable. Vinyl acetate, vinyl amide and ethylene belong to this group. This section will begin with a bibliographic introduction on the controlled radical polymerizations of vinyl acetate, followed by vinyl amides to end with ethylene controlled polymerizations.

a) Poly(vinyl acetate) state of art

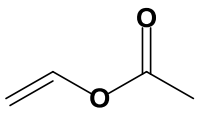

Figure 18: Vinyl acetate monomer (VAc).

Vinyl acetate (VAc, Figure 18) can only be polymerized by a radical pathway. Though control of the radical polymerization of this monomer has recently made great progress, there are still interesting questions to be addressed.[122,123] The vinyl acetate radical is very reactive due to the lack of stabilizing substituent. It is also characterized by low steric bulk thus leading to fast propagation (k_p ~ 3 000 $L \cdot mol^{-1} \cdot s^{-1}$ at 20°C).[124] Poly(vinyl acetate) (PVAc) is of interest due to the facile hydrolysis to poly(vinyl alcohol) (PVOH) which is the largest volume of water-soluble polymer produced commercially.[125] PVOH is a non-toxic, non-carcinogenic and biocompatible material. Cross-linking PVOH gives access to gels that have been investigated for their suitability as drug delivery systems.[126,127] Consequently, control of vinyl acetate polymerization is of considerable importance. We discuss herein the specificity of each main radical polymerization mechanism toward vinyl acetate.

The first example of controlled radical polymerization of vinyl acetate was reported in 1994 by Matyjaszewski and coworkers using Al(*i*Bu)$_3$/bPy/TEMPO.[128] The involvement of a persistent hexacoordinated aluminum radical was proposed to rationalize the level of control. However, this system was found complicated and the results were difficult to reproduce. The "living" radical character of the polymerization was contradicted by further NMR and EPR

investigations.[129] The same group reported later the polymerization of VAc using CCl_4 as the initiator in the presence of $[Fe(OAc)_2]$/PMDETA. A detailed kinetic study revealed that the polymerization does not follow the expected ATRP behavior but is rather a redox-initiated radical telomerization apparently based on the irreversible activation of a C-Cl bond. The polymer molecular weight is determined by the $[VAc]_0/[CCl_4]_0$ molar ratio and is independent on monomer conversion. PVAc with a wide range of predictable molecular weights were synthesized in high yields (ca. 70%) and the resulting PVAc (M_n = 3 600, Đ = 1.81) was successfully used as a macroinitiator for the synthesis of block copolymers with *n*BA (M_n = 11 000, Đ = 1.41) and St (M_n = 24 300, Đ = 1.42).[130] In 2002, PVAc with low dispersity (Đ = 1.4) was obtained using the dinuclear iron complex $[Fe(Cp)(CO)_2]_2$ as a catalyst in the presence of an iodo initiator $[(CH_3)_2C(CO_2Et)I]$ and an additive like $[Al(Oi\text{-}Pr)_3]$ or $[Ti(OiPr)_4]$ in anisole at 60°C.[131] Without the additive, the polymerization was very slow and no polymerization took place in the absence of either the iron complex or the iodo alkyl initiator. The authors proposed a mechanism via the metal-catalyzed activation (homolysis) of the initiator C-I bond (Scheme 14). This was the first example of a radical polymerization of VAc in which a metal-catalyzed system leads to a linear increase of M_n with monomer conversion. Although the contribution of the iodine-transfer process cannot be fully excluded, this polymerization is undoubtedly triggered by the metal catalyst. The conversion reached 70% with molar masses up to 1 500 g/mol and a broad dispersity of 1.4-2. Copper-mediated ATRP of VAc using [CuBr(*t*Py)] or [CuCl(*t*Py)] (*t*Py = 2,2';6',2''-terpyridine) as a catalyst and ethyl-2-bromoisobutyrate was reported in 2009 by Tang and coworkers.[132] The polymerization produces PVAc with controlled molecular weights until high conversions. The dispersity was relatively narrow at low conversion (Đ = 1.4 at 16% conversion) and slightly broadened at high conversion (Đ = 1.7, 80%).

To date, the ATRP of VAc is still not very successful except for the terpyridine Copper(I)halide system described above. Carbon-halogen bonds (C-Br, C-Cl) of the dormant chains are indeed too strong to be homolytically activated even by the highly active ATRP catalyst [CuBr(Me_6TREN)] (Me_6TREN = tris[2-(dimethylamino)ethyl]amine). Other factors, like side reactions, may explain the difficulties encountered in ATRP of vinyl acetate. Decomposition of the halogen-capped chains (Figure 19)[133] and reduction of the radical growing chain via an outer-sphere electron transfer process (Figure 20) have been suggested.[134]

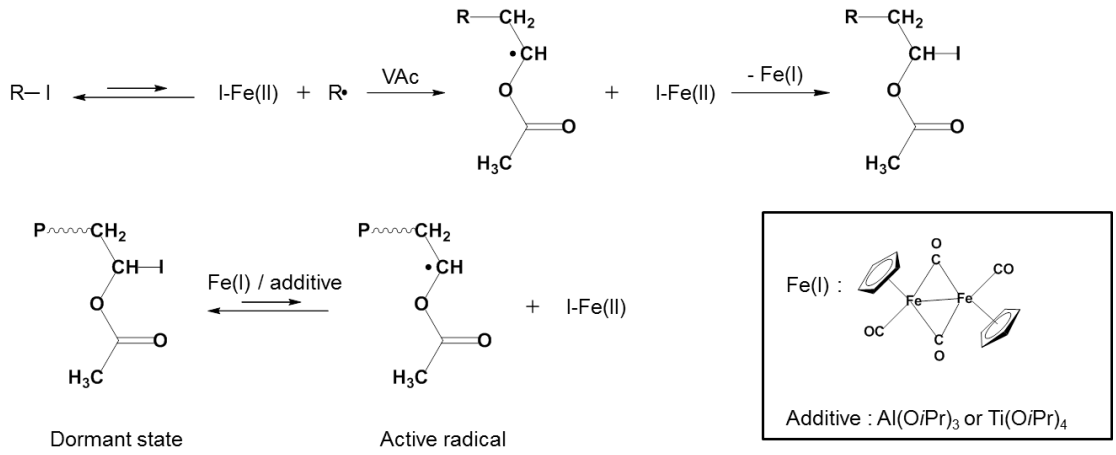

Scheme 14: Proposed mechanism of iron catalyzed vinyl acetate polymerization

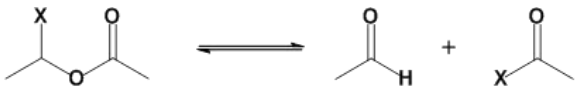

Figure 19: Decomposition of the halogen-capped chains in ATRP of VAc.

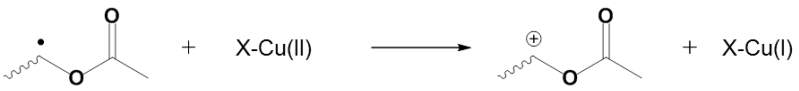

Figure 20: Reduction of the radical growing chains in ATRP of VAc.

Although NMP is a largely employed RDRP technique, there is no report of nitroxides able to control vinyl acetate polymerization to the best of our knowledge. Though, RAFT is one of the most studied processes for polymerization of vinyl acetate. Charmot and coworkers reported in 2000 the first controlled polymerization of VAc using the RAFT agent I in Figure 21. PVAc with relatively low dispersity was obtained (M_n = 3 200, Đ = 1.30).[135] One year later, the group of Moad succeeded in obtaining PVAc in high yield with even lower dispersity using a thiocarbonylthio compound (II in Figure 21) (Conv. = 66%, M_n = 7 030, Đ = 1.18).[136] After having optimized all the experimental parameters (temperature, concentrations…), excellent control of the molecular weight distribution can be achieved using one of the four RAFT agent represented in Figure 21 (III-VI), leading to PVAc of molecular weights exceeding 50 000 g/mol.[137] Đ values as low as 1.24 were obtained using the dithiocarbamate VII in Figure 21.[138]

Stenzel and coworkers studied the influence of the Z activating group of the xanthate transfer agent ZC(S)SR (Figure 22) toward vinyl acetate polymerization.[137] It was concluded that the improved control of polymerization is correlated with the increasing of the electron density on the central carbon of the xanthate, and this was thought to correspond to the decreased stability of the RAFT-adduct radical. However, the xanthate with the least electron-withdrawing Z substituent (agent H in Figure 22) actually inhibited the polymerization of vinyl acetate for up to 2 days. Surprised by this result, Coote's group used ab initio molecular

orbital calculations to explore the effect of the alkoxy group OZ' (Z' = Me, Et, *i*Pr, *t*Bu).[139] It appears that the increase in donation to the electron-deficient center may be stabilizing (rather than destabilizing as previously supposed) the RAFT-adduct radical, thereby leading to the observed increase in fragmentation enthalpies from Me to *t*Bu. Instead, the rate retardation observed with RAFT agent H appears to be the result of the preferred fragmentation of the O-C bond in the *tert*-butoxy group (see Figure 23). This fragmentation pathway is not normally favored in RAFT polymerization. However, in this particular system, the combination of the vinyl acetate being a poor leaving group with the *tert*-butyl acetate being a good leaving group changes the balance in favor of this abnormal fragmentation.

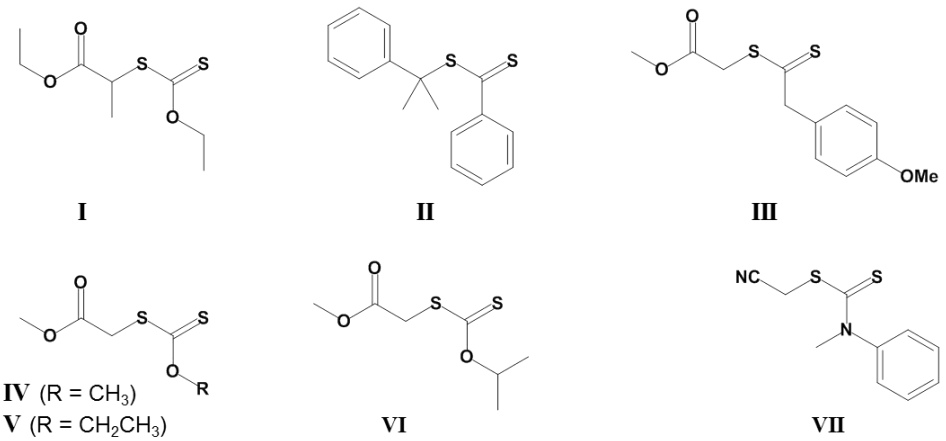

Figure 21: RAFT agents able to control vinyl acetate polymerization.

From an industrial point of view the controlled radical polymerizations conducted in suspension, emulsion and mini-emulsion are much more attractive than the bulk polymerizations because of a series of advantages such as better control of the heat transfer, absence of volatile organic solvents… The RAFT polymerization of VAc is possible in emulsion up to 40% conversion, after which the polymer gels[93] as well as in miniemulsion.[140] In general, the dispersity values were low at low conversions (< 1.2) and then increased. This was proposed to result from chain transfer to monomer and polymer.

RAFT also enabled the synthesis of three and four-arm PVAc stars which could be hydrolyzed into PVOH stars, as reported by Stenzel's group.[141,142] The methodology invokes the synthesis of a core with arms terminated by a thiocarbonylthio function. A "classic" RAFT process was then used to let the linear PVAc grow and give the desired stars with low dispersity (Scheme 15).

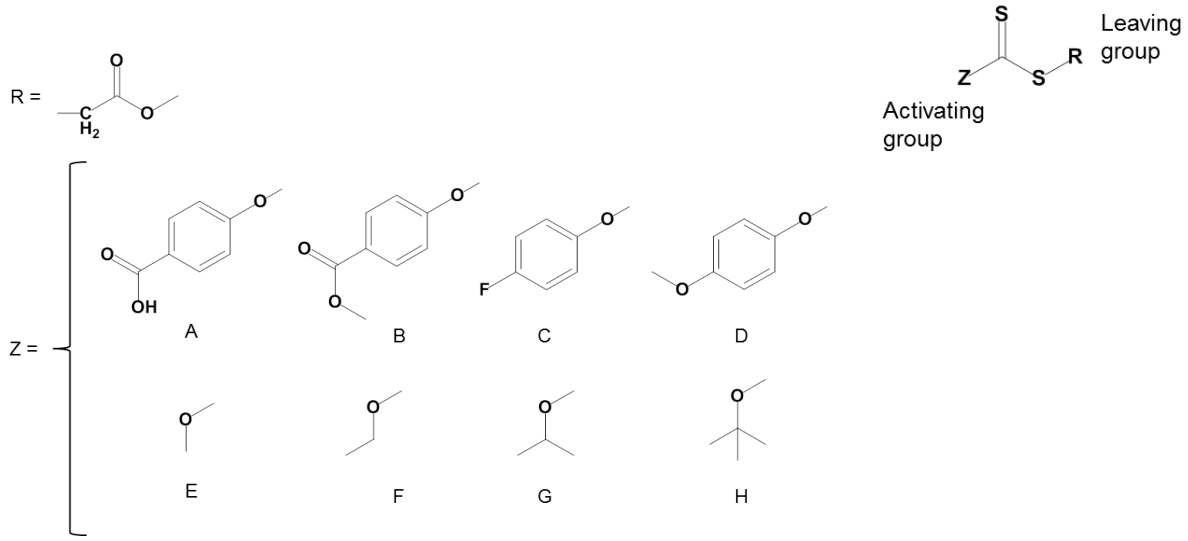

Figure 22: Xanthate agents considered in the reference 137.

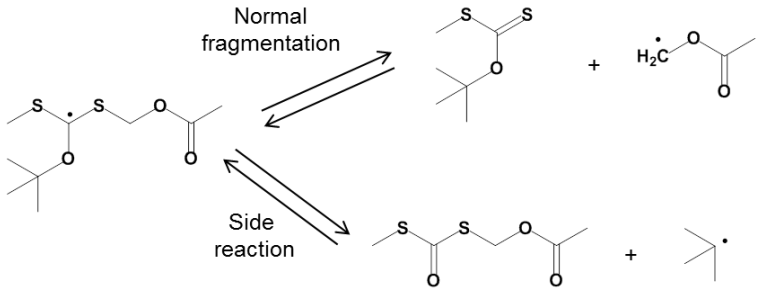

Figure 23: Normal fragmentation pathway and side reaction expected by ab initio calculations for VAc RAFT polymerization using *t*BuO as an activating group.

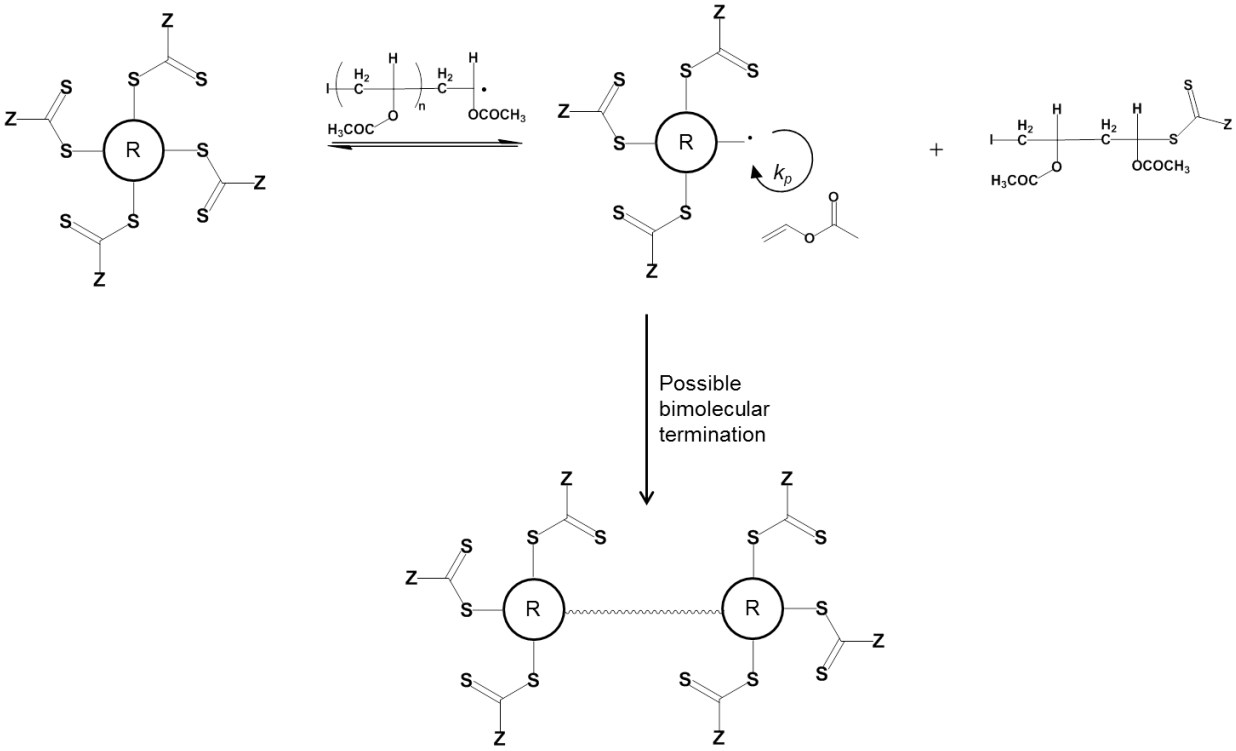

Scheme 15: Methodology for the synthesis of four-arm PVAc stars.

The TERP of VAc, using ethyl 2-methyltellanyl-2-methylpropionate (EMA-TeMe) and AIBN as initiator, provides polymers with a low dispersity at low degrees of polymerization (M_n = 3100, Đ = 1.28), but the controllability decreased at high DPs (M_n = 8 500, Đ = 1.5).[121] The broadening of the SEC curves was explained by the significant formation of the primary adduct (-CH_2-TeMe) following head-to-head additions and its too slow reactivation. Organostibine were also succesfully employed (conv. = 92%, M_n = 2 800, Đ = 1.26). The radical pathway was confirmed[143] but the same limitations as exposed for TERP occurred. The dispersity increased as the molecular weight of PVAc increased due to the occurrence of head-to-head addition.[118]

Ueda *et al*. attempted the synthesis of PVAc by using either iodoform[144] or iodoperfluorohexane.[145,146,147] Finally, PVAc with a low dispersity were obtained using iodoacetate as a transfer agent (M_n = 20 000, Đ < 1.5).[104] Analysis of the polymer chain ends showed that the iodo end groups were not stable and decomposed during the reaction to yield aldehyde-terminated polymer.[133,148,149] Moreover, the head-to-head addition form primary alkyl iodide which are more stable than their secondary counterparts, thus retard the polymerization. Kamigaito and coworkers have nicely succeeded the simultaneous control of the molecular weight and tacticity of PVAc for the first time by conducting the iodine transfer radical polymerization of VAc in fluoroalcohols.[150] The stereospecific chain growth is likely to be due to the hydrogen-bonding or coordinative interaction of the solvent molecules with the carbonyl groups of the monomer and/or the growing chains which induce steric hindrance. PVAc with a low dispersity value (M_n = 8 000, Đ = 1.2) and a relatively high syndiotacticity (r = 59%) were recovered using *m*-$C_6H_4\{C(CF_3)_2OH\}_2$ and $CH_2I(CO_2Et)$ in the presence of V-70 at 20°C.

The best method reported so far to control the polymerization of VAc is OMRP making use of [$Co(acac)_2$] as CA. This was discovered by Jérôme and coworkers while they were studying Quinone Transfer Radical Polymerization catalyzed by cobalt complexes.[71] They discovered that the polymerization was better controlled in the absence of the quinone, with the cobalt complex only. A good agreement between theoretical and experimental molecular weights was obtained with a low dispersity value (Đ ≤ 1.33). The highest PVAc weight synthesized was 99 000 $g.mol^{-1}$ with Đ = 1.33. The phenomenology of this process has already been presented in the previous section. The authors proposed a RDARP mechanism of control and interpreted the long induction period as the result of the presence of the larger concentration of residual Co(II), suppressing the dissociative OMRP equilibrium by the mass effect until all

of the [Co(acac)$_2$] complex was transformed to the Co^{III} adduct. Poli and coworkers, however, proposed an alternative explanation of the observed induction period.[72] Their work actually allowed revealing a previously unsuspected interplay between the dissociative RDARP and the associative degenerative transfer (DT) pathways in OMRP (Scheme 16). The cobalt-mediated radical polymerization (Co-MRP) mechanism of VAc in bulk in the presence of [Co(acac)$_2$] changes from degenerative chain transfer (pathway a) to reversible termination (pathway b) upon addition of neutral electron donor (ED) molecules like water or pyridine.

From a historical point of view, cobalt porphyrins have been the first metallic complexes reported as OMRP CAs. Developed by Wayland and coworkers, these compounds were also tested for the control of vinyl acetate polymerization. While no polymerization occurred under RDARP conditions (the PVAc radical chain trapping process is irreversible), a controlled polymerization was reported under DT conditions with the organocobalt(III) complex acting as transfer agent and diazocompounds as radical initiators. Cobalt(II) tetramesitylporphyrin and a mixture of V-70 and AIBN were used at 60°C to shorten the induction period (rapid decomposition of V-70) while keeping an approximately constant influx of radicals for a longer time from AIBN.[151] Theoretical and experimental molecular weights were in good agreement even if the GPC traces showed a low molecular tail which increased with conversion. The low molecular weight shoulder consists of terminated oligomers and short cobalt-capped polymer chains resulting from reinitiation that uses cobalt(II) produced in the radical termination events.[152] Cobalt-mediated radical polymerization is the most studied system for OMRP but other transition metals have demonstrated effective control of vinyl acetate polymerization, such as chromium β-diketiminato complexes (Figure 24).[153] The single-component OMRP with the alkyl chromium(III) compound [CpCr(NacNac^{XylXyl})(CH_2CMe_3)] (Figure 25) gave a controlled polymerization at room temperature yielding a PVAc with M_n = 16 200 and Đ = 1.46, but the polymerization was quite slow and the kinetic monitoring showed a slowdown which was attributed to the formation of stronger Cr─C bonds in the dormant species after head-to-head monomer additions.[66] A faster polymerization took place when using the Cr^{II} complex with the *iso*propyl substituents on the NacNac ligand (1), attributed to the steric labilization of the Cr─PVAc bond in the dormant species. Attempts to speed up the polymerization for the xylyl derivative (2) by warming led to decomposition of the controlling system to the inactive acetate complex CpCr(NacNac^{XylXyl})($OCOCH_3$). Similar results were also obtained with complexes (3), (4) and (5).

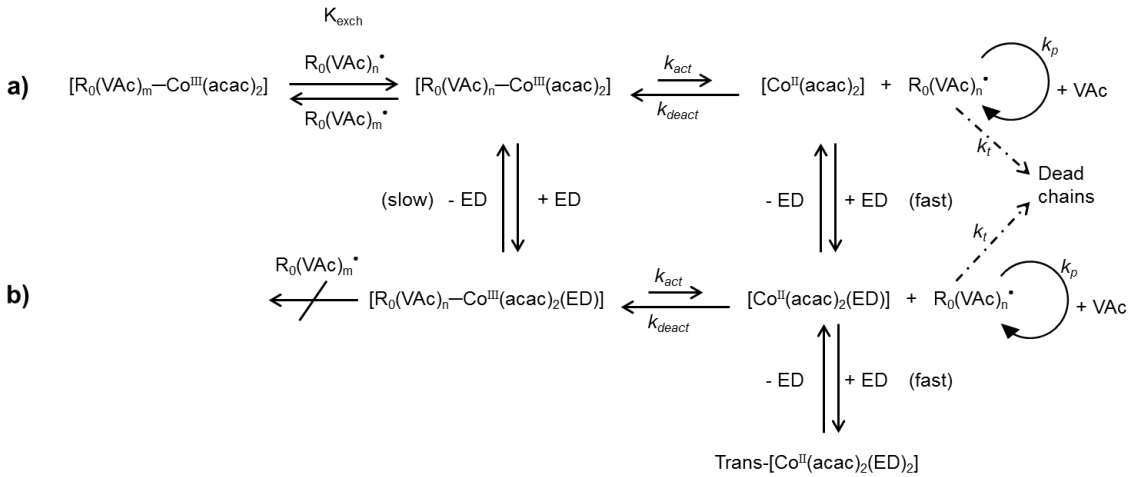

Scheme 16: Proposed general mechanism for the CMRP of VAc mediated by [Co(acac)$_2$] complex in the a) absence and b) presence of EDs.

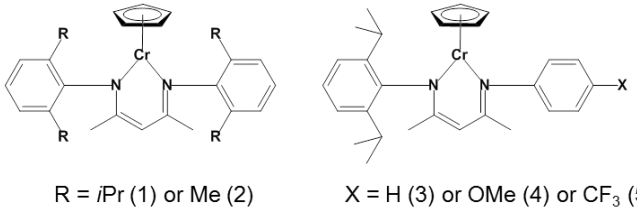

Figure 24: Chromium(II) complexes with β-diketiminato and cyclopentadienyl ligands.

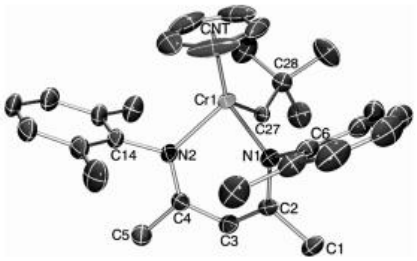

Figure 25: [*neo*pentyl-CpCr^{III}(NacNac^{XylXyl})] complex used as a single-component OMRP reagent in reference 66.

It has to be noticed that contrary to the cobalt(II)acetylacetonate[72] and cobalt(II) tetramesitylporphyrin systems,[151] those chromium complexes are not capable of mediating an associative degenerative transfer process. This is consistent with the absence of vacant sites on the Cr atom in the Cr(III)-capped dormant chains.

Jérôme and coworkers succeeded in polymerizing vinyl acetate with [Co(acac)$_2$] in miniemulsion, for the first time with the formation of very stable PVAc latexes of solid contents ranging from 25 to 30 wt%.[154] PVAc with a molar mass as high as 81 000 g.mol^{-1} and a high monomer conversion (94%) was collected in only 1 h at 30 °C after ultrasonication for 6 min. They also reported the Co-MRP of vinyl acetate initiated by a PVAc macroinitiator in suspension in water. High conversion were reached along with high molar mass and a relatively low dispersity value (conv.= 95%, M_n = 60 500, Đ = 1.35).[155]

b) Vinyl amides monomers

Contrary to acryl amides, vinyl amides (Figure 26) possess an alkene unit which is not conjugated with the C=O functional group. The latter is a member of the family of so-called less reactive monomers (LRM), for which the corrresponding radical is not stabilized. Thus, the controlled polymerization of vinyl amides is difficult. Poly(vinyl amides) (PVA) are of interest mainly because of their biocompatibility and absence of toxicity. PVA are in most cases thermoresponsive materials[156,157] which can undergo fast and reversible solubility changes as a function of temperature. PVA have received much attention because of their potential in a wide range of applications including controlled drug delivery,[158,159,160] separation processes,[161] and tissue engineering.[162]

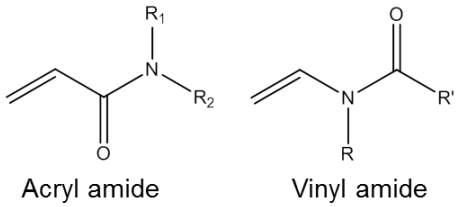

Figure 26: General formula of two isomers: acryl amide and vinyl amide (R_1, R_2, R, R' = alkyl group).

The RDRP of six vinyl amide monomers has been reported so far (see Figure 27). The controlled radical homopolymerizations of N-vinyl formamide (NVF), N-vinyl pyrrolidone (NVP), N-vinyl-2-piperidone (NVPip), and N-vinyl caprolactam (NVCl) have been described as detailed below, whereas *N*-vinyl acetamide (NVA) and *N*-methyl-*N*-vinylacetamide (NMVA) have only been statistically copolymerized with NVCl via Co-MRP.[163] Among those monomers, NVP is, by far, the most studied. It gives an important water-soluble polymer which has attracted significant attention in the medical field. The NVP controlled polymerization has been mainly reported by MADIX with xanthates (Figure 28),[164] but also by RAFT with trithiocarbonate (Figure 29),[165] or dithiocarbamate derivative (Figure 30).[166]

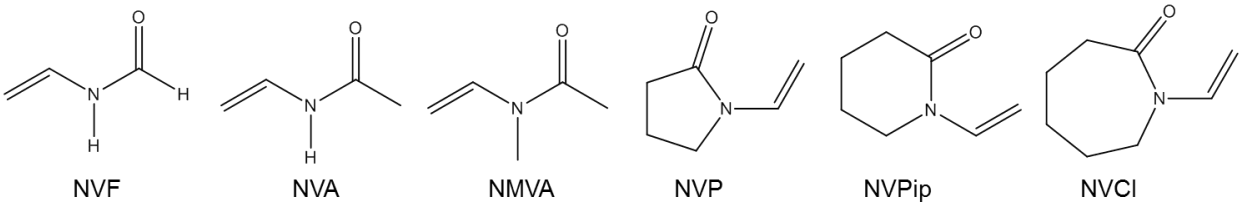

Figure 27: Chemical structures of vinyl amides for which a RDRP is reported in literature: *N*-vinyl formamide (NVF), *N*-vinylacetamide (NVA), *N*-methyl-*N*-vinylacetamide (NMVA), *N*-vinyl pyrrolidone (NVP), *N*-vinyl-2-piperidone (NVPip), and *N*-vinyl caprolactam (NVCl).

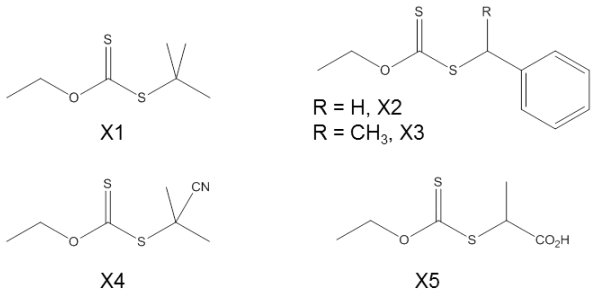

Figure 28: Xanthates used for the NVP polymerization by MADIX.

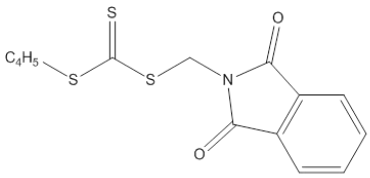

Figure 29: Trithiocarbonate used for the RAFT polymerization of NVP in reference 165.

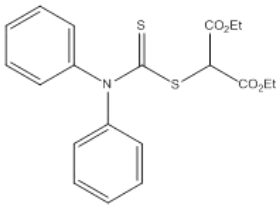

Figure 30: Diphenyldithiocarbamate of diethylmalonate (DPCM) used for RAFT of NVP in reference 166.

The characteristics of poly(*N*-vinyl pyrrolidone) (PNVP) synthesized via the MADIX/RAFT process are summarized in Table 6. Relatively low dispersity values have been obtained (Đ = 1.3-1.74) with moderate molecular weight ($M_{n,exp}$ = 9 800 – 31 900 g/mol). Klumperman *et al*. have shown evidence of selective initiation from X4 (Figure 28) (i.e. the formation of the single monomer adduct of xanthate is a highly selective reaction).[167] At the end of the initiation process, a slight but sudden decrease in the rate of monomer consumption occurs. The xanthates X1 and X5 (Figure 28), on the other hand, do not give rise to a selective initiation process. Moreover, Fandrich and coworkers have observed a competitive chain transfer to the solvent (1,4-dioxane or anisole) when using xanthate X5 (Figure 28).[168]

Yamago and coworkers have reported the RDRP of NVP using organostibine[169] and organobismuthine[120] CAs. With organostibine as mediator (Figure 31), the dispersity value of PNVP is low (Đ = 1.1) when the targeted molecular weight is relatively low (M_n < 15 000 g/mol), but it slowly increases as the targeted molecular weight becomes higher (M_n = 100 000 g/mol, Đ < 1.3). Deuterium-labeling experiments suggested that occurrence of the head-to-head addition is the major course of the loss of the controllability upon the increase of

the amount of NVP used. A variety of diblock copolymers containing a PNVP segment were also synthesized in a controlled manner.[169]

Table 6: Characteristics of PNVPs synthesized via the MADIX/RAFT technique.

Entry	Xanthate	NVP conversion	$M_{n,exp}$	Đ	Reference
1 [a]	X1	48%	31 900	1.74	167
2 [b]	X2	68%	12 400	1.47	164
3 [b]	X3	80%	16 900	1.26	164
4 [a]	X4	27%	14 400	1.32	167
5 [a]	X5	26%	15 500	1.34	167
6 [c]	CT1	48%	26 700	1.41	165
7 [d]	DPCM	64%	9 800	1.3	167

[a] $[NVP]_0/[X1/X4/X5]_0/[AIBN]_0$ = 450:1:0.1, bulk, 60°C; [b] $[NVP]_0/[X2/X3]_0/[AIBN]_0$ = 150:1:0.2, bulk, 60°C; [c] $[NVP]_0/[CT1]_0$ = 151:1, $[AIBN]_0$ = 3.08×10^{-3} M, bulk, 60°C ; [d] $[NVP]_0/[DPCM]_0/[AIBN]_0$ = 100:1:0.0625, in anisole, 80°C.

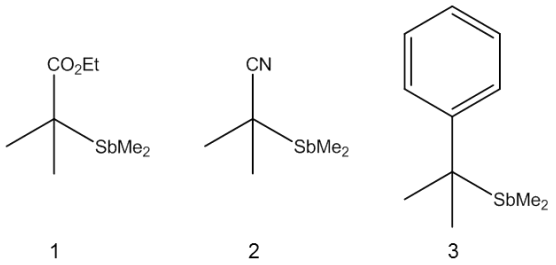

Figure 31: Organostibines used in reference 169 to control the polymerization of NVP.

With organobismuthine (Figure 32), the polymerization of NVP proceeded smoothly at 60°C in the presence of AIBN, whereas it did not proceed efficiently without AIBN at 100°C. This result is attributed to the strong C-Bi bond of the corresponding dormant polymer species, from which the radical was not generated efficiently at this temperature. A block copolymer was successfully synthesized by using the living polymer end. Thus, the treatment of a polystyrene macro-mediator (M_n = 6 000 g/mol, Đ = 1.07, Figure 33) with NVP (100 equiv) in the presence of AIBN (0.2 equiv) in DMF at 60°C afforded the corresponding diblock copolymer in 93% yield (M_n = 15 100 g/mol, Đ = 1.16).

The NMP of NVP was also reported using either 2,2,6,6-tetramethyl-1-(phenylethoxy)piperidine (Figure 34) as a unimolecular initiator or AIBN/TEMPO (Figure 35) as a bimolecular initiation system.[29] The polymerizations were conducted at high temperatures in the presence of acetic anhydride, which acted as an accelerator. However, the

PNVP dispersity value was high at low conversion and continued to increase with conversion (Đ = 1.7-2.2).

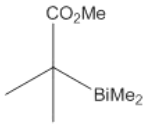

Figure 32: Organobismuthine used in reference 120 to control the polymerization of NVP.

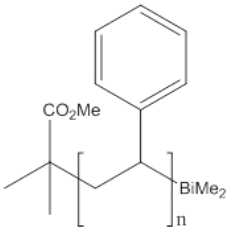

Figure 33: Macro-mediator used in reference 120 to synthesized PS-*b*-PNVP.

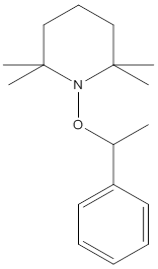

Figure 34: 2,2,6,6-tetramethyl-1-(phenylethoxy)piperidine used as a unimolecular initiator for NVP polymerization in reference 29.

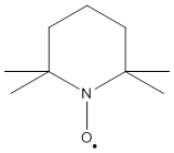

Figure 35: (2,2,6,6-tetramethylpiperidin-1-yl)oxidanyl (TEMPO).

The polymerization of NVP by ATRP at room temperature was reported using Me_6Cyclam as ligand, methyl-2-chloropropionate (MCP) as initiator, and copper(I) chloride and copper(II) chloride as catalysts (see Figure 36).[170] The PNVP had low dispersity values (Đ = 1.2-1.4) and the molecular weights were quite close to the theoretical values. New fluorescent amphiphilic block copolymers were synthesized by ATRP from a PNVP─Cl macroinitiator and *N*-meth-acryloyl-N'-(α-naphthyl)thiourea (MANTU, Figure 37) as the hydrophobic monomer.

Finally, the Co-MRP of NVP was introduced by Matyjaszewski's group.[171] After a short induction period (~ 1 h), the rate of polymerization initiated by [$Co(acac)_2$] and V-70 exhibited a second-order curvature with time. The polymerization was conducted until 55% conversion. Molecular weights, although higher than the theoretical ones, increased with conversion and the dispersity values of PNVP were relatively low (Đ = 1.3-1.7). Moreover, statistical PVAc-co-PNVP block copolymers were prepared in a controlled manner. The

degree of control for NVP was inferior to VAc, most likely because of the lower deactivation rate of the PNVP growing chains by the [Co(acac)$_2$]. PVAc-*b*-PNVP block copolymers were synthesized later by Detrembleur and coworkers who used a [Co(acac)$_2$-PVAc] macroinitiator.[172] The length of the two blocks could be tuned by the [VAc]/[Co(acac)$_2$] and the [NVP]/[PVAc] ratios for the synthesis of the macroinitiator and the polymerization of the second monomer, respectively. The use of cobalt-mediated radical coupling (CMRC, Scheme 17) with butadiene affords triblock copolymers PVAc-*b*-PNVP-*b*-PVAc.[173] The same strategy of combining Co-MRP with CMRC with addition of ε-caprolactone ring opening polymerization (ROP) gave access to well-defined telechelic PNVP as well as amphiphilic diblock and symmetrical triblock copolymers containing biocompatible PNVP and biodegradable poly(ε-caprolactone) segments (PCl).[174]

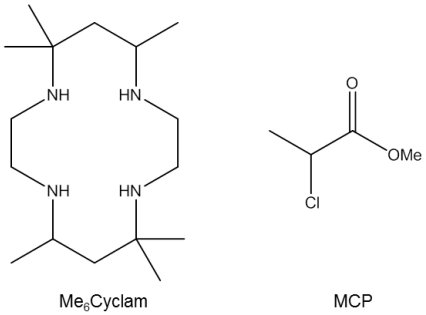

Figure 36: Chemical structures of the ligand (Me_6Cyclam) and initiator (MCP) for ATRP of NVP.

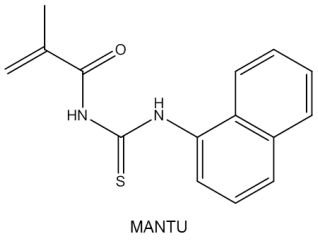

Figure 37: Representation of the fluorescent MANTU monomer.

N-vinyl formamide (NVF, Figure 27) is the simplest vinyl amide and poly(*N*-vinylformamide) (PNVF) is a water-soluble polymer[175] that, because of problems in the needed preliminary monomer purification, has not received wide attention. PNVF is not only a water-soluble polymer but also an important precursor for preparing poly(vinylamine) which is a potential polyelectrolyte candidate for many industrial applications. To date, PNVF and its derivatives have been used in water treatment,[176] papermaking, and radiation cure coating.[177] Only one paper dealing with the controlled radical polymerization of NVF was reported in 2003 by Beckman *et al.*[178] Attempts by these authors to employ the ATRP methodology with NVF were unsuccessful. However, after having synthesized a precise

macro-RAFT agent made of poly(ethyleneglycol) (PEG) (M_n = 2 100 g/mol, Đ = 1.09) the NVF controlled polymerization to yield a PEG-*b*-PNVF block copolymer (M_n = 6 100 g/mol, Đ = 1.7 after purification) was successful. The broad dispersity value of the NVF block copolymers was attributed to the greater chain transfer of NVF propagating radical to monomer and polymer.[179] Indeed, the chain transfer constant of NVF is $C_{tr} = 9.53 \times 10^{-4}$ at 60 °C,[180] which is slightly higher than that of vinyl acetate ($C_{tr} = 1.75 - 2.85 \times 10^{-4}$).

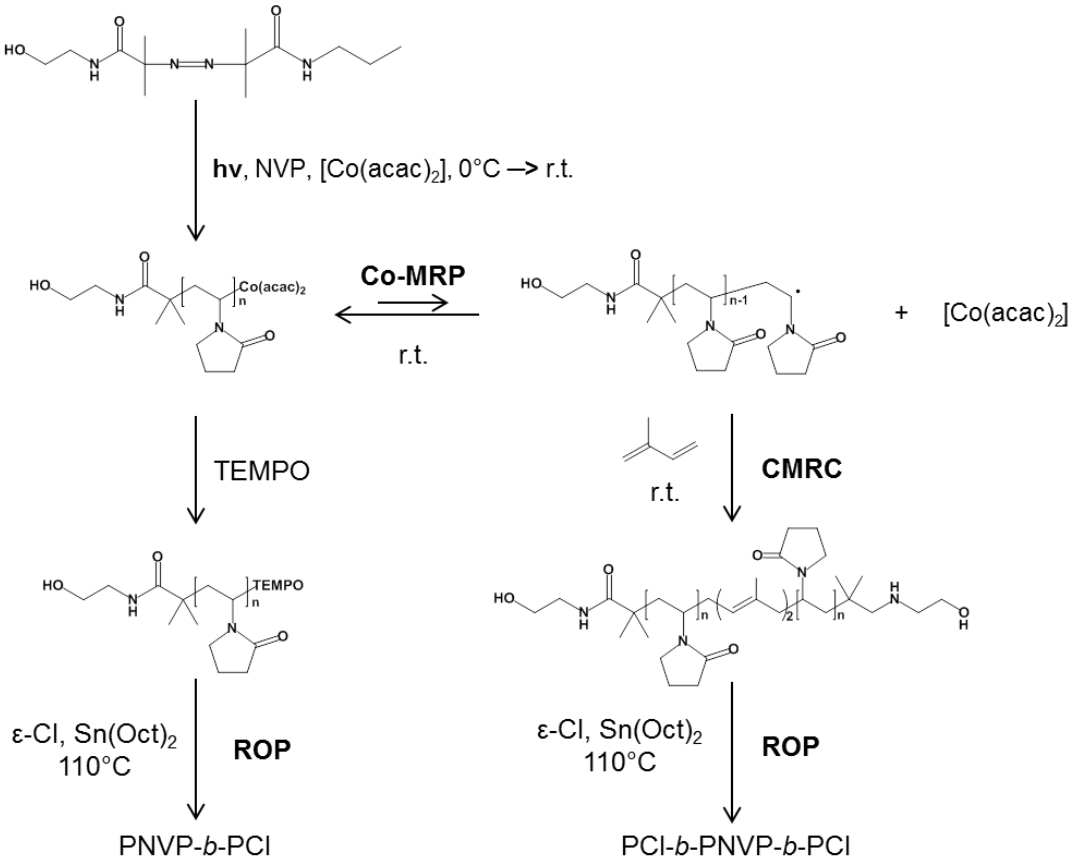

Scheme 17: Synthetic strategy combining photoinitiated Co-MRP, CMRC and ROP.

O'Reilly and coworkers have published the first MADIX polymerization of *N*-vinyl-2-piperidone (NVPip, Figure 27)[181] using the xanthate depicted in Figure 38. The controlled nature of the NVPip polymerization was confirmed by the pseudo-first-order kinetic plot. However, linear kinetics were consistently observed only up to ca. 50% conversion and in all cases the rate of polymerization leveled off after reaching ca. 70%. The apparent molecular weight was observed to increase linearly with conversion. A series of homopolymers with control over M_n (4 500 – 83 000 g/mol) were prepared by varying the monomer-to-CTA ratios. All the poly(*N*-vinyl-2-piperidone) (PNVPip) obtained possessed fairly low dispersity (Đ < 1.3) as well as xanthate end groups. These PNVPip all exhibited sharp reversible cloud points (in the range 68-87°C for M_n ~ 82 000 and 6 400 g/mol respectively). The authors also succeeded to make amphiphilic ($PNVPip_x$-*b*-$PVAc_y$) diblock copolymers by chain extension

of PNVPip. For example, before chain extension the PNVPip molecular weight was 7 600 g/mol (Đ = 1.28) and after chain extension the PNVPip-*b*-PVAc molecular weight was increased to 11 400 g/mol (Đ = 1.27). Depending on the composition, $PNVPip_x$-*b*-$PVAc_y$ exhibited a phase transitions at 62°C (with x:y = 75:25) or 55°C (with x:y = 66:34) in water.

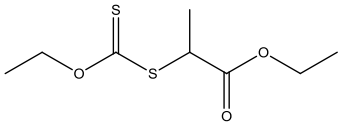

Figure 38: Chain transfer agent used to control NVPip radical polymerization in reference 181.

N-vinylcaprolactam (NVCl, Figure 27) can only be polymerized by the radical mechanism. Poly(*N*-vinylcaprolactam) (PNVCl) is a thermoresponsive polymer and has a lower critical solution temperature (LCST) close to the physiological temperature (33 – 46°C).[182,183] Controlled polymerization was achieved via RAFT or MADIX techniques or via Co-MRP. A few examples of successful RAFT (CTA1)[184] and MADIX (X1, X2, X3)[185] agents for NVCl controlled polymerization are depicted in Figure 39. The corresponding characteristics of the PNVCl obtained are summarized in Table 7.

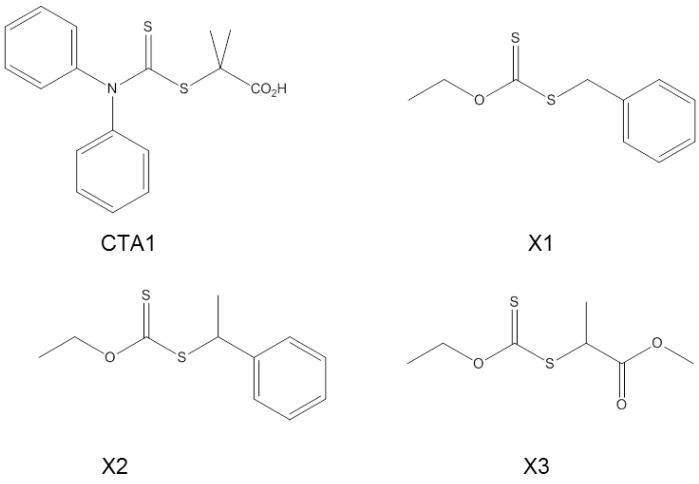

Figure 39: Chain transfer agent used for NVCl polymerization by RAFT or MADIX processes.

The molecular weight increased along with the monomer conversion and relatively low dispersity values were obtained (Đ = 1.1 – 1.5). Moreover, the presence of chain-end functionalities was confirmed by chain extension with vinyl acetate. However, this chain extension process was less well controlled. The apparent molecular weight of the resulting diblock copolymer increased but the dispersity value also increased with the VAc conversion (Đ = 1.6 – 1.7). The GPC trace showed a long tail at the low-molecular weight side which was attributed to the contribution of the dead PNVCl chains produced by radical coupling, bearing no dithiocarbamate group and thus being non extensible.

Table 7: Characteristics of the PNVCl obtained by RAFT and MADIX (references 184 and 185).

Entry	CTA	time (h)	yield (%)	$M_{n,theor}$ [a]	$M_{n,exp}$ [b]	Đ [b]
1	none	4	52.4	-	7 400	2.7
2	CTA1 [c]	14	23.2	4 800	3 100	1.4
3	CTA1 [c]	48	50.2	10 500	5 000	1.5
4	X1 [c]	12	30.3	6 500	3 400	1.4
5	X1 [c]	16	52.1	11 100	4 200	1.5
6	X2 [c]	12	28.2	6 100	3 300	1.4
7	X2 [c]	16	50.7	10 800	4 100	1.3
8	X3 [d]	20	-	16 000	18 000	1.1
9	X3 [d]	20	-	45 000	50 000	1.1
10	X3 [d]	20	-	80 000	71 000	1.2
11	X3 [d]	20	-	150 000	150 000	1.1

[a] the theoretical molecular weights were calculated by the formula: $M_{n,theor} = ([NVCl]_0/[CTA]_0) \times MW_{NVCl} \times conversion + MW_{CTA}$; [b] Experimental number-average molecular weight ($M_{n,exp}$) and dispersity values were determined by GPC in THF; [c] bulk polymerization at 60°C with $[NVCl]_0/[CTA]_0/[AIBN]_0 = 150: 1: 0.2$; [d] polymerization in 1,4-dioxane at 60°C.

The Co-MRP of NVCl was reported by Detrembleur et al.[186] who used a preformed [PVAc-$Co(acac)_2$] macroinitiator to initiate the polymerization of NVCl, yielding well-defined PVAc-*b*-PNVCl copolymers of varying compositions, depending on the [NVCl]/[PVAc] initial ratio. Block copolymers with a molecular weight as high as 87 000 g/mol and a low dispersity value (Đ = 1.1) could be prepared by this process. The livingness of the copolymerization was further assessed by the cobalt-mediated radical coupling (CMRC) reaction that resulted in the formation of PVAc-*b*-PNVCl-*b*-PVAc symmetrical triblock copolymers. PVAc-*b*-PNVCl is also the precursor of PVOH-*b*-PNVCl through hydrolysis. These novel copolymers are double-hydrophilic at room temperature and become amphiphilic when heated at 36–42°C, depending on their composition. The same group also reported the statistical copolymerization of NVCl with hydrophilic *N*-vinylamide (NMVA, NVA) or hydrophobic vinylester (VAc, Vinyl pivalate) monomers in order to precisely tune the LCST of the resulting copolymers.[163]

c) Current development of poly(ethylene) and related copolymers

Polyethylene (PE) is one of the World-wide most produced plastic by mass as it represents 50 to 110 million metrics tons depending on the source.[187] It has many applications: from packaging to the medical field or automotive area (in 2001, French cars were made of about 25%w of plastic materials).[188] The raw material is inexpensive (~500-2000 $/ton) and represents less than 1% of the total crude oil and natural gas production. We describe herein the two basic industrial processes. The “High Pressure” process involves a free radical polymerization of ethylene under high pressure and high temperature. Low-density

polyethylene (LDPE) is produced with a wide molecular weight distribution and a high branching proportion (one branch every 20-50 carbons) leading to a density of 0.91-0.94 g/cm^3 and a low crystallinity (50-60%). A major drawback of this industrial process is the known thermal runaway phenomena leading to a pressure and temperature increase and a consequent reactor shutdown for security reasons.[189] The "Low Pressure" process involves the use of a third row metal catalyst (Ti, V, Cr, Fe, Co, Ni…), often activated by a main group co-catalyst or deposited on a solid. There are many versions of the low pressure process, referred to as Ziegler-Natta or Phillips process when respectively titanium or chromium are employed. The proposed mechanism is a coordination-insertion of ethylene into the metal-alkyl bond of an active center.[190,191] The resulting high-density polyethylene (HDPE) has a much lower level of chain branching (less than one side chain per 200 carbons) which increase its stiffness, the density (0.95-0.97 g/cm^3) and the crystallinity (> 90%). Linear low-density polyethylene (LLDPE) can be obtained by copolymerizing ethylene with a small amount of another monomer (mainly hexene or octene). The disadvantages of this process are the relatively high quantity of catalyst needed and more specifically the high viscosity of the media leading to difficulties of heat transfer.

In 2012, Nicol claimed a new process for making low density polyethylene at a relatively low temperature (150°C to 200°C) and high pressure (500 to 3 000 bar), which is based on the use of a peroxide (Figure 40) as initiator.[192] The productivity (mass of PE produced *vs* mass of initiator) is increased and the ethylene conversion remains at 13 to 25% but there is no indications about the PE characteristics. Other authors patented the use of stable free radicals or nitroxide to control ethylene polymerization under high temperature and high pressure leading to PE of high dispersity (M_n > 20 000 g/mol, Đ > 3)[193,194] or moderate dispersity (5 000 < M_n < 1 000 000 g/mol, 1 < Đ < 2).[195]

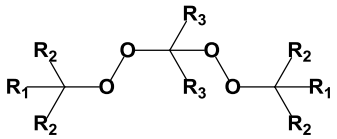

Figure 40: peroxide initiator (R_1=C_2-C_6 alkyl group, R_2=C_1-C_5 alkyl group, R_3=C_1-C_6 alkyl group).

In 2009, Monteil *et al.* have reported the radical polymerization of ethylene under mild conditions (P < 100 bar, T= 70°C). They demonstrated the strong influence of the solvent: polymerization occurred at significant rates in THF down to 10 bar of ethylene, an unusual pressure range for the free radical polymerization of ethylene.[196] The molecular weight of the resulting PE is controlled by transfer to solvent. Carbonates are solvents with lower radical

chain transfer constants, thus leading to molecular weights up to 15 000 g/mol. The authors proposed the solvent activation effect to be mainly due to the Keesom interaction of the solvent on the macroradical.[197]

The formation of branches during free radical polymerization of ethylene is due to two types of reaction. The first one, called backbiting, is an intramolecular chain transfer where the growing radical chain curls back on its own chain to form a six- or seven-membered ring. A hydrogen atom is abstracted and the radical is transferred along the chain resulting in the formation of short chains (butyl or pentyl).[198] Shorter branches are formed through double backbiting.[199] The second reaction is an intermolecular hydrogen transfer leading to long chain branches.

Because the molecular weight (along with the dispersity) and the crystallinity (related to the level of chain branching) directly affect the properties, control of the polyethylene chain growth is of crucial importance.Controlled radical polymerization of ethylene could overcome those limitations. However, a small number of papers have been reported on this challenging topic. For example, there are no experimental results on the RAFT homopolymerization of ethylene, although computational work suggests that fluorodithioformates (Figure 41) should be able to control the ethylene polymerization.[200]

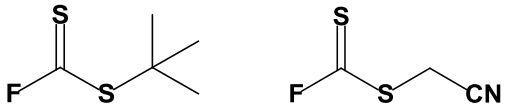

Figure 41: Fluorothioformates.

Moreover, copolymers of ethylene and polar monomers such as vinyl acetate and acrylates are currently produced by FRP. Controlled random copolymerization of α-olefins has apparently been examined only with methyl (meth)acrylate (M(M)A) by using ATRP, RAFT, TERP and ITP. Table 8 reports some significant results obtained for the copolymerization of MA or MMA with 1-alkenes. Structurally well-controlled copolymers were obtained with low dispersity but only for a low degree of polymerization and low olefin insertion ratio (MF_{alkene}). The copolymers dispersity starts to increase with increasing molecular weight. This is due to the accumulation of dormant species terminated with α-alkene monomer units, which less efficiently undergo reactivation to form radical polymer chains than those terminated with acrylate monomers do.[201,202] Nevertheless, this side reaction is not too significant, presumably because the cross-polymerization with acrylate is significantly faster than irreversible termination. Thus, the copolymerizations are still “controlled” with dispersity

values as narrow as 1.07 for lower molecular weight MA/1-hexene copolymers (see entry 8 in Table 8).

Table 8: Reported systems for the RDRP of M(M)A and 1-alkenes.

Entry	Controlling system	1-Alkene	Polar monomer	MF_{alkene} (mol%)	Mn (g/mol)	Đ	Ref.
1	CuBr/EBP/PMDETA	ethylene	MA	8.6	10 400	1.5	208
2	CuBr/EBP/PMDETA	ethylene	MA	8.1	7 100	1.10	206
3	CuBr/EBP/PMDETA	octene	MA	23.6	4 000	1.2	208
4	CuBr/EBP/PMDETA	octene	MA	10.4	19 000	1.3	206
5	CuCl/TCE/PMDETA	octene	MMA	7	6 200	1.3	203
6	MeTe-R / V-601	6-methylene undecane	MA	22	3 400	1.26	205
7	MeTe-R / V-601 +$(CF_3)_2CHOH$	6-methylene undecane	MA	32	4 800	1.18	205
8	RAFT1	hexene	MA	20.2	4 400	1.07	201
9	RAFT1	hexene	MA	12.4	60 400	2.03	201
10	RAFT1	ethylene	MA	Nd	51 600	1.96	201
11	$CHI_3/AlCl_3$/AIBN	ethylene	MA	Nd	5 700	1.38	201
12	$CHI_3/AlCl_3$/AIBN	ethylene	MA	Nd	80 600	2.4	201
13	CA1/I1	ethylene	MA	13.6	9 000	1.19	204
14	CA1/I1	octene	MA	8	4 900	1.13	204

MeTe-R = 2-methyl-2-methyltellanylpropionate (MeTe-$C(CH_3)_2(CO_2Me)$); V-601 = dimethyl-2,2′-azobis(2-methylpropionate); RAFT1 = benzyl-1-pyrrolcarbodithioate; CA1 = 2,2,5-trimethyl-4-phenyl-3-azahexane-3-nitroxide and I1 = 2,2,5-trimethyl-3-(1-phenylethoxy)-4-phenyl-3-azahexane. All compounds are represented in Figure 42.

The living character of the RAFT process was assessed by the chain extension of a macro-chain tranfer agent (poly(methylacrylate)-*co*-(6-methyleneundecane), poly(MA)-*co*-(6MU), Mn = 5000, Đ = 1.18, MF_{6MU} = 31%, entry 7 in Table 8) with styrene or NVP in the presence of an azo-initiator or by photoirradiation. The desired block copolymers poly[(MA-*co*-6MU)-*block*-St] and poly[(MA-*co*-6MU)-*block*-NVP] with Mn = 21 900, Đ = 1.41 and Mn = 31 000, Đ = 1.22 respectively were obtained.[205] In the same way, poly(MA-co-hexene) (M_n = 4 400, Đ = 1.07, MF_{hexene} = 20.2 mol%) was succesfully used as a macro-CTA in chain extension reaction with MA to afford poly[(MA-*co*-hexene)-*b*-(MA)] (M_n = 13 900, Đ = 1.21).[201] ATRP with CuBr/EBP/PMDETA afforded the diblock terpolymer, poly[(MA-*co*-ethylene)-*b*-(MA-*co*-nonafluorohexene)], by sequential addition of ethylene and nonafluoro-1-hexene to an acrylate copolymerization system.[206] The same strategy allowed the synthesis of poly[(MA-*co*-ethylene)-*b*-(MA-co-propene)] with high molar mass (M_n = 48 000), low dispersity (Đ = 1.1) and MA/E/P composition equal to 86.6/2.2/11.2 (mol%).[207]

Furthermore, some Lewis-acid based system such as $AlCl_3$[208] and $Sc(OTf)_3$[209] and Brønsted acids, such as $(CF_3)_2CHOH$ and $(CF_3)_3COH$,[201] enabled the synthesis of nearly alternating

copolymers made of non polar olefins and polar monomers such as (meth)acrylates under FRP conditions. Although the mechanism is not fully understood, the control was proposed to be due to the coordination of the Lewis-acid to the carbonyl function of the acrylic monomer and its corresponding radical. Thus, the electron density of the vinyl group decreases and the cross-propagation to the non polar olefin is enhanced. The resultant highly electron-deficient monomer forms a 1:1 alternating copolymer with 1-alkenes in the presence of radical initiators and a significant increased alkene insertion from 20% to 50% could be observed.[205] Thus, the addition of Lewis acids was attempted under RDRP conditions. It was reported that insertion of 6MU into the copolymer could be increased to nearly 40% by adding fluoroalcohols as a Brønsted acid in TERP process without losing control of the copolymer dispersity (Entry 7, Table 8). However, the addition of $AlCl_3$ to the RAFT polymerization of MA and ethylene led to less controlled behavior with high molecular weight and broad dispersity for the resultant material (Entry 10, Table 8). It was proposed that the reactivity of the RAFT agent is adversely affected by the coordination of its thiocarbonyl group to $AlCl_3$.[201]

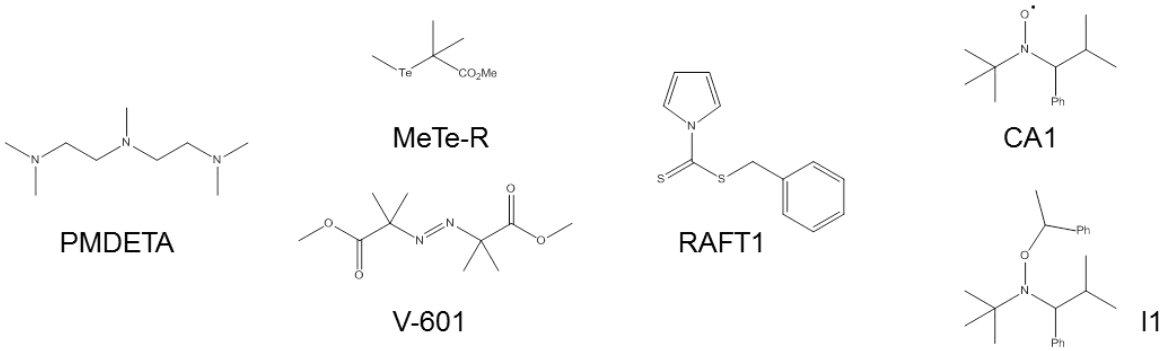

Figure 42: Compounds used for RDRP of α-olefins and methyl (meth)acrylate (see Table 8).

In conclusion, systems able to bring the controlled radical homo- and co-polymerization of ethylene closer to a living polymerization are still lacking.

3) Objectives

The control of polar non-conjugated monomers (like vinyl acetate and vinyl amides) which would allow the synthesis of well-defined polymers is an industrial challenge. Moreover, the controlled radical copolymerization of ethylene with polar monomers remains, so far, unsatisfactory. On the basis of the promising results obtained for the OMRP of vinyl acetate and vinyl amides using $[Co(acac)_2]$, we decided to explore copper complexes as controlling agents under OMRP conditions. Copper is an interesting metal for large scale applications because of its low cost. As described above, an OMRP pathway involves the dynamic equilibrium between a metal complex in its lower oxidation state plus a radical and an

organometallic species with the metal in the higher oxidation state. The paucity of stable alkylcopper(II) complexes in the literature suggests that the alkyl-Cu^{II} bond is homolytically fragile and could therefore be suitable for a reversible activation/deactivation equilibrium of OMRP type with reactive radicals. In addition, previous investigations by Matyjaszewski have shown that the Cu^{I} complexes that are active catalysts for the polymerization of reactive monomers such as styrene and acrylates are not capable of trapping efficiently these weak radical to form dormant Cu^{II}-capped chains. However, a slowdown of the free radical polymerization rate indicated a certain degree of radical trapping, insufficient to establish an efficient persistent radical effect.[56] At variance with the enormous amount of results available on the copper-mediated polymerization by ATRP, there is no report so far on the use of copper in RDRP within an OMRP approach but, given the expected trend of bond strengths, we suspected that copper may have the potential to yield a controlled radical polymerization of the LRM's. Therefore, we have focused on the copper(I)/copper(II) couple coordinated by nitrogen based ligands. The coordination sphere of the selected complexes must fulfill a few conditions. First of all, it should not be too crowded in order to allow the addition of the polymer chain and formation of the new copper(II)-carbon bond. Secondly, it should be flexible enough to adapt to both preferred geometries when going from one copper oxidation state to the other one. Copper(I) is known to adopt, in most cases, a tetrahedral geometry, although planar tri-coordinated and linear dicoordinated complexes are also known, whereas copper(II) complexes are generally isolated as 4-coordinate distorted square planar, 5-coordinate trigonal bipyramidal or square pyramidal or 6-coordinate octahedral complexes, the latter ones being more or less distorted (usually by axial elongation) by the Jahn-Teller effect. The third attribute is the absence of halide ligands to avoid any unwanted ATRP pathway (vide supra). Moreover, the ligands should be easily modified to introduce different electronic and/or steric effects in order to tune the catalyst activity. We arrived at the conclusion that the nitrogen analogues of acetylacetonate as well as the tripodal scorpionates, tris(pyridylmethyl)amine and tris(pyridylthiomethanide) should be promising ligands and they were therefore selected for investigation in this thesis (Figure 43). In a first part of this thesis (Chapter I), the formation and stability of copper(II)-alkyl compounds were investigated then copper(I) complexes with the above ligands were synthesized and tested as controlling agents for vinyl acetate, vinyl amide and ethylene polymerization under OMRP conditions (Chapter II). Finally, Chapter III reports a theoretical studies aimed at better understanding the reasons of the [$Co(acac)_2$] success for the polymerization of VAc as well as certain specific reactivity trends that are experimentally observed in the controlled polymerization of a variety of vinyl

amides. The experimental work on which this last chapter is based was conducted in the group of Dr. Antoine Debuigne at the "Centre d'Etude et de Rercherches sur les Macromolécules" of the University of Liège and the joint research work has made the object of two publications.[210,211]

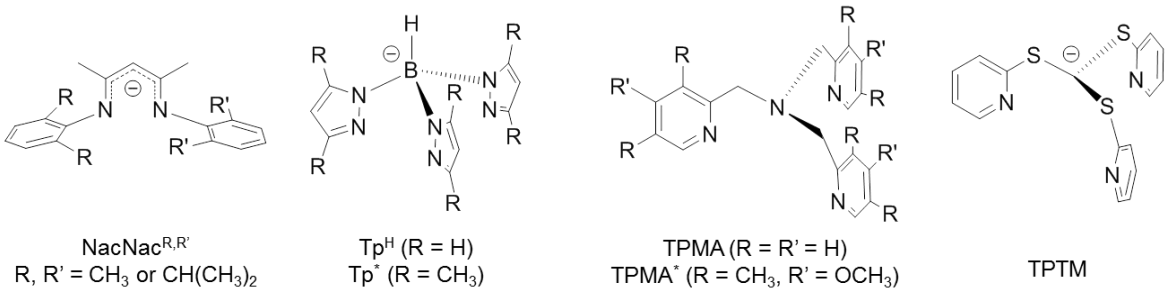

Figure 43: Ligand families investigated in this study.

CHAPTER I

ELUSIVE ALKYL COPPER(II) SPECIES

CHAPTER I: ELUSIVE ALKYL COPPER(II) SPECIES

The presumed Copper-Mediated Radical Polymerization (Cu-MRP) pathway involves the formation of organometallic copper(II) species (LCu^{II}—P) in the dormant state (Scheme 18). The copper-carbon bond has to be photolytically or thermally labile to allow a sufficient rapid activation so that the radical chains can propagate, and at the same time it must be sufficiently stable to shift the equilibrium toward the dormant state. We have explored the possibility to synthesize and isolate an organometallic copper(II) model compound. The alkyl polymer chain (P) was modelled by a methyl radical ($CH_3^{\bullet}$), which should bind more strongly to the copper metal center than the radical of a poly(vinyl acetate) (PVAc) or poly(vinyl amide) (PVA) growing chain and similarly to the polyethylene (PE) chain. The isolation of one such copper(II) compound would also be of great interest as it could serve as a unimolecular precursor for Cu-MRP. Indeed, mixing LCu^{II}—CH_3 and a monomer followed by thermal- or photo-activation would be a simple procedure for controlled radical polymerization and would allow us to investigate the activation kinetics. This synthetic target is not expected to be straightforward, because stable compounds with Cu^{II}—C bonds are rare (see next section). However, the previous work on Co-MRP has taught us that the metal-carbon bond strength can be tuned by the ligand coordination sphere, particularly going from an oxygen-based coordination sphere in $[Co(acac)_2]$ to a nitrogen-based coordination sphere in Co(porphyrin) system, the Co^{III}-C bond strengthens. Thus, it was hoped that using the N-based ligands outlined in the general introduction (Figure 43) would give us a chance to stabilize sufficiently one such compound. Furthermore, even if a sufficiently stable compound could be generated in solution, the isolation of such product may still be challenging. For instance, attempts to isolate a model compound of the dormant species for the cobalt(II)acetylacetonate-mediated OMRP of vinyl acetate, the cobalt(III) complex $[(acac)_2Co(CHMeOOCCH_3)]$, has not so far met with success.[212] On the other hand, a low-molecular-weight cobalt adduct (Figure 44) could be synthesized by decomposing V-70 in the presence of vinyl acetate and a large amount of $[Co(acac)_2]$, isolated and used as unimolecular initiator for the polymerization of vinyl acetate in a direct OMRP approach. A similar strategy has therefore been explored for copper.

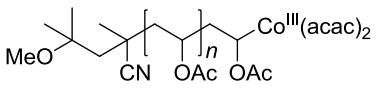

Figure 44: Cobalt adduct (n~3).

This chapter is divided in four parts. The first one is a bibliographic introduction depicting the organometallic copper(II) compounds described in the literature. Then electron paramagnetic resonance (EPR) spectroscopy, with emphasis on the cupric ion, is introduced to the reader. The third section reports our attempted synthesis of organometallic copper(II) model compounds. This chapter ends with a mechanistic investigation of a dormant species involved in a polymerization of butyl acrylate were an interplay between ATRP and OMRP is suggested.

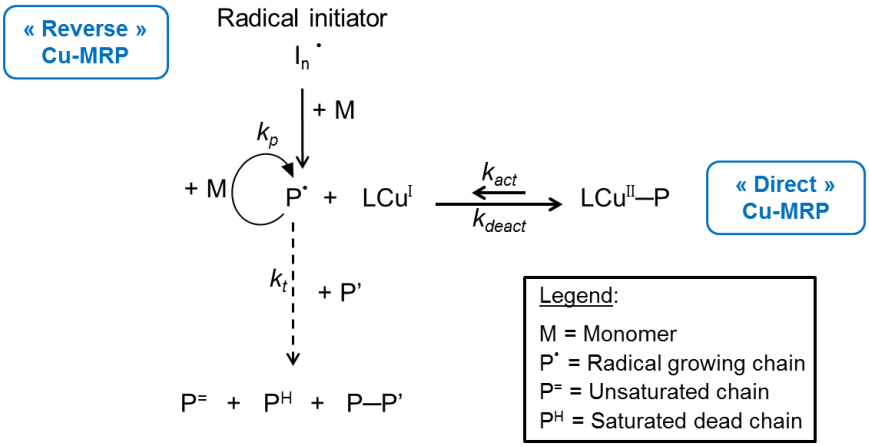

Scheme 18: Copper-Mediated Radical Polymerization (Cu-MRP).

1) Organometallic copper(II) compounds: state of art

In contrast to copper(I), few examples of organometallic compounds of copper(II) have been reported to date and these are either elusive species or benefit from special stabilizing effects. Transient σ–alkyl adducts of copper(II) have been postulated in the azide-alkyne cycloaddition reaction (called Glaser/Eglinton coupling, see Figure 45 and Figure 46),[213,214] in the copper-catalyzed methoxylation of tolylboronic ester (called Chan-Evans-Lam coupling),[215] and in the modified Ullmann reaction.[216] Moreover, the reaction of cuprous ions with alkyl radicals in aqueous solution has been extensively studied by Meyerstein and coworkers. They concluded that $[Cu^{II}CH_2OH]^+$ is formed in the equilibrium reaction **(1)** and that the stability constants for the corresponding complexes $[Cu^{II}CH(CH_3)OH]^+$ and $[Cu^{II}C(CH_3)_2OH]^+$ are rather small and thus these intermediates are not observed.[217]

$$Cu^{+}_{(aq)} + {}^{\bullet}CH_2OH \rightleftharpoons [Cu^{II}–CH_2OH]^+ \qquad (1)$$

The same equilibrium with the methyl radical gives $[Cu^{II}CH_3]^+$ which has a maximum absorption at λ_{max} = 375 nm. More interestingly, it was observed that the decomposition of $[Cu^{II}CH_2OH]^+$ followed a homolytic process[218] whereas $[Cu^{II}CH_3]^+$ decomposed at pH = 3.7

rather by a methyl transfer reaction followed by a fast reductive elimination which produces ethane.[219]

Finally, heterolysis of the copper-carbon σ-bond occurs mainly when electron-withdrawing groups are bound to the α-carbon. This mechanism is acid catalyzed. Homolysis of the copper-carbon σ-bond also occurs and this mechanism is enhanced if the free radical formed is stabilized by resonance and by steric hindrance imposed by the ligand, or by substituents on the aliphatic residue. The reaction of two transient complexes with each other to form a carbon-carbon bond between the two aliphatic residues is also possible.[220]

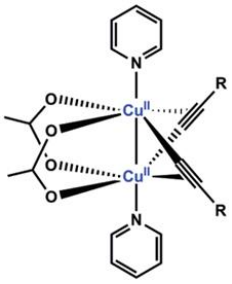

Figure 45: Postulated bimetallic copper(II)-alkyne intermediate in the Glaser/Eglinton coupling sequence enabled by [Cu(OAc)$_2$]/pyridine complex. A delocalized negative charge is implied in the drawing of the acetate.

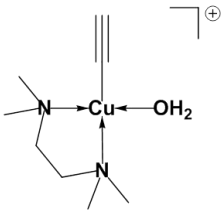

Figure 46: Postulated Intermediate for the Hay modification of the Glaser reaction based on DFT study.

In 2000, Latos-Grażyński's group opened the route toward organometallic copper(II) species stabilized by N-confused porphyrins. The inverted porphyrins 2-aza-5,10,15,20-tetraphenyl-21-carbaporphyrin ($CTPPH_2$) and its methylated derivatives 2-aza-2-methyl-5,10,15,20-tetraphenyl-21-carbaporphyrin (2-N(CH_3)CTPPH) were used to stabilize copper(II) complexes.[221] Three copper(II) complexes were synthesized but only characterized by EPR and NMR spectrometries (Scheme 19). The Cu-C(sp^2) bond in the N-confused porphyrin is stabilized by the π-delocalization effect in the porphyrin ring.

Almost one year later, Furuta and coworkers reported the first X-ray structure of a complex of this family (Figure 47),[222] which was synthesized by refluxing the correponding protonated N-confused porphyrin ligand with copper(II) acetate in chloroform. The structure exhibits a coordination geometry with only small deviations of the pyrrole rings from coplanarity. This

complex formed, in the solid state, a dimeric structure through hydrogen bonding between the peripheral amide groups.

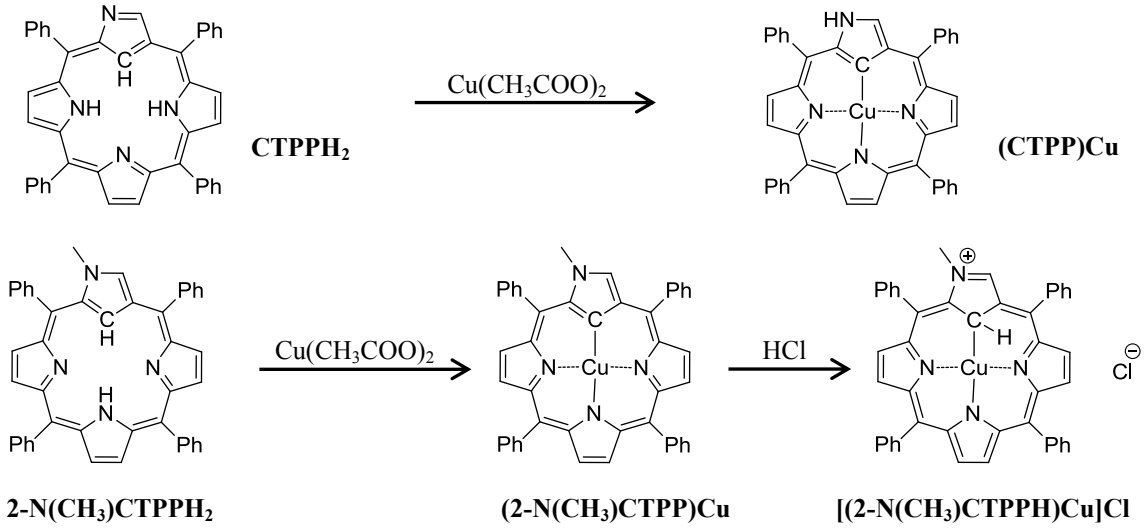

Scheme 19: Proposed structures of confused-porphyrin copper(II) complexes.

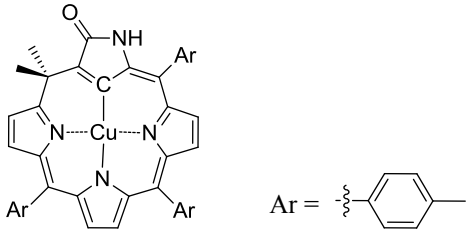

Figure 47: First crystallographically characterized compound containing a copper(II)-carbon bond.

Derived from this first reported structure, two additional examples of divalent copper coordinated by porphyrin-type ligands have been described later by the same group, which first reported the electrochemical interconversion of two N-confused porphyrin copper complexes (Scheme 20).[223] At that time, only the X-ray structure of the copper(III) species was reported. However, the planar copper(II) complex was reported later as a reddish product (Figure 48).[224] The EPR parameters (g_{iso} = 2.09, $g_{\|}$ = 2.12, [$A_{\|}$] = 168 Gauss) in toluene at 77 K are consistent with the square-planar structure determined by X-ray crystallography. When examining the CIF file included in the publication as supporting information, the copper structure (depicted in Figure 49) is actually different from that discussed by Furuta in the paper: it does not contain any copper-carbon bond but rather a four-nitrogen environment of a regular porphyrin ligand around the copper center. This is surprising as it would suggest that reduction of the Cu^{III} complex induces a carbon-carbon and a carbon-hydrogen bond breaking at two adjacent ring carbon atoms and swapping of these two bonds. However, there might be simply a mistake in the crystallographic files deposited at the Cambridge Structural Database and included in the supporting information.

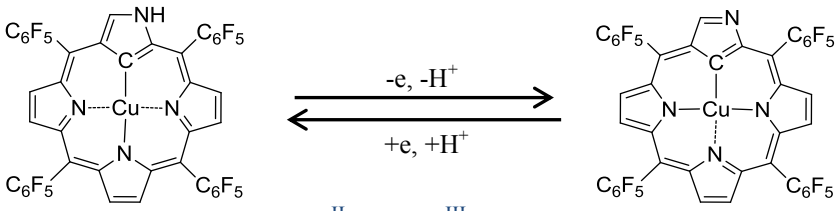

Scheme 20: Interconversion between Cu^{II} and Cu^{III} complexes by detachment and attachment of the peripheral NH.

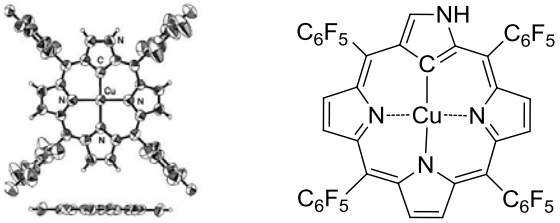

Figure 48: Structure of the copper(II) complex discussed by Furuta in reference 224 (X-ray top and side view and schematic view depicted in the paper).

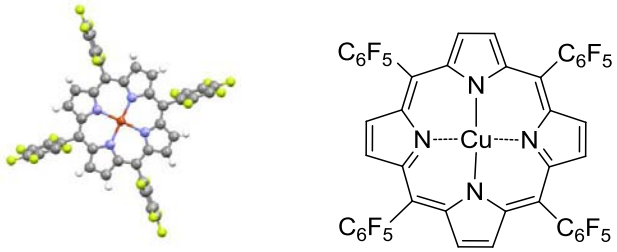

Figure 49: Structure from CIF file with schematic representation.

Latos-Grażyński's group reported in 2007 the X-ray structure of an organometallic copper(II) compound coordinated by a modified porphyrin-type ligand (Figure 50).[225] The macrocycle is only slightly distorted from planarity. The Cu^{II}–C bond length equals 1.939(4) Å. They also reported another structure (Figure 51) with a weak copper-carbon bond[226] and an EPR spectrum characterized by typical parameters for the square planar copper(II) electronic structure ($g_{\parallel} = 2.158$, $g_{\perp} = 2.041$, $g_{\circ} = 2.082$, $A_{\parallel}^{Cu} = 164$ gauss, $A_{\perp}^{Cu} = 25$ gauss, $A_{\circ}^{Cu} = 65.9$ gauss, $A_{\circ}^{N} = 13.7$ gauss), resembling those of N-confused porphyrin copper(II) derivatives. The superhyperfine coupling pattern indicates the presence of three pyrrolic nitrogen donor atoms in the first coordination sphere. The coordination environment of copper(II) is square-pyramidal with the equatorial positions occupied by three nitrogen atoms plus one carbon atom and the apical position is occupied by the oxygen atom of the phosphine oxide. Importantly, the carbon atom located in the equatorial position approaches the copper(II) ion at a much shorter distance (2.2322 Å) than the sum of van der Waals radii (3.1 Å) reflecting the formation of a weak copper-carbon bond (red bond in Figure 51).

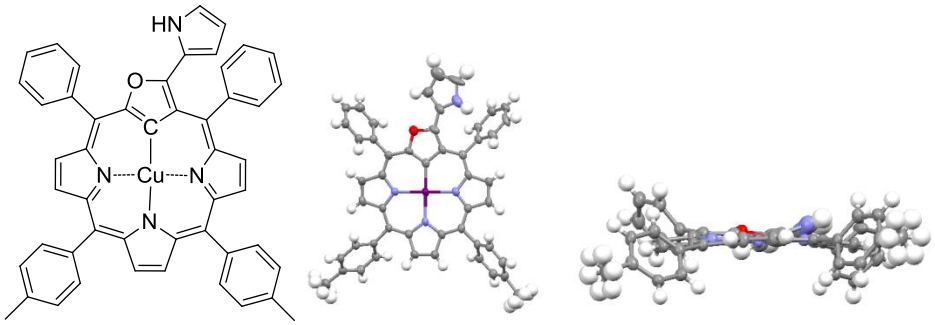

Figure 50: Copper(II) structure reported by Latos- Grażyński (schematic view and 50% thermal ellipsoids: perspective and side view) from reference 225.

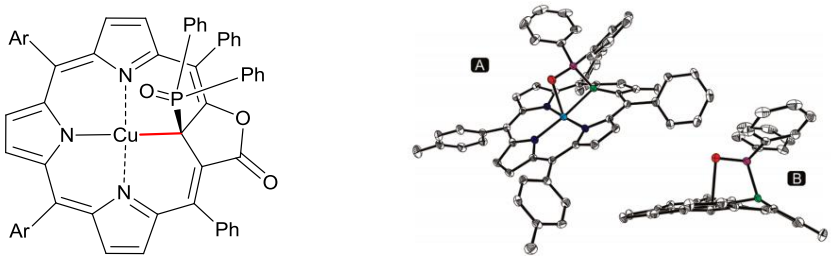

Figure 51: Schematic view and X-ray structure of a copper(II) complex bearing a weak Cu-C bond (from reference 226).

A different type of stable organometallic copper(II) species, containing bonds between a copper(II) center and neutral N-heterocyclic carbene (NHC) ligands, has been first described by Meyer and coworkers in 2003, with the isolation of complex $[(TIMEN^{Bz})Cu](OTf)_2$ (Figure 52).[227] Unfortunately this complex was not characterized by X-ray analysis but elemental analysis, low-temperature X-band EPR spectroscopy, and variable temperature SQUID magnetization measurements were reported. It should be remarked, however, that since the carbyl ligand in these complexes is a 2-electron donor (L-type ligand according to the Green nomenclature) rather than a one-electron (X-type) ligand such as an organic radical, these compounds cannot serve as model of OMRP dormant species or as unimolecular OMRP initiators.

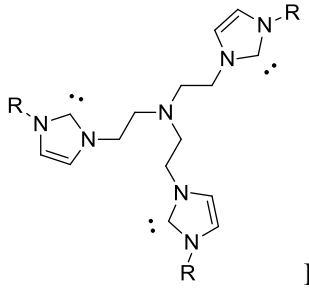

R = benzyl

Figure 52: Structure of tris-[2-(3-benzylimidazolium-1-yl)ethyl]amine carbene $[TIMEN^{Bz}]$.

The first X-ray structure of a copper(II) NHC complex was reported by Hoveyda's group.[228] It is a dimeric complex (Figure 53), isolated as a dark red air-stable solid. The copper atoms are

in a twisted configuration, between square planar and tetrahedral and the two copper-carbon bonds are 1.926(8) and 1.964(8) Å.

The second X-ray structure of a copper(II) NHC complex was described by Long and coworkers.[229] They isolated an air-stable purple monomeric copper(II) triflate salt (Figure 54). The 1.889(4) Å copper-carbon bond is, so far, the shortest one reported for an organometallic copper(II) compound. The EPR spectrum in frozen solution has apparent axial symmetry, with $g_{\perp} \approx 2$ .23 and $g_{||} \approx 2.08$. The copper ion resides slightly above the plane defined by the pyridine donors. Significant elongation (~0.2 Å) of two trans Cu─N bonds in the Py_4 plane is observed.

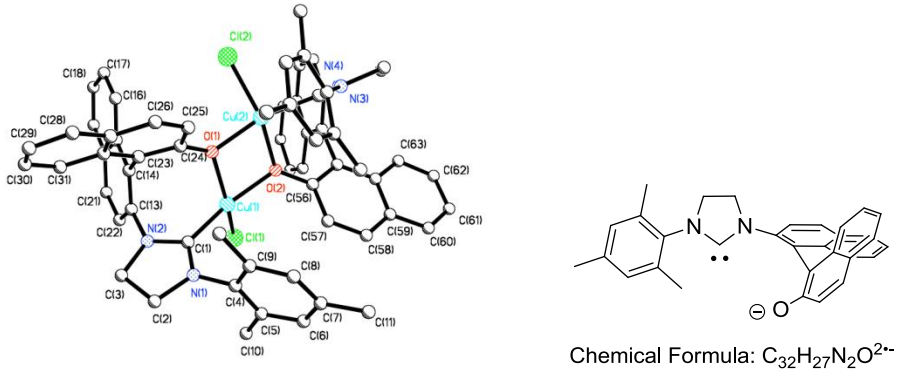

Figure 53: X-ray of the copper(II) complex and bidentate NHC ligand structure.

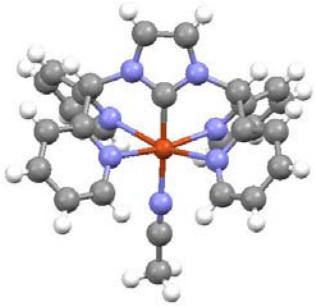

Figure 54: Structure of $[(Py_4Im)Cu(MeCN)](CF_3SO_3)_2$. The two counter anions and two THF molecules are omitted for clarity.

The last type of organometallic copper(II) species reported by Kinoshita and coworkers is a family of $[Cu^{II}(TPTM)X]$ complexes (TPTM = tris(2-pyridylthio)methanide; X = F, Cl, Br, I), which feature a novel Cu^{II}─$C(sp^3)$ bond with a trigonal bipyramidal structure (

Figure 55).[230,231] Only the X-ray structure of the cationic mononuclear complex $[Cu(TPTM)(MeCN)]PF_6$ was reported (Figure 56) with a Cu-C bond length equal to 2.004(3) Å. The structure indicates the presence of strong axial coordination causing a (dz^2) ground state. These complexes were synthesized by an uncommon general procedure with use of a starting copper(I) reagent mixed with the neutral TPTMH ligand under aerobic conditions, to form the copper(II) complex coordinated by the deprotonated TPTM ligand (

Scheme 21). The reaction was proposed to be catalyzed by copper(I).

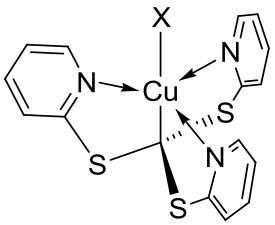

Figure 55: Structure of [Cu(TPTM)X] reported by Kinoshita in reference 230 (X = F, Cl, Br, I).

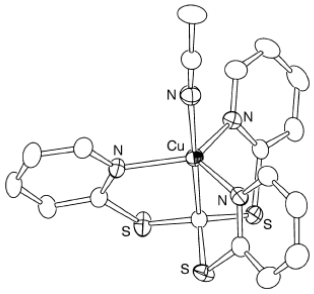

Figure 56: X-ray structure of [Cu(TPTM)(MeCN)]PF_6, counterion omitted.

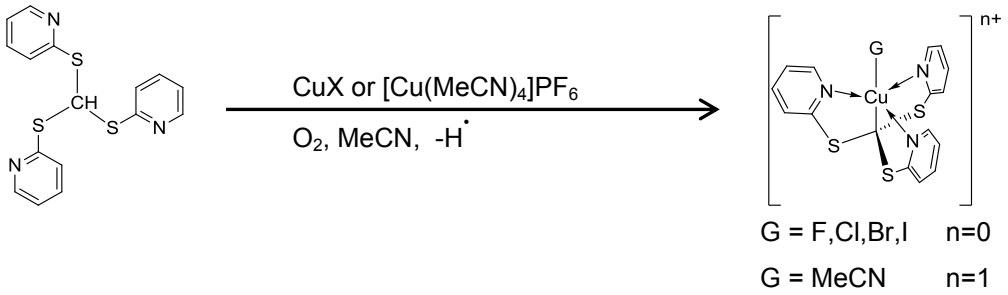

Scheme 21: Synthetic procedure for the family of copper complexes coordinated by TPTM.

In conclusion, seven crystallographic data collections of organometallic copper(II) compounds were found in the litterature. When the copper atom is surrounded by a confused porphyrin, the geometry is in the four cases square planar (Figure 47, Figure 48, Figure 50, and Figure 51). Trigonal bypiramidal (Figure 56) and distorted four-coordinate (Figure 53) or pseudo-octahedral (Figure 54) structures were reported when the copper atom is respectively coordinated by the anionic tris(2-pyridylthio)methanide and neutral NHC ligands.

2) General EPR features of copper(II) complexes

The Electron Paramagnetic Resonance (EPR) technique is similar to Nuclear Magnetic Resonance (NMR). The difference is that EPR probes the electron spin properties whereas NMR looks at the nuclear spin. EPR spectroscopy can be applied to organic molecules, inorganic materials or transition metal complexes so long as they possess at least one unpaired electron. It is the analysis of choice and a powerful tool in the study of the structure and environment of the cupric ion (electronic configuration $3d^9$). The theory, based on quantum mechanics, is not detailed here but the principal EPR spectrum characteristics are briefly

explained. The electron has mainly two types of motion. The first one is spinning around the nucleus, which brings about orbital magnetic moment. The other one is spinning around its own axis and gives spin magnetic moment. For a copper(II) ion, the total spin angular momentum is S = ½ with two possible projections along the z axis m_S = +½ and -½. There will be two degenerate energy states $E_{-1/2} = E_{1/2}$ but when an external magnetic field (B_0) is applied the degeneracy of the two energy states is removed (electronic Zeeman effect) (Figure 57).

Nuclei possessing a spin angular momentum exhibit additional splitting due to the nuclear Zeeman effect. Thus, when a nuclear spin of quantum number I interacts with the electronic spin, it perturbs the energy of the system in such a way that each electronic state is split into 2I+1 sublevels. Since the nuclear magneton is about 1000 times smaller than the Bohr magneton, the nuclear magnetic interactions are weak, so the energy separations between sublevels are small. Transitions involving these states give rise to hyperfine splitting in a well-resolved spectrum which is designated by "a". The hyperfine patterns are highly valuable when it comes to determining the spatial structure of paramagnetic species. Naturally abundant copper has two magnetic (I = 3/2) isotopes (^{63}Cu, 69.17%; ^{65}Cu, 30.83%) with very close values of the gyromagnetic ratio, giving rise to a single envelope of four resonances ((2 x N x I) + 1 = 4 with N = number of nuclei) in a 1:1:1:1 ratio for a mononuclear complex. In addition, the nuclear spin of nitrogen is also well known to interact with the spin angular momentum. The most abundant isotope of natural nitrogen ^{14}N (99.63%) has a spin of 1 and gives rise to a superhyperfine splitting designated by "a_N"

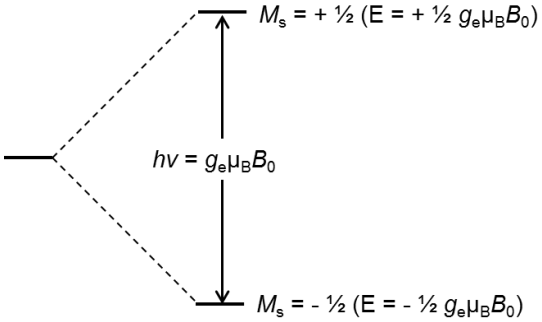

g_e = Free electron g factor = 2.0023193
μ_B = Bohr magneton = 9.274 x 10^{-24} J/T
B_0 = Applied external field (T)

Figure 57: Electronic Zeeman energy-level diagram.

Along this work, the g values were calculated using the formula $g = \frac{h\nu}{\mu B}$, where h = 6.626 × 10^{-34} J.s, μ = 9.274 × 10^{-24} J/T, ν = 9.5 GHz for the X-band microwave frequency used by our EPR instrument, and B is the field position where the g values are measured. Moreover, from quantum mechanics a simplified relation can be extracted for finding the modification of the g

value under the influence of spin-orbit coupling:

$$g_i = g_e \pm \frac{k\lambda}{E0-En} \qquad \text{where } i = x, y, z.$$

The signs + or – refer, respectively, to the mixing of the electron with an empty or filled orbital. The constant k defines the degree of orbital mixing the value of which can be taken from the magic pentagon (Scheme 22). E_0 and E_n are the energies of the ground state (where the electron stands) and the excited states (with which it may mix by spin-orbit coupling) so (E_0 - E_n) is always a negative value. The λ parameter is the spin-orbit coupling constant, which is negative for the d^9 configuration of the Cu^{II} ion where the unpaired electron can be either in the $d_{x^2-y^2}$ or in the d_{z^2} orbital. For a complex having a compressed octahedral, a tetragonal or a trigonal bipyramid symmetry, an unpaired electron residing in the d_{z^2} orbital yields $g_{\parallel} = g_e$ and $g_{\perp} = g_e + (6\lambda / (E(d_{z^2}) - E(d_{xz} \text{ or } d_{yz})))$. On the other hand, for an elongated octahedral, a square pyramid or a square planar symmetry, the unpaired electron resides in $d_{x^2-y^2}$; one can write $g_{\parallel} = g_e + (8\lambda / (E(d_{x^2-y^2}) - E(d_{xy})))$ and $g_{\perp} = g_e + (2\lambda/(E(d_{x^2-y^2}) - E(d_{xz} \text{ or } d_{yz})))$. According to this formula, both g values for tetragonal copper(II) complexes should always be greater than the free electron g value ($g_{\parallel}$, $g_{\perp} > g_e = 2.0023$).

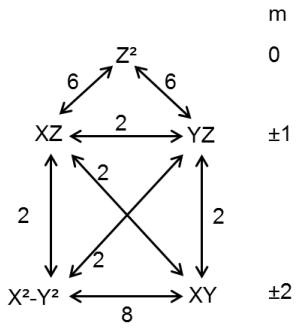

Scheme 22: Magic pentagon used to evaluate the value of k.

3) Studies on copper(II) alkyl complexes

Despite numerous efforts, we failed to isolate any copper(II) alkyl complex. We describe here the attempted experiments that partially confirmed the formation of copper(II) alkyl species thanks to EPR spectroscopy. Starting from copper(II) halides we have tried to exchange the halogen atom by a methyl group using either methyl lithium (MeLi) or a Grignard reagent. Cationic copper complexes were also investigated for the targeted alkylation reaction as they have a less bulky coordination sphere.

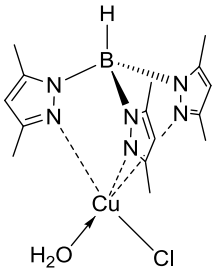

Figure 58: Proposed monomeric structure of [Tp*CuCl] hydrate inspired by the reported structure of [Tp^{iPr}CuCl(DMF)] in reference 232.

The first strategy attempted was a methylation using methyl Grignard reagent. To a brownish solution of dry [Tp*CuCl] was added at -40°C a solution of MeMgI ([Tp*CuCl] compound is brownish-blue solid. When completely dry and dissolved in a solvent it gives rise to a brown solution whereas when hydrated, the THF solution is more blue as in the case of [$CuCl_2$]). A white precipitate appeared which could be potentially assigned to MgICl salt (the expected side product). After the work-up (at -40°C) a solid which turned out to be a mixture of green and blue solids was recovered. The EPR spectrum of this solid is depicted as a blue line in Figure 59 together with the spectrum of the [Tp*CuCl] starting material. One can see that these two EPR spectra are completely different with a shift to higher fields upon alkylation. The spectrum of [Tp*CuCl] appears of low symmetry with a probable orthorhorbic g tensor, whereas the spectrum of the product appears of essentially tetragonal symmetry with $g_{\|}$ = 2.067, $g_{\perp}$ = 2.282, and a measurable Cu hyperfine coupling for the parallel component of approximatively $a_{Cu\|} \approx 160$ G. The g tensor values and hyperfine coupling constants are also reported in Table 9, page 100. The EPR spectrum of the reaction product was succesfully simulated using Easyspin® whereas the starting [Tp*CuCl] simulation was attempted with no success. A reason of the difficulties encountered for [Tp*CuCl] EPR spectrum simulation is the potential presence of two different species (i.e. a tetracoordinated [Tp*CuCl] and a pentacoordinated [Tp*CuCl(THF)]) which yield a complex EPR spectrum made of a mix of two different EPR prints. Indeed, Kitajima and Moro-oka have reported a marked difference for the EPR spectra of [Tp^{iPr}CuCl] recorded in dichloromethane (DCM) and in DMF solution.[232] The EPR spectrum was either orthorombic in DCM (spectrum A in Figure 60) or axial in DMF (spectrum B in Figure 60) because of the coordination of a DMF molecule to the copper center. The coordination geometry of [Tp^{iPr}CuCl] is described as a slightly elongated tetrahedron whereas the pentacoordinated [Tp^{iPr}CuCl(DMF)] has a square-pyramidal geometry with one pyrazole nitrogen atom as an apical donor. Only one additional EPR study appears to be reported in the literature for a scorpionate copper(II) chloride complex, [$CuTp^{H}Cl]_2$, which remains as a chloride-bridged dimer in DCM solution. The

geometry about each copper approximates that of a distorted square pyramid and the EPR spectrum exhibits two poorly resolved lines at g = 2.10 and g = 2.29 and, in addition, a ΔM_s = 2 transition is seen at g = 4.19 in agreement with a copper(II) dimer.[233]

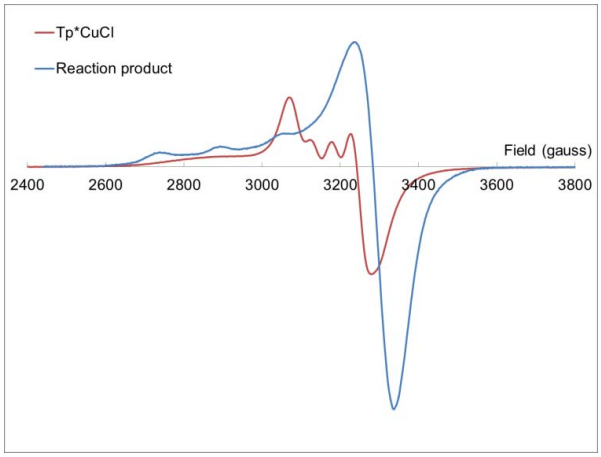

Figure 59: EPR spectra of [Tp*CuCl] and of the methylation product (THF solution, 150K).

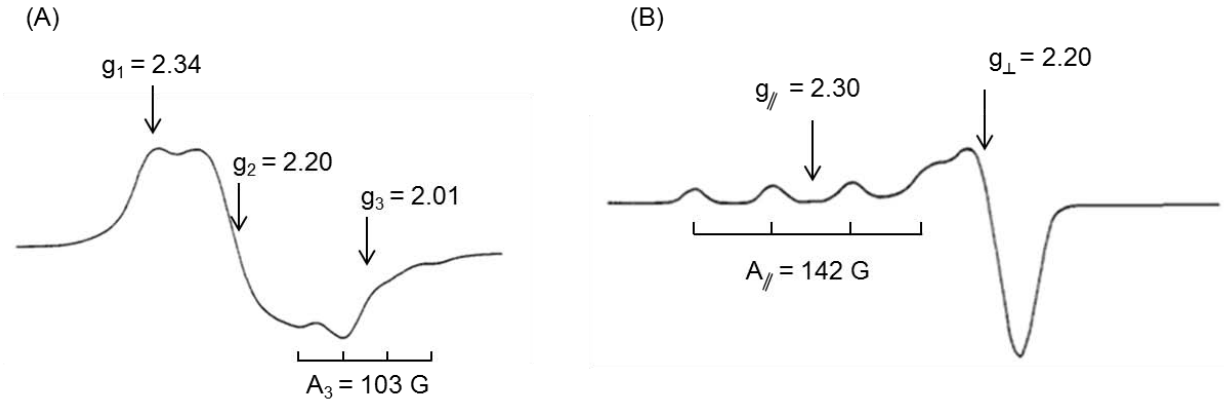

Figure 60: EPR spectra recorded at 77 K: (A) [Tp^{iPr}CuCl] in CH_2C1_2; (B) [Tp^{iPr}CuCl(DMF)] in DMF. Taken from reference 232.

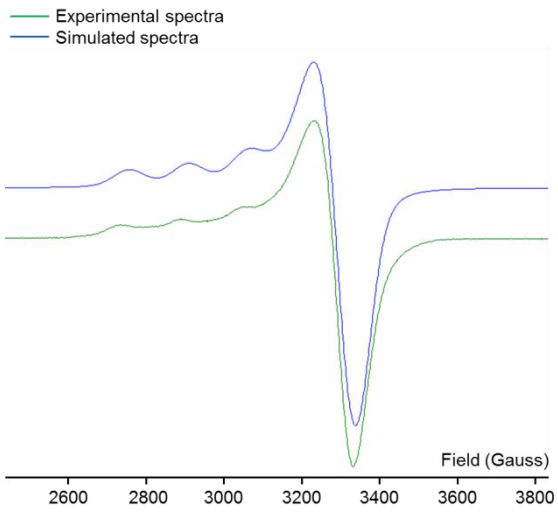

Figure 61: Experimental and simulated spectrum of the reaction product. Spectrum have been shifted along the ordinate for clarity.

Both simulated and experimental spectra for the alkylation product, Tp*Cu(CH_3), are superimposed in Figure 61. There is an excellent correlation between both spectra with a root-mean-square-deviation (RMSD) below 0.34. The simulated spectrum has an almost perfect axial symmetry with $g_\perp$ = 2.055 (± 0.001) and $g_\parallel$ = 2.266. The perpendicular hyperfine coupling component ($a_\perp$) has been set to zero for consistency. When $a_\perp$ was allow to vary, its value was very close to zero without affecting the RMSD value so much ($\Delta_{RMSD} < 0.01$). The parallel component $a_\parallel$ is equal to 471.591 MHz i.e. 149.7 Gauss.

No direct indication of the presence of the putative methyl group attached to copper can be seen on the spectrum (e.g. superhyperfine coupling with the H atoms). However, it is clear that a reaction occurs between [Tp*CuCl] and MeMgI and that the product is stable at least below -40°C. Indeed, when the solid product was allow to warm up at room temperature, the color changed which probably indicates a degradation of the product.

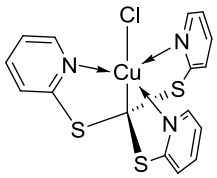

Figure 63: Structure of [(TPTM)CuCl].

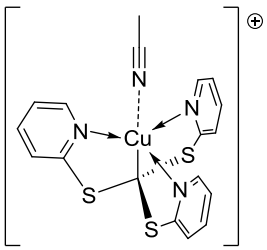

Figure 62: Structure of [(TPTM)Cu(MeCN)]BF_4, counterion omitted.

We have subsequently investigated the alkylation of the known [(TPTM)CuCl] complex (Figure 63)[230] by MeLi at -30°C. No visible color change was observed. The EPR spectrum, of essentially cubic symmetry, shows only minor differences compared to the sarting copper halide (Figure 64), suggesting that essentially no reaction took place in this case (values are reported in Table 9, page 100).

On the other hand, when MeLi was added to [(TPTM)Cu(MeCN)]BF_4 (Figure 63) at -50°C, there was no visible color modification but the EPR spectrum revealed a significant change (Figure 65). The spectrum of [(TPTM)Cu(MeCN)]BF_4 has a nearly cubic g tensor, with g_{iso} = 2.083 whereas the EPR spectrum of the product shows tetragonal symmetry with $g_\perp$ = 2.084, $g_\parallel$ = 1.995 and hyperfine coupling constants ranging from 11 to 15 gauss (values are reported in Table 9, page 100). This rich hyperfine structure is consistent with the interaction of the unpaired electron with the three nitrogen atoms and/or with the methyl group H atoms. However, the complexity of the spectrum did not allow a satisfactory simulation in order to

discern the exact nature of the nuclear spin system. The solution mixture was allowed to slowly warm up from -50°C to +1°C over a few days. The EPR monitoring showed that the product is stable for almost 2 days at -25°C, but then a dramatic change occurred upon warming to +1°C, the final spectrum being close to that of the sarting material except for a shoulder at high field (Figure 66).

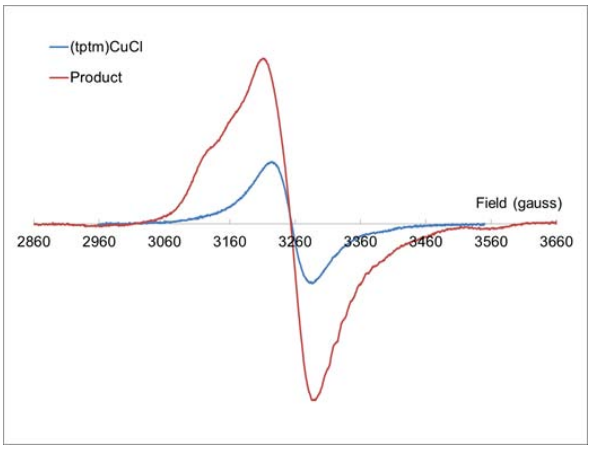

Figure 64: EPR spectra of [(TPTM)CuCl] and of the methylation product (THF solution, 150K).

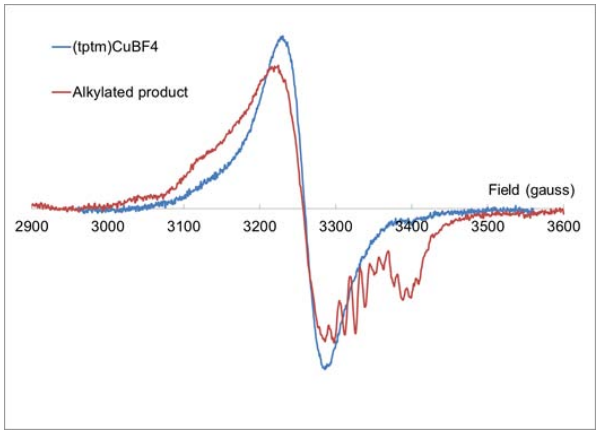

Figure 65: EPR spectra of [(TPTM)Cu(MeCN)]BF_4 and its methylated product (THF solution, 150K).

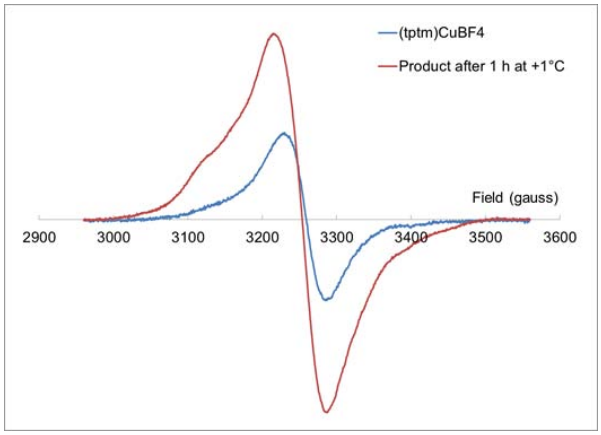

Figure 66: Decomposition of the methylated product.

We can conclude from this experiment that the putative [(TPTM)CuMe] complex is stable below -20°C but suffers from thermal degradation at higher temperatures. The methylation reaction seems less favoured on the copper(II) halide than on the cationic complex [(TPTM)Cu(MeCN)]BF_4. This is understandable since the coordination sphere is full in the chloride complex and the chloride ligand is strongly bound, whereas a coordination site is more accessible in [(TPTM)Cu(MeCN)]BF_4 since only a weakly binding acetonitrile molecule has to be displaced.

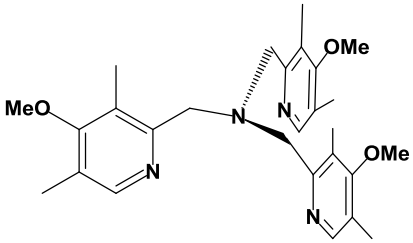

Figure 67: Tris((4-methoxy-3,5-dimethylpyridin-2-yl)methyl)amine, TPMA*.

Following this interesting results with copper complexes coordinated by TPTM ligand, another cationic copper complex was investigated. In situ generated [(TPMA*)CuCl]PF_6 (ligand depicted in Figure 67) was reacted with 1.2 equivalent of MeMgBr solution. The starting bright yellow solution of copper complex turned more pale yellow (slightly greenish). When a drop of the Grignard solution fell into the copper solution, a green color diffused from the whirl indicating that a reaction occurred. The reaction was monitored by EPR before and after the dropwise addition of the Grignard reagent (Figure 68, Table 9, page 100). A comparison of the two spectra shows that the global intensity has decreased to about half and the spectra resolution has increased but there is close correspondence between all minima and maxima in the two spectra, suggesting that the reaction occurs with a 2:1 stoichiometry (2 MeMgBr molecules per each $[(TPMA^*)CuCl]^+$ ion). The product of this reaction is not visible in the spectrum, suggesting that it is not a soluble paramagnetic complex. A possible interpretation of this phenomenon is that, following a first alkylation reaction to yield a putative $[(TPMA^*)Cu(CH_3)]^+$ complex, a second Me group is added to the system, possibly under the Coulombic driving force, to yield an unstable dimethyl species $[(TPMA^*)Cu(CH_3)_2]$ that decomposes immediately by ethane reductive elimination with formation of a Cu^0 precipitate. An alternative possibility is the intervention of a single electron transfer (SET) process between the first Cu^{II} intermediate, $[(TPMA^*)Cu(CH_3)]^+$, and a second equivalent of MeLi, leading to a diamagnetic $(TPMA^*)Cu^I(CH_3)$ product and a methyl radical which is then rapidly quenched. This pathway would be promoted by the very

strong electron donating power of the TPMA* and CH_3^- ligands, making the first Cu^{II} intermediate very easily reducible.

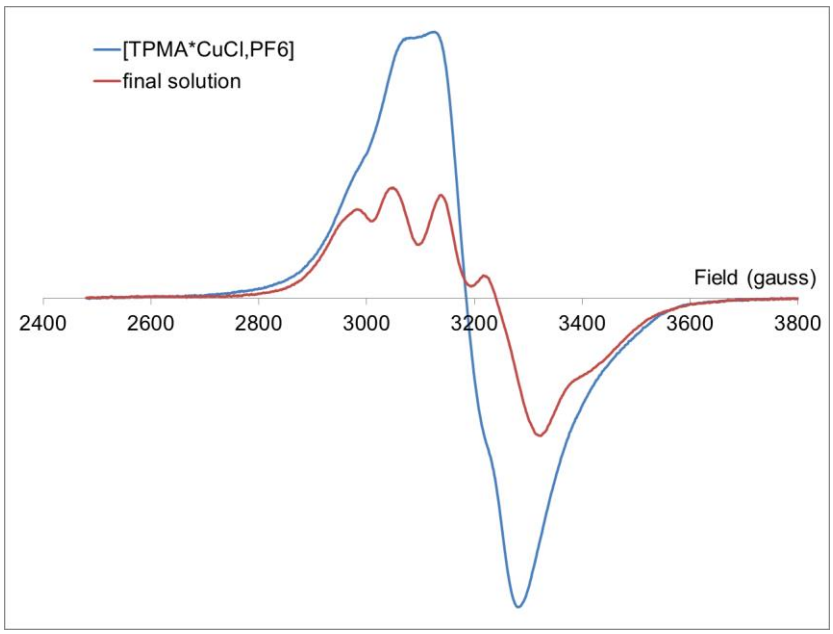

Figure 68: EPR spectra of the initial [(TPMA*)CuCl]PF_6 solution and of the final solution after reaction with 1 equivalent of MeMgBr (THF solution, 150K).

In conclusion, depending on the ligand surrounding the copper atom, more or less clear evidence of copper-carbon bond formation by alkylation of suitable Cu^{II} cationic or neutral chloride precursors has been obtained by EPR spectroscopy. Although we failed to isolate any copper(II)-alkyl species, we are now conviced that such a species can be formed and that an OMRP equilibrium can be established with the complexes studied under appropriate conditions. The copper complex with Tp* ligand has shown interesting properties toward alkylation. Thus, the copper(I) complex $[Tp^*Cu]_2$, which is in fact dinuclear as an isolated solid,[234] gave promising results for the OMRP of either ethylene or vinyl acetate as described in the second chapter.

4) Studies on copper species during polymerization

As already discussed in the general introduction, different mechanisms of control can interplay during polymerization. We have shown along this work that copper(I) complexes can trap radical growing chains to form an alkyl copper(II) dormant species. Copper is also the metal of choice for ATRP and could be, moreover, involved in a CCT mechanism. The Cu(I) complex obtained in situ from Cu(I) and tris((4-methoxy-3,5-dimethylpyridin-2-yl)methyl)amine (TPMA*, Figure 67) is currently the most reducing and the most active catalyst for ATRP. Matyjaszewski, Poli and coworkers have recently shown that this complex

(obtained in situ) is strongly slowing down the polymerization rate of butyl acrylate (BA) when used under OMRP conditions.[235] In addition to the rate moderation effect, however, it was found that the rate of polymerization and also the average molecular weight of the isolated polymer are inversely proportional to the concentration of the copper species. On the basis of these results, the authors concluded that the metal is also responsible for an additional and previously not appreciated phenomenon, a catalytic action on the bimolecular radical termination process. The phenomenon is due to the formation of an organometallic copper(II) complex which is capable to intercept an additional radical species and/or due to a catalytic chain transfer reaction which involves the formation a copper-hydride complex, which is in turn able to intercept a radical (Scheme 23).

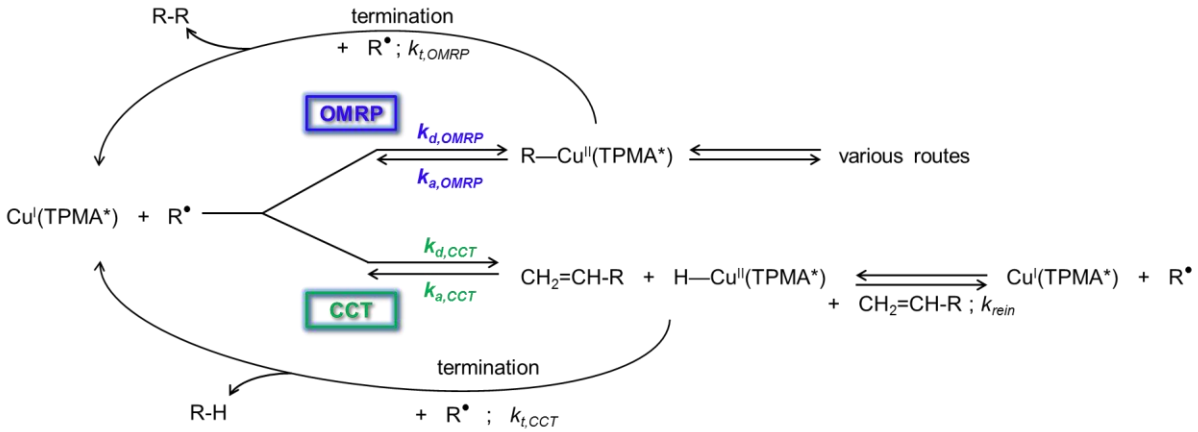

Scheme 23: Proposed mechanism pathway of AIBN initiated BA polymerization.

We decided to check which of the OMRP and/or CCT pathway was involved (i.e. the presence of either alkyl copper(II) and/or copper-hydride complexes) by direct EPR analysis of the medium under the same experimental conditions. With a [BA]/[AIBN]/[TPMA*]/[Cu(MeCN)$_4$]BF$_4$ ratio of 160 : 0.2 : 0.06 : 0.016 the solution color changed rapidly from colorless to light purple at 60°C. After 20 hours reaction, the polymerization was stopped and a sample was taken for the EPR analysis in THF frozen solution. First of all, the purple color of the medium is reminiscent of the colors reported for various organometallic copper(II) complexes (dark-red,[228] purple[229,230]). The recorded EPR spectrum (Figure 69) is complex, showing seven lines correponding to hyperfine coupling constant to copper. Therefore, this EPR spectrum confirms presence of copper(II) complex(es) in the polymerization reaction. However, the formation of either a copper-alkyl complex [R-Cu^{II}/TPMA*] and/or a copper-hydride [H-Cu^{II}/TPMA*] could not be elucidated.

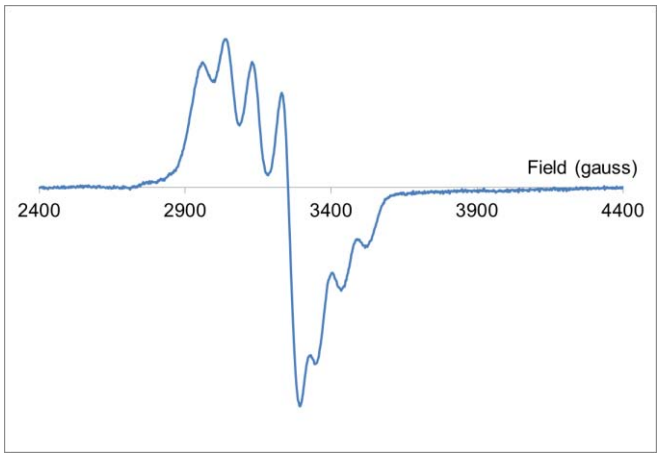

Figure 69: Spectrum of the polymerization medium for the polymerization of BA initiated by AIBN in the presence of $[Cu(MeCN)_4]^+$/TPMA* (THF solution, 150K).

In conclusion of this study on « elusive alkyl-copper(II) », the reader would agree that "elusive" can now be omitted. Indeed, we have fully described the seven crystallographic data reported in the litterature on isolated copper complexes containic a cupric-carbon bond. Although we have shown spectroscopic evidences of the targeted alkyl-copper(II) formation, more work is needed to isolate a species which could serve as a unimolecular initiator under OMRP conditions. However, copper(I) complexes are well-known and can be synthesized and used along with radical initiators under "Reverse" OMRP conditions. This is indeed what we have done in the next chapter.

Table 9 : RPE parameters extracted from spectra discussed in this section.

Copper complex	g tensor		Hyperfine couplings	Figures
[Tp*CuCl] [a]	$g_{\|\|}$ = 2.086	$g_{\perp}$ = 2,151	$a_{\perp} \approx$ 50 G	59
[Tp*Cu-Me] [b]	$g_{\|\|}$ = 2.067	$g_{\perp}$ = 2.282	$a_{\|\|} \approx$ 160 G	59, 61
[Tp*Cu-Me] simulated	$g_{\|\|}$ = 2.055	$g_{\perp}$ = 2.266	$a_{\|\|} \approx$ 150 G	61
[(TPTM)CuCl] [a]	g_{iso} = 2.085			64
$[(TPTM)Cu(MeCN)]BF_4$ [a]	g_{iso} = 2.083			65
[(TPTM)Cu-Me] [b]	$g_{\|\|}$ = 1.995	$g_{\perp}$ = 2.084	$a_{\|\|} \approx$ 11-15 G	65, 66
$[(TPMA^*)CuCl]PF_6$ [a]	$g_{\|\|}$ = 2.095	$g_{\perp}$ = 2,192	$a_{\perp} \approx$ 68-80 G	68

All spectra recorded in THF at 150 K. [a] Experimental spectra of isolated complexes. [b] Experimental spectra of the crude product of alkylation.

CHAPTER II

COPPER IN CONTROLLED RADICAL POLYMERIZATION OF LESS REACTIVE MONOMERS

CHAPTER II: COPPER IN CONTROLLED RADICAL POLYMERIZATION OF LESS REACTIVE MONOMERS

In this chapter, copper(I) complexes are, for the first time, investigated as controlling agents (CA) for vinyl acetate (VAc) and ethylene polymerization under an OMRP strategy (Scheme 18, page 84). The copper-catalyzed ATRP of VAc has been attempted but is generally unsuccessful[130] except for the terpyridine Copper(I)halide system[132] which yield PVAc with high conversion (~ 75%) and moderate dispersity value (Đ = 1.7) for a low degree of polymerization (X_n = ~ 120). The polymerization of ethylene catalyzed by copper complexes was reported by the groups of Stibrany and Gibson employing either [(bisbenzimidazole)$CuCl_2$] systems[236,237] or [(α-diimine)$CuCl_2$].[238] Since then, several other reports have emerged of [$LCu^{II}Cl_2$] or [L_2Cu^{II}] complexes employing salicylaldiminato,[239] pyrazolylpyrimidine,[240,241] and chiral pyrazolylquinoline ligands[242] that were also active for ethylene polymerization. In all cases, methylaluminoxane was used as a cocatalyst with moderate to very low activities and high polymer molecular weights reported. No mechanism for polymerization was deduced, although a coordination/insertion mechanism was postulated in some cases. However, the contribution of copper in this coordination/insertion mechanism has been questioned.[243]

Our target is to obtain a living polymerization which is indicated by polymers with an ideal dispersity (*i.e.* as close as possible to Đ = 1), the predictability of the molecular weight from the CA/initiator ratio, a linear molecular weight-conversion profile (*i.e.* a constant radical concentration), and the possibility to synthesize block or higher molecular weight polymers by further monomer addition.

1) Vinyl acetate polymerization

Copper complexes are heavily used in ATRP (see general introduction). In 1998, a report pointed to the possibility of an interaction between an organic radical and a copper(I) complex in the absence of halogen atoms.[56] Diminished polymerization rates for methyl acrylate initiated by AIBN[114] were observed in the presence of [$Cu^{I}OTf$] complexes with di-*tert*-butyl-2,2′-bipyridine ligand (Figure 70), implying a reversible trapping of the growing radical chains by the metal. Fourteen years later, while studying on the potential interplay between ATRP, OMRP, and CCT mechanisms, Matyjaszewski *et al.* proposed the reversible formation

[114] AIBN half-life in toluene at 60°C equal 2 000 min or 33 h 20.

of a dormant [R-Cu^{II}(TPMA*)] species and this is consistent with our EPR studies reported in the last section of chapter I.

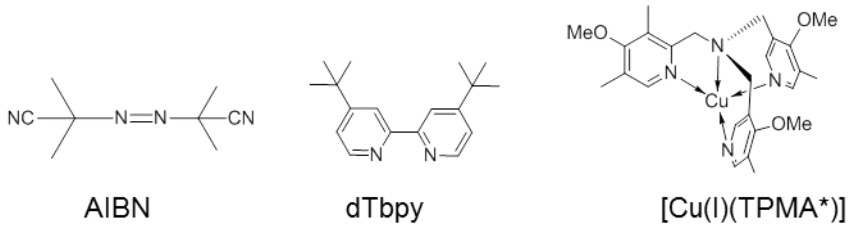

Figure 70: Compounds used in former studies on OMRP ; AIBN = 2,2'-azobiisobutyronitrile ; dTbpy = di-*tert*-butyl-2,2′-bipyridine; TPMA* = tris((4-methoxy-3,5-dimethylpyridin-2-yl)methyl)amine.

For our study of vinyl acetate polymerization under OMRP conditions, we decided to investigate the copper(I) complexes depicted in Figure 71. Anionic tris(pyrazolyl)borate (scorpionate)[244] and β-diketiminato ligands have been chosen. The β-diketiminato ligand framework is commonly called NacNac$^{RR'}$ (with R and R' being the two substituents on the nitrogen atoms) in reference with its oxygen analogue: the acetylacetonato (acac). NacNac ligands can be easily synthesized by condensation of the appropriate amine with acetylacetone.[245] All the complexes used are free from any halogen atom to avoid any unwanted ATRP process.

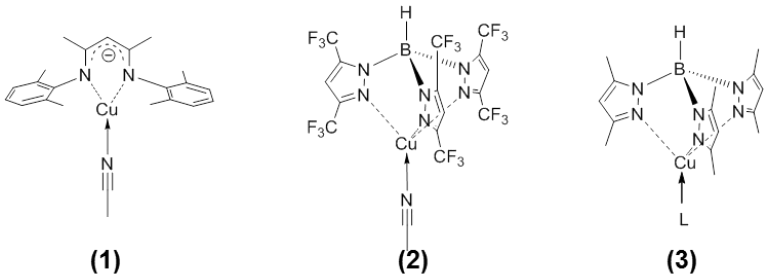

Figure 71: Copper(I) complexes tested in OMRP, (1) = (*N*-[3-[(2,6-dimethylphenyl)amino]-1-methyl-2-buten-1-ylidene]-2,6-dimethyl-benzenamine)(acetonitrile)copper(I) [CuNacNac^{XylXyl}(MeCN)]; (2) = Hydrotris(3,5-bis(trifluoromethyl)pyrazol-1-yl)-borato](acetonitrile)copper(I) [CuTp^{CF3}(MeCN)]; (3) = Hydrotris(3,5-dimethylpyrazol-1-yl)-borato]copper(I) with L = H_2O, MeCN, THF [CuTp*L] or no L gives the dimer [CuTp*]$_2$.

Complex **(1)** (Figure 71) was the first system screened as a controlling agent for the OMRP of vinyl acetate. By analogy with the reported x-ray structure of the neutral ethylene adduct[246] or triphenylphosphine adduct[247] of copper(I) complexes coordinated by the NacNac^{XylXyl} ligand, we propose that our synthesized acetonitrile adduct[248,249] should have a trigonal planar geometry with coordination of two nitrogen atoms from the NacNac^{XylXyl} ligand and one oxygen atom from the THF molecule. If the growing PVAc radical chains are trapped by this copper(I) complex, an organometallic copper(II) dormant species will be formed with a

coordination number of three or four (depending on the possible chelation via the carbonyl group of the Cu-bonded monomer from the PVAc chain or coordination of a solvent molecule). Three-coordinate copper(II) complexes are known to adopt a trigonal geometry, whereas four-coordinate complexes adopt usually a distorted square planar geometry. In any case, no considerable rearrangement of the coordination sphere is needed during this radical trapping process.

The VAc polymerization was first conducted in toluene with a [Cu] / VAc / V-70 ratio of 1 : 500 : 0.7 and a VAc/toluene ratio of 15:85 v/v. Started at 30°C, the polymerization rate was rather slow because of the highly diluted system. Indeed, only 1% of the monomer was consumed after 48 hours. However, the solution color changed from a clear yellow to a more brownish color, potentially indicating the transformation of the copper(I) complex into a copper(II) organometallic dormant state. The radical initiator used (V-70) has a 10 hours half-life time in toluene at 30°C. Moreover, because of cage effect,[250] its efficiency factor is equal to 0.6 in benzene[73] meaning that 40 % of the radicals produced by decomposition of the V-70 terminate by bimolecular coupling and are thus unable to initiate the polymerization of VAc. After 48 hours at 30°C, approximatively 95 % of the radicals have been produced (100 % radicals produced = total decomposition of the 0.7 equivalent of V-70). When comparing with a blank reaction in the absence of copper (VAc / V-70 ratio of 500 : 0.7; VAc/toluene = 40:60 v/v), the medium became too viscous and the reaction had to be stopped after 47 hours at 30°C yielding 34 % of monomer conversion. Hence, the polymerization is much slower in the presence of copper, confirming the occurrence of radical trapping processes. In consequence, the medium temperature was gradually increased to reach 50°C to probe for the reversibility of the radical trapping. The VAc conversion rate increased when the polymerization temperature was raised to 40 and 45°C but then seemed to slow-down again when the temperature was set at 50°C (Figure 72). The accuracy of the measurement for such low conversions (~ 3%) may be in question. Anyway, the polymerization definitely continues beyond 100 h and without the addition of any fresh initiator, after being set at 40 and then 45°C for ca. 50 h. The V-70 radical initiator has a half-life of 3 hours at 40°C. We can consider that, with the applied temperature, there is no more V-70 after 60 hours of reaction time but VAc is still consumed (albeit very slowly) after this period which means that radicals continue to be reversibly generated from a dormant species. Nevertheless, the molecular weights obtained are around ten times higher than the theoretical one (Figure 73) which implies poor control. As copper complexes are studied as OMRP controlling agents for VAc for the first time, we can only compare the results with PVAc obtained by OMRP with

cyclopentadienyl chromium β-diketiminate complexes [$CpCr^{II}(NacNac^{XylXyl})$] which is coordinated by the same NacNac ligand or by [$Co^{II}(acac)_2$] which gives the best control so far (see general introduction pages 63-66). The Cr^{II} complex leads to about 15% conversion after ca. 400 h at room temperature (polymerization initiated by [$CpCr^{II}(NacNac^{XylXyl})(CH_2tBu)$],[66] whereas [$Co(acac)_2$] gives rise to a faster polymerization, the rate of which depends on the nature of ligand additives. For instance, in the presence of 60 equiv of DMSO the conversion was ca. 60% at 30°C after 7h.[251] This suggests that the OMRP equilibrium is more shifted toward the dormant species for [PVAc-$Cu^{II}(NacNac^{XylXyl})$] than for [PVAc-$Cr^{III}Cp(NacNac^{XylXyl})$] and especially [PVAc-$Co^{III}(acac)_2$] or otherwise stated that the PVAc-Cu^{II} bond is stronger than the other bonds. In conclusion, our results show the ability of the copper complex [$Cu^{I}(NacNac^{Xyl,Xyl})(MeCN)$] to trap the growing PVAc radical chains and to release them back into solution, but the polymerization rate and the controlling ability of this system are way too limited.

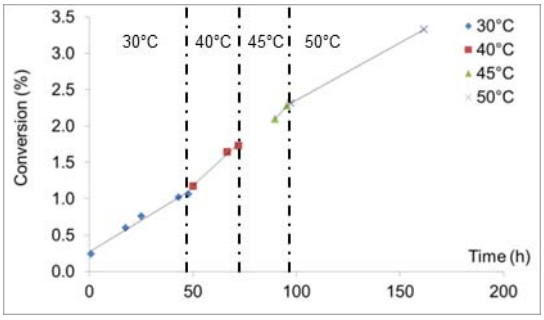

Figure 72: Conversion of vinyl acetate vs. time (conditions: 30-50°C, [Cu(NacNacXylXyl)(MeCN)] / VAc / V-70 = 1 : 500 : 0.7; VAc/toluene = 15:85 v/v).

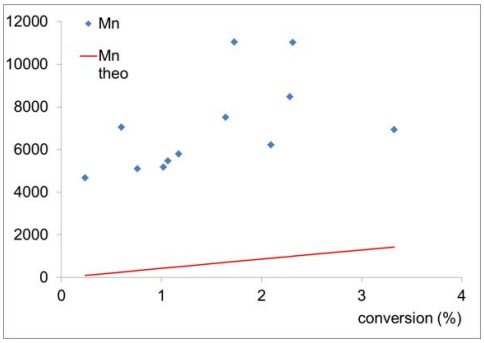

Figure 73: PVAc experimental (blue dots) and theoretical (red line) molecular weights (conditions: [Cu($NacNac^{Xyl,Xyl}$)(MeCN)] / VAc / V-70 = 1 : 500 : 0.7; VAC/toluene = 15:85 v/v).

In extension of the discussed results with the β-diketiminate copper(I) complex, additional copper(I) complexes with three coordinated scorpionates ligands were investigated. This type of complexes possesses a higher coordination number compared to the β-diketiminate copper(I) complex. The crystallographic structure of [$Cu(Tp^{CF3})$(MeCN)] reported by Pintauer *et al*. shows a distorded tetrahedral geometry.[252] With a [Cu] / VAc / V-70 ratio of 1 :

500 : 0.8, the bulk polymerization at 30°C led to a >70% conversion in 25 h at 30°C. This immediately proves that the [PVAc-$Cu^{II}(Tp^{CF3})$] bond, if it forms, is much weaker than the [PVAc-$Cu^{II}(NacNac^{XylXyl})$] bond. The polymerization rate is essentially identical to the control experiment realized under the same conditions but without the presence of copper (Figure 74). Therefore, we cannot make clear conclusions about the trapping of the PVAc radical chains by the [$Cu(Tp^{CF3})$(MeCN)] complex. The polymerization was characterized by an essentially linear molecular weight – conversion profile (Figure 75) although the extrapolated M_n value at zero conversion is not zero. The M_n values are compared with the theoretical ones shifted by 82 330 g/mol (the origin value of the experimental linear fit curve). This is consistent with the poorly effective trapping of the growing radical chains by the copper(I) complex. The PVAc dispersity was low and remained more or less constant (Đ = 1.2-1.3) throughout the polymerization, indicating that perhaps a small degree of control on the polymerization process is imparted by the copper complex.

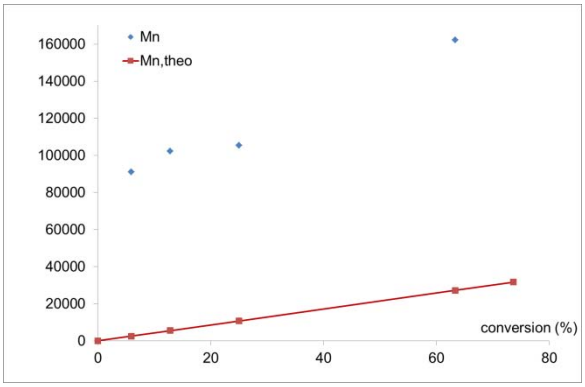

Figure 74: PVAc molecular weights evolution with VAc conversion ([$Cu(Tp^{CF3})$(MeCN)] / Vac / V-70 = 1 : 500 : 0.8 in bulk) (Blue dots). Theoretical molecular weights (red line).

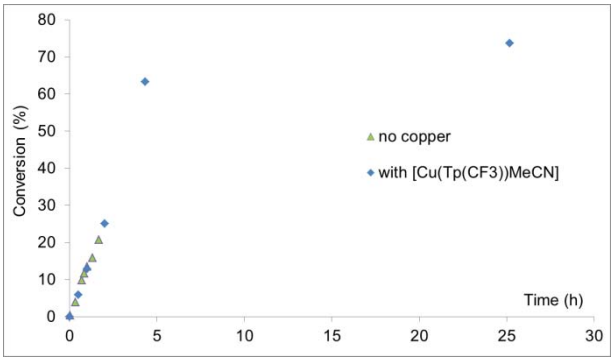

Figure 75: Kinetic profile of VAc polymerizations with [$Cu(Tp^{CF3})$(MeCN)] and without copper ([Cu] / VAc / V-70 = 1 : 500 : 0.8 or VAc / V-70 = 500 : 0.8 in bulk at 30°C).

The same conditions ([$Cu(Tp^{CF3})$(MeCN)] / VAc / V-70 = 1 : 500 : 0.8) were repeated in a diluted medium (with 75% weight of toluene), however the results did not show any living polymerization behavior: the ($\ln([Vac]_0/[Vac])$ *vs.* time plot is not linear although it could be seen as the sum of two linear curves with two different slopes (Figure 76) and the molecular weights did not increase linearly with conversion. However, the polymer dispersity continuously decreased with conversion to yield a PVAc final dispersity value around 1.5.

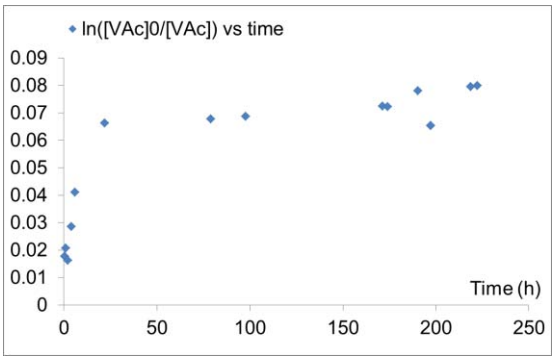

Figure 76: Linear correlation of $\ln([VAc]_0/[VAc])$ *vs*. time in diluted polymerization of VAc with [30°C, $Cu(Tp^{CF3})(MeCN)$] (30°C, [Cu] / VAc / V-70 / THF = 1 : 500 : 0.8 : 75%w).

More interesting results were obtained with the methyl analogue, $[CuTp^*]_2$.[234] The trifluoromethyl groups on the pyrazole rings are replaced by methyl groups leading to a substantial change of the ligand electronic properties but no significant steric change. The methyl groups are rather electron donating whereas the trifluoromethyl groups are electron-withdrawing. Thus the three nitrogen atoms of Tp* are more strongly coordinated to the copper center than those of Tp^{CF3}. Indeed, the copper-nitrogen bonds in $[CuTp^*(C_2H_4)]$[253] are shorter than in $[CuTp^{CF3}(C_2H_4)]$[254] with average values of 2.073 Å and 2.108 Å respectively. If the Tp* ligand is more electron donating, then the copper(II) state should be more stabilized shifting the OMRP equilibrium toward the dormant state and the polymerization should be slower. Indeed, with [CuTp*] in bulk at 30°C ($[CuTp^*]_2$ / Vac / V-70 = 0.5 : 500 : 0.7), the apparent rate of polymerization was slower than the rate of polymerization using $[Cu(Tp^{CF3})(MeCN)]$ and slower than in the control experiment without the copper complex. Moreover, there is a linear correlation between $\ln([Vac]_0/[Vac])$ and time (*i.e.* a constant radical concentration) (Figure 77). Judging from the rate of polymerization, the [PVAc-$Cu^{II}(Tp^*)$] bond is stronger than the [PVAc-$Cu^{II}(Tp^{CF3})$] bond, although much weaker than the [PVAc-$Cu^{II}(NacNac^{xyl,xyl})$] bond.

Again, when the system was diluted in toluene (~ 20:80 v/v), the control of the polymerization was not improved. The radical concentration was constant as shown by the linearity of the first order kinetic plot, but the molecular weight of the polymer did not increase linearly with the monomer conversion. However, we still observed a decrease of the polymer dispersity along with the monomer conversion with a final value at 1.8 (Figure 78).

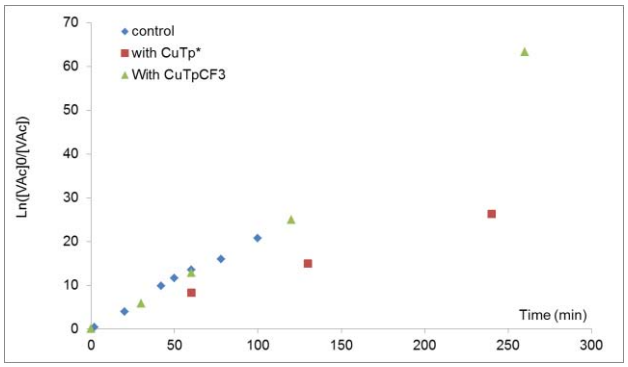

Figure 77: Linear correlation of ln([VAc]$_0$/[VAc]) *vs*. time in bulk polymerizations of VAc with [Cu(Tp^{CF3})(MeCN)], [CuTp*]$_2$ and without copper (30°C, [Cu] / VAc / V-70 = 1 : 500 : 0.7).

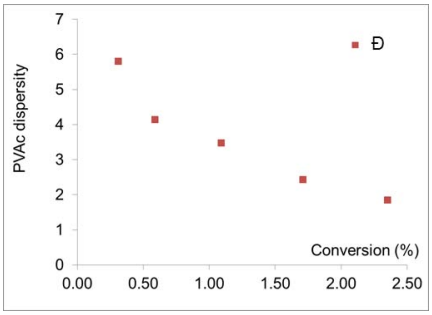

Figure 78: Dispersity evolution of PVAc obtained from polymerization [CuTp*]$_2$ in diluted medium (30°C, [CuTp*]$_2$ / VAc / V-70 / toluene = 0.5 : 500 : 0.7 : 80%v).

The polymerization rate decrease, when [CuTp*] was added in the medium compared to the experiment without copper is evidence of PVAc radical chain trapping by the copper complex. However, the variation of the M_n with conversion and the high Đ values demonstrate poor control. The temperature influence during bulk polymerization of VAc using [CuTp*]$_2$ as controlling agent was investigated.

At 50°C ([CuTp*]$_2$ / VAc / V-70 = 0.5 : 500 : 0.7), the apparent rate of polymerization was again lower in the presence of [CuTp*]$_2$ than with the absence of copper. The less pronounced retardation, compared to the polymerization experiment at 30°C, is consistent with a greater activation equilibrium constant ($K_{OMRP}(50°C) = k_{act}/k_{deact} > K_{OMRP}(30°C)$). Moreover, there is still a linear correlation between ln([Vac]$_0$/[Vac]) and time (Figure 79).

At 70°C, the apparent rate of polymerization is also lower than the one of the control experiment with no copper and the retardation is even less pronounced than at 50°C (Figure 80). There is again a linear correlation between ln([Vac]$_0$/[Vac]) and time (Figure 81).

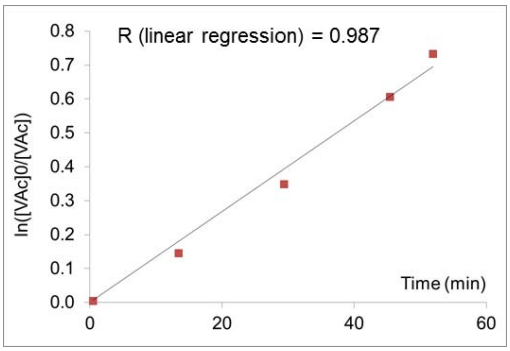

Figure 79: Linear correlation of $\ln([VAc]_0/[VAc])$ *vs*. time in bulk polymerizations of VAc with [CuTp*] (50°C, $[CuTp^*]_2$ / VAc / V-70 = 0.5 : 500 : 0.7).

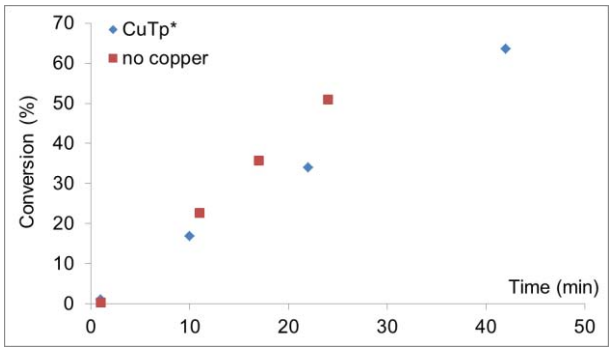

Figure 80: Kinetic profile of the bulk polymerizations of VAc with [CuTp*] and without copper (70°C, $[CuTp^*]_2$ / VAc / V-70 = 0.5 : 500 : 0.7 and VAc / V-70 = 500 : 0.7).

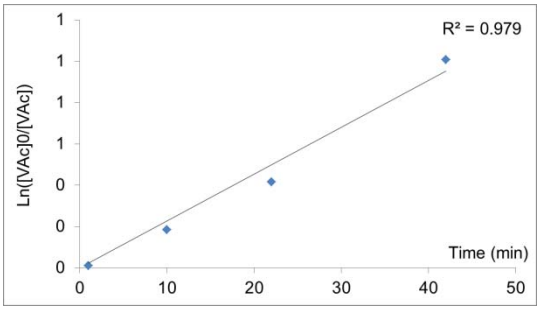

Figure 81: Linear correlation of $\ln([VAc]_0/[VAc])$ *vs*. time in bulk polymerizations of VAc with [CuTp*] (70°C, $[CuTp^*]_2$ / VAc / V-70 = 0.5 : 500 : 0.7).

In conclusion, we have shown for the first time that even if the control was sometimes poor, copper(I) complexes are indeed able to slow down the polymerization of vinyl acetate and give PVAc with low dispersity values (Đ < 1.5). The bulky tridentate scorpionate ligands provide a moderate trapping efficiency and yield poor control, whereas the bidentate β-diketiminate counterparts yield a much more stable dormant species which does not reactivate very efficiently. Two different substituted (trispyrazolylborato)copper(I) complexes have been investigated and better control was obtained with the methyl group compared to the electron-withdrawing trifluoromethyl group. The fine tuning of the copper-carbon bond strength could be done by modifying the steric effects on the ligand coordination sphere. Indeed, Poli's group has shown the influence of methyl and *iso*propyl substituents on the OMRP of VAc

using [CpCr(NacNac)] type of complexes and concluded that the polymerization runs faster in the presence of the bulkier coordination sphere while keeping the same level of control.[66] Since the [Cu(NacNac^{xyl,xyl})(MeCN)] system seems to trap the PVAc chains too tightly, use of the bulkier [Cu(NacNac^{Dipp,Dipp})(THF)] complex could be of interest. On the other hand, with [CuTp*]$_2$ the PVAc chains are not sufficiently restrained. Therefore, the ligand should be less hindered than Tp*. Complex [CuTp^H] where the six methyl groups on the scorpionate ligand are replaced by hydrogen atoms could be screened as controlling agent for vinyl acetate polymerization under OMRP conditions. In the next part, we detail the investigation on the copper(I) complexes abilities as controlling agent for ethylene radical polymerization.

2) Ethylene polymerization

As shown in the bibliographic introduction, the control of ethylene polymerization (and copolymerization with certain polar monomers) is still a challenge. In principle, a PE-Mt bond is expected to be stronger than a PVAc-Mt bond. [CuTp*]$_2$ was considered as the most interesting candidate as a controlling agent for ethylene polymerization since is gave a small but definitely non zero trapping equilibrium with the PVAc chains. Therefore, we decided to extend our investigations of this complex to the controlled radical polymerization of ethylene but other scorpionate ligands as well as the above mentionned NacNac^{XylXyl} ligand were also screened.

The operating conditions were inspired by the recent work of Monteil *et al.*.[196] Blank experiments of ethylene free radical polymerization (FRP) were performed using AIBN as radical initiator and THF or toluene as a solvent (Table 10). Differential Scanning Calorimetry (DSC) analysis of the polyethylenes gave their melting temperatures and degrees of crystallinity (through the measurement of the enthalpy of fusion and its normalization to the known enthalpy of fusion of the theoretical perfect crystal). The crystallinity of the PE obtained by FRP is around 40% which is the value for low density polyethylenes made by the FRP high-pressure process. One PE sample made in THF was also analyzed by high-temperature NMR. According to the PE peaks attribution made by Monteil and coworkers,[196] we can calculate the average number of carbon atoms per chain as well as the ratio of terminal methyl and tetrahydrofuryl groups. The differences between the experiments run in THF and toluene in total PE masses recovered as well as the short size of PE chains formed in THF are in agreement with the conclusion of Monteil et al[196]: THF allows a faster polymerization and leads to much more chain transfer to solvent.

Table 10: conditions: THF or toluene / AIBN / ethylene, 90°C, 24 h.

solvent	[AIBN] (mM)	solid PE (g)	total PE mass (g)	T_{melt} (°C)	crystallinity	CH_3/THF ratio	number of carbons
THF	2.23	1.18	2.18	87.3	38.20%	2.4	34
toluene	2.23	0.03	0.31	98.1	41.80%	nd	nd

[a] The total PE mass is divided in two parts: the solid part and the more or less viscous liquid part which is made of short PE chains (< 30 carbons) and is referred as oligomers.

The results of the attempted controlled radical polymerization of ethylene using copper(I) complexes as CA under OMRP conditions are summarized in Table 11. Four different copper complexes were investigated: $[CuTp^*]_2$, $[CuTp^{CF3}(MeCN)]$ and $[Cu(NacNac^{XylXyl})MeCN]$ which have already been discussed in the previous section and $[CuTp^{H}(THF)]$ which is another scorpionate based ligand with no substituents on the three pyrazolyl units (represented in Figure 82).

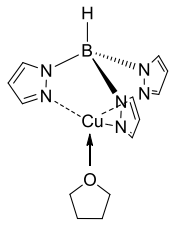

Figure 82: Hydrotris(pyrazol-1-yl)-borato]copper(I) THF solvate, $[CuTp^{H}(THF)]$.

The total PE mass recovered is completely different for the four copper(I) complexes used. Under the same experimental conditions (except for the nature of the copper complex), the polymerization with $[Cu(NacNac^{XylXyl})(MeCN)]$ yielded 940 mg of polymers (i.e. 43 %w compared to the blank experiment without copper) (see entry 3, Table 11), suggesting that the polymerization is slowed down by the presence of the metal complex. Moreover, even if the NMR analysis is lacking, we can qualitatively conclude to the formation of longer PE chains (oligomers represent only 36 % w of the recovered PE mass whereas they represent 46 % w in the blank experiment). It has to be noticed that PE produced after the polymerization in THF solution were recovered by adding 250 mL of methanol to the medium to allow PE precipitation. The solid part was recovered by filtration and dry under vacuum whereas oligomers (PE chains below 30 carbon atoms) which were still soluble in the THF/MeOH mixture were recovered by evaporation of the solvents. When using the scorpionate copper complexes, the total mass of PE recovered was greater and decreased with the ligand substituents CF_3 > H > CH_3 (2.04 g, 1.88 g and 1.57 g respectively, see entries 1, 2 and 5 in Table 11). As for the trend previously observed for the polymerization of VAc in the presence of the scorpionate copper complexes, Tp* ligand shows greater trapping efficiency than Tp^{CF3} but the steric pressure release in Tp^{H} did not yield the expected better controlling capacity

(vide supra). Among the substituted trispyrazolylborate ligands, Tp* is again giving the strongest effect in terms of polymerization rate decrease. After 2 hours of reaction (Entry 6 in Table 11), the PE obtained with $[CuTp^*]_2$ as controlling agent showed a higher density as seen by its high degree of crystallinity (79.5 %) (*i.e.* a lower level of chain branching resulting in a closer packing of the chains). However, when the polymerization was allowed to continue for 24 hours (Entry 5 in Table 11), the measured degree of crystallinity was radically lower (42.9 %) and reached the value of the blank experiment run without copper complex. $[CuTp^*]_2$ is expected to neither suppress nor promote the backbiting and transfer to polymer phenomena that are present in the FRP of ethylene. In principle, only an effect on the average degree of polymerization could be expected if $[CuTp^*]_2$ also operates as a chain transfer catalyst via the formation of transient $[H\text{-}Cu^{II}Tp^*]$ and unsaturated chain ends. However, the presence of unsaturated chain ends is not clearly detected in the ^1H NMR spectra of the recovered PE oligomers. Moreover, the PE infrared spectra do not show any double bond related vibrations. All the peaks can be assigned to the vibrations of alkane C─H bonds plus one broad peak around 1070 cm^{-1} which is assigned to C─O stretching of the tetrahydrofuryl chain-end.

Table 11: OMRP of ethylene with copper(I) complexes (conditions: [Cu] ≈ 1.7 mM in THF, 90°C, 55-60 bars) solid recovered = solid PE chains; total PE mass = solid PE mass + oligomers mass.

Entry	Ligand	LCu / AIBN	initial ethylene pressure (bar)	reaction time (h)	solid recovered (g)	total PE mass (g)	DSC T_{melt} (°C)	crystallinity
1	Tp^H	1 : 1.4	60	24	1.28	1.88	97.1	56.8%
2	Tp^{CF3}	1 : 1.4	55	24	0.84	2.04	96.5	70.1%
3	$NacNac^{XylXyl}$	1 : 0.7	55	24.5	0.34	0.94	nd	-
4	Tp*	1 : 0.0	58	24	0.11	0.62	89.6	40.6%
5		1 : 1.4	58	24	0.77	1.57	89.3	42.9%
6		1 : 1.4	60	2	0.02	0.61	97.3	79.5%

To further investigate the "living" character of ethylene polymerization by Copper-Mediated Radical Polymerization (Cu-MRP), a start-stop experiment was realized. A first polymerization was performed using $[CuTp^*]_2$ and AIBN as initiator in THF yielding PE (T_{melt} = 98.8 °C, 46.5 % crystallinity) and oligomers. Part of the green liquid oligomers (190 mg) were recovered under controlled atmosphere then used in a second polymerization test run in the absence of any additional initiator and copper complex. From this polymerization run, solid PE and a greater amount of oligomers were recovered (20 mg and 350 mg,

respectively). The PE recovered from this experiment had the highest melting temperature reached in our study (T_{melt} = 100.5 °C) with a 60.5 % level of crystallinity. This result suggest that the oligomers recovered under an argon atmosphere are end-capped by the copper complex [PE-CH_2─Cu^{II}Tp*] and are able to release a radical polyethylene chain to allow further polymerization without addition of any azo-initiator.

A control experiment was done without initiator and in the presence of the CA $[CuTp^*]_2$, ethylene and THF only. The initial ethylene pressure was set at 58 bars and the autoclave was heated at 90°C for 24 hours (Entry 4 in Table 11). Surprisingly, the ethylene pressure decreased by 10 bars and a total mass of 615 mg of PE were recovered including 110 mg of solid PE having a low level of crystallinity (40.6 %) whereas no polymerization was expected. The experiment was repeated under the same conditions and an autoclave was charged with $[CuTp^*]_2$ in THF (30 mL) and 57 bars of ethylene at 90°C. After 24 hours of reaction, without any radical initiator, the pressure decreased by 20 bars. Considering that the free volume of the autoclave is around 70 mL, this pressure drop is approximately equal to a consumption of 46 mmol of ethylene (1.3 g according to the perfect gas law) but this time, a total of 575 mg of PE including only 5 mg of solid PE were recovered (equivalent to 20 mmol of ethylene). The large difference in the solid part isolated with 110 mg in the first experiment and 5 mg in the second one can be simply explained by the amount of methanol used to precipitate the PE which is equal to 250 mL in the first case and 150 mL in the second one. However, the total PE mass recovered in both experiments are almost identical with a value of 600 ± 20 mg. The green color of the recovered oligomers indicates the presence of the copper complex. As no external radical initiator was added to the reaction mixture, the polymerization must be initiated by the THF solvent or by impurities coming from either the solvent or the ethylene tank which could explain the poor reproducibility of the experiment. The α C-H bond of THF is the weakest bond in the molecule and the hydrogen abstraction could give the tetrahydrofuryl radical (Figure 83) which can initiate polymerization.[197,255,256]

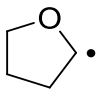

Figure 83: Tetrahydrofuryl radical.

To check the possibility of spontaneous radicals formation from THF, the autoclave was charged with THF and TEMPO (a stable free radical, see Figure 84, [TEMPO] = 0.19 M) then heated at 90 °C for 24 hours. Analysis of the resulting red solid by positive TOFMS, GC and NMR spectroscopy demonstrated that the product was a mixture of the radical TEMPO and the protonated $TEMPO^H$ which could originate from the reaction of TEMPO and THF (Figure

84). As TEMPO was in excess (relative to the amount of radicals generated under the same conditions as calculated from the number average degree of polymerization and the total mass of polymer), we could expect the formation of the TEMPO-THF adduct (Figure 85) if tetrahydrofuryl radicals were formed, but this compound was not observed. Therefore, it seems that tetrahydrofuryl radical are not produced spontaneously from THF only. The reaction of TEMPO with THF was repeated but with addition of an initial ethylene pressure ([TEMPO] = 75 mM). After 24 hours at 90°C, the final apparent pressure was the same as the initial one but 240 mg of oligomers and 5 mg of polyethylene were collected, showing that the amount of TEMPO used not sufficient to trap all the radicals produced. The ethylene tank supplier guarantees a molecular oxygen level below 300ppm but after a simplified arithmetic we conclude that about 0.04 mmol of O_2 could be present in the autoclave under our experimental conditions.

Figure 84: Putative reaction of THF and (2,2,6,6-Tetramethylpiperidin-1-yl)oxyl (TEMPO) to give $TEMPO^H$ and tetrahydrofuryl radical.

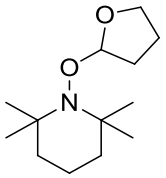

Figure 85: TEMPO-THF adduct.

The influence of ethylene pressure and reaction temperature over the formation of polyethylene by self-initiation in THF (*i.e.* no initiator in the medium) was investigated without the presence of any copper complex. According to the work of Monteil and coworkers, the THF-ethylene system is biphasic for all the experiments except the one at 90°C and pressure over 100 bars (see Phase diagram in Figure 86).[257,258,259]

Figure 87 shows the mass of solid polyethylene obtained from the experiments at 90°C while varying the ethylene pressure. One can see that below 100 bars the higher the ethylene pressure the more PE is recovered. The ethylene solubility in THF at 70°C was experimentally determined by Grau and Monteil.[258] From 50 to 75 bars, the solubility increase approximately from 150 g/L to 250 g/L. Thus, the higher the ethylene pressure the higher ethylene concentration in the liquid phase and the more PE is produced. But above 100 bars, the quantity of PE produced is much less. In the case of a putative monophasic system,

ethylene is the major compound and the higher the pressure the smaller the THF concentration in the medium.

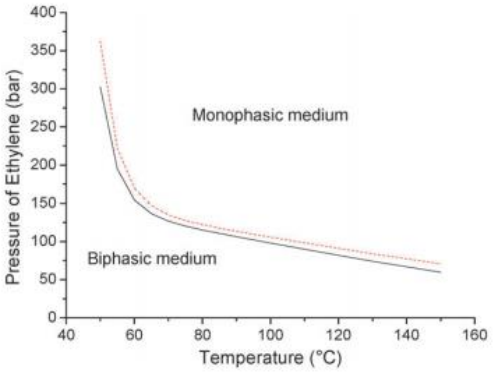

Figure 86: Phase diagram of ethylene/solvent system in a 230 mL reactor with 50 mL THF (black line) and 50 mL toluene (dashed red line) from reference 258.

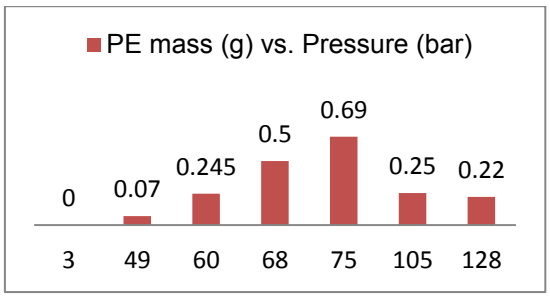

Figure 87: Variation of PE self-production under various ethylene pressure (conditions: THF / ethylene, T = 90°C).

The results of the same study, performed this time with a constant ethylene pressure (51 ± 2 bars) and a variable temperature (from 50 °C to 110 °C), are given in Figure 88. At such a low pressure, the system is assumed to be biphasic. Whatever the mechanism of self-initiation, this is effective only above 50°C because no polymer was recovered below this temperature. Otherwise, a lower amount of PE was produced as the temperature was increased. This could be explained by the decreased solubility of ethylene when increasing the temperature. In terms of polymerization kinetics, in fact, it is well known that the propagation rate in ethylene free radical polymerization, which is proportional to $k_p(k_d/k_t)^{1/2}$ (k_p = propagation rate constant; k_d = initiator decomposition rate constant; k_t = termination rate constant), increases with temperature.

Thus, we can conclude that some self-initiation of ethylene radical polymerization occurs under our experimental conditions, for reasons that we have not further explored. However, the experiments of ethylene OMRP carried out in the presence of $[CuTp^*]_2$ and radical initiator (AIBN) were conducted at 90°C and 50 bars, where the amount of PE produced by the background reaction is 70 mg, which is very low relative to the polymer produced in the

presence of the radical initiator. Hence, the effect of the Cu complex in moderating the polymer production is real.

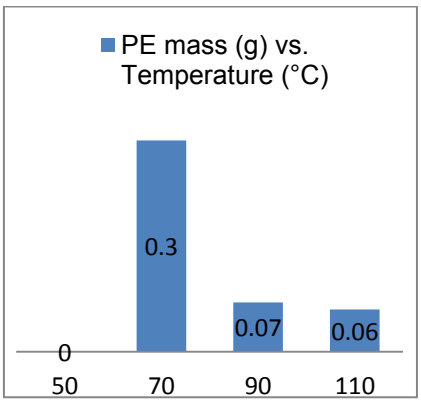

Figure 88: Variation of PE self-production under various temperature (conditions: THF / ethylene, P = 51 ± 2 bars).

3) Conclusion and perspectives

In this chapter, we have investigated, for the first time, the use of copper(I) complexes as controlling agents for the polymerization of less reactive monomers under OMRP conditions. An acceptable degree of control was not achieved but all the investigated copper(I) complexes revealed a more or less pronounced retardation effect on vinyl acetate and ethylene polymerization. In addition, polymer formation continued in the case of VAc beyond the time needed to fully decompose the radical initiator, demonstrating the presence of a dynamic reversible trapping of polymer chains by copper(I) complexes to yield labile dormant species. Among the β-diketiminate and scorpionates ligands studied, the hydrotris(3,5-dimethylpyrazol-1-yl)-borate ligand (Tp*) gave the most interesting results under "reverse" OMRP conditions leading to the isolation of a PVAc with relatively low dispersity values ($1.2 < Đ < 1.5$) but the molecular weight was much higher than expected for a controlled process. For both VAc and ethylene polymerizations, the degree of control was assessed by successful start-stop experiments and by analysis of the polymer dispersity and of the molecular weight-conversion profile. From our preliminary results, we can conclude that the ligand structure has an effect on the OMRP equilibrium with the more electron-donating substituents leading to more efficient trapping. The lower coordination number of the NacNac ligand (bidentate) relative to the tris(pyrazolyl)borate ligand (tridentate) leads to much stronger PVAc-Cu^{II} bonds. In perspective, the steric effects on NacNac and scorpionate ligands should be investigated to fine tune the copper-carbon bond strength and consequently the OMRP equilibrium constant. A screening of other bidentate and tridentate nitrogen ligands could potentially allow the discovery of more efficient copper complexes. Vinyl acetate and

ethylene copolymerization should also be investigated and the experimental set-up already used for ethylene homopolymerization could be modified to eliminate the observed self-initiation from the solvent or monomer impurities. Other solvents could also be investigated in order to limit the chain transfer reactions to solvent that are favored by the high reactivity of the PE radical chains.

CHAPTER III

THEORETICAL STUDIES USING DENSITY FUNCTIONAL THEORY

CHAPTER III: THEORETICAL STUDIES USING DENSITY FUNCTIONAL THEORY

Density functional theory (DFT) is a tool of great help for chemical systems that are difficult to explore by experimental studies, or as complementary tool to verify or rationalize available experimental data. The approach is to compute the electronic structure of molecules in which the electron density distribution plays a central role. Walter Kohn and John Pople won the Nobel Prize in 1998 for their respective work on the development of the density-functional theory and on computational methods in quantum chemistry. This area is growing every year (see Figure 89).

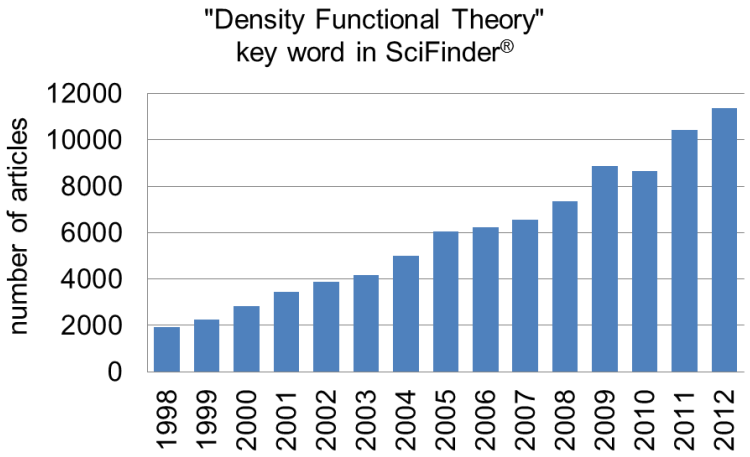

Figure 89: Evolution of the number of publications dealing with DFT.

With the help of DFT, we aim at better understanding why cobalt-mediated radical polymerization is so far giving the best results for vinyl acetate and at rationalizing certain observed reactivity trends in the controlled radical polymerization of vinyl amides. This chapter is divided into two parts. The first one reveals a generalization of the intramolecular metal chelation phenomenon discovered for vinyl acetate to the poly(vinyl amide)s. The second part explores the head-to-head and head-to-tail addition of vinyl acetate polymerization during cobalt-mediated radical polymerization (Co-MRP).

1) Intramolecular metal chelation and hydrogen bonding

We have described in the general introduction how organometallic-mediated radical polymerization (OMRP), is particularly well developed with cobalt complexes (Co-MRP, Scheme 24) and is very efficient for controlling the polymerization of less reactive non conjugated monomers such as vinyl acetate (VAc), *N*-vinyl caprolactam (NVCl) or *N*-vinyl pyrrolidone (NVP). The choice of the ligand coordination sphere is crucial as we have seen in

the previous chapter. Moreover, in the case of Co-MRP, it has been shown that the cobalt-carbon bond strength can be modulated by the addition of Lewis base additives that are able to coordinate to the metal center such as pyridine, water, dimethylformamide (DMF) or dimethyl sulfoxide (DMSO).[72] The major activating effect of the coordinating agents involves stabilization of the released cobalt(II) with formation of bis-adducts. It is therefore possible to use such additives to change the activation/deactivation equilibrium and operate an efficient switch in the build-up of block copolymers. Importantly, in the absence of external coordinating agents, an intramolecular cobalt chelation phenomenon involving coordinating groups on the polymer chains becomes possible, as verified for the polymerization of vinyl acetate (VAc) mediated by bis(acetylacetonato)cobalt(II), [$Co(acac)_2$] (see Figure 90).[212] Such a double linkage between the controlling agent and the polymer chains, through a covalent bond and a dative bond, has so far been evidenced only for this [$Co(acac)_2$]-mediated polymerization of vinyl acetate in the entire field of RDRP. It is a uniquely powerful lever for fine tuning the equilibrium between "dormant" and active species involved in the controlled polymerization. A DFT study of the VAc polymerization mentioned above (reference 212) in the presence of [$Co(acac)_2$] suggested that the ester moiety of the last VAc unit of the dormant species chelates the cobalt(III) at the end of the chain and forms a five-member ring, which provides an extra stabilization of about 3 kcal.mol^{-1} (calculated by a DFT method) to the cobalt-polymer bond. However, very few experimental data support this assumption at the moment.

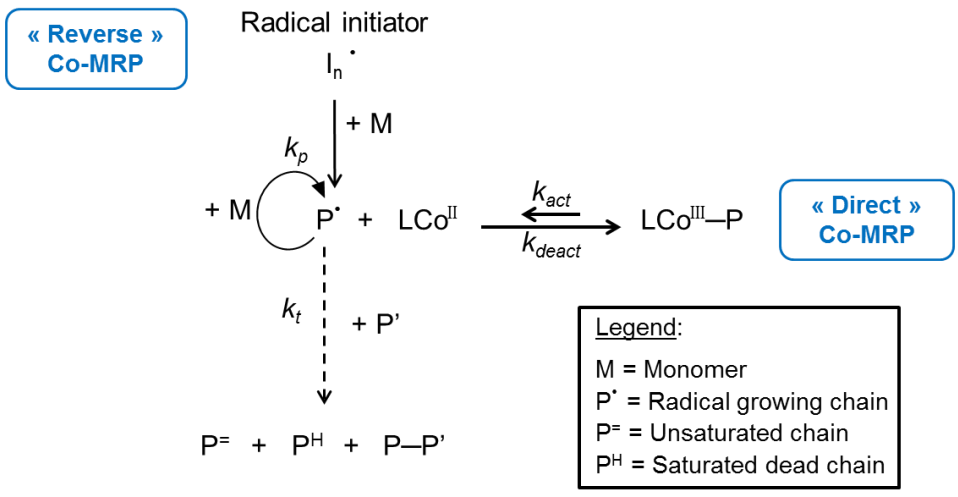

Scheme 24: Simplified mechanism of cobalt-mediated radical polymerization (Co-MRP).

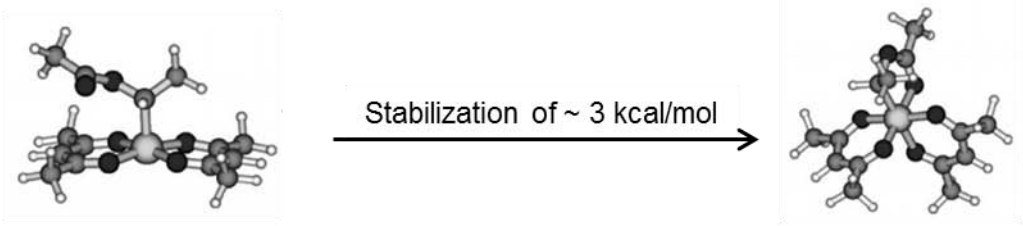

Figure 90: DFT-optimized geometries of the model compounds [VAc–Co(acac)$_2$] from reference 212.

Although amides are known to be stronger Lewis bases than esters because of their more electron-rich carbonyl group, the possible effect of an intramolecular chelation of the cobalt center on the course of the NVP and NVCl polymerization has never been considered. Regardless of the conditions used, the Co-MRP of these monomers have always been presented as a simple reversible capping of the radical chains by the metal following the equilibrium between species 1 and 2 in Scheme 25.

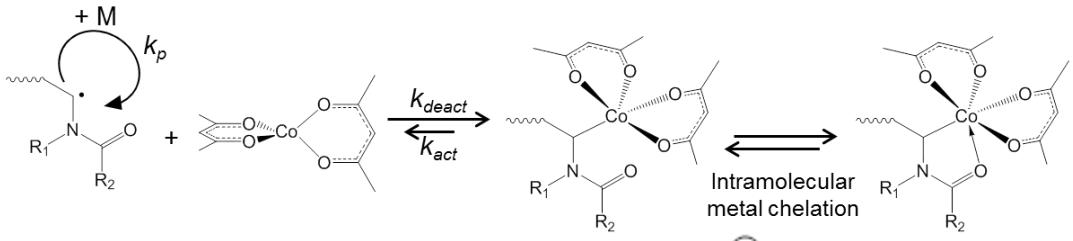

Scheme 25: Metal chelation in the Co-MRP of vinyl amides (= acac).

In collaboration with Antoine Debuigne and coworkers from Christine Jérôme's team at the Center for Education and Research on Macromolecules (CERM),[260] we explored the Co-MRP of a series of *N*-vinyl amides (see Figure 91) to evidence the preponderance of the chelated species (3 in Scheme 25) in the Co-MRP mechanism based on kinetics data and theoretical calculations. When considering the structural differences of the five investigated monomers, we note that NMVA, NVP and NVCl have a fully alkyl-substituted nitrogen atom (i.e. they are tertiary amides), whereas NVF and NVA are secondary amides. The N-bonded H atom has a different electronic effect and is a possible source of hydrogen bonding with the carbonyl functions. The first three monomers should have very similar electronic properties, but whereas NVP and NVCl are cyclic, NMVA is acyclic and ring tension may play a role in the generation of the dormant species.

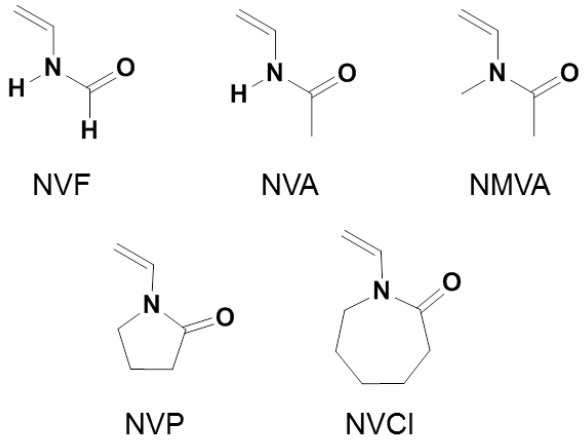

Figure 91: Structure of the five unconjugated *N*-vinyl amides studied by Debuigne and coworkers (NVF = *N*-vinyl formamide, NVA = *N*-vinyl amide, NMVA = *N*-methyl-*N*-vinyl acetamide, NVP = *N*-vinyl pyrrolidone, NVCl = *N*-vinyl caprolactam).

Debuigne and coworkers carried out the polymerization of those five *N*-vinyl amides (Figure 91) under bulk OMRP conditions in the presence of [$Co(acac)_2$]. The evolution of the molecular parameters (M_n and Đ) of the resulting polymers and the monomer consumption were monitored to determine the level of control and the kinetics of the polymerization, thus allowing comparison with the polymerization of vinyl acetate. They used a preformed alkyl-cobalt derivative as initiator (as seen above, Figure 44, page 83). Thermal treatment of this alkyl-cobalt derivative promotes homolytic cleavage of the Co─C bond and the release of both the initiating radical and the controlling agent in the polymerization medium (Direct OMRP, Scheme 24). Although both degenerative chain transfer and reversible termination contributions are reported for Co-MRP, the former requires an influx of radicals along the polymerization, which is not the case when an alkyl-cobalt derivative is used.

While Co-MRP of NVP has already been investigated with some success,[171,172,173,174] the polymerization was carried out either in the presence of a co-monomer or in solution (anisole or methanol) at low temperature (below 30°C). Here, a solution of the [R─$Co(acac)_2$] initiator in NVP was heated at 40°C (Table 12, entry 2). The polymerization was very fast but not deprived of any control, as illustrated by the increase in the M_n with the conversion and the moderate dispersity value (ca. 1.3). Considering the results obtained for VAc under the same conditions (Table 12, entry 1), the deactivation of the PNVP growing chains by [$Co(acac)_2$] is clearly not as efficient as for PVAc. The overlay of the kinetic curves presented in Figure 92 clearly emphasizes the drastic difference in the polymerization rates of VAc and NVP.

The Co-MRP of NVCl, another cyclic vinyl amide with a seven-membered lactam ring, was then considered. A recent report deals with the radical polymerization of this monomer by using the same [PVAc-$Co(acac)_2$] initiator at 30°C in DMF yielding well-defined PNVCl (Đ

= 1.2).[186] Because NVCl is characterized by a melting point of around 37°C, its bulk polymerization at 40°C was carried out by first melting NVCl at 40°C under an inert atmosphere, followed by addition of the [R-Co(acac)$_2$] initiator (Table 12, entry 3). The kinetics of the Co-MRP of NVCl was intermediate between those of VAc and NVP (see Figure 92), that is, 40 % monomer conversion in 3 h. From the control point of view, the bulk process is much better for NVCl than the previously described solution procedure in DMF. The low PNVCl dispersity values observed until molar mass as high as 65 000 g/mol suggest that Co-MRP is a technique of choice for the controlled polymerization of this monomer. Finally, it is striking that the slight structural differences between NVCl and NVP, two vinyl lactams, lead to such contrasting kinetics and quality of control.

Table 12: Co-MRP of VAc and *N*-vinyl amides in bulk ([Monomer]/[RCo(acac)$_2$] = 380). [a]Measured by SEC in THF using a PS calibration. [b]Measured by SEC in DMF using a MALLS detector.

Entry	Monomer	T (°C)	Time	Conversion (%)	M_n (g/mol)	Đ
1	VAc	40	4 h	16	5 000 [a]	1.05
			8 h	28	9 300 [a]	1.09
			16 h	60	19 300 [a]	1.18
2	NVP	40	2.5 min	8	12 700	1.12
			3.5 min	33	25 000	1.30
3	NVCl	40	1 h	21	10 200	1.04
			2 h	31	17 800	1.03
			3 h	40	24 200	1.02
4	NMVA	40	2 h	14	4 800	1.07
			7 h	32	12 700	1.08
			14 h	62	24 700	1.14
5	NMVA	60	20 min	19	9 300	1.05
			40 min	31	13 800	1.12
			1 h	48	24 800	1.30
6	NVF	20	2 min	67	20 200	1.40
7	NVA	60	few sec.	~ 100	62 400	2.34

The Co-MRP of a noncyclic *N*-alkyl vinyl amide was also considered in this study, that is, *N*-methyl-*N*-vinyl acetamide (NMVA, Figure 91). In spite of the very interesting properties of the parent polymer (PNMVA), until now, no report had addressed the controlled homopolymerization of this monomer (see general introduction). For the sake of comparison, the polymerization was conducted under the same experimental conditions (bulk at 40°C; Table 12, Entry 4). In this case, the polymerization rate was very similar to that of VAc (Figure 92) and the polymerization control was excellent; the molar mass was strictly dictated

by the monomer conversion and the [NMVA]/[R-Co(acac)$_2$] molar ratio, and the dispersity value was low (between 1.1 and 1.2). The control of the NMVA polymerization was confirmed by the clear shift of the SEC peaks with time towards higher molecular weight.

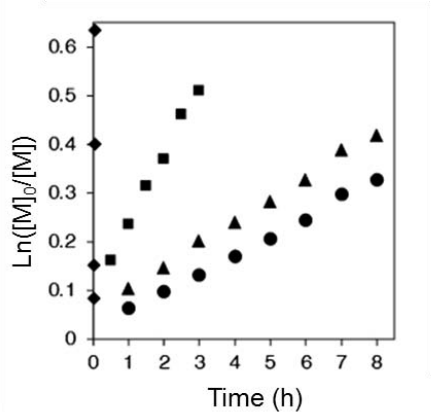

Figure 92: Time dependence of ln([M]$_0$/[M]) (M = monomer) for the Co-MRP of VAc (●), NVP (♦), NVCl (■), and NMVA (▲) initiated in bulk at 40°C by a low molecular weight alkyl cobalt adduct; [M]/[Co(acac)$_2$(PVAc)] = 380 (from reference 210).

Debuigne and coworkers then studied the Co-MRP of *N*-vinyl formamide (NVF, Figure 91) and *N*-vinyl acetamide (NVA, Figure 91), two monomers bearing a hydrogen atom on the nitrogen atom of the amide group. After mixing the NVF with the [R-Co(acac)$_2$] initiator at room temperature, a highly exothermic reaction occurred and the mixture became extremely viscous within two minutes. The monomer conversion reached 67 % and the molecular parameters of the PNVF were determined by aqueous SEC (M_n = 20 200 g/mol, Đ = 1.4) (Table 12, Entry 6). Indeed, no control can be claimed for NVF under these conditions. The bulk polymerization of NVA could not be carried out at 40°C because the melting point of this crystalline monomer is 55°C. The Co-MRP of NVA was thus realized at 60°C in the melted monomer phase and the monomer consumption was almost complete within a few seconds after addition of the melted NVA onto the [R-Co(acac)$_2$] initiator (M_n = 62 400 g/mol, Đ = 2.34) (Table 12, entry 7). For the sake of comparison, the polymerization of NMVA was also performed at 60°C (Table 12, Entry 5) and, as expected, the polymerization was much faster than that at 40°C, but the cobalt complex still exerted some control on the polymerization as illustrated by the regular shift of the SEC chromatograms with the polymerization time. Therefore, it is clear that the substitution of the methyl group of NMVA by a hydrogen atom is sufficient to alter the control of the polymerization.

Finally, the Debuigne group examined the effect of the addition of NVA on the course of the Co-MRP of NMVA. This copolymerization initiated at 40°C in bulk ([NMVA]/[NVA] = 1) by [R-Co(acac)$_2$] was quite fast compared with the homopolymerization of NMVA but

controlled, as assessed by the shift of narrow SEC peaks towards higher molar masses with time. The composition of a PNVA-*co*-PNMVA copolymer prepared under the same conditions was evaluated by ^{1}H NMR in D_2O (NVA/NMVA molar ratio in the copolymer = 55 : 45). In this copolymerization, trapping of the radical chains having NMVA as last unit by [$Co(acac)_2$] is efficient enough to produce well-defined statistical copolymers containing NVA units.

To summarize the experimental polymerization investigation made by Debuigne and coworkers, the vinyl amide monomers shown in Figure 91 polymerize at a wide range of rates under similar conditions in spite of their relatively similar electronic structure, featuring the same CH2=CH-N(R^1)-CO-R^2 framework. The bulk polymerization becomes faster in the order NMVA < NVCl < NVP < NVA < NVF.

To rationalize this order of polymerization rate, we performed a DFT investigation of all these systems, in comparison with the previously published study of the VAc system.[251] On the basis of the previously published computational results for the VAc polymerization (Figure 93) as a guide,[212] the first question was the relative strength of the Co^{III}-chain bond and any extra stabilization provided by chelation. As for the VAc system, the polymer chain was modeled by a hydrogen atom beyond the Co-bonded monomer unit, as shown in Figure 94.

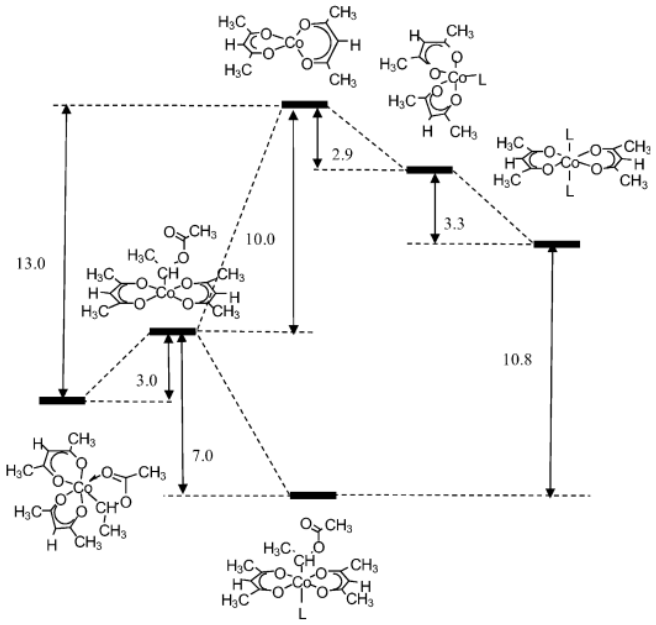

Figure 93: Energy diagram related to the OMRP equilibrium in the [$Co(acac)_2$]-mediated polymerization of VAc in the presence of DMF (L = DMF). Values are ΔH in kcal.mol^{-1} calculated by DFT with use of the BPW91* functional. Data are taken from reference 212.

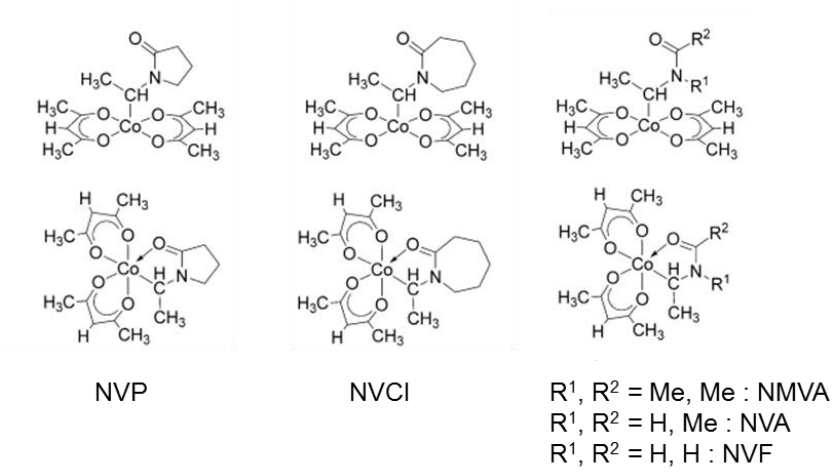

Figure 94: Models of the five- and six-coordinate Co^{III} dormant species for the polymerization of the vinyl amide monomers.

The calculations were carried out at the same level of theory as those previously reported for the VAc system. The selection of the BPW91* as functional to investigate this system will be briefly commented here. The [Co(acac)$_2$] complex, which is actually a stable species, is characterized by three unpaired electrons. Otherwise stated, it adopts a spin quartet state (S = 3/2). When this system binds the radical and generates the alkylcobalt(III) dormant species, the spin changes to zero (diamagnetic). Special care has to be taken in DFT calculations when there is a spin state change. To summarize, it is known by experience that functionals based on the local density approximation (LDA) and on the generalized gradient approximation (GGA) have a bias in favor of lower spin state and hybrid functionals have a bias in favor of the higher spin state.[261,262] Therefore, special functionals such as BPW91* have been developed to cope with this problem.[263] The BPW91* is a hybrid functional derived from the popular B3PW91 functional which combines the three-parameter hybrid exchange-correlation functional developed by Becke[264] with the non-local correlation provided by Perdew/Wang 91,[265] where the exact Hartree−Fock exchange contribution is reduced from 25 to 15%. Calculations were carried out on the three processes illustrated in Scheme 26 for all the above mentioned amide monomers and afford the results summarized in Table 13. For comparison, the Co─CH_3 bond dissociation enthalpy in [Co(acac)$_2$(CH_3)] has also been calculated. A first observation is that the intrinsic Co─C bond strength in the dormant chain models (enthalpy of Co─C bond formation to yield the K^1:C product, in the 7.3-10.0 kcal/mol range) is only slightly smaller than in the [Co(acac)$_2$(VAcH)] model (see Figure 93, Table 13 and black values in Figure 95) and much smaller than in [Co(acac)$_2$(CH_3)]. The radicals containing an N-H bond (from the NVA and NVF monomers) yield slightly weaker bonds, comparable in strength to that of the radical from VAc. The NVPH radical gives the smaller intrinsic Co─C

bond strength, probably because of ring tension. The five-membered pyrrolidone ring is less flexible than the seven-membered caprolactone ring yielding a slightly stronger intrinsic Co─C bond for NVClH. The two methyl groups in NMVAH take more space and the radical is constrained by the Co-CH=N angle requirement to remain in close proximity to the acetylacetonate ligands (see view in Figure 95).

However, the chelation resulting from coordination of the carbonyl group change deeply the total Co─C bond strength values (enthalpy of chelation in the 3.0-7.8 kcal/mol range, see blue values in Figure 95). Indeed, the greatest stabilization is obtained for the dialkyl amide systems (in the order NMVA > NVCl > NVP) and less for the monoalkyl amides (NVA > NVF). This can be attributed to the inductive effect of the second alkyl substituent, rendering the carbonyl oxygen atom a better electron donor. The greater chelating ability of NVA relative to NVF can also be attributed to an inductive effect (Me group bonded to the CO donor function). The reason for the relative order of chelation strength for the dialkyl-substituted amides may be attributed to ring tension, which is non-existent for NMVA, intermediate for NVCL, and greater for NVP, making the latter system an even poorer donor than NVA.

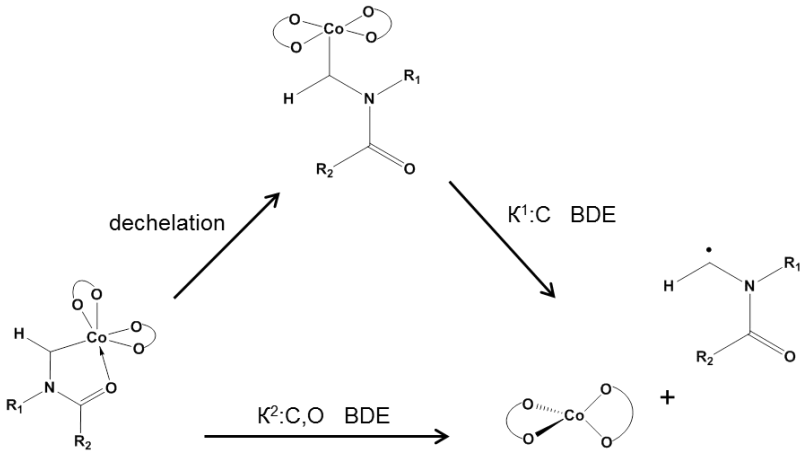

Scheme 26: Dechelation and homolytic bond cleavage processes for the dormant species in [Co(acac)$_2$]-mediated polymerization of vinyl amide monomers (= acac).

Finally, when the carbonyl group chelation is taken into account, the total enthalpies of the Co─C bond formation to yield the more stable K^2:C,O product are all greater than that of VAc (13.0 kcal/mol) except for the NVPH radical (in the 11.6-16.5 kcal/mol range, see red values in Figure 95). The enthalpy difference between the dormant and activated species (1 and 3 in Scheme 25) becomes smaller in the order NMVAH > NVClH > NVAH > NVFH = VacH > NVPH.

Table 13: Calculated enthalpy changes (in kcal.mol^{-1}) for the processes shown in Scheme 26.

Complex	Dechel.	K^1:C BDE	K^2:C,O BDE
[Co(acac)$_2$(NVPH)]	4.3	7.3	11.6
[Co(acac)$_2$(NVClH)]	5.2	9.5	14.7
[Co(acac)$_2$(NMVAH)]	7.8	8.7	16.5
[Co(acac)$_2$(NVAH)]	4.7	9.4	14.1
[Co(acac)$_2$(NVFH)]	3.0	10.0	13.0
[Co(acac)$_2$(VAcH)]	3.0	10.0	13.0
[Co(acac)$_2$(CH$_3$)]	-	20.1	-

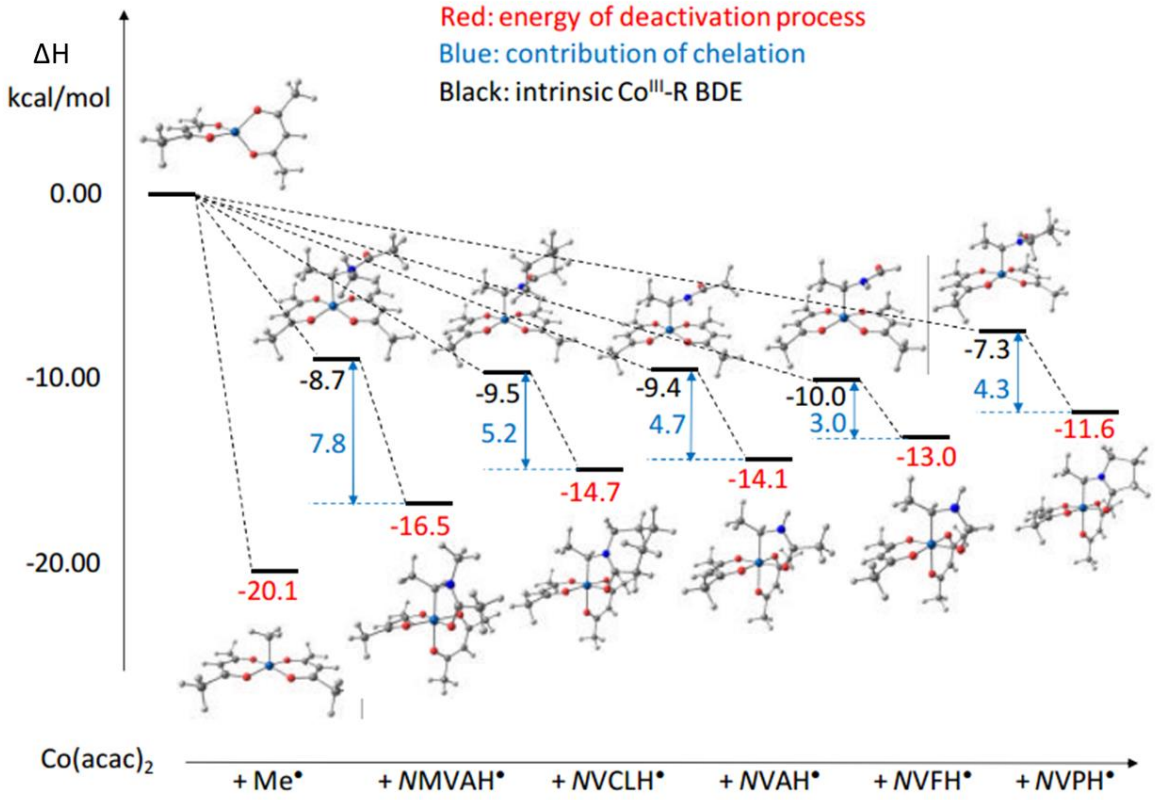

Figure 95: Relative enthalpies in kcal/mol and views of the optimized geometries of the K^1:C and K^2:C,O [Co(acac)$_2$(alkyl)] complexes with the model radicals of the growing chains resulting from the polymerization of N-vinyl amide monomers, as well as for the [Co(acac)$_2$(CH$_3$)] complex.

As shown in Figure 93, the OMRP equilibrium must take into account the possible coordination of ligands to the Co^{II} and Co^{III} species. In the case of the [Co(acac)$_2$]-mediated VAc polymerization, the monomer itself is a poor ligand and calculations have indicated that its coordination to the five-coordinate Co^{III} complex is less favored than the chain end chelation, whereas coordination to [Co(acac)$_2$] is largely unfavored. Better ligands such as DMF (in Figure 93), DMSO, pyridine, or water, on the other hand, can indeed coordinate to both species. The polymerizations of the vinyl amide monomers were in fact carried out in bulk, in the absence of potentially donor additives. However, the vinyl amide monomers

examined here are by themselves better donors than the ester function of VAc due to the greater contribution of the polar mesomeric $CH_2=CH-N^+(R^1)=C(R^2)O^-$ form, but their donor ability relative to ligands such as DMF is not clear. To evaluate the contribution of monomer coordination, additional calculations were carried out on the six-coordinate mono-adduct of the Co^{III} system and on the bis-adduct of the Co^{II} system. The five-coordinate $[Co(acac)_2(monomer)]$ complex, being less relevant to the thermodynamic balance, was not calculated.

The enthalpy balance of the two equilibria (Equations (1) and (2); M = monomer ; MH = radical associated with the monomer, model of the polymer chain) are shown in Table 14, and graphically in Figure 96a-e.

$$[K^1\text{:C-Co(acac)}_2\text{(MH)}] + M \longrightarrow [Co(acac)_2(MH)(M)] \quad (1)$$

$$[Co(acac)_2] + 2M \longrightarrow [Co(acac)_2(M)_2] \quad (2)$$

Table 14: Calculated enthalpy changes (in kcal/mol) of the monomer coordination to the Co^{III} and Co^{II} species.

Monomer	[Eq. (1)]	[Eq. (2)]
NVP	+ 1.1	-0.4
NVCl	+ 7.1	+ 2.1
NMVA	0	+ 0.2
NVA	- 1.2	- 1.8
NVF	- 2.6	- 2.2

The results show that the vinyl amide monomers, although indeed better ligands than VAc as expected, bind less strongly than DMF to both Co^{III} and Co^{II} (Figure 93). The monoalkyl amides NVA and NVF afford mildly exothermic interactions in both oxidation states, whereas the dialkyl amides afford thermoneutral (NMVA) or endothermic (NVP, NVCl) interactions. In this respect, it is interesting to note that whereas the literature contains numerous X-ray structures of bis-L adducts of di(β-diketonato)cobalt(II), the only members of this family containing a carbonyl-based ligand (ketone, ester, amide, etc.) are those for which L = DMF.[266,267,268]

The observed trend of binding enthalpies can once again be attributed to the steric pressure exerted by the alkyl substituents. Given these results, it seems that the contribution of monomer coordination to the dormant species and to the $[Co(acac)_2]$ trapping complex is negligible or very small. In fact, coordination to the alkylcobalt(III) system is less favorable, for all five monomers, than chelation by the carbonyl functionality. Therefore, the best parameter to describe the radical controlling equilibrium is the enthalpy difference between

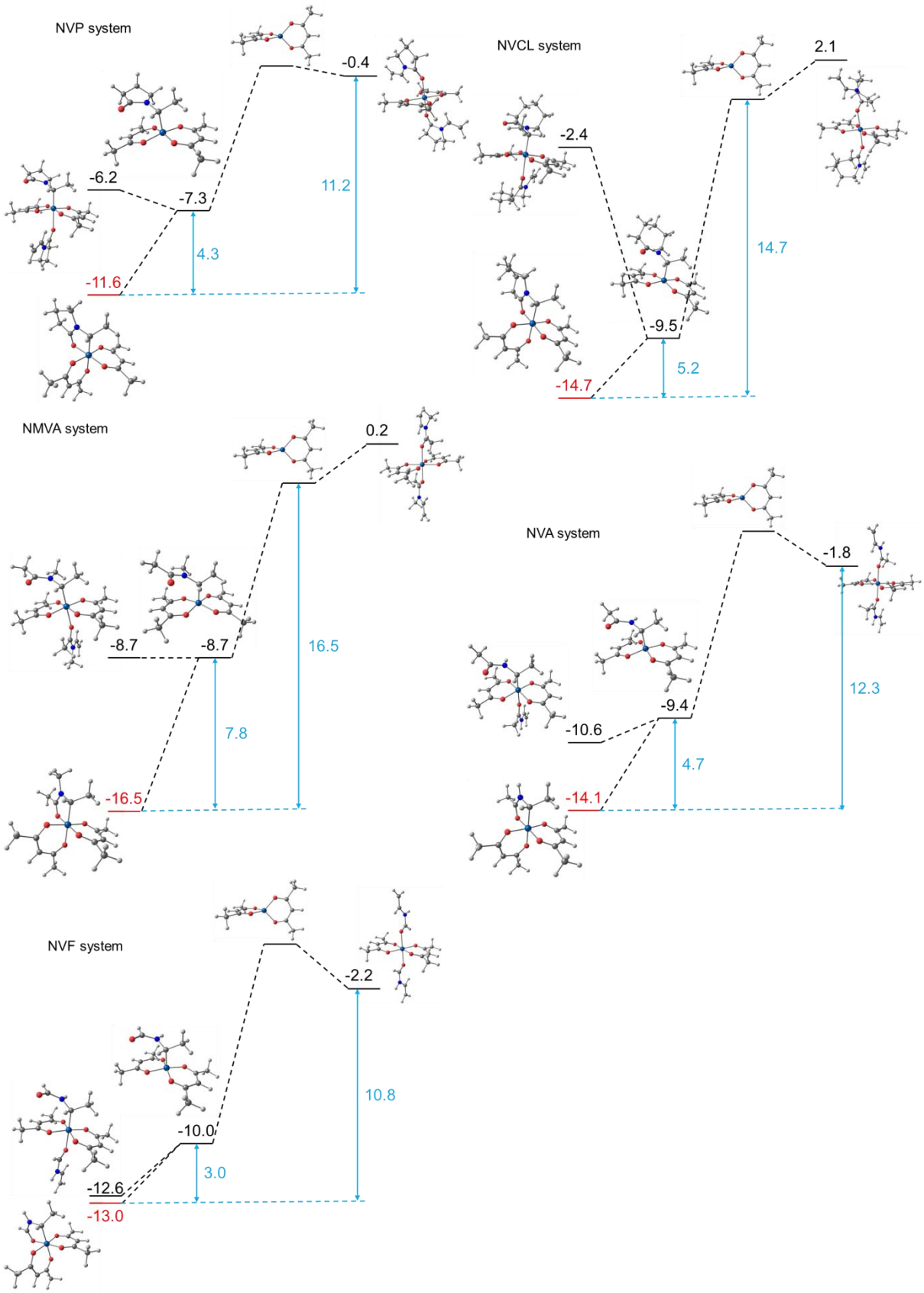

Figure 96: Relative enthalpies in kcal/mol and views of the optimized geometries of the monomer addition products to K^1:C─[Co(acac)$_2$(MH)] and [Co(acac)$_2$]. For comparison, the K^2:C,O─[Co(acac)$_2$(MH)] system is also shown.

the chelated [K^2:C,O -Co(acac)$_2$(MH)] complex and the separate [Co(acac)$_2$] and MH$^\bullet$ radical species (i.e., the K^2:C,O BDE in the last column of Table 14), except perhaps for the NVA and especially NVF systems in which the Co^{II} stabilization by coordination of a monomer unit may result in an accelerating effect. It should be noted that these calculated enthalpic parameters are not a direct measure of the ligand association/dissociation equilibria because the entropic component is not included. However, because the -TS contribution is small and not greatly different for the various systems, the trend of the calculated ΔH should be representative of the real trend of ΔG. The enthalpy difference between dormant and trapping complexes is therefore ranked in the following decreasing order (values in kcal/mol): NMVA (16.5) > NVCl (14.7) > NVA (12.3) > NVP (11.6) > NVF (10.8).

The only apparent disagreement between the bond strength order and the rate of polymerization (the slower NMVA < NVCl < NVP < NVA < NVF the faster) appears to be the relative positioning of NVP, the polymerization of which, although quite fast, is not as fast as those of NVA and NVF. It seems that the enthalpy differences analyzed above are overvalued for the two latter monomer systems. Possible differences in the propagation rate constant may be invoked to explain the discrepancy, but according to the literature,[180,269,270] the k_p values for NVP and NVF are not too different under similar conditions. We therefore wondered whether the discrepancy could be explained by the intervention of hydrogen bonding. The possibility for the free monomer to establish hydrogen bonds can further affect the OMRP equilibria for the NVA and NVF systems. Indeed, as shown in Scheme 27, both the free radical and the cobalt K^1:C have three possible ways to establish a hydrogen bond with the free monomer: N─H(radical)···O=C(monomer), N─H(monomer)···O=C(radical), and a cyclic structure with both types of interactions. The latter is, in principle, energetically preferred although it forces a less favorable *s*-E conformation around the N─C(O) bond in both radical and monomer. On the other hand, the chelated hexacoordinated complex, with the carbonyl function tied up in cobalt coordination and therefore unavailable for hydrogen bonding, can only form the N-H(radical)··· O=C(monomer) interaction and therefore suffers from reduced stabilization. This argument predicts that hydrogen bonding will stabilize the free radical + [Co(acac)$_2$] to a greater extent than the chelated dormant state, with a net accelerating effect for the polymerization. The calculations qualitatively confirm this view. The stabilization of the dormant species on the enthalpy scale is worth only 2.4 kcal.mol^{-1} for the NVA system and 3.2 kcal.mol^{-1} for the NVF system, whereas the free radical is indeed most stabilized by the double interaction, as shown in Scheme 27, by 13.1 kcal.mol^{-1} for the NVA system and by 15.1 kcal.mol^{-1} for the NVF system. Complete energy diagrams for the

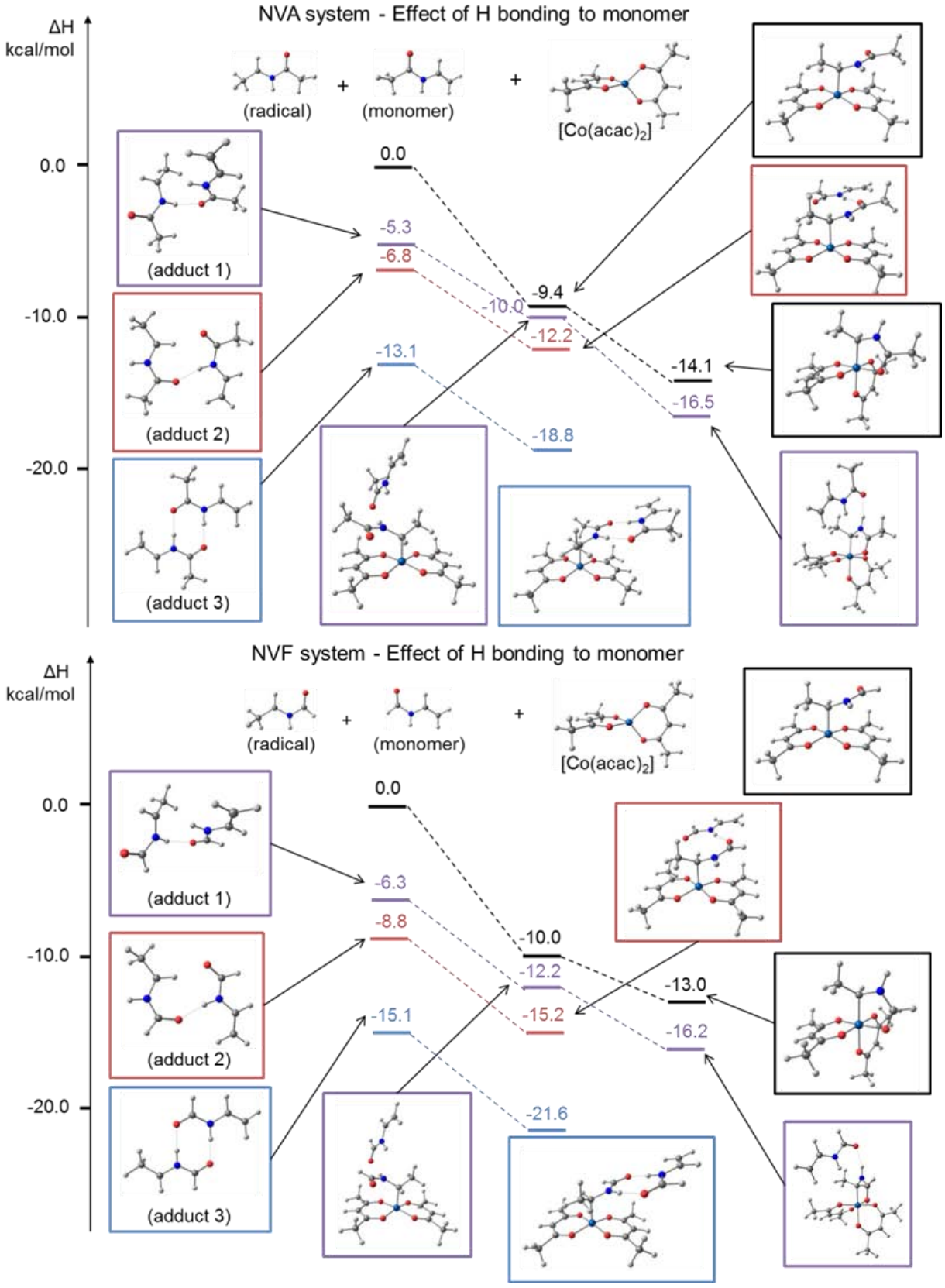

Figure 97: Effect of H bonding on the energy of latent and free radical for the NVA and NVF systems in $Co(acac)_2$-mediated radical polymerization.

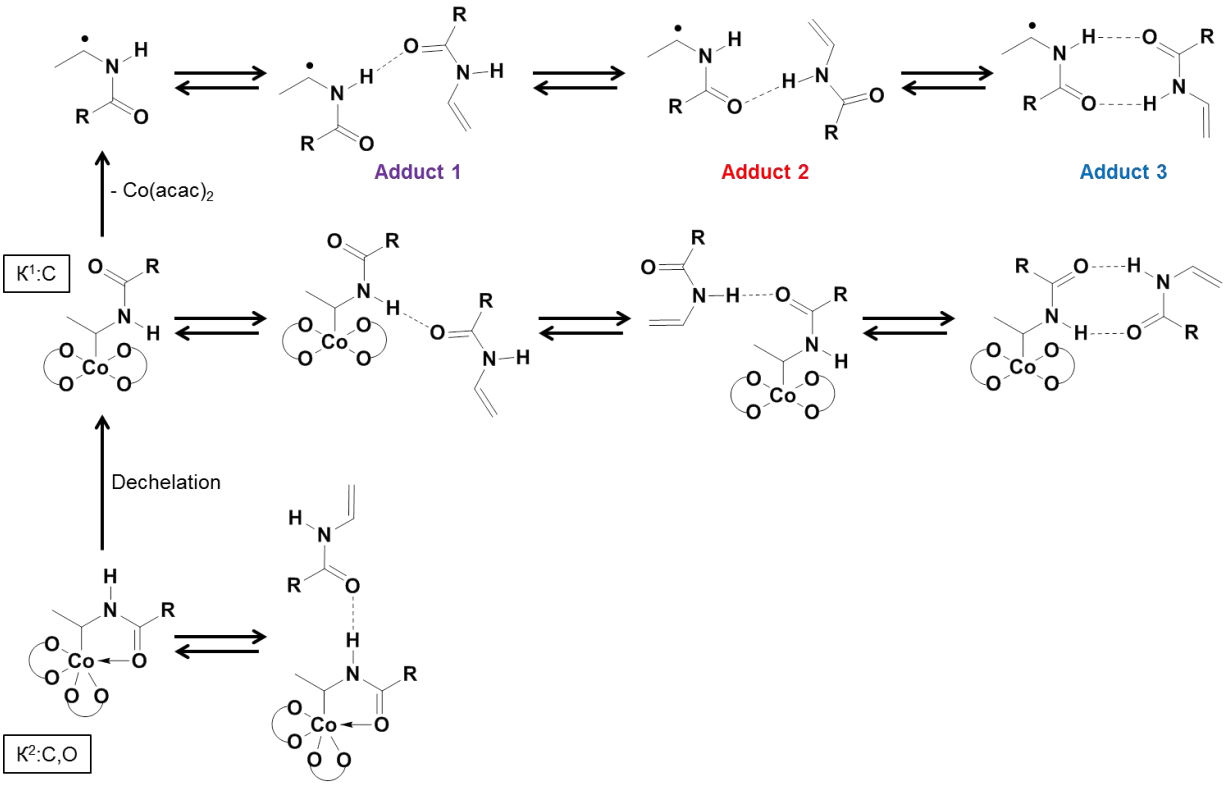

Scheme 27: Effect of hydrogen bonding on the dechelation and homolytic bond cleavage processes for the formant species in [Co(acac)$_2$]-mediated polymerization of NVA (R = CH$_3$) and NVF (R = H) ; the acetylacetonate ligands are simplified for clarity.

two systems and views of the optimized geometries are depicted in Figure 97. This substantial difference in relative stabilization largely affects the position of the equilibrium between latent and free radical and rationalizes the very large difference in polymerization rate between the NVA and NVF systems on one side and the NVP on the other side.

In light of the above computational results, it is also possible to rationalize the good level of control achieved for the statistical copolymerization of NVA and NMVA, with a polymerization rate not much greater than that of the NMVA homopolymerization and much smaller than that of the NVA homopolymerization. According to our computational model, the [Co(acac)$_2$] controlling agent is able to efficiently moderate the concentration of the NMVA related radicals and much less that of the NVA related radicals. Therefore, the longer-life dormant chain in the copolymerization will contain a [Co(acac)$_2$]-bonded NMVA monomer unit. Given the 50:50 ratio in the comonomer feed and a nearly equivalent ratio found in the polymer, the reactivity ratios are probably quite close to unity and the polymerization rate should ideally be multiplied by a factor of two. On the other hand, even though the NVA comonomer can establish hydrogen bonds with both dormant and active chains, the extent of these interactions should be nearly identical when the chain is terminated

by an NMVA unit and the energetic scheme for the activation/deactivation equilibrium should remain essentially unaltered.

In conclusion, this DFT study has revealed that intramolecular chelation of the cobalt by the amide moiety in the last monomer unit of the dormant species, generating a five-membered ring, provides a reasonable rationalization for the observed differences in the kinetics and the control of *N*-vinyl amides. Such coordination contributes to the stabilization of the dormant species and slows down the polymerization, making polymerization control more efficient. The absence of ring tension in the NMVA explains the preponderance of the chelation effect in the polymer-cobalt(III) derivative in contrast to NVP. The NVCl is intermediate because its lactam ring is larger and less strained than that of NVP. The competitive coordination of the cobalt(III) dormant species and cobalt(II) trapping complex by the free monomer was also considered but evaluated as being negligible or very small. This intramolecular chelation phenomenon is, however, insufficient to describe the behavior of monoalkyl *N*-vinyl amides, that is, NVF and NVA. The polymerization of these monomers is extremely fast and suffers from either poor or no control. In these polymerizations, the different ability of the free monomer, through the formation of N─H···O=C hydrogen bonds, to stabilize the dormant chains (only as proton donor) and the growing radical chains (both as proton donor and as proton acceptor) excessively shifts the equilibrium towards the propagating radical form. Nevertheless, these monomers are not precluded from use in the Co-MRP because addition of NMVA as a comonomer leads to controlled copolymerization. This detailed mechanistic study and the essential role played by this unique intramolecular chelation phenomenom and by hydrogen bonding is a crucial step in the development of an efficient synthetic platform for a wide range of well-defined poly(*N*-vinyl amide) (co)polymers of high interest.

2) Vinyl acetate head-to-head addition

Despite the great progress made concerning vinyl acetate controlled radical polymerization (see general introduction), all the reported systems show either an increase of the PVAc dispersity values with conversion or a slowdown in the polymerization rate (in some cases, the polymerization even stops) except for the [$Co(acac)_2$] controlling agent. Table 15 shows the characteristics of the PVAc reported in a few of the relevant contributions. The most interesting indicators for our purposes are the length of the polymer chain (as expressed by the number-average degree of polymerization, X_n) and the dispersity (Đ). Only OMRP using [$Co(acac)_2$] as controlling agent leads to chain growth that remains well controlled up to very high degrees of polymerization and high conversions (entry 10). In many of the other cases,

Table 15: Reported Systems for the RDRP of VAc and Characteristics of the Resulting Polymer.

Entry	Method	Controlling system	Initiator	X_n[a]	Đ[a]	Remarks	Ref.
1	ATRP (?)	$[Fe(OAc)_2]$/PMDETA[b]	CCl_4	~ 170	~ 2	telomerization by transfer to CCl4	130,271
2	ATRP	$[CpFe(CO)_2]_2$/M(O*i*Pr)$_n$	$(CH_3)_2C(CO_2Et)I$	~ 120	~ 2	slowdown, max. conv. = 60%	131
3	ATRP	[CuCl]/PMDETA	$CH_3CH(CO_2Me)Br$	7.5	1.6	stopped at 14 % conv.	130
4	ATRP	[CuCl] or [CuBr]/*t*py	$(CH_3)_2C(CO_2Et)Br$	~ 120	1.7	linear first-order plot (~75% conv.)	132
5	RAFT	$Ph_2NC(S)SCH(CO_2Et)_2$	AIBN	57	1.56	Đ increases with conv. (up to 73%)	272
6	RAFT	$EtOC(S)SCH_2CN$	AIBN	~ 127	1.31	linear first-order plot (77% conv.)	165
7	RAFT	$EtOC(S)SCH_2CO_2Me$	AIBN	~ 580	1.18	Đ at 25% conv. (max conv. ~ 56%)	137
8	ITP	$CH_3CH(CO_2Et)I$	CPD[b]	~ 400	1.45	slowdown, max. conv. = 57%	104
9	TERP	$(CH_3)_2C(CO_2Et)TeMe$	AIBN	34	1.28	slowdown at low conversions	121
10	OMRP	$[R_0{-}(CH_2CHOAc)_{<4}{-}Co(acac)_2]$[c]	-	~ 1630	1.27	linear first-order plot (52% conv.)	212
11	OMRP	$[CpCr(NacNac^{Xyl,Xyl})(CH_2tBu)]$	-	175	1.46	slowdown, max conv. = 14%	66
12	OMRP	[(TMP)Co]	AIBN	~ 660	1.27	max conv. = 10%	151

[a] Highest reported number-average degree of polymerization (X_n) and dispersity (Đ) at maximum conversion. [b] CPD = α-cumyl peroxyneodecanoate. [c] R_0 = initiating fragment of V-70.

including OMRP with other metal complexes (e.g., entry 11), the polymerization of vinyl acetate slows down or stops completely before all monomer is consumed and the resulting polymers show higher dispersity, often increasing with conversion. Of note is also the tetramesitylporphyrin system (TMP)Co (entry 12), which leads to a PVAc of relatively high molecular weight and low dispersity making use of the degenerate transfer approach, but only low conversions were achieved. Among many reasons that have been advanced to rationalize these difficulties, some of them valid only for a specific technique (e.g., ATRP), others of general applicability, are the low equilibrium constant for the activation process from the dormant species, the decomposition of the dormant species, the oxidation of the growing radicals to carbocations, the chain transfer to solvent or to polymer. However, limitations in the level of control for VAc radical polymerization have also been attributed to the formation of a stronger PVAc─CHOAc─CH_2─X bond in the dormant species following the inverted monomer insertion by head-to-head addition, which gives a more reactive primary radical. The stronger bond formed by this radical with the trapping agent makes the new dormant species more difficult to reactivate, rationalizing the slowdown of the reaction and the increase of the dispersity index with conversion. The degree of head-to-head addition in VAc polymerization was shown to be small but significant, and to increase with temperature: from about 1.23% at 25°C to 1.95% at 110°C.[273] Hence, for a suitable system in terms of activation/deactivation equilibrium for the weaker latent secondary radical, it is reasonable to expect control at low conversions, but accumulation of the stronger latent primary radicals at

higher conversions slows down the polymerization and broadens the molecular weight distribution.

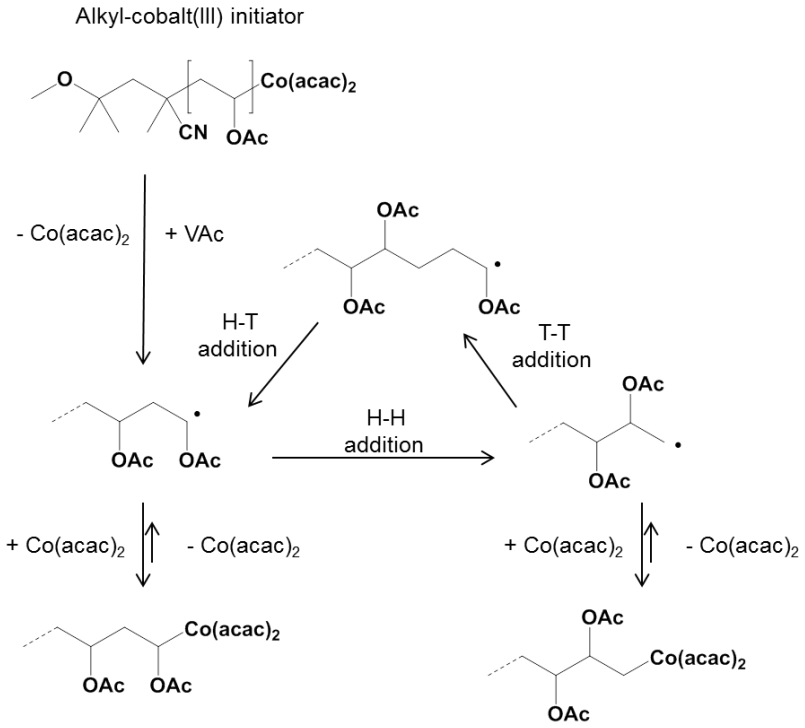

Scheme 28: Head-to-Tail (H─T) and Head-to-Head (H─H) Additions in Co-MRP

Although this explanation seems reasonable, it does not answer the question why the slowdown is more accentuated for certain systems (e.g., TERP, ATRP with certain Cu complexes) than for others (e.g., RAFT/MADIX) and especially why does the OMRP system using [$Co(acac)_2$] not suffer from any slowdown at all. It is notable that Đ remains quite low for this system, whereas other systems, for which a slowdown was not observed or was not reported, show poorer control as suggested by the polymer higher Đ. Thus, either [$Co(acac)_2$] is able to somewhat alter the radical reactivity by reducing the incidence of the head-to-head additions, or the dormant species must allow facile reactivation of the latent primary radical. The possibility of a reduction of head-to-head additions for the Co-MRP has been explored by Debuigne and coworkers, who have carried out an NMR analysis of PVAc made by $Co(acac)_2$-mediated radical polymerization.[211] The presence of the expected fraction of inverted monomer units resulting from head-to-head addition in free radical polymerization was confirmed, in agreement with the notion that the action of the controlling agent is only that of trapping the active radical into the inactive dormant state, whereas the propagation step occurs on the free radical and consequently the same propagation rate constant, stereochemical characteristics, and degree of monomer inversion as in free radical polymerization should result. Therefore, the reason for the excellent level of control observed

in VAc polymerization until high degrees of polymerization when using this controlling agent must be a rapid reactivation of the dormant species of the latent primary radical, with a rate not too much smaller than the reactivation of the latent secondary radical. This situation contrasts with that of the dormant species in ATRP, ITP, and TERP and to a certain extent also RAFT. Alkylcobalt(III) complexes that can be taken as models of each type of dormant species are presently unavailable. Therefore, information on any difference in the reactivation rate is not at reach from experimental investigations. Useful information can only be gathered from theoretical calculations.

In order to find out the reason for the similar reactivation rates from both types of [PVAc-$Co(acac)_2$] dormant species, we have carried out computational investigations on models of these two species and we have also calculated the relative bond strengths for the other R−X bonds in the dormant species generated by ATRP, RAFT/MADIX, ITP, and TERP in order to gain a comprehensive view of the effect of this monomer inversion in RDRP.

The chosen computational model is rather simple. In order to keep the computational cost low without significantly affecting the quality of the result, the polymer structure beyond the last monomer unit at the capped chain end was simplified to an H atom as shown in Scheme 29 (as already done in previously published work[72,212] as well as in the calculations presented in the previous section). Previous calculations of M−X bond strengths for H−M−X and H−M′−M−X models (M, M′ = monomer; X = Cl, Br), carried out in order to evaluate penultimate effects in ATRP [M and M' were restricted to propene (P), methyl acrylate (MA) and methyl methacrylate (MMA)] led to the conclusion that a significant change was only present on going from H−MMA−X to H−MMA−MMA−X, which could be mainly attributed to steric destabilization by van der Waals repulsion between the two bulky MMA units.[274] This result confirmed the known penultimate effect in the ATRP of MMA.[275] Two adjacent VAc monomers should not exert any greater pressure on each other than two MA monomers. Hence, a large penultimate effect is not expected for PVAc and the H−VAc−X BDE should be representative of the BDE in the X-capped PVAc chain.

For the OMRP system, this bond is directly regulating the activation/deactivation equilibrium. For the ATRP system implicating a Mt^n catalyst and the corresponding Mt^{n+1}−Cl trapping agent, the equilibrium is related to BDE(PVAc−Cl) − BDE(Mt^{n+1}−Cl). However, since the latter bond strength is common to the two equilibria, the differences can be evaluated from the individual PVAc─Cl bond strengths, modeled by the H−VAc−Cl isomers. The other three systems (ITP, TERP and RAFT) work on the degenerative transfer principle for which the

controlling criterion is different. However, the same BDE(HVAc−X) difference is once again relevant to evaluate slowdown effects. This can be easily appreciated from Scheme 30 which illustrates the reactivation of the stronger primary latent radical by the nondegenerative exchange with the secondary active radical. Although in reality the exchange occurs associatively, the enthalpy difference of the process is formally identical to the difference of bond dissociation enthalpies. The greater this difference, the harder to reactivate the dormant species formed after head-to-head addition.

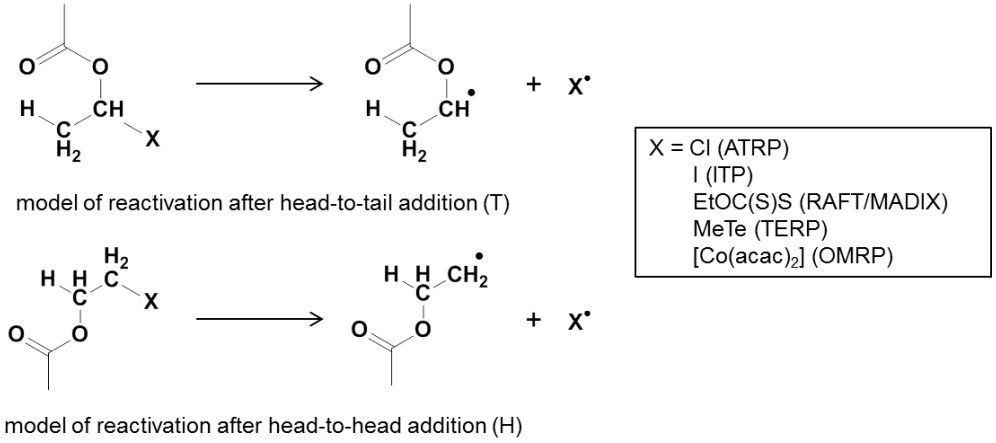

Scheme 29: Models used for the DFT calculations.

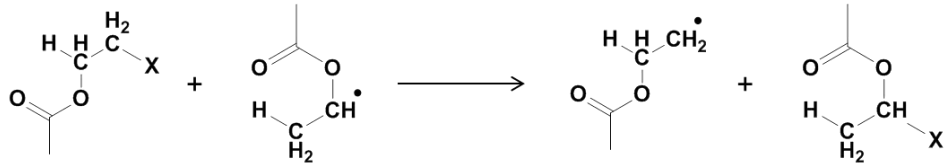

Scheme 30: Reactivation in degenerate exchange.

The OMRP system with X = $[Co(acac)_2]$ deserves two special comments. One of them concerns the different spin state change, already alluded to in the previous section of this chapter. Contrary to the other capping agents ($Cl^{\bullet}$, $I^{\bullet}$, $EtOC(S)S^{\bullet}$ and $MeTe^{\bullet}$) that have radical character (spin state S = 1/2), the $[Co(acac)_2]$ complex is characterized by three unpaired electrons and the total spin state changes from 2 or 1 (ferro- or antiferromagnetic combination of the 3/2 spin of $[Co(acac)_2]$ with the ½ spin of the organic radical) to zero during the formation of the Co-C bond . Al already discusses above, special care has to be taken in DFT calculations when there is a spin state change. Therefore, we have decided to apply a variety of functionals to span all possible scenarios for the analysis of this problem. In particular, we have used BPW91, which is a GGA functional; B3PW91, a popular hybrid functional; the above-mentioned BPW91*, as well as two recently developed functionals (M06, which is a hybrid functional recommended for application in organometallic chemistry and M06L, a local density functional performing well in transition metal energetics). The second special

comment concerns the structure of the polymer chain-end for the $Co(acac)_2$-capped PVAc. As already detailed in the first section of this chapter (see species I, Figure 98), under bulk conditions, chelation with carbonyl coordination of the last monomer unit bonded to the $[Co(acac)_2]$ chain end is preferred. It can therefore be imagined that a similar chelation may occur for the alternative dormant species generated after a head-to-head addition, forming a 6-membered chelate ring (II in Figure 98). For all latent PVAc radicals generated by the other RDRP methods, no such chelation is possible. The enthalpic results of the calculations are summarized in Table 16 and figures of all optimized geometries are provided in Figure 99-Figure 103.

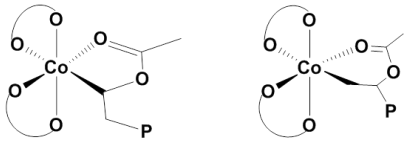

I II

Figure 98: Structure of $[PVAc{-}Co(acac)_2]$ chain end.

Table 16: Calculated bond dissociation enthalpies (kcal/mol) of HVAc−X bonds using different functionals (Values are BDE(HVAc─X) in kcal/mol. H─T = head-to-tail coupling model (secondary radical); H─H = head-to-head coupling model (primary radical); Δ = BDE(H─H) – BDE(H─T).) [a] Δ = enthalpy difference between the two isomeric free radicals.

X		BPW91	BPW91*	B3PW91	M06	M06L
-	Δ[a]	8.2	7.7	7.3	7.2	6.6
Cl (ATRP)	H–T	74.2	75.7	73.9	79.4	78.7
	H–H	81.8	83	81	85.8	84
	Δ	7.6	7.3	7.1	6.4	5.3
I (ITP)	H–T	47.1	46.2	46.6	54.2	51.7
	H–H	56.3	55.5	55.7	62.7	59
	Δ	9.2	9.3	9.1	8.5	7.3
MeTe (TERP)	H–T	41.8	43.5	42.5	52.8	50.2
	H–H	50.1	50.9	49.8	58.9	55.4
	Δ	8.3	7.4	7.3	6.1	5.2
EtOC(S)S (RAFT)	H–T	46.8	51.3	50.6	57.7	54.7
	H–H	52.4	56.4	55.3	61.5	57.9
	Δ	5.6	5.1	4.7	3.8	3.2
$Co(acac)_2$ (OMRP)	H–T	28.2	17.3	9.3	18.5	34.2
	H–H	29.1	18.3	10.2	19.9	34.3
	Δ	0.9	1	0.9	1.4	0.1

The first line (X = -) shows the enthalpy difference between the two isomeric free radicals. As expected, the primary radical (H−H) is less stabilized than the secondary one (H−T), the

computed difference being relatively independent of the type of functional used in the calculation (6.6 −8.2 kcal/mol range). The BDE(HVAc−X) for each isomer, related to each X group with radical nature (S = 1/2), namely the dormant species in ATRP, ITP, TERP and RAFT, is also quite similar for all functionals that involve the PW91 correlation part, whereas it is slightly higher (by 4−10 kcal/mol depending on X) when using Truhlar's M06 and M06L functionals, with M06 always yielding higher BDEs relative to M06L. The special [Co(acac)$_2$] case will be analyzed separately below. The BDE difference (Δ) between the isomeric bonds is however always in a narrow range (within 3 kcal/mol), M06 and M06L always giving slightly smaller differences. These Δ values are not too different than the enthalpy difference between the isomeric free radicals, which is not totally unexpected. The Δ values associated with Cl and MeTe are indeed very close to the enthalpy difference between the isomeric free radicals, whereas they are slightly greater for the ITP dormant species (there is an extra stabilization in the HVAc-I bond for the H−H isomer, or a destabilization for the H−T isomer) and slightly smaller for the RAFT dormant species. In the latter case, however, the difference remains relatively high (from 3.2 kcal/mol at the M06L level to 5.6 kcal/mol at the BPW91 level), too high to account for an equally rapid reactivation from the dormant species with the primary radical. Nevertheless, the calculations predict that the slowdown effect in RAFT using xanthates should be less pronounced relative to ATRP, TERP, and particularly ITP, in line with the experimental evidence.

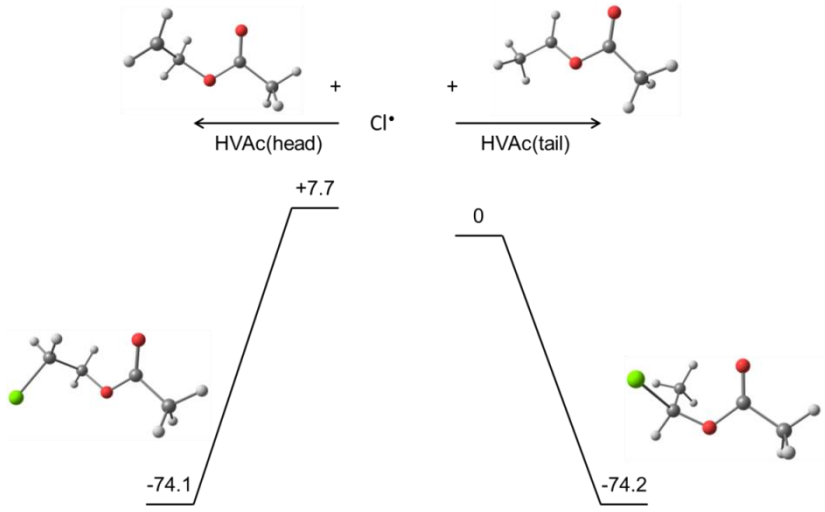

Figure 99: Relative BPW91* enthalpies (in kcal/mol) and optimized geometries of the species implicated in the deactivation process of the T and H PVAc radical models by ATRP (X = Cl•).

The [Co(acac)$_2$] case is more interesting, because there is a greater variation of BDE among different functionals, the greatest difference being 25 kcal/mol for the H-T isomer between the calculations with B3PW91 and M06-L. The calculated BDE that are reported in Table 16

(page 141) are based on the chelated structures shown in I and II (Figure 98) for the dormant species. The greater variation of BDE between different functionals is caused by the change of spin state on going from the Co^{III} dormant species (S = 0) to the separate fragments (S = ½ for the organic radical and 3/2 for $[Co^{II}(acac)_2]$. As expected from the typical performance in problems involving a spin state change, the highest computed BDE for each isomer is associated with the local M06L functional and, to a lesser extent, with the generalized gradient BPW91 functional, whereas the lowest BDE is given by the hybrid functional B3PW91. The "ad hoc" BPW91* functional yields intermediate BDE values. The M06 functional yields results closer to those of the "ad hoc" BPW91* functional than to those of the B3PW91 functional. The most important point, however, is that all functionals yield essentially the same Δ for the organocobalt(III) dormant species, just like for the other dormant species with the radical-type X groups.

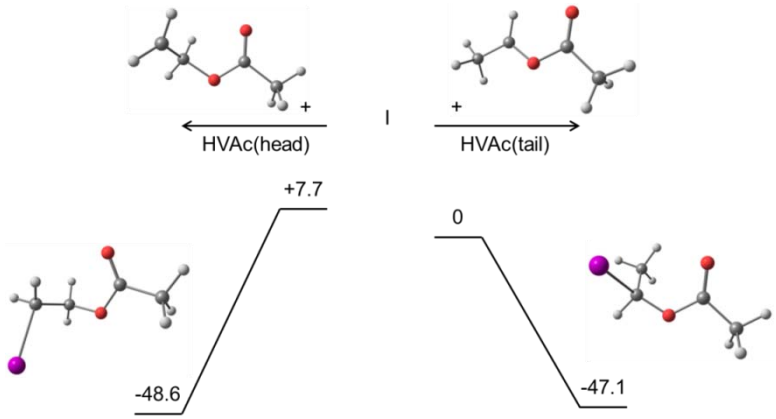

Figure 100: Relative BPW91* enthalpies (in kcal/mol) and optimized geometries of the species implicated in the deactivation process of the T and H PVAc radical models by ITP (X = I).

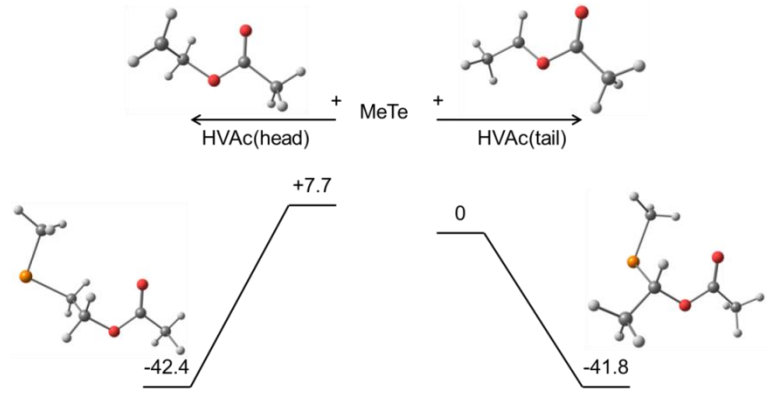

Figure 101: Relative BPW91* enthalpies (in kcal/mol) and optimized geometries of the species implicated in the deactivation process of the T and H PVAc radical models by TERP (X = MeTe•).

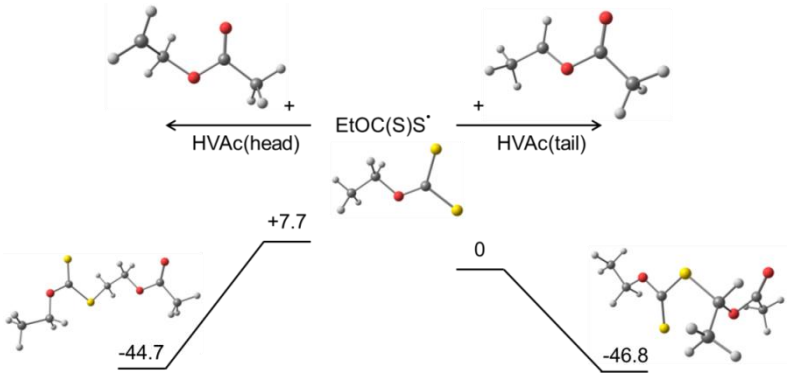

Figure 102: Relative BPW91* enthalpies (in kcal/mol) and optimized geometries of the species implicated in the deactivation process of the T and H PVAc radical models by RAFT (X = EtOC(S)S•).

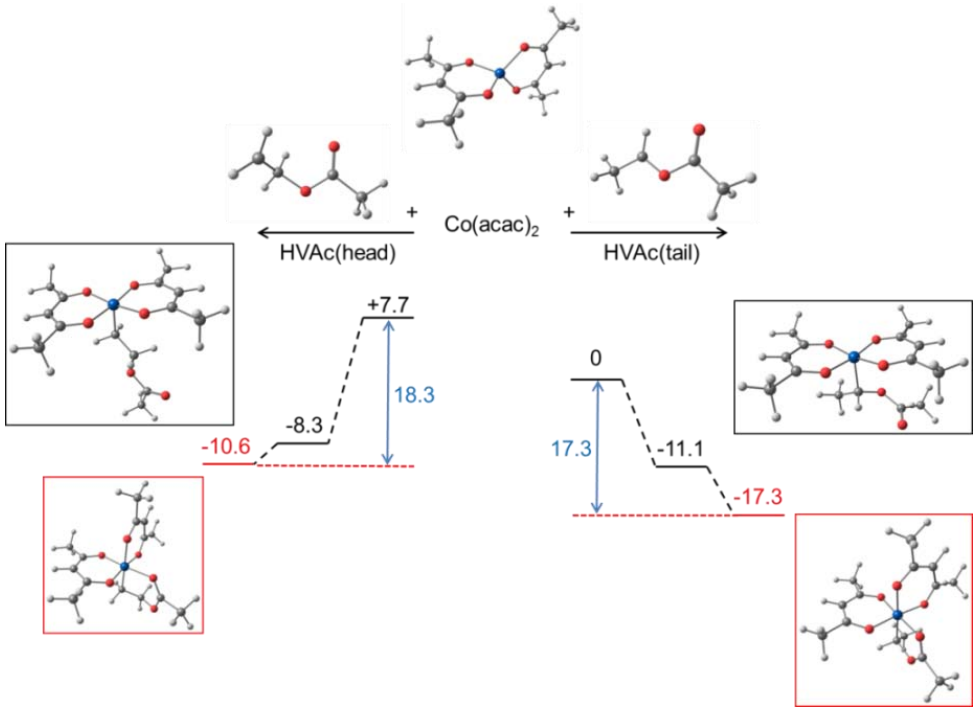

Figure 103: Relative BPW91* enthalpies (in kcal/mol) and optimized geometries of the species implicated in the deactivation process of the T and H PVAc radical models by OMRP (X = [$Co(acac)_2$]).

The point that is now of interest is the very different Δ for the $Co(acac)_2$-capped polymer chain models (close to zero) relative to the ATRP, RAFT, ITP, and TERP dormant chain models. This means that an essentially equivalent energetic cost is predicted for the reactivation of both types of dormant species, comforting the experimental evidence of the absence of slowdown and good control for the $Co(acac)_2$-mediated VAc polymerization, contrary to ATRP, ITP, TERP, OMRP with other metal complexes and to a certain extent RAFT with xanthates. In order to rationalize this large difference in relative stabilization, the radical releasing process has been analyzed in more details to evaluate the individual contributions of the chelation and the intrinsic Co^{III}–C BDE. This analysis has only been

carried out using the BPW91* functional and the result is graphically shown in Figure 103. Going from [$Co(acac)_2$] (in the top middle) to the [$HVAc{-}Co^{III}(acac)_2$] dormant species (regular H−T isomer toward the right and inverted H−H isomer toward the left), the process can be split into two separate steps: first, bond formation yields a five-coordinate alkylcobalt-(III) intermediate that has a S = 0 ground state and a square pyramidal geometry with the alkyl group in the apical position. The spin state change occurs in this step. Subsequently, the arrangements of the two acac ligands changes from planar to butterfly, in order to move the empty coordination site from trans to cis relative to the alkyl group and to allow coordination of the carbonyl function. The calculations indicate that the bond formation is more exothermic, as could be anticipated, for the more reactive primary radical (16.0 kcal/mol for the H−H isomer *vs* 11.1 kcal/mol for the H−T isomer). The difference of 4.9 kcal/mol in these intrinsic BDEs is rather similar to that calculated for the RAFT dormant species with the same functional (5.1 kcal/mol). However, the much more favorable chelation to make a five-membered ring for the H-T isomer (worth 6.2 kcal/mol on the enthalpy scale) provides additional stabilization to the H−T dormant species relative to the H−H isomer, for which chelation leading to a six-membered ring is only worth 2.3 kcal/mol of stabilization. Therefore, the compensation of a weaker bond by a more stable chelate renders the stabilization of the H−T dormant species equivalent to that of the more reactive H−H isomer and both dormant species can be reactivated with similar rates. Note that this compensation effect is only possible when the metal complex has the possibility to make a coordination site available for chelation in an adjacent position (cis) to the metal−carbon bond, which is the case for [$Co(acac)_2$] and not for other metal complexes such as CpCr(NacNac) (see Figure 25, page 65). The porphyrin compound (TMP)Co (see Figure 8, page 46) equally forbids or prevents chelation because of the rigidity of the planar porphyrin ligand.

In conclusion, we have used theoretical calculations to gain a comprehensive view of the impact of the inverted head-to-head addition mode in the RDRP of vinyl acetate. In general, the primary head-to-head radicals lead to a more stable dormant species compared to the regular secondary head-to-tail adducts that, because of its more difficult reactivation, leads to a slowdown or inhibition of the polymerization and to an increase of the molar mass distribution. However, these problems are not observed for the $Co(acac)_2$-mediated polymerization. NMR study made by Debuigne and coworkers has revealed a similar fraction of head-to-head sequences in the PVAc produced by Co-MRP and FRP under the same experimental conditions. This proves that the cobalt complex has no effect on the VAc insertion mode. Moreover, no abnormal accumulation of these repeated units was observed at

the chain-end.[211] Therefore, both types of dormant species must be reactivated at similar rates. This assumption was corroborated by DFT calculations which predict similar enthalpic stabilizations for the secondary H−T−Co and primary H−H−Co dormant species. The stronger Co−C σ-bond formed by the H−H adduct is compensated by a weaker stabilization from the formation of the 6-membered chelate ring with the carbonyl function of the metal-bonded monomer. On the other hand, the regular H−T−Co dormant species contains a weaker Co−C σ-bond and a stronger 5-membered chelate ring. The combination of both effects yields a similar reactivation rate from both dormant species. This peculiar structural feature is specific for the $Co(acac)_2$-terminated dormant chains, at variance with the PVAc−X dormant chains of other RDRP techniques like ATRP, RAFT/MADIX, ITP, and TERP, for which the C−X bond to the primary H− H radical is significantly stronger and therefore more difficult to reactivate.

GENERAL CONCLUSION

GENERAL CONCLUSION

In conclusion, we have explored for the first time the use of copper complexes as controlling agent for the organometallic-mediated radical polymerization (OMRP) of vinyl acetate and ethylene. We have focused on the copper(I)/copper(II) couple coordinated by nitrogen based ligands: *β*-diketiminate (NacNac), substituted tripodal scorpionates (Tp), tris(pyridylmethyl)amine (TPMA) and tris(pyridylthiomethanide) (TPTM). Although we were not able to isolate any copper(II)-alkyl species, we have shown with evidence from EPR spectroscopic studies that depending on the ligand surrounding the copper atom, copper-carbon bond could be formed by alkylation of suitable Cu^{II} cationic or neutral chloride precursors. We are now convinced that an organometallic copper(II) species can be formed and that an OMRP equilibrium can be established with these complexes studied. In particular, a copper complex with the hydrotris(3,5-dimethylpyrazol-1-yl)-borate (Tp*) ligand, [Tp*CuCl], has shown interesting properties toward alkylation. All the investigated copper(I) complexes have revealed a more or less pronounced retardation effect on vinyl acetate (VAc) and ethylene polymerizations. In the case of VAc, the most interesting results were obtained with the Tp* ligand showing a certain degree of control and a recovered PVAc with relatively low dispersity values ($1.2 < Đ < 1.5$) under "reverse" OMRP conditions. In addition, polymer formation continued beyond the time needed to fully decompose the radical initiator, demonstrating the presence of a dynamic reversible trapping of polymer chains by copper(I) complexes to yield labile dormant species. For both VAc and ethylene polymerizations, the degree of control was assessed by start-stop experiments, analysis of the polymer dispersity and molecular weight-conversion profile. From our preliminary results, we can conclude that the ligand structure has an effect on the OMRP equilibrium with the more electron-donating substituents leading to more efficient trapping. The lower coordination number of the NacNac ligand (bidentate) relative to the tris(pyrazolyl)borate ligand (tridentate) leads to much stronger PVAc-Cu^{II} bonds.

In perspective, the steric effects of the NacNac and scorpionate ligands should be investigated to finely tune the copper-carbon bond strength and consequently the OMRP equilibrium constant. A screening of other bidentate and tridentate nitrogen ligands could potentially allow the discovery of more efficient copper complexes for OMRP of VAc and ethylene. Vinyl acetate and ethylene copolymerization should also be investigated and the experimental set-up already used for ethylene homopolymerization could be modified to eliminate the observed self-initiation from the solvent or monomer impurities. Other solvents could also be

investigated in order to limit the chain transfer reactions to solvent that are favored by the high reactivity of the PE radical chains. Although we have shown spectroscopic evidences of the targeted alkyl-copper(II) formation, more work is needed to isolate a species which could serve as a unimolecular initiator under OMRP conditions.

In addition, we have used theoretical calculations to gain a comprehensive view of the successful cobalt-mediated radical polymerization processes. The impact of the inverted head-to-head addition mode in the RDRP of vinyl acetate has been investigated. Although this "inverted" monomer addition frequency is low, the primary head-to-head radicals lead to a more stable dormant species compared to the regular secondary head-to-tail adducts that, because of its more difficult reactivation, leads to a slowdown or inhibition of the polymerization and to an increase of the molar mass distribution. However, the $Co(acac)_2$-mediated radical polymerization of VAc does not seem to be severely affected by these problems. In collaboration with Debuigne and coworkers, we have given an interpretation to this remarkable $Co(acac)_2$-mediated polymerization feature. Indeed, the cobalt has no effect on the VAc insertion mode but according to DFT calculations, both types of dormant species are reactivated at similar rates because of a unique coordination of the carbonyl group from the last monomer unit of the trapped chain to the cobalt center. The stronger Co−C σ-bond formed by the head-to-head adduct is compensated by a weaker stabilization from the formation of the 6-membered chelate ring with the carbonyl function of the metal-bonded monomer. On the other hand, the regular head-to-tail dormant species contains a weaker Co−C σ-bond and a stronger 5-membered chelate ring. The combination of both effects yields a similar reactivation rate from both dormant species. This peculiar structural feature is specific for the $Co(acac)_2$-terminated dormant chains, at variance with the PVAc−X dormant chains of other RDRP techniques like ATRP, RAFT/MADIX, ITP, and TERP, for which the C−X bond to the primary H− H radical is significantly stronger and therefore more difficult to reactivate. With the perspective of finding complexes able to provide good control for the VAc polymerisation under OMRP condition, this unique coordination phenomenon must be taken into consideration.

Although amides are known to be stronger Lewis bases than esters, the Co-MRP of these monomers have, so far, always been presented as a simple reversible capping of the radical chains by the metal. In light of the above results with VAc polymerization, we have subsequently investigated the possible effect of an intramolecular chelation of the cobalt center on the course of a series of *N*-vinyl amides [*N*-vinyl formamide (NVF), *N*-vinyl amide

(NVA), *N*-methyl-*N*-vinyl acetamide (NMVA), *N*-vinyl pyrrolidone (NVP), *N*-vinyl caprolactam (NVCl)]. The rate of polymerization order obtained experimentally by Debuigne and coworkers (the slower NMVA < NVCl < NVP < NVA < NVF the faster) has been rationalized by DFT studies. Indeed, the intrinsic Co─C bond strength in the dormant chain models (in the 7.3-10.0 kcal/mol range) is only slightly smaller than in the [$Co(acac)_2$(VAcH)] model but the chelation resulting from coordination of the carbonyl group change deeply the total Co─C bond strength values (enthalpy of chelation in the 3.0-7.8 kcal/mol range). Finally, when the carbonyl group chelation is taken into account, the total enthalpies of the Co─C bond formation to yield the more stable K^2:C,O product are all greater than that of VAc (13.0 kcal/mol) except for the NVPH radical (in the 11.6-16.5 kcal/mol range). The enthalpy difference between the dormant and activated species becomes smaller in the order NMVAH > NVClH > NVAH > NVFH = VAcH > NVPH. The only apparent disagreement between the bond strength order and the rate of polymerization observed experimentally appears to be the relative positioning of NVP and NVF. Indeed, the enthalpy differences analyzed above are overvalued for the two latter monomer systems because of hydrogen bondings. The calculations predict that hydrogen bonding with the monomer will stabilize the free radical + [$Co(acac)_2$] to a greater extent (13.1 and 15.1 $kcal.mol^{-1}$ for the NVA and NVF system, respectively) than the chelated dormant state (2.4 and 3.2 $kcal.mol^{-1}$ for the NVA and NVF system, respectively), with an accelerating effect for the polymerization.

EXPERIMENTAL PART

EXPERIMENTAL PART

Materials.

All chemicals were purchased from commercial sources and used as received if not stated otherwise. 2,2'-azobis(isobutyronitrile) (AIBN, $C_8H_{12}N_4$; > 98% ; ACROS); 2,2'-azobis(4-methoxy-2,4-dimethylvaleronitrile) (V-70, $C_{16}H_{28}N_4O_2$; 95% ; Wako); butyl acrylate ($C_7H_{11}O_2$; 99% ; Sigma-Aldrich); calcium hydride (CaH_2 ; 99 % ; Aldrich); copper(II) chloride ($CuCl_2$; 99 % ; Fluka); copper(I) trifluoromethanesulfonate benzene complex ($[Cu(OTf)]_2,C_6H_6$; 98 % ; Strem Chemicals); ethylene (in a gas tank, C_2H_4 ; > 99.8 % ; Linde Gas); methyl lithium (MeLi, 1M in cumene ; Aldrich); methylmagnesium bromide (MeMgBr, 3M in diethyl ether ; Strem Chemicals); methylmagnesium iodide (MeMgI, 3M in diethyl ether ; Acros Organics); sodium hexafluorophosphate ($NaPF_6$; > 98% ; Fluka); tetrahydrofuran (THF, C_4H_8O ; > 99.9 % ; Aldrich); 2,2,6,6-(tetramethylpiperidin-1-yl)oxyl (TEMPO, $C_{10}H_{19}O$; > 98% ; Acros Organics); toluene (C_7H_8 ; 99.7% ; Aldrich); vinyl acetate (Vac, $C_4H_6O_2$; 99% ; Acros Organics). We are grateful to Prof. Krzysztof Matyjaszewski for providing us with a sample of the TPMA* ligand, synthesized in his laboratory by Dr. Kristin Schröder.[276]

The following organic molecules and complexes were synthesized according to published procedure and the analysis of the product obtained were in agreement with the reported analysis: tetrakis(acetonitrile)copper(I) tetrafluoroborate $[Cu(CH_3CN)_4]BF_4$,[277] (hydro-tris(pyrazol-1-yl)borato)copper(I) dimer, $[CuTp^*]_2$,[234] chloro(hydrotris(3,5-dimethyl(pyrazol-1-yl))borato)copper(II), [CuTp*Cl],[278] potassium tris(3,5-bis(trifluoromethyl)pyra-zolyl)borate, KTp^{CF3},[279] (hydrotris(3,5-(trifluoromethyl)pyrazol-1-yl)borato)(acetonitrile) copper(I), $[Cu(Tp^{CF3})(MeCN)]$,[252] chlorotris(pyridylthio)methanidocopper(II), [Cu(TPTM)Cl] .[230] THF and diethyl ether solvents were distilled over sodium and benzophenone, under an argon atmosphere, prior to use. Dichloromethane and toluene were distilled under an argon atmosphere over calcium hydride and sodium respectively. Deuterated benzene used for NMR analyses (C_6D_6) was purchased as sealed vial under argon from Eurisotop.

Instrumentation.

Vacuum Pump

The pump used is a "Edwards" model RV5, A653-01-903 which allow a pressure below 100 mbar.

Gel permeation chromatography (GPC)

GPC was used to determine number-average molecular weight (M_n) and dispersity values (Đ). The GPC was conducted with a gel PL type guard column (50 x 7.5 mm; particles size 5µm) and a mixt PL-gel separation column (D 5µm; 300x 7.5 mm; Polymer Laboratories) in tetrahydrofuran as an eluent (previously filtered on a 200nm pore diamenter membrane) at a flow rate of 1 mL/min at 20°C. Samples were dissolved in THF at concentration around 5 mg/mL and ultrasonicated for 5 min. Their dissolution were followed by a 4 hours to 24 hours resting time before being filtered over a teflon microfilter (200 nm). Molecular weights were determined by a Multi-angle diffusion light scattering detector (MALLS minidawn Tristar Wyatt Technology Corporation) coupled with a differential refractometer (RI2000 Sopares). The dn/dc parameter for PVAc is 0.0502 ml/g in THF at 23 °C.[280]

Nuclear magnetic resonance (NMR) spectrometry

The special case of PE sample is detailed below. Otherwise, ^{1}H NMR spectra were recorded using a Bruker Avance 300 MHz and/or a Bruker Avance 400 MHz spectrometers at 20°C. Acquisition conditions used: *zg60* pulse program; number of scans ≥ 6; relaxation time ≥ 1s. ^{13}C spectra were recorded using a Bruker Avance 500 instrument operating at 100.56 MHz. Acquisition conditions used: *zg60gd* or dept135 pulse program; number of scans ≥ 200; relaxation time = 4s. ^{19}F spectra were recorded using a Bruker Avance 500 instrument operating at 282.4 MHz. Acquisition conditions used: *zg60* pulse program; number of scans ≥ 16; relaxation time = 4s. ^{11}B spectra were recorded using a Bruker Avance 500 instrument operating at 121.5 MHz. Acquisition conditions used: *zg60* pulse program; number of scans = 32; relaxation time = 4s. The ^{1}H chemical shifts are reported in ppm relative to tetramethylsilane (δ = 0 ppm) by internal standardization with the residual solvent peak. Abbreviations used for the NMR resonances are: br. broad, s singlet, d doublet, t triplet, m multiplet.

The PE NMR analyses were carried out by ^{1}H and ^{13}C NMR at 363K with a tetrachloroethylene/deuterated benzene (50/50 v/v) solvent mixture.
The ^{1}H NMR spectra were recorded at 500 MHz with the (30°)-acquisition (Zg30) pulse sequence. Spectral width, 4.5 kHz; FID size, 30K; time between pulses (d1+AQ), 13.3 s; number of scans, 8; acquisition time, 2 min 13 s.

The ^{13}C NMR spectra were recorded at 125 MHz with a ^{1}H decoupled pulse sequence to allow integration (zgig60). Spectral width, 25 kHz; FID size, 50K; time between pulses (d1+AQ), 6 s; number of scans, 7056; acquisition time, 12 hours.

Mass spectrometry

The masse spectra analyses were performed by ‘‘Service commun de spectrométrie de masse’’ of the Université Paul-Sabatier, Toulouse, France (GCT 1er Waters for DCI, CH_4; UPLC Xevo G2 Q-TOF (Waters) for ES+).

Electron Paramagnetic Resonance (EPR) spectrometry

Solutions of the starting copper complex or of the reaction medium were diluted to 0.1-1 mM in THF. Samples were frozen in quartz tubes and data were acquired using an Elexsys E 500 Bruker spectrometer, operating at a microwave frequency of approximately 9.5 GHz. All spectra were recorded using a microwave power of 20 mW with a modulation amplitude of 5 G. The sweep width varied with experiments but was between 600 G and 1400 G (centered at 325 ± 5 mT). Experiments were carried out at 110 K using a liquid nitrogen cryostat.

EPR spectra simulations

Simulations of the EPR spectra were performed using the MATLAB r2012b Easyspin® tool box and the Pepper function.

Computational details.

The computational work was carried out using the Gaussian03 or Gaussian09 suite of programs.[281,282] The geometry optimizations were performed without any symmetry constraint by using the BPW91, BPW91*, B3PW91*, M06 and M06L functionals. The BPW91* is a modified version of the B3PW91 functional, in which the c3 coefficient in Becke’s original three parameter fit to thermochemical data was changed to 0.15.[283] The 6-31G** basis functions were used for all light atoms (H, C, Cl, N, O, S) and the Co, I and Te atoms were treated with the LANL2DZ function augmented by an f polarization function ($\alpha = 3.78$)[284] for Co and by a d polarization function for Te ($\alpha = 0.252$) and for I ($\alpha = 0.289$).[285] The unrestricted formulation was used for open-shell molecules, yielding only minor spin contamination ($< S^2 >$ at convergence was very close to the expected value of 0.75 for the radical species and 3.75 for the spin quartet species). All final geometries were characterized as local minima by verifying that all second derivatives of the energy were positive. Thermochemical corrections were obtained at 298.15 K on the basis of frequency calculations, using the standard approximations (ideal gas, rigid rotor and harmonic oscillator).

Synthesis of tris(pyridylthio)methanido(acetonitrile)copper(II) tetrafluoroborate: $[Cu(TPTM)(CH_3CN)]BF_4$, was synthesized following the same procedure reported for the synthesis of $[Cu(TPTM)(MeCN)]PF_6$[230] except that $[Cu(CH_3CN)_4]PF_6$ was replaced by $[Cu(CH_3CN)_4]BF_4$.

Synthesis of (*N*-[3-[(2,6-dimethylphenyl)amino]-1-methyl-2-buten-1-ylidene]-2,6-dimethyl-benzenamine)(acetonitrile)copper(I) [Cu(NacNac^{XylXyl})MeCN]: To a suspension of tetrakis(acetonitrile)copper(I) tetrafluoroborate (557 mg, 1.77 mmol) in 4 mL of THF was added dropwise a solution of LiNacNac^{XylXyl} (553 mg, 1.77 mmol) in 4 mL of THF to yield a bright yellow solution and an orange precipitate, which may correspond to $LiBF_4$. The mixture was stirred at room temperature overnight and filtered through Celite. The solvent was removed under reduced pressure to yield a brownish solid. Pentane (12 mL) was added and the resulting orange solution was again filtered through Celite. The volume of the filtrate was reduced to 3 mL and stored in the freezer to give white yellowish solid with 17 % yield (110 mg). ^{1}H NMR (C_6D_6, 300 MHz): δ 7.2 (m, 4H), 7.1 (m, 4H), 4.9 (s, 1H), 2.1 (s, 12H), 1.8 (s, 6H), 0.5 (s, 3H).

Polymerizations.

General procedure for vinyl acetate polymerizations: The monomer was dried over calcium hydride overnight then distilled over calcium hydride. A typical polymerization procedure was as follows: in a Schlenk tube equipped with a stirrer was introduced the copper complex, vinyl acetate and freshly distilled solvent (toluene or tetrahydrofuran). The mixture was then freeze-pumped three times (with a vacuum pressure below 100 mbar). The initiator (usually V-70) was added under an argon flow on the top of the freezed mixture before the last pump cycle. The Schlenk tube was immersed in an oil bath at the desired temperature (starting time t_0). Whenever samples were withdrawn during the polymerization, they were collected under an argon flow by a syringe followed by quenching of the polymerization by bubbling air into the sample. Conversions were determined by weight after removal of the monomer under reduced pressure until the residue reached constant weight.

General procedure for ethylene polymerizations: Ethylene was used as received without further purification. In a Schlenk tube was prepared a mixture containing THF (usually 30 mL), the initiator (usually AIBN) and the copper complex. This mixture was deoxygenated by several freeze-pump cycles then transferred into a dry and degassed autoclave equipped with a stirrer via a cannula. The autoclave was then connected to the vacuum line for less than a second to remove the argon atmosphere and then charged with ethylene while stirring the

liquid phase to allow dissolution of the ethylene into the solvent. The autoclave was heated if necessary with a heating-collar and the temperature was monitored by an electro-thermometer connected into the autoclave. After the reaction time, the autoclave was cooled down to room temperature, depressurized and open in the air. The liquid was transferred into an Erlenmeyer flask, a large excess of methanol was added and the whole mixture was stored at 5°C overnight to allow the polymer precipitation. The solid polyethylene was finally recovered by filtration on a paper filter and dried under vacuum until the sample weight was constant. The oligomers were still soluble in the THF/MeOH mixture. They were recovered by evaporation of the filtrate solvent under reduced pressure to yield a viscous paste (colorless or green when copper was used).

Chain extension of the PE: A classical ethylene polymerization was set-up as described above (initial ethylene pressure 30 bars at 14°C, polymerization temperature 90°C). After the 24 hours reaction time, the autoclave was cooled down to room temperature, depressurized and the 30 mL liquid mixture was transfer into a Schlenk tube under an argon flow. Degassed methanol (60 mL) was added to allow the polymer chains to precipitate. The PE was recovered by filtration via a cannula equipped with a paper filter. The filtrate solvent was removed by evaporation under reduced pressure to yield 310 mg of a slightly green viscous liquid (*i.e*. PE oligomers). Part of this recovered PE oligomer sample (112 mg) was put into a Schlenk tube under an argon flow and 30 mL of dry and distilled THF were added. This solution was then cannula transferred into a dry and degassed autoclave equipped with a stirrer. The autoclave was then depressurized for less than a second to remove the argon atmosphere and then charged with ethylene while stirring the liquid phase to allow dissolution of ethylene into the solvent (initial ethylene pressure 32 bars at 16°C). The autoclave was heated to 90°C with a heating collar and the temperature was monitored by an electro-thermometer connected to the autoclave. After the reaction time, the autoclave was cooled down to room temperature, depressurized and open in the air. Dry and degassed methanol (60 mL) was added. After filtration, 17 mg of solid PE and 350 mg of oligomers were recovered.

Procedure for butyl acrylate polymerization and EPR analysis:

Butyl acrylate was filtered on basic alumina to remove the radical polymerization inhibitor prior to use. The same protocol described earlier by Matyjaszewsky was adopted (BA = 10 mL, 68.9 mmol; AIBN = 14.3 mg, 87.1 µmol; TPMA* = 12 mg, 26 µmol; $[Cu(MeCN)_4]BF_4$ = 2.2 mg, 7µmol).[286] After 4 h and 45 min at 60°C, the Schlenk tube was cooled down to room temperature and 10 mL of distilled and degassed (by several freeze-pump cycles) THF

was added to yield a solution with [Cu] = 0.56 mM. A 0.5 mL aliquot of this diluted solution was transferred into a quartz tube and analyzed by EPR (see conditions above).

Alkylation experiments

Alkylation of [Tp*CuCl] by MeMgI: [Tp*CuCl] (40 mg, 0.1 mmol) was dissolved into 10 mL of dry and degassed diethyl ether to yield a clear brownish solution. Argon was bubbled for 10 more min. The Schlenk tube was immersed into a cold bath at -40°C and a solution of MeMgI (3M in diethyl ether; 30 µL, 0.1 mmol) was added dropwise by syringe. After the first drop fell into the solution, an immediate color change to dark blue was noted at the spot where the drop hit the solution, then the solution became yellow-brownish after the 2nd and 3rd drop and a white precipitate appeared. At the end of the MeMgI solution addition, the solution was yellow. The mixture was stirred for 40 additional min at -40°C, during which time it became a bright green suspension. The blue-green solid part was separated by filtration over Celite at -40°C and stored at -80°C before the EPR analysis. This solid is neither soluble in diethyl ether nor in pentane.

Alkylation of [(TPTM)CuCl] by MeLi: A purple THF solution of [(TPTM)CuCl] was prepared (4.4 mg, 0.01 mmol, V = 20 mL). A THF solution of methyl lithium (0.016 mol/L; 1.0 mL, 0.016 mmol) were added into the copper solution. Both solutions were previously cooled down and kept at -50°C during the reaction. There was no noticeable color change upon addition of the methyl lithium. A sample was taken under argon flow for the EPR analysis.

Alkylation of [(TPTM)Cu(CH_3CN)BF_4] by MeLi: The same protocol as for [(TPTM)CuCl] was used (starting copper solution [Cu] = 0.43 mM, 20mL; methyl lithium solution [MeLi] = 16 mM, 0.7 mL added *i.e.* 1.3 eq.). No noticeable color change could be observed but the reaction was monitored by EPR while increasing temperature from -50°C to +1°C.

Alkylation of [(TPMA*)CuCl]PF_6 by MeMgBr: TPMA* (48 mg, 0.103 mmol) was dissolved into 10 mL of THF giving a yellow solution. In another Schlenk tube was prepared a THF solution of $CuCl_2$ (12 mg, 0.9 eq., 80 mL). The TPMA* solution was then added into the copper solution, turning its color from pale yellow to an intense bright yellow. The mixture was stirred at room temperature for 1 hour then a THF solution of $NaPF_6$ (18 mg, 1.1 eq., 20 mL) was added and the mixture was stirred for 2 additional hours at r.t.. The solution was then cooled down at -50°C before dropwise addition of a MeMgBr THF solution (1 mL, [MeMgBr] = 0.15 M, 1.5 eq.) that had previously been cooled down to -50°C. The solution turned progressively from bright yellow to yellow brownish and yellow greenish. When a

drop of the Grignard reagent fell into the copper solution, a dark green color appeared in the whirl before diffusion. Samples were directly taken from the solution to be analyzed by EPR.

REFERENCES

REFERENCES

[1] S. Gaynor, D. Greszta, D. Mardare, M. Teodorescu, K. Matyjaszewski, *J. Macromol. Sci., Pure Appl. Chem*., **1994**, *A31*, 1561-1578
[2] A. D. Jenkins, R. G. Jones, G. Moad, *Pure Appl. Chem*., **2010**, *82*, 483-491
[3] A. H. E. Müller, R. Zhuang, D. Yan, G. Litvinenkos, *Macromolecules*, **1995**, *28*, 4326-4333
[4] D. H. Solomon, E. Rizzardo, P. Cacioli (CSIRO) EP 0135280, **1985**
[5] M. K. Georges, R. P. N. Veregin, P. M. Kazmaier, G. K. Hamer, *Macromolecules*, **1993**, *26*, 2987-2988
[6] G. Moad, E. Rizzardo, *Macromolecules*, **1995**, *28*, 8722-8728
[7] B. Yamada, Y. Miura, Y. Nobukane, M. Aota, *ACS Symp. Ser*., **1998**, *685*, 200-213
[8] S. Grimaldi, J. P. Finet, A. Zeghdaoui, P. Tordo, D. Benoit, Y. Gnanou, M. Fontanille, P. Nicol, J. F. Pierson, *Polym. Prepr*., **1997**, *38*, 651-652
[9] L. Marx, P. Hemery, *Polymer*, **2009**, *50*, 2752-2761
[10] A. Studer, K. Harms, C. Knoop, C. Muller, T. Schulte, *Macromolecules*, **2004**, *37*, 27-34
[11] D. Benoit, S. Grimaldi, S. Robin, J.-P. Finet, P. Tordo, Y. Gnanou, *J. Am. Chem. Soc*., **2000**, *122*, 5929-5539
[12] Y. Guillaneuf, D. Gigmes, S. R. A. Marque, P. Astolfi, L. Greci, P. Tordo, D. Bertin, *Macromolecules*, **2007**, *40*, 3108-3114
[13] N. L. Hill, R. Braslau, *Macromolecules*, **2005**, *38*, 9066-9074
[14] C. J. Hawker, G. C. Barclay, A. Orellana, J. Dao, W. Devonport, *Macromolecules*, **1996**, *29*, 5245-5554
[15] F. Chauvin, P.-E. Dufils, D. Gigmes, Y. Guillaneuf, S. R. A. Marque, P. Tordo, D. Bertin, *Macromolecules*, **2006**, *39*, 5238-5250
[16] A. Fischer, A. Brembilla, P. Lochon, *Macromolecules*, **1999**, *32*, 6069-6072
[17] I. Chalari, S. Pispas, N. Hadjichristidis, *J. Polym. Sci. Part A: Polym. Chem*., **2001**, *39*, 2889-2895
[18] X. Z. Ding, A. Fischer, A. brembilla, P. Lochon, *J. Polym. Sci. Part A: Polym. Chem*., **2000**, *38*, 3067-3073
[19] D. Benoit, V. Chaplinski, R. Braslau, C. J. Hawker, *J. Am. Chem. Soc*., **1999**, *121*, 3904-3920
[20] C. Tang, T. Kowalewski, K. Matyjaszewski, *Macromolecules*, **2003**, *36*, 1465-1473
[21] L. Couvreur, C. Lefay, J. Belleney, B. Charleux, O. Guerret, S. Magnet, *Macromolecules*, **2003**, *36*, 8260-8267
[22] T. N. T. Phan, D. Bertin, *Macromolecules*, **2008**, *41*, 1886-1895
[23] J. Ruehl, N. L. Hill, E. D. Walter, G. Milihauser, R. Braslau, *Macromolecules*, **2008**, *41*, 1972-1982
[24] D. Benoit, E. Harth, P. Fox, R. M. Waymouth, C. J. Hawker, *Macromolecules*, **2000**, *33*, 363-370
[25] S. Harrisson, P. Couvreur, J. Nicolas, *Macromolecules*, **2011**, *44*, 9230-9238
[26] M. Baumert, J. Fröhlich, M. Stieger, H. Frey, R. Mülhaupt, H. Plenio, *Macromol. Rapid Commun*., **1999**, *20*, 203-209
[27] W. A. Braunecker, K. Matyjaszewski, *Prog. Polym. Sci*., **2007**, *32*, 93-146
[28] J.-F. Lutz, P. Lacroix-Desmazes, B. Boutevin, C. Le Mercier, D. Gigmes, D. Bertin, P. Tordo, *Polym. Prepr*., **2002**, *43*, 287-288
[29] P. Bilalis, M. Pitsikalis, N. Hadjichristidis, *J. Polym. Sci. Part A: Polym. Chem*., **2006**, *44*, 659-665
[30] A. Gaudel-Siri, D. Siri, P. Tordo, *Chem. Phys. Chem*., **2006**, *7*, 430-438
[31] M. V. Ciriano, H.-G. Korth, W. B. von Scheppingen, P. Mulder, *J. Am. Chem. Soc*., **1999**, *121*, 6375-6381
[32] S. Marque, H. Fischer, E. Baier, A. Studer, *J. Org. Chem*., **2001**, *66*, 1146-1156
[33] K. Matyjaszewski, J.-S. Wang, *J. Am. Chem. Soc*., **1995**, *117*, 5614-5615
[34] M. Kato, M.Kamigaito, M. Sawamoto and T.Higashimura, *Macromolecules*, **1995**, *28*, 1721-1723
[35] D. Xiao, M. J. Wirth, *Macromolecules*, **2002**, *35*, 2919-2925
[36] K. Matyjaszewski, S. Mu Jo, H.-J. Paik, S. G. Gaynor, *Macromolecules*, **1997**, *30*, 6398-6400
[37] J. Xia, X. Zhang, K. Matyjaszewski, *Macromolecules*, **1999**, *32*, 3531-3533
[38] S. Coca, K. Matyjaszewski, *Polym. Prepr*., **1996**, *37*, 573-574
[39] R. M. Johnson, C. Ng, C. C. M. Samson, C. L. Fraser, *Macromolecules*, **2000**, 33, 8618-8628
[40] K. Matyjaszewski, B. Göbelt, H.-J. Paik, C. P. Horwitz, *Macromolecules*, **2001**, *4*, 430-440
[41] S. Maria, F. Stoffelbach, J. Mata, J.-C. Daran, P. Richard, R. Poli, *J. Am. Chem. Soc*., **2005**, *127*, 5946-5956
[42] S. H. Chan, L. S. Man Lam, C. W. Tse, K. Y. Kitty Man, W. T. Wong, A. B. Djurišić, W. K. Chan, *Macromolecules*, **2003**, *36*, 5482-5490
[43] K. Matyjaszewski, M. Wei, J. Xia, N. E. McDermott, *Macromolecules*, **1997**, *30*, 8161-8164
[44] T. Opstal, F. Verpoort, *Angew. Chem. Int. Ed*., **2003**, *42*, 2876-2879
[45] C. Moineau, M. Minet, P. Teyssié, R. Jérôme, *Macromolecules*, **1999**, 32, 8277-8282
[46] P. Lecomte, I. Drapier, P. Dubois, P. Teyssié, R. Jérôme, *Macromolecules*, **1997**, 30, 7631-7633
[47] T. Opstal, J. Zednik, J. Sedlacek, J. Svoboda, J. Vohlidal, F. Verpoort, *Col. Czec. Chem. Commun*., **2002**, *67*, 1858-1871
[48] Y. Shen, H. Tang, S. Ding, *Prog. Polym. Sci*., **2004**, *29*, 1053-1078
[49] S. Chul Hong, K. Matyjaszewski, *Macromolecules*, **2002**, *35*, 7592-7605

[50] W. Jakubowski, K. Min, K. Matyjaszewski, *Macromolecules*, **2006**, *39*, 39-45
[51] J. Hyun Jeong, J. H. Youk, S. H. Ahn, J. H. Choi, K. S. Cho, *Macromol. Res*., **2009**, *17*, 240-244
[52] S.-I. Yamamoto, K. Matyjaszewski, *Polym. J*., **2008**, *40*, 496-497
[53] K. Min, H. Gao, K. Matyjaszewski, *Macromolecules*, **2007**, *40*, 1789-1791
[54] M. J. Nasrullah, V. V. Sonalkar, R. M. Hoshaw, D. C. Webster, *Polym. Prepr*., **2008**, *49*, 20-21
[55] Y. Kwak, K.Matyjaszewski, *Polym. Int*., **2009**, *58*, 242-247
[56] K. Matyjaszewski, B. E. Woodworth, *Macromolecules*, **1998**, *31*, 4718-4723
[57] E. Le Grognec, J. Claverie, R. Poli, *J. Am. Chem. Soc*., **2001**, *123*, 9513-9524
[58] V. C. Gibson, R. K. O'Reilly, D. F. Wass, A. J. P. White, D. J. Williams, *Macromolecules*, **2003**, *36*, 2591-2593
[59] M. P. Shaver, L. E. N. Allan, H. S. Rzepa, V. C. Gibson, *Angew. Chem. Int . Ed*., **2006**, *45*, 1241-1244
[60] M. P. Shaver, L. E. N. Allan, V. C. Gibson, *Organometallics*, **2007**, *26*, 4725-4730
[61] L. E. N. Allan, J. P. MacDonald, A. M. Reckling, C. M. Kozak, M. P. Shaver, *Macromol. Rapid commun*., **2012**, *33*, 414-418
[62] A. Debuigne, J.-R. Caille, R. Jérôme, *Macromolecules*, **2005**, *38*, 5452-5458
[63] B. B. Wayland, L. Basickes, S. L. Mukerjee, M. Wei, M. Fryd, *Macromolecules*, **1997**, *30*, 8109-8112
[64] B. B. Wayland, G. Poszmik, and S. L. Mukerjee *J. Am. Chem. Soc.*, **1994**, *116*, 7943-7944
[65] M. R. Perry, L. E. N. Allan, A. Decken, M. P. Shaver, *Dalton Trans*., **2013**, *42*, 9157-9165
[66] Y. Champouret, K. C. MacLeod, U. Baisch, B. O. Patrick, K. M. Smith, R. Poli, *Organometallics*, **2010**, *29*, 167-176
[67] W. A. Braunecker, Y. Itami, K. Matyjaszewski, *Macromolecules*, **2005**, *38*, 9402-9404
[68] For an interesting historic perspective, see: A. Gridnev, *J. Polym. Sci. Part A: Polym. Chem*., **2000**, *38*, 1753-1766
[69] A. A. Gridnev, S. D. Itell, *Chem. Rev*., **2001**, *101*, 3611-3659
[70] L. D. Arvanitopoulos, M. P. Greuel, H. J. Harwood, *Polym. Prepr*., **1994**, *35*, 549-550
[71] A. Debuigne, J.-R. Caille, R. Jérôme, *Angew. Chem. Int. Ed*., **2005**, *44*, 1101-1104
[72] S. Maria, H. Kaneyoshi, K. Matyjaszewski, R. Poli, *Chem. Eur. J*., **2007**, *13*, 2480-2492
[73] B. B. Wayland, C.-H. Peng, X. Fu, Z. Lu, M. Fryd, *Macromolecules*, **2006**, *39*, 8219-8222
[74] A. Debuigne, J.-R. Caille, N. Willet, R. Jérôme, *Macromolecules*, **2005**, *38*, 9488-9496
[75] D. N. Bunck, G. P. Sorenson, M. K. Mahanthappa, *J. Polym. Sci. Part A: Polym. Chem*., **2011**, *49*, 242-249
[76] R. Bryaskova, C. Detrembleur, A. Debuigne, R. Jérôme, *Macromolecules*, **2006**, *39*, 8263-8268
[77] C. Detrembleur, R. Jérôme, Y. Piette, A. Debuigne, V. Sciannamea, *Chem. Commun.,* **2006**, 4180
[78] A. H. Janowicz (E.I. DuPont de Nemours and Co.) EP 261942, **1988**
[79] A. H. Janowicz (E.I. DuPont de Nemours and Co.) EP 222619, **1987**
[80] G. P. Abramo, J. R. Norton, *Macromolecules*, **2000**, *33*, 2790-2792
[81] G. P. Abramo, J. R. Norton, Book Abstr., 216th ACS Nat. Meet., 1998, INOR-423
[82] J. R. Norton, G. P. Abramo, Book Abstr., 220th ACS Nat. Meet., 2000, INOR-313
[83] J. Chiefari, Y. K. Chong, F. Ercole, J. Krstina, J. Jeffery, T. P. T. Le, R. T. A. Mayadunne, G. F. Meijs, C. L. Moad, G. Moad, E. Rizzardo, S. H. Thang, *Macromolecules*, **1998**, *31*, 5559-5562
[84] D. Colombani, P. Chaumont, *Prog. Polym. Sci*., **1996**, *21*, 439-503
[85] G. F. Meijs and E. Rizzardo, *Makromol. Rapid. Commun*., **1988**, *9*, 547-551
[86] M. Destarac, C. Brochon, J.-M. Catala, A. Wilczewska, S. Z. Zard, *Macromol. Chem. Phys*., **2002**, *203*, 2281-2289
[87] J. Chiefari, R. T. A. Mayadunne, C. L. Moad, G. Moad, E. Rizzardo, A. Postma, M. A. Skidmore, S. H. Thang, *Macromolecules*, **2003**, *36*, 2273-2283
[88] Y. K. Chong, J. Krstina, T. P. T. Le, G. Moad, A. Postma, E. Rizzardo, and S. H. Thang, *Macromolecules*, **2003**, *36*, 2256-2272
[89] G. Moad, E. Rizzardo, S. H. Thang, *Aust. J. Chem*., **2005**, 58, 379-410
[90] C. McCormick and A. B. Lowe, *Acc. Chem. Res*., **2004**, 37, 312-325
[91] S. Perrier, T. P. Davis, A. J. Carmichaelb and D. M. Haddleton, *Chem. Commun*., **2002**, 2226-2227
[92] T. Arita, S. Beuermann, M. Buback, P. Vana, *E-Polymers*, **2004**, 003
[93] I. Uzulina, S. Kanagasabapathy, J. Claverie, *Macromol. Symp*., **2000**, *150*, 33-38
[94] S. Nozari, K. Tauer, *Polymer*, **2005**, *46*, 1033-1043
[95] A. Butté, G. Storti, and M. Morbidelli, *Macromolecules*, **2001**, *34*, 5885-5896
[96] B. Charleux, *Macromolecules*, **2000**, *33*, 5358-5365
[97] J. Rzayev and J. Penelle, *Angew. Chem. Int. Ed*., **2004**, *43*, 1691-1694
[98] M. J. Monteiro, R. Bussels, S. Beuermann and M. Buback, *Aust. J. Chem*., **2002**, *55*, 433-443
[99] [a] S. Saricilar, R. Knott, C. Barner-Kowollik, T. P. Davis, J. P.A. Heuts, *Polymer*, **2003**, *44*, 5169-5176; [b] T. Krasia, R. Soula, H. G. Börner, H. Schlaad, *Chem. Commun*., **2003**, 538-539; [c] X. Hao, J. P. A. Heuts, C. Barner-Kowollik, T. P. Davis, E. Evans, *J. Polym. Sci. A, Polymer Chem*., **2003**, *41*, 2949-2963; [d] E. N. Savariar, S. Thayumanavan, *J. Polym. Sci. A, Polymer Chem*., **2004**, *42*, 6340-6345
[100] A. Postma, T. P. Davis, G. Moad, M. S. O'Shea, *Macromolecules*, **2005**, *38*, 5371-5374
[101] M. Tatemoto, Y. Yutani, K. Fujiwara (Daikin Industries, Ltd) EP 272698, **1988**

[102] C. Boyer, D. Valade, P. Lacroix-Desmazes, B. Ameduri, B. Boutevin, *J. Polym. Sci. Part A: Polym. Chem*., **2006**, *44*, 5763-5777
[103] A. W. Barnes (Imperial Chemical Industries, Ltd) GB 674060, **1952**
[104] M. C. Iovu, K. Matyjaszewski, *Macromolecules*, **2003**, *36*, 9346-9354
[105] S. G. Gaynor, J.-S. Wang, K. Matyjaszewski, *Macromolecules*, **1995**, *28*, 8051-8056
[106] P. Lacroix-Desmazes, R. Severac, B. Boutevin, V. Bodart, V. Kurowsky (Solvay SA) WO 03097704, **2003**
[107] D. E. P. Mestach, R. H. G. Brinkhuis, P. J. M. D. Elfrink (Akzo Nobel N.V.) WO 2004009648, **2004**
[108] P. Lacroix-Desmazes, R. Severac, B. Boutevin, *Macromolecules*, **2005**, *38*, 6299-6309
[109] C. Boyer, P. Lacroix-Desmazes, J.-J. Robin, B. Boutevin, *Macromolecules*, **2006**, *39*, 4044-4053
[110] J. Tonnar, P. Lacroix-Desmazes, *Polym. Prepr*., **2008**, *49*, 66-67
[111] A. Butté, G. Storti, M. Morbidelli, *Macromolecules*, **2000**, *33*, 3485-3487
[112] S. Yamago, H. Miyazoe, J. Yoshida, *Tetrahedron Lett*., **1999**, *40*, 2339-2342
[113] S. Yamago, K. Iida, J.-I. Yoshida, *J. Am. Chem. Soc*., **2002**, *124*, 2874-2875
[114] W. G. Skene, S. T. Belt, T. J. Connolly, P. Hahn, J. C. Scaiano, *Macromolecules*, **1998**, *31*, 9103-9105
[115] S. Yamago, K. Iida, and J.-I. Yoshida, *J. Am. Chem. Soc*., **2002**, *124*, 13666-13667
[116] A. Goto, Y. Kwak, T. Fukuda, S. Yamago, K. Iida, M. Nakajima, and J.-I Yoshida, *J. Am. Chem. Soc*., **2003**, *125*, 8720-8721
[117] S. Yamago, B. Ray, K. Iida, J.-I. Yoshida, T. Tada, K. Yoshizawa, Y. Kwak, A. Goto, T. Fukuda, *J. Am. Chem. Soc*., **2004**, *126*, 13908 -13909
[118] S. Yamago, *J. Polym. Sci. Part A: Polym. Chem*., **2006**, *44*, 1-12
[119] Y. Kwak, A. Goto, T. Fukuda, S. Yamago, B. Ray, *Z. Phys. Chem*., **2005**, *219*, 283-293
[120] S. Yamago, E. Kayahara, M. Kotani, B. Ray, Y. Kwak, A. Goto, T. Fukuda, *Angew. Chem. Int. Ed*., **2007**, *46*, 1304-1306
[121] Y. Kwak, A. Goto, T. Fukuda, Y. Kobayashi, S. Yamago, *Macromolecules,* **2006**, *39*, 4671-4679
[122] M. Ouchi, T. Terashima, M. Sawamoto, *Chem. Rev*., **2009**, *109*, 4963-5050
[123] K. Matyjaszewski, B. Sumerlin, N. V. Tsarevsky, Progress in Controlled Radical Polymerization: Materials and Applications; Am. Chem. Soc., Washington, D.C., **2012**; ISBN: 978-0-8412-2756-9
[124] R. A. Hutchinson, J. R. Richards, M. T. Aronson, *Macromolecules*, **1994**, *27*, 4530-4537
[125] E. Chiellini, A. Corti, S. D'Antone and R. Solaro, *Prog. Polym. Sci*., **2003**, *28*, 963-1014
[126] C. M. Hassan, N. A. Peppas, *Adv. Polym. Sci*., **2000**, *153*, 37-65
[127] K. Y. Lee, D. J. Mooney, *Chem. Rev*., **2001**, *101*, 1869-1879
[128] K. Matyjaszewski, D. Mardare, *Macromolecules,* **1994**, *27*, 645-649
[129] C. Granel, R. Jérôme, P. Teyssié, C. B. Jasieczek, A. J. Shooter, D. M. Haddleton, J. J. Hastings, D. Gigmes, S. Grimaldi, P. Tordo, D. Greszta, K. Matyjaszewski, *Macromolecules*, **1998**, *31*, 7133-7141
[130] K. Matyjaszewski, H.-J. Paik, J. Xia, *Macromolecules,* **1999**, *32*, 8310-8314
[131] M. Sawamoto, M. Kamigaito, T. Ando, K.-Y. Baek, M. Wakioka, *Macromolecules,* **2002**, *35*, 330-333
[132] H. D. Tang, M. Radosz, Y. Q. Shen, *AIChE J.*, **2009**, *55*, 737-746
[133] E. K. Euranto, A. Noponen, T. Kujanpää, *Acta Chem. Scand*., **1966**, *20*, 1273-1280
[134] K. Matyjaszewski, *Macromolecules*, **1998**, *31*, 4710-4717
[135] D. Charmot, P. Copart, H. Adam, S. Z. Zard, T. Biadatti, G. Bouhadir, *Macromol. Symp*., **2000**, *150*, 23-32
[136] E. Rizzardo, J. Chiefari, R. Mayadunne, G. Moad, S. Thang, *Macromol. Symp*., **2001**, *174*, 209-212
[137] P. Vana, T. P. Davis, G. E. Roberts, L. Cummins, M. H. Stenzel, *Macromol. Chem. Phys.,* **2003**, *204*, 1160-1168
[138] S. Perrier, P. Takolpuckdee, *J. Polym. Sci. Part A: Polym. Chem.,* **2005**, *43*, 5347-5393
[139] M. L. Coote, L. Radom, *Macromolecules*, **2004**, *37*, 590-596
[140] M. F. Cunningham, T. P. Davis, R. W. Simms, *Macromol. Rapid Commun.,* **2005**, *26*, 592-596
[141] M. H. Stenzel,T. P. Davis, C. Barner-Kowollik, *Chem. Commun*., **2004**, 1546-1547
[142] J. Bernard, A. Favier, L. Zhang, A. Nilasaroya, T. P. Davis, C. Barner-Kowollik, M. H. Stenzel, *Macromolecules*, **2005**, *38*, 5475-5484
[143] A. K. Srivastave, A. K. Chaurasia, S. Sharma, G. Mishra, *J. Sci. Indus. Res*., **2006**, *65*, 514-517
[144] N. Ueda (Sekisui Chemical Co. Ltd.) JP 10060021, **1998**
[145] N. Ueda (Sekisui Chemical Co. Ltd.) JP 11255827, **1999**
[146] N. Ueda (Sekisui Chemical Co. Ltd.) JP 11171926, **1999**
[147] N. Ueda (Sekisui Chemical Co. Ltd.) JP 11147914, **1999**
[148] B. Boutevin, J. P. Hugon, Y. Pietrasanta, A. Sideris, *Eur. Polym. J*., **1978**, *14*, 353-356
[149] R. Adams, W. V. Wirth, H. E. French, *J. Am. Chem. Soc*., **1918**, *40*, 424-431
[150] Y. Okamoto, M. Kamigaito, K. Satoh, K. Koumura, *Macromolecules* **2006**, *39*, 4054
[151] B. B. Wayland, M. fryd, S. Li, J. Scricco, C.-H. Peng, *Macromolecules,* **2008**, *41*, 2368-2373
[152] S. Li, B. de Bruin, C.-H. Peng, M. Fryd, B. B. Wayland, *J. Am. Chem. Soc*., **2008**, *130* , 13373-13381
[153] Y. Champouret, U. Baisch, R. Poli, L. Tang, J. L. Conway, K. M. Smith, *Angew. Chem. Int. Ed.,* **2008**, *47*, 6069-6072
[154] R. Jérôme, B. Charleux, R. Bryaskova, A. Debuigne, C. Detrembleur, *Macromol. Rapid Commun.,* **2006**, *27*, 37-41

[155] A. Debuigne, J.-R. Caille, C. Detrembleur, R. Jérôme, *Angew. Chem. Int. Ed*., **2005**, *44*, 3439-3442
[156] S. Dai, P. Ravi, K. C. Tam, *Soft Matter*, **2009**, *5*, 2513-2533
[157] C. de las Heras Alarcón, S. Pennadam, C. Alexander, *Chem. Soc. Rev*., **2005**, *34*, 276-285
[158] A. B. Lowe, C. L. McCormick, *Prog. Polym. Sci*., **2007**, *32*, 283-351
[159] D. Schmaljohann, *Adv. Drug Delivery Rev*., **2006**, *58*, 1655-1670
[160] A. K. Bajpai, S. K. Shukla, S. Bhanu, S. Kankane, *Prog. Polym. Sci*., **2008**, *33*, 1088-1118
[161] A. Kikuchi, T. Okano, *Prog. Polym. Sci*., **2002**, *27*, 1165-1193
[162] G. Chan, D. J. Mooney, *Trends Biotechnol*., **2008**, *26*, 382-392
[163] A. Kermagoret, C.-A. Fustin, M. Bourguignon, C. Detrembleur, C. Jérôme, A. Debuigne, *Polym. Chem*., **2013**, *4*, 2575-2583
[164] D. Wan, K. Satoh, M. Kamigaito, Y. Okamoto, *Macromolecules*, **2005**, *38*, 10397-10405
[165] A. Postma, T. P. Davis, G. Li, G. Moad, M. S. O'Shea, *Macromolecules*, **2006**, *39*, 5307-5318
[166] R. Devasia, R. L. Bindu, R. Borsali, N. Mougin, Y. Gnanou, *Macromol. Symp*., **2005**, *229*, 8-17
[167] G. Pound, J. B. McLeary, J. M. McKenzie, R. F. M. Lange, B. Klumperman, *Macromolecules*, **2006**, *39*, 7796-7797
[168] N. Fandrich, J. Falkenhagen, S. M. Weidner, D. Pfeifer, B. Staal, A. F. Thünemann, A. Laschewsky, *Macromol. Chem. Phys*., **2010**, *211*, 869-878
[169] B. Ray, M. Kotani, S. Yamago, *Macromolecules*, **2006**, *39*, 5259-5265
[170] X. Lu, S. Gong, L. Meng, C. Li, S. Yang, L. Zhang, *Polymer*, **2007**, *48*, 2835-2842
[171] H. Kaneyoshi, K. Matyjaszewski, *Macromolecules*, **2006**, *39*, 2757-2763
[172] A. Debuigne, N. Willet, R. Jérôme, C. Detrembleur, *Macromolecules*, **2007**, *40*, 7111-7118
[173] A. Debuigne, R. Poli, J. De Winter, P. Laurent, P. Gerbaux, J.-P. Wathelet, C. Jérôme, C. Detrembleur, *Macromolecules*, **2010**, *43*, 2801-2813
[174] A. Debuigne, M. Schoumacher, N. Willet, R. Riva, X. Zhu, S. Rütten, C. Jérôme, C. Detrembleur, *Chem. Commun*., **2011**, *47*, 12703-12705
[175] R. J. Badesso, A. F. Nordquist, R. K. Pinschmidt, D. J. Sagl, Hydrophilic Polymers: Performance with Environmental Acceptance; Glass, J. E., Ed.; Am. Chem. Soc., Washington, D.C., **1996**; DOI:10.1021/ba-1996-0248
[176] F. Brunnmueller, R. Schneider, M. Kroener, H. Mueller, F. Linhart, H. Burkert, K. H. Beyer (BASF A.-G., Fed. Rep. Ger.) EP 71050, **1983**
[177] R. K. Pinschmidt, N. Chen, *Polym. Prepr*., **1998**, *39*, 639
[178] L. Shi, T. M. Chapman, E. J. Beckman, *Macromolecules*, **2003**, *36*, 2563-2567
[179] L. Gu, S. Zhu, A. N. Hrymak, R. H. Pelton, *Macromol. Rapid Commun*., **2001**, *22*, 212-214
[180] L. Gu, S. Zhu, A. N. Hrymak, R. H. Pelton, *Polymer*, **2001**, *42*, 3077-3086
[181] N. S. Ieong, M. Redhead, C. Bosquillon, C. Alexander, M. Kelland, R. K. O'Reilly, *Macromolecules*, **2011**, *44*, 886-893
[182] Y. E. Kirsh, Water Soluble Poly(N-Vinyl Amides), Synthesis and Physicochemical Properties; Wiley, **1998**; ISBN: 978-0-471-97630-1
[183] A. C. W. Lau, C. Wu, *Macromolecules*, **1999**, *32*, 581-584
[184] D. Wan, Q. Zhou, H. Pu, G. Yang, *J. Polym. Sci. Part A: Polymer Chem*., **2008**, *46*, 3756-3765
[185] M. Beija, J.-D. Marty, M. Destarac, *Chem. Commun*., **2011**, *47*, 2826-2828
[186] M. Hurtgen, J. Liu, A. Debuigne, C. Jérôme, C. Detrembleur, *J. Polym. Sci. Part A: Polymer Chem*., **2012**, *50*, 400-408
[187] E. Jonhson, M. Arne, Chemistry & Industry (London, United Kingdom) **2009**, 14, 23-24
[188] Ressources PSA Peugeot Citroën – Renault ADEME
[189] J. Albert, G. Luft, *Chem. Eng. Proc*., **1998**, *37*, 55-59
[190] D. P. Gates, S. A. Svejda, Enrique Oñate, C. M. Killian, L. K. Johnson, P. S. White, M. Brookhart, *Macromolecules*, **2000**, *33*, 2320-2334
[191] L. Deng, P. Margl, T. Ziegler, *J. Am. Chem. Soc*., **1999**, *121*, 6479-6487
[192] P. Nicol, S. Hub (Arkema France, Fr.) FR 2971510 A1, **2012**
[193] M. Buback, E. Minaux, T. Senninger, J.-M. Le Blevec (Elf Atochem S.A., Fr.) WO 2000020469, **2000**
[194] E. Minaux, L. Greci, M. Buback, P. Tordo, T. Senninger, P. Stipa, P. Carloni, E. Damiani, G. Tommasi (ATOFINA, Fr.) EP 1120430, **2001**
[195] K. A. Moffat, M. D. Saban, R. P. N. Veregin, M. K. Georges, G. K. Hamer, P. M. Kazmaier (Xerox corp.) US5449724A, **1994**
[196] E. Grau, J.-P. Broyer, C. Boisson, R. Spitz, V. Monteil, *Macromolecules*, **2009**, *42*, 7279-7281
[197] E. Grau, J.-P. Broyer, C. Boisson, R. Spitz, V. Monteil, *Polym. Chem.*, **2011**, *2*, 2328-2333
[198] D. E. Dorman, E. P. Otocka, F. A. Bovey, *Macromolecules*, **1972**, *5*, 574-577
[199] R. S. Lehrle, C. S. Pattenden, *Polym. Degrad. Stab*., **1999**, *63*, 153-158
[200] M. L. Coote, E. I. Izgorodina, G. E. Cavigliasso, M. Roth, M. Busch, C. Barner-Kowollik, *Macromolecules*, **2006**, *39*, 4585-4591
[201] S. Liu, B. Gu, H. A. Rowlands, A. Sen, *Macromolecules*, **2004**, *37*, 7924-7929

[202] R. Venkatesh, S. Harrisson, D. M. Haddleton, B. Klumperman, *Macromolecules*, **2004**, *37*, 4406-4416
[203] R. Venkatesh, B. Klumperman, *Macromolecules*, **2004**, *37*, 1226-1233
[204] B. Gu, S. Liu, J. D. Leber, A. Sen, *Macromolecules*, **2004**, *37*, 5142-5144
[205] E. Mishima, T. Tamura, S. Yamago, *Macromolecules*, **2012**, *45*, 2989-2994
[206] S. Borkar, A. Sen, *Macromolecules*, **2005**, *38*, 3029-3032
[207] S. Liu, S. Elyashiv, A. Sen, *J. Am. Chem. Soc*., **2001**, *123*, 12738-12739
[208] S. Liu, A. Sen, *J. Polym. Sci., Part A: Polym. Chem*., **2004**, *42*, 6175-6192
[209] M. Nagel, D. Poli, A. Sen, *Macromolecules*, **2005**, *38*, 7262-7265
[210] A. Debuigne, A. N. Morin, A. Kermagoret, Y. Piette, C. Detrembleur, C. Jérôme, R. Poli, *Chem. Eur. J*., **2012**, *18*, 12834-12844
[211] A. N. Morin, C. Detrembleur, C. Jérôme, P. De Tullio, R. Poli, A. Debuigne, *Macromolecules*, **2013**, *46*, 4303-4312
[212] A. Debuigne, Y. Champouret, R. Jérôme, R. Poli, C. Detrembleur, *Chem. Eur. J*., **2008**, *14*, 4046-4059
[213] G.-C. Kuang, P. M. Guha, W. S. Brotherton, J. T. Simmons, L. A. Stankee, B. T. Nguyen, R. J. Clark, L. Zhu, *J. Am. Chem. Soc*., **2011**, *133*, 13984-14001
[214] L. Fomina, B. Vazquez, E. Tkatchouk, S. Fomine, *Tetrahedron*, **2002**, *58*, 6741-6747
[215] A. E. King, T. C. Brunold, S. S. Stahl, *J. Am. Chem. Soc*., **2009**, *131*, 5044-5045
[216] E. Sperotto, G. P. M. van Klink, G. van Koten, J. G. de Vries, *Dalton Trans*., **2010**, *39*, 10338-10351
[217] M. Freiberg, W. A. Mulac, K. H. Schmid, D. Meyerstein, *J. C. S. Faraday I*, **1980**, *76*, 1838-1848
[218] H. Cohen, D. Meyerstein, *Inorg. Chem*., **1987**, *26*, 2342-2344
[219] H. Cohen, D. Meyerstein, *Inorg. Chem*., **1986**, *25*, 1505-1506
[220] N. Navon, G. Golub, H. Cohen, D. Meyerstein, *Organometallics*, **1995**, *14*, 5670-5676
[221] P. J. Chmielewski, L. Latos-Grażyński , I. Schmidt, *Inorg. Chem*., **2000**, *39*, 5475-5482
[222] H. Furuta, T. Ishizuka, A. Osuka, Y. Uwatoko, Y. Ishikawa, *Angew. Chem. Int. Ed*., **2001**, *40*, 2323-2325
[223] H. Maeda, Y. Ishikawa, T. Matsuda, A. Osuka, H. Furuta, *J. Am. Chem. Soc*., **2003**, *125*, 11822-11823
[224] H. Maeda, A. Osuka, Y. Ishikawa, I. Aritome, Y. Hisaeda, H. Furuta, *Org. Lett*., **2003**, *5*, 1293-1296
[225] M. Pawlicki, I. Kańska, L. Latos-Grażyński, *Inorg. Chem*., **2007**, *46*, 6575-6584
[226] N. Grzegorzek, M. Pawlicki, L. Szterenberg, L. Latos-Grażyński, *J. Am. Chem. Soc*., **2009**, *131*, 7224-7225
[227] X. Hu, I. Castro-Rodriguez, K. Meyer, *J. Am. Chem. Soc*., **2003**, *125*, 12237-12245
[228] A. O. Larsen, W. Leu, C. N. Oberhuber, J. E. Campbell, A. H. Hoveyda, *J. Am. Chem. Soc*., **2004**, *126*, 11130-11131
[229] J. M. Smith, J. R. Long, *Inorg. Chem*., **2010** , *49*, 11223-11230
[230] I. Kinoshita, L. J. Wright, S. Kubo, K. Kimura, A. Sakata, T. Yano, R. Miyamoto, T. Nishioka, K. Isobe, *Dalton Trans*., **2003**, 1993-2003
[231] R. Miyamoto, R. Santo, T. Matsushita, T. Nishioka, A. Ichimura, Y. Teki, I. Kinoshita, *Dalton Trans*., **2005**, 3179-3186
[232] N. Kitajima, K. Fujisawa, Y. Moro-oka, *J. Am. Chem. Soc*., **1990**, *112*, 3210-3212
[233] S. G. N. Roundhill, D. M. Roundhill, D. R. Bloomquist, C. Landee, R. D. Willett, D. M. Dooley, H. B. Gray, *Inorg. Chem*., **1979**, *18*, 831-835
[234] C. Mealli, C. S. Arcus, J. L. Wilkinson, T. J. Marks, J. A. Ibers, *J. Am. Chem. Soc*., **1976**, *98*, 711-718
[235] K. Schröder, D. Konkolewicz, R. Poli, K. Matyjaszewski, *Organometallics*, **2012**, *31*, 7994-7999
[236] R. Stibrany, D. Schultz, S. Kacker, A. Patil, (Exxon Researchand Engineering) WO 9930822, **1999**
[237] R. T. Stibrany, D. N. Schulz, S. Kacker, A. O. Patil, L. S. Baugh, S. P. Rucker, S. Zushma, E. Berluche, J. A. Sissano, *Macromolecules*, **2003**, *36*, 8584-8586
[238] V. C. Gibson, A. Tomov, D. F. Wass, A. J. P. White, D. J. Williams, *J. Chem. Soc., Dalton Trans*., **2002**, 2261-2262
[239] A. M. R. Gallette, C. Carlini, S. Giaiacopi, M. Martinelli, G. Sbrana, *J. Polym. Sci. Part A: Polym. Chem*., **2007**, *45*, 1134-1142
[240] M. B. Bushuev, V. P. Krivopalov, N. V. Semikolenova, Y. G. Shvedenkov, L. A. Sheludyakova, G. G. Moskalenko, L. G. Lavrenova, V. A. Zakharov, S. V. Larionov, *Russ. J. Coord. Chem*., **2007**, *33*, 601-606
[241] M. B. Bushuev, V. P. Krivopalov, N. V. Semikolenova, E. V. Peresypkina, A. V. Virovets, L. A. Sheludyakova, L. G. Lavrenova, V. A. Zakharov, S. V. Larionov, *Russ. J. Coord. Chem*., **2006**, *32*, 199-207
[242] S. V. Larionov, Z. A. Savel'eva, N. V. Semikolenova, R. F. Klevtsova, L. A. Glinskaya**,** E. G. Boguslavskii, V. N. Ikorskii, V. A. Zakharov, S. A. Popov, A. V. Tkachev, *Russ. J. Coord. Chem*., **2007**, *33*, 436-448
[243] J. A. Olson, R. Boyd, J. W. Quail, S. R. Foley, *Organometallics*, **2008**, *27*, 5333-5338
[244] S. Trofimenko, *Polyhedron*, **2004**, *23*, 197-203
[245] L. Bourget-Merle, M. F. Lappert, J. R. Severn, *Chem. Rev*., **2002**, *102*, 3031-3065
[246] X. Dai, T. H. Warren, *Chem. Commun*., **2001**, 1998-1999
[247] J. T. York, V. G. Young, Jr., W. B. Tolman, *Inorg. Chem*., **2006**, *45*, 4191-4198
[248] X. Dai, T. H. Warren, *Chem. Commun*., **2001**, 1998-1999
[249] L. D. Amisial, X. Dai, R. A. Kinney, A. Krishnaswamy, T. H. Warren, *Inorg. Chem*., **2004**, *43*, 6537-6539
[250] H. P. Waits, G. S. Hammond, *J. Am. Chem. Soc*., **1964**, *86*, 1911-1918

[251] A. Debuigne, R. Poli, R. Jérôme, C. Jérôme, C. Detrembleur, *ACS Symp. Ser*., **2009**, *1024*, 131-148
[252] M. N. C. Balili, T. Pintauer, *Acta Cryst*., **2007**, *E63*, m988-m990
[253] J. S. Thompson, R. L. Harlow, J. F. Whitney, *J. Am. Chem. Soc*., **1983**, *105*, 3522-3527
[254] H. V. R. Dias, H.-L. Lu, H.-J. Kim, S. A. Polach, T. K. H. H. Goh, R. G. Browning, C. J. Lovely, *Organometallics*, **2002**, *21*, 1466-1473
[255] M.-K. Wang, Z.-L. Zhou, R.-Y. Tang, X.-G. Zhang, C.-L. Deng, *Synlett*, **2013**, *24*, 737-740
[256] H. Sun, Y. Zhang, F. Guo, Z. Zha, Z. Wang, *J. Org. Chem*., **2012**, *77*, 3563-3569
[257] R. C. Reid, J. M. Prausnitz, B. E. Poling, inThe Properties of Gases and Liquids, ed. R. C. Reid, J. M. Prausnitz and B. E. Poling, McGraw-Hill Book Company, Singapore, **1988**, pp. 74–84
[258] E. Grau, J.-P. Broyer, C. Boisson, R. Spitz, V. Monteil, *Phys. Chem. Chem. Phys*., **2010**, *12*, 11665–11669
[259] L.-S. Lee, H.-J. Ou, H.-L. Hsu, *Fluid Phase Equ*., **2005**, *231*, 221-230
[260] Located at Liège, Belgium, website: http://www.cerm.ulg.ac.be
[261] M. R. Bray, R. J. Deeth, V. J. Paget, P. D. Sheen, *Quantum Chem*., **1998**, *61*, 85-91
[262] M. Reiher, *Inorg. Chem*., **2002**, *41*, 6928-6935
[263] J. N. Harvey, M. Aschi, *Faraday Discuss*., **2003**, *124*, 129-143
[264] A. D. Becke, *J. Chem. Phys*., **1993**, *98*, 5648-5652
[265] J. P. Perdew, J. A. Chevary, S. H. Vosko, K. A. Jackson, M. R. Pederson, D. J. Singh, C. Fiolhais, *Phys. Rev. B*, **1992**, *46*, 6671-6687
[266] A. Debuigne, C. Michaux, C. Jerome, R. Jerome, R. Poli, C. Detrembleur, *Chem. Eur. J*., **2008**, *14*, 7623-7637
[267] J. Casabó, J. Marquet, M. Moreno-Manas, M. Prior, F. Teixidor, F. Florencio, S. Martinez-Carrera, S. Garcia-Blanco, *Polyhedron*, **1987**, *6*, 1235-1238
[268] G. Arom, C. Boldron, P. Gamez, O. Roubeau, H. Kooijman, A. L. Spek, H. Stoeckli-Evans, J. Ribas, J. Reedijk, *Dalton Trans*., **2004**, 3586-3592
[269] E. Senogles, R. Thomas, *J. Polym. Sci. Part C: Polym. Symp*., **1975**, *49*, 203-210
[270] M. Stach, I. Lacík, C. Jr. Dušan, M. Buback, P. Hesse, R. A. Hutchinson, L. Tang, *Macromolecules*, **2008**, *41*, 5174-5185
[271] H.-J. Paik, M. Teodorescu, J. Xia, K. Matyjaszewski, *Macromolecules*, **1999**, *32*, 7023-7031
[272] M. Destarac, D. Charmot, X. Franck, S. Z. Zard, *Macromol. Rapid Commun*., **2000**, *21*, 1035-1039
[273] P. J. Flory, F. S. Leutner, *J. Polym. Sci*., **1948**, *3*, 880-890
[274] C. Y. Lin, M. L. Coote, A. Petit, P. Richard, R. Poli, K. Matyjaszewski, *Macromolecules*, **2007**, *40*, 5985-5994
[275] A. K. Nanda, K. Matyjaszewski, *Macromolecules*, **2003**, *36*, 8222-8224
[276] K. Schröder, R. T. Mathers, J. Buback, D. Konkolewicz, A. J. D. Magenau, K. Matyjaszewski, *ACS Macro. Lett*., **2012**, *8*, 1037-1040
[277] X. Tang, S. Woodward, N. KrauseEur., *J. Org. Chem*., **2009**, 2836-2844
[278] S. T. Handy, A. Ivanow, *Inorg. Chim. Acta*, **2009**, *362*, 4468-4471
[279] H. V. R. Dias, H.-L. Lu, R. E. Ratcliff, S. G. Bott, *Inorg. Chem*., **1995**, *34*, 1975-1976
[280] American Polymer Standards Corporation
[281] **Gaussian 03, Revision C.02**, M. J. Frisch, G. W. Trucks, H. B. Schle-gel, G. E. Scuseria, M. A. Robb, J. R. Cheeseman, J. Montgomery, J. A. , T. Vreven, K. N. Kudin, J. C. Burant, J. M. Millam, S. S. Iyen-gar, J. Tomasi, V. Barone, B. Mennucci, M. Cossi, G. Scalmani, N. Rega, G. A. Petersson, H. Nakatsuji, M. Hada, M. Ehara, K. Toyota, R. Fukuda, J. Hasegawa, M. Ishida, T. Nakajima, Y. Honda, O. Kitao, H. Nakai, M. Klene, X. Li, J. E. Knox, H. P. Hratchian, J. B. Cross, C. Adamo, J. Jaramillo, R. Gomperts, R. E. Stratmann, O. Yazyev, A. J. Austin, R. Cammi, C. Pomelli, J. W. Ochterski, P. Y. Ayala, K. Morokuma, G. A. Voth, P. Salvador, J. J. Dannenberg, V. G. Zakrzewski, S. Dapprich, A. D. Daniels, M. C. Strain, O. Farkas, D. K. Malick, A. D. Rabuck, K. Raghavachari, J. B. Fores-man, J. V. Ortiz, Q. Cui, A. G. Baboul, S. Clifford, J. Cioslowski, B. B. Stefanov, G. Liu, A. Liashenko, P. Piskorz, I. Komaromi, R. L. Martin, D. J. Fox, T. Keith, M. A. Al-Laham, C. Y. Peng, A. Na-nayakkara, M. Challacombe, P. M. W. Gill, B. Johnson, W. Chen, M. W. Wong, C. Gonzalez, J. A. Pople, Gaussian, Inc., Wallingford CT, **2004**.
[282] **Gaussian 09, Revision A.02**, M. J. Frisch, G. W. Trucks, H. B. Schlegel, G. E. Scuseria, M. A. Robb, J. R. Cheeseman, G. Scalmani, V. Barone, B. Mennucci, G. A. Petersson, H. Nakatsuji, M. Caricato, X. Li, H. P. Hratchian, A. F. Izmaylov, J. Bloino, G. Zheng, J. L. Sonnenberg, M. Hada, M. Ehara, K. Toyota, R. Fukuda, J. Hasegawa, M. Ishida, T. Nakajima, Y. Honda, O. Kitao, H. Nakai, T. Vreven, J. A. Montgomery, Jr., J. E. Peralta, F. Ogliaro, M. Bearpark, J. J. Heyd, E. Brothers, K. N. Kudin, V. N. Staroverov, R. Kobayashi, J. Normand, K. Raghavachari, A. Rendell, J. C. Burant, S. S. Iyengar, J. Tomasi, M. Cossi, N. Rega, J. M. Millam, M. Klene, J. E. Knox, J. B. Cross, V. Bakken, C. Adamo, J. Jaramillo, R. Gomperts, R. E. Stratmann, O. Yazyev, A. J. Austin, R. Cammi, C. Pomelli, J. W. Ochterski, R. L. Martin, K. Morokuma, V. G. Zakrzewski, G. A. Voth, P. Salvador, J. J. Dannenberg, S. Dapprich, A. D. Daniels, O. Farkas, J. B. Foresman, J. V. Ortiz, J. Cioslowski, and D. J. Fox, Gaussian, Inc., Wallingford CT, **2009**.
[283] M. Reiher, *Inorg. Chem*. **2002**, *41*, 6928-6935

[284] A. W. Ehlers, M. Boehme, S. Dapprich, A. Gobbi, A. Hoellwarth, V. Jonas, K. F. Koehler, R. Stegmann, A. Veldkamp, G. Frenking, *Chem. Phys. Lett*., **1993**, *208*, 111-114
[285] A. W. Ehlers, M. Boehme, S. Dapprich, A. Gobbi, A. Hoellwarth, V. Jonas, K. F. Koehler, R. Stegmann, A. Veldkamp, G. Frenking, *Chem. Phys. Lett*., **1993**, *208*, 237-240
[286] K. Schröder, D. Konkolewicz, R. Poli, K. Matyjaszewski, *Organomet*., **2012**, *31*, 7994-7999

RESUME EN FRANCAIS

Ces travaux de thèse portent sur la polymérisation radicalaire contrôlée (PRC) des esters et amides de vinyle. L'une des possibilités de contrôle est le piégeage dynamique réversible des chaînes radicalaires croissantes ($P^{\bullet}$) par un agent de contrôle (T) formant une espèce dormante (P─T'). La concentration en radicaux dans le milieu peut alors diminuer dramatiquement de sorte que les réactions indésirables de terminaisons soient négligeables et que le contrôle de la masse molaire des polymères soit atteint avec un faible indice de dispersité. L'utilisation de complexes métalliques, pouvant s'oxider et former une liaison métal-carbone, comme agent de piégeage des radicaux est une manière de réaliser ce contrôle. La PRC est alors appelée Polymérisation Radicalaire Contrôlée par voie Organométallique (OMRP) (Schéma 1). A ce jour, plusieurs métaux de transitions ont été utilisés avec plus ou moins de succès en OMRP. Lors de cette étude, nous avons synthétisé des complexes de cuivre(I) et testé leurs performances pour l'OMRP de l'acétate de vinyle et de l'éthylène. Nous avons également utilisé des outils de chimie théorique pour mieux comprendre pourquoi le cobalt(II) acetylacetonate est, jusqu'à aujourd'hui, le meilleur agent de contrôle pour la polymérisation de l'acétate de vinyle et des amides de vinyle. Grâce à la théorie de la fonctionnelle de densité (DFT), nous avons mis en lumière le rôle crucial de la coordination sur le cobalt des groupements carbonyles des monomères étudiés.

MOTS CLEFS : Polymérisation radicalaire contrôlée (PRC), Polymérisation Radicalaire Contrôlée par voie Organométallique (OMRP), théorie de la fonctionnelle de densité (DFT), Cuivre, Acétate de vinyle, éthylene.

ENGLISH RESUME

This thesis focus on Controlled Radical Polymerization (CRP) of vinyl esters and vinyl amides. One of the possibilities to achieve this control is a dynamic reversible trapping of the growing radical chains ($P^{\bullet}$) by a controlling agent (T) to form a dormant species (P─T'). The radical concentration in the medium can be dramatically reduced so that the unwanted terminations are disfavored and polymers with controlled molecular weights and low dispersity can be obtained. A way to achieve this control is the use of metallic complexes, which can oxidize and form a metal-carbon bond, as trapping agent in the so-called Organometallic Mediated Radical Polymerization (OMRP) (Scheme 1). So far, different transition metals have been used with gretaer or smaller success. In this study, the synthesis of copper(I) complexes and their investigation for the vinyl acetate and ethylene polymerization under OMRP conditions were performed. We also used computational chemistry as a tool to better understand why the cobalt(II) acetylacetonate ($Co(acac)_2$) has, so far, given the best results for either vinyl acetate or vinyl amides polymerization. Thanks to Density Functional Theory (DFT), the crucial role of the monomer carbonyl group coordination to cobalt was pointed out.

KEY WORDS : Controlled Radical Polymerization (CRP), Organometallic Mediated Radical Polymerization (OMRP), Density Functional Theory (DFT), Copper, Vinyl acetate, ethylene.

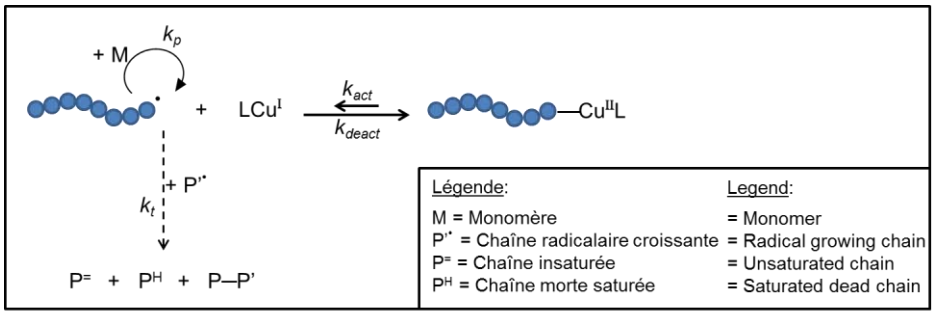

Schéma 1 : équlibre de l'OMRP / Scheme 1 : OMRP equilibrium